



Pseudo- C_3 -Symmetric Titanium Complexes For Asymmetric Catalysis

Philip Axe

A thesis submitted for the degree of Doctor of Philosophy

University of Bath

Department of Chemistry

September 2008

COPYRIGHT

Attention is drawn to the fact that copyright of this thesis rests with its author. A copy of this thesis has been supplied on condition that anyone who consults it is understood to recognise that its copyright rests with the author and they must not copy it or use material from it except as permitted by law or with the consent of the author.

This thesis may be made available for consultation within the University Library and may be photocopied or lent to other libraries for the purposes of consultation

Signed

Date

Acknowledgements

Firstly, I would like to thank Dr. Steve Bull for his continual support and guidance, without which, this thesis would never have seen the light of day. I am truly grateful. I would also like to thank Diane for her initial work in the area which made my project possible. Thanks also to Carly and Matthew Jones for their help in synthesising the metal complexes.

I would like to thank Dr. Tony James and Dr. John Fossey for the work opportunity that saw me getting to grips with working with dendrimers. Thanks also to GSK for providing my funding and to Dr. Bill Mitchell and Kam Jandu at GSK Harlow for their support during my three month placement there.

I would like to thank the entire Bull group, both past and present, who have helped me through good times and bad times, and made chemistry so much fun. Special thanks to Matt (for showing me the ropes (and the local beer!)), Sonia (for your crazy Spanish sense of humour!), Gan (for your caring and fun nature), Iwan (for being there from beginning to end-it means a lot to me), Paul (for putting up with me at the end), Mike (for providing much entertainment) and Rachel. Also, a big thanks to the people from the rest of the department, there are too many of you to mention here, but you know who you are! Thanks also to all the players, past and present, from the mighty Chemistry Football Team for all the good times!

I would also like to thank Andrew, Ewan and Steve P., my former housemates from Second Avenue, as well as Jo, Lee, Jill and Mark my current housemates at The Coach House for making my stay in Bath a good one. Thanks also to Isabel and Peter at Grove Lodge B&B for taking me on and being there with a glass of wine when things went wrong!

Special thanks to my friends Amy (for being the rock I could depend upon), Vicky and Andrew, and all the boys from back home (Pete, Dan, Robin, Sanjay and Tom).

Finally, I would like to thank all my family (Mum, Dad, Jenny and Giles, and Rob and Tanya) for all the love and support that you gave me. I couldn't have done it without you.

Abbreviations and Acronyms

Å	Ångström
Ac	acetyl
AcAc	acetylacetone
AIBN	azobisisobutyronitrile
app	apparent
Ar	aryl
BINAP	2,2'-bis(diphenylphosphino)-1,1'-binaphthyl
BINOL	1,1'-bi-2-naphthol
Bn	benzyl
BOX	bisoxazoline
bp	boiling point
br	broad
Boc	<i>tert</i> -butoxycarbonyl
°C	degree Celsius
CDCl ₃	deuterated chloroform
CI	chemical ionisation
CHP	cumene hydroperoxide
cm ³	cubic centimetre
cm ⁻¹	wavenumbers
COD	1,5-cyclooctadiene
COSY	correlated spectroscopy
Cp	cyclopentadiene
δ	chemical shift in parts per million
Δ	heat
2D	two dimensional
D	deuterium (² H)
d	doublet
dd	doublet of doublets
DCE	1,2-dichloroethane
DCM	dichloromethane
de	diastereomeric excess
DET	diethyl tartrate
DIBAL-H	diisobutylaluminium hydride

DiPAMP	(2-methoxyphenyl)-[2-[(2-methoxyphenyl)-phenylphosphanyl]ethyl]-phenylphosphane
DKR	dynamic kinetic resolution
dm ³	cubic decimetre
DMAP	4-dimethylaminopyridine
DMF	<i>N,N</i> -dimethylformide
DMSO	dimethyl sulfoxide
L-DOPA	3,4-dihydroxy-L-phenylalanine
EDCI	1-ethyl-3-(3-dimethylaminopropyl)carbodiimide
ee	enantiomeric excess
EI	electron impact
ES+	positive phase electrospray ionisation
Et	ethyl
EtOAc	ethyl acetate
EtOH	ethanol
eq.	equivalent
FAB	fast atom bombardment
g	gram
G _{R/S}	chiral guest molecule
h	hours
H	host
<i>hν</i>	incident light
HLADH	horse liver alcohol dehydrogenase
HNL	hydroxynitrile lyase
HOBt	hydroxybenzotriazole
HPLC	high performance liquid chromatography
HRMS	high resolution mass spectrometry
<i>i</i> -Pr	<i>iso</i> -propyl
<i>i</i> -PrOH	<i>iso</i> -propanol
<i>J</i>	coupling constant
<i>K</i>	stability constant
kg	kilogram
kJ	kilojoules
λ	wavelength
L	ligand

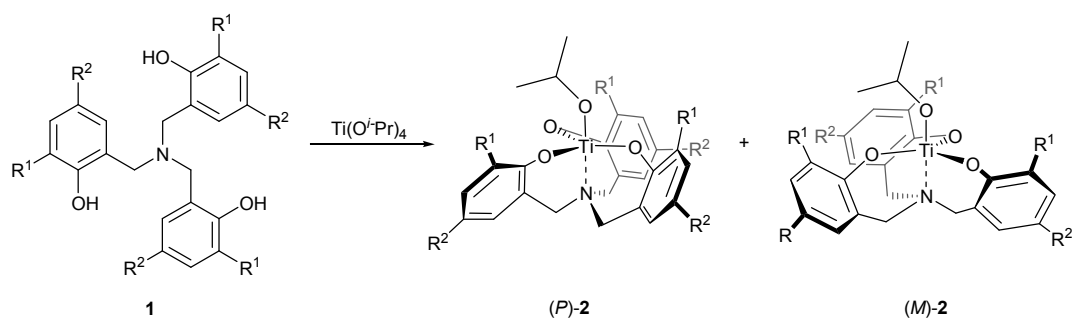
LHMDS	lithium hexamethyldisilazide
lit	literature
LRMS	low resolution mass spectrometry
μL	microlitre
<i>m</i>	<i>meta</i>
m	unresolved multiplet / minutes
M	molar (moles per cubic decimetre)
$[\text{M}]^+$	parent molecular ion
MAO	methylaluminoxane
Me	methyl
MeOD	deuterated D4 methanol
MeOH	methanol
mg	milligram
MHz	megahertz
mmol	millimole
M_n	number average molecular weight
mol	mole
mp	melting point
MS	molecular sieves
M_w	weight average molecular weight
<i>m/z</i>	mass-to-charge ratio
ν	infrared
NAD^+	nicotinamide adenine dinucleotide
NADH	nicotinamide adenine dinucleotide, reduced form
NBD	norbornadiene
NMR	nuclear magnetic resonance
NOE	nuclear overhauser effect
<i>o</i>	<i>ortho</i>
<i>p</i>	<i>para</i>
P	protecting group
PDI	polydiversity index
PE	petroleum ether
Ph	phenyl
ppm	parts per million
PTC	phase transfer catalyst

q	quartet
R_f	retardance factor
ROP	ring opening polymerisation
rt	room temperature
s	singlet / second
SDS	sodium dodecyl sulphate
L-Selectride	lithium tri- <i>sec</i> -butylborohydride
K-Selectride	potassium tri- <i>sec</i> -butylborohydride
sept	septet
t	triplet
TBHP	<i>tert</i> -butyl hydroperoxide
TBS/TBDMS	<i>tert</i> -butyldimethylsilyl
<i>t</i> -Bu	<i>tert</i> -butyl
Tf	triflate, trifluoromethanesulfonyl
TFA	trifluoroacetic acid
THF	tetrahydrofuran
TLC	thin layer chromatography
TMS	trimethylsilyl
TOF	turnover frequency
TP-TACN	trispyrrolidine-1,4,7-triazacyclononane
Ts	tosyl, <i>p</i> -toluenesulfonyl
TS	transition state
<i>p</i> -TsOH	<i>p</i> -toluenesulfonic acid
UV	ultraviolet
wt%	weight percent

Abstract

The use of C_2 -symmetric chiral ligands to promote selectivity in transition metal catalysed asymmetric transformations has been well documented over the last few decades.¹ In recent years, more and more interest has been focused on C_3 -symmetric chiral ligands and complexes and their applications in this field.² It has been proposed, for a number of reasons, that transition metal complexes derived from C_3 -symmetric ligands have even greater potential for asymmetric catalysis than their C_2 -symmetric counterparts.³

This project is focused on the development of a new, chiral family of amine tris(phenolate) ligands, such as **1**. Despite ligand **1** being achiral, it has been shown that it forms a chiral (but racemic) monomeric complex with titanium such as **2** (**Scheme 1**).⁴ The chirality is due to its propeller-like structure, leading to both the *P* and *M* isomers. Complexes of this type have been shown to catalyse a number of organic transformations.⁵

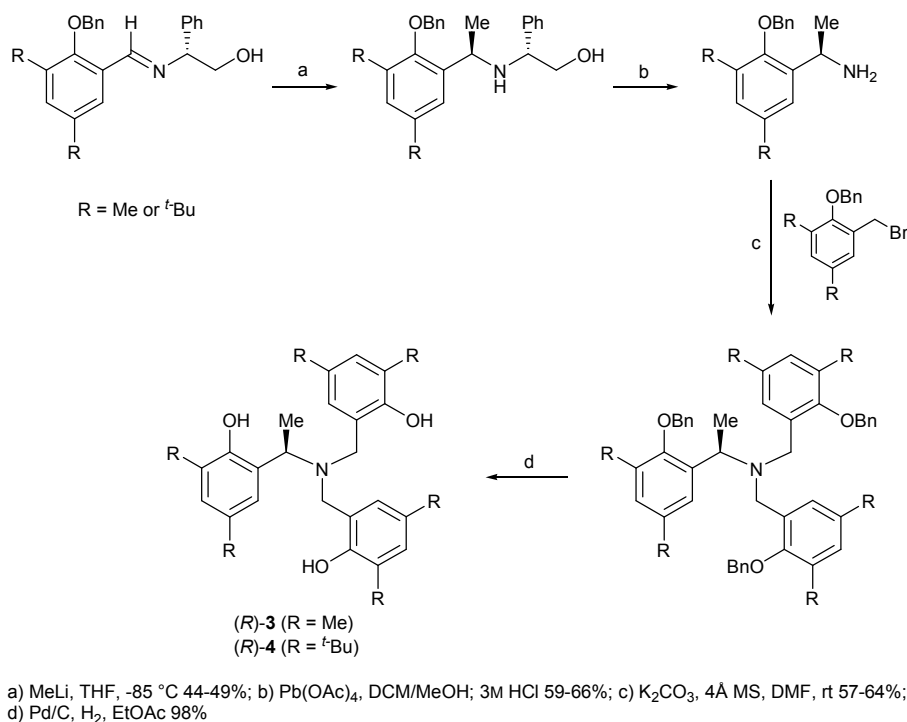


Scheme 1. Formation of complex (*rac*)-**2**

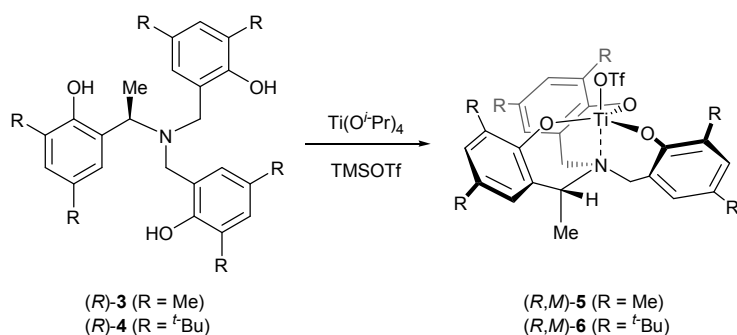
In light of this, the design and synthesis of chiral pseudo- C_3 -symmetric ligands (*R*)-**3** and (*R*)-**4** was completed *via* the protocol depicted in **Scheme 2** using a chiral auxiliary controlled addition to an imine, followed by oxidative cleavage and bisalkylation of the primary amine and subsequent hydrogenolytic deprotection of

¹ J. K. Whitesell, *Chem. Rev.*, 1989, **89**, 1581-1590; ² S. E. Gibson and M. P. Castaldi, *Chem. Commun.*, 2006, 3045-3062; ³ (a) C. Moberg, *Angew. Chem. Int. Ed.*, 1998, **37**, 248-268; (b) S. T. Handy, *Curr. Org. Chem.*, 2000, **4**, 363-395; ⁴ M. Kol, M. Shamis, I. Goldberg, Z. Goldschmidt, S. Alfi and E. Hayut-Salant, *Inorg. Chem. Commun.*, 2001, **4**, 177-179; ⁵ (a) S. D. Bull, M. G. Davidson, A. L. Johnson, D. E. J. E. Robinson and M. F. Mahon, *Chem. Commun.*, 2003, 1750-1751; (b) G. Licini, M. Mba and L. J. Prins, *Org. Lett.*, 2007, **9**, 21-24

the benzyl protecting groups. Upon coordination to titanium, the chirality of the ligands effectively locked the conformation of the propeller-like complex, such that the α -methyl group occupied its predicted pseudoaxial orientation (**Scheme 3**).

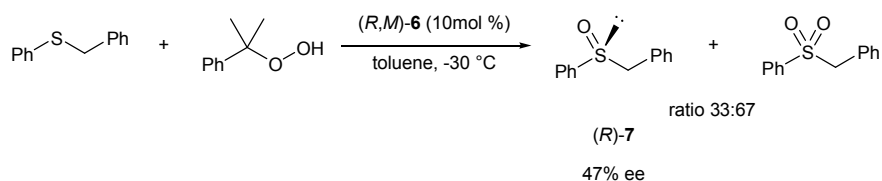


Scheme 2. Synthesis of ligands (*R*)-**3** and (*R*)-**4**



Scheme 3. Formation of complexes (*R,M*)-**5** and (*R,M*)-**6**

In the screening of these titanium complexes in a number of organic transformations (*R,M*)-**6** showed moderate selectivity in the oxidation of aryl alkyl sulfides, delivering the (*R*)-sulfoxide in enantioselectivities of up to 47% ee (**Scheme 4**).



Scheme 4. Sulfoxidation reaction catalysed by (*R,M*)-**6**

Contents

Acknowledgements	i
Abbreviations and Acronyms	ii-v
Abstract	vi-vii
Contents	viii-xiii
Chapter 1: Introduction	1
1 Introduction	2
1.1 Chirality	2
1.2 Asymmetric Synthesis	3
1.2.1 Chiral Pool Approach	3
1.2.2 Resolution of Racemates	5
1.2.3 Chiral Auxiliaries	8
1.2.4 Asymmetric Catalysis	9
1.3 Ligand Symmetry	17
1.4 C₃-Symmetry in Chemistry	19
1.4.1 Applications of C ₃ -Symmetric Molecules in Molecular Recognition	19
1.4.2 Applications of C ₃ -Symmetric Ligands in Catalysis	27
1.5 Conclusion	72
Chapter 2: Results and Discussion I	73
2 Results and Discussion I	74
2.1 Amine Tris(phenolate) Ligands	74
2.1.1 Introduction	74
2.1.2 Titanium Complexes of Amine Tris(phenolate) Ligands and their Applications in Catalysis	76
2.1.3 Screening of (<i>rac</i>)- 194b and (<i>rac</i>)- 195a -Previous Work within the Group	80
2.2 Design of a Chiral Amine Tris(phenolate) Ligand	86
2.2.1 Novel C ₃ -Symmetric Amine Tris(phenolate) Ligands	86
2.2.2 Pseudo-C ₃ -Symmetric Ligands	89

2.3	Previous Work within the Group-Attempted Synthesis of Chiral Ligand (R)-231	91
2.4	Work towards the Synthesis of (R)-232 and (R)-236	93
2.4.1	Literature Precedent	93
2.4.2	Preparation of Benzyl Protected Aldehyde 245	95
2.4.3	Synthesis of Imines (R)- 241 and (R)- 246	95
2.4.4	Addition of Alkyl Lithium to Imines (R)- 241 and (R)- 246	96
2.4.5	Attempted Cleavage of Methyl Aryl Ether of Amine (R,R)- 247	97
2.4.6	Successful Cleavage of Benzyl Aryl Ether of Amine (R,R)- 248	98
2.5	Synthesis of Chiral Amines (R)-255a-c	99
2.5.1	Preparation of Aldehyde 261	99
2.5.2	Synthesis of Benzyl Protected Aldehyde 256	101
2.5.3	Formation of Imine (R)- 262	102
2.5.4	Diastereoselective Addition of Alkyl Lithium to Imine (R)- 262	102
2.5.5	Oxidative Cleavage of Amines (R,R)- 263a and (R,R)- 263b	103
2.6	Synthesis of Chiral Ligand (R)-254a	105
2.6.1	Attempted Formation of Amine (R)- 266b via a Two Step Reductive Amination	105
2.6.2	Alternative Strategy for the Synthesis of Amines (R)- 254a and (R)- 254b	106
2.6.3	Preparation of Benzyl Bromide 267	106
2.6.4	Formation of Amines (R)- 266a and (R)- 266b via a Bisbenzylation Reaction	107
2.6.5	Deprotection of Tertiary Amines (R)- 266a and (R)- 266b	110
2.7	Conclusion	113
 Chapter 3: Results and Discussion II		 114
3	Results and Discussion II	115
3.1	Formation of Titanium tris(phenolate) <i>iso</i>-Propoxide Complex (R,M)-271	115
3.2	Formation of Titanium tris(phenolate) Triflate Complex (R,M)-272	119
3.3	Initial Screening of the Chiral Titanium Complexes of (R,M)-271 and (R,M)-272	120

3.3.1	Diethyl Zinc Addition to Benzaldehyde	120
3.3.2	Aza-Diels Alder Reaction	123
3.4	Synthesis of Chiral Ligand (<i>R</i>)-278	126
3.4.1	Synthesis of Aldehyde 282 and Imine (<i>R</i>)- 283	127
3.4.2	Diastereoselective Addition of Methyl Lithium to Imine (<i>R</i>)- 283	128
3.4.3	Oxidative Cleavage of Amine (<i>R,R</i>)- 284	128
3.4.4	Preparation of Benzyl Bromide 280	129
3.4.5	Formation of the tertiary amine (<i>R</i>)- 286	129
3.4.6	Deprotection of Tertiary Amine (<i>R</i>)- 286	131
3.5	Formation of Titanium Complex (<i>R,M</i>)-287	133
3.6	Formation of Titanium Complex (<i>R,M</i>)-288	135
3.7	Conclusion	137
Chapter 4: Results and Discussion III		139
4	Results and Discussion III	140
4.1	Aza-Diels Alder Reaction	140
4.2	Sulfoxidation Reaction	141
4.2.1	Titanium-Catalysed Asymmetric Oxidation of Sulfides	141
4.3	Sulfoxidation Reaction Catalysed by (<i>rac</i>)-195b, (<i>R,M</i>)-287 and (<i>R,M</i>)-288	151
4.3.1	Synthesis of Racemic Benzyl Phenyl Sulfoxide (<i>rac</i>)- 292q	151
4.3.2	Screening of (<i>rac</i>)- 195b in the Oxidation of Benzyl Phenyl Sulfide 291q	153
4.3.3	Screening of (<i>R,M</i>)- 287 and (<i>R,M</i>)- 288 in the Oxidation of Benzyl Phenyl Sulfide 291q	155
4.3.4	Solvent Screen in the Oxidation of Benzyl Phenyl Sulfide 291q Catalysed by (<i>R,M</i>)- 288	157
4.3.5	Addition of 4Å Molecular Sieves to the Oxidation of Benzyl Phenyl Sulfide 291q	159
4.3.6	Kinetic Resolution of Racemic Benzyl Phenyl Sulfoxide (<i>rac</i>)- 292q	160
4.3.7	Monitoring the Oxidation of Benzyl Phenyl Sulfide 291q Catalysed by (<i>R,M</i>)- 288	161

4.3.8	NMR Studies	162
4.4	Screening of Sulfides 291 in the Reaction Catalysed by (<i>R,M</i>)-288	166
4.4.1	Synthesis of Sulfides 291	166
4.4.2	Synthesis of Racemic Sulfoxides (<i>rac</i>)-292	167
4.4.3	Screening of Sulfides 291 in the Sulfoxidation Reaction Catalysed by (<i>R,M</i>)-288	168
4.5	Conclusion	170
4.6	Future Work	170
Chapter 5: Experimental		173
5	Experimental	174
5.1	General Experimental	174
5.2	General Procedures	176
5.2.1	General Procedure A: Preparation of Benzyl Protected Aldehydes	176
5.2.2	General Procedure B: Preparation of Imines	176
5.2.3	General Procedure C: Addition of Alkyl Lithium to Imines	176
5.2.4	General Procedure D: Preparation of Primary Amines	177
5.2.5	General Procedure E: Preparation of Benzyl Alcohols	177
5.2.6	General Procedure F: Preparation of Benzyl Bromide Analogues	177
5.2.7	General Procedure G: Preparation of Tertiary Amines <i>via</i> bis- <i>N,N</i> -alkylation	178
5.2.8	General Procedure H: Removal of Benzyl Protecting Groups	178
5.2.9	General Procedure I: Preparation of Sulfides	178
5.2.10	General Procedure J: Preparation of Racemic Sulfoxides	179
5.3	Results and Discussion I	179
5.3.1	Synthesis of Chiral Amines (<i>R,R</i>)-247 and (<i>R,R</i>)-248	179
5.3.2	Attempted Cleavage of Methyl Aryl Ether of (<i>R,R</i>)-247	182
5.3.3	Removal of Benzyl Protecting Group of (<i>R,R</i>)-248	182
5.3.4	Preparation of Chiral Amines (<i>R</i>)-255a and (<i>R</i>)-255b	183
5.3.5	Attempted Preparation of (<i>R</i>)-266b <i>via</i> Reductive Amination ((<i>R</i>)-265b Formed)	188
5.3.6	Preparation of Benzyl Bromide 267	189
5.3.7	Synthesis of Chiral Ligand (<i>R</i>)-254a	190

5.4	Results and Discussion II	194
5.4.1	Preparation of Titanium Complexes (<i>R,M</i>)- 271 and (<i>R,M</i>)- 272	194
5.4.2	Addition of Diethyl Zinc to Benzaldehyde Catalysed by (<i>R,M</i>)- 271 and (<i>R,M</i>)- 272	195
5.4.3	Aza-Diels Alder Reaction Catalysed by (<i>R,M</i>)- 272	196
5.4.4	Attempted aza-Diels Alder Reaction Catalysed by (<i>R</i>)- 254a	197
5.4.5	Synthesis of Chiral Amine (<i>R</i>)- 279	198
5.4.6	Preparation of Benzyl Bromide 280	200
5.4.7	Synthesis of Chiral Ligand (<i>R</i>)- 278	201
5.4.8	Preparation of Titanium Complexes (<i>R,M</i>)- 287 and (<i>R,M</i>)- 288	203
5.5	Results and Discussion III	206
5.5.1	Aza-Diels Alder Reaction Catalysed by (<i>rac</i>)- 195b and (<i>R,M</i>)- 288	206
5.5.2	Synthesis of Racemic Benzyl Phenyl Sulfoxide (<i>rac</i>)- 292q	207
5.5.3	Screening of (<i>rac</i>)- 195b in the Oxidation of Benzyl Phenyl Sulfide 291q	207
5.5.4	Screening of (<i>R,M</i>)- 287 and (<i>R,M</i>)- 288 in the Oxidation of Benzyl Phenyl Sulfide 291q	208
5.5.5	Solvent Screen in the Oxidation of Benzyl Phenyl Sulfide 291q Catalysed by (<i>R,M</i>)- 288	209
5.5.6	Addition of 4Å Molecular Sieves to the Oxidation of Benzyl Phenyl Sulfide 291q	210
5.5.7	Kinetic Resolution of Racemic Benzyl Phenyl Sulfoxide (<i>rac</i>)- 292q	211
5.5.8	Monitoring the Oxidation of Benzyl Phenyl Sulfide 291q Catalysed by (<i>R,M</i>)- 288	211
5.5.9	Synthesis of Sulfides 291	212
5.5.10	Synthesis of Racemic Sulfoxides (<i>rac</i>)- 292	214
5.5.11	Screening of Sulfides 291 in the Sulfoxidation Reaction	216
Chapter 6:	References	219
6	References	220

Chapter 7: Appendix	229
7 Appendix	229
7.1 Selected NMR Spectra	229
7.2 Crystal Structure Data for (<i>R,M</i>)-271 and the Co-crystallised Trimetallic Amine (trisphenolate)-oxo-alkoxide Complex	242
7.3 Crystal Structure Data for (<i>R,M</i>)-287	263

Chapter 1:

Introduction

1 Introduction

1.1 CHIRALITY

A molecule is considered to be chiral if it is non-superimposable on its mirror image. As many compounds associated with living organisms are chiral (eg DNA, enzymes, antibodies and hormones), the way in which enantiomers of a molecule interact can have markedly different biological activities. This is true for limonene, a compound which is formed naturally in both *R* and *S* forms, with one of the enantiomers, (*S*)-limonene **1** smelling of lemons, while its mirror image, (*R*)-limonene **1** smells of oranges (**Figure 1**).¹

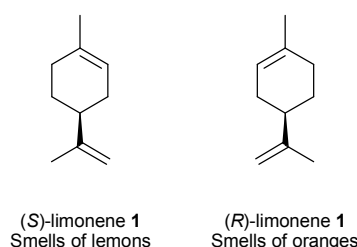


Figure 1. (*S*)-limonene and (*R*)-limonene **1**

Another example found in nature is the unusual case of the pheromone activity of olean **2**, the female sex pheromone of the olive fruit fly (*Bactrocera oleae*).² After both enantiomers were synthesised and bioassayed it was found that the (*R*)-enantiomer stimulated the male fruit flies, while the (*S*)-enantiomer stimulated the females.³ Analysis of the natural olean showed it to be a racemic mixture; thus, the female produced pheromone stimulates both male fruit flies and the female herself.

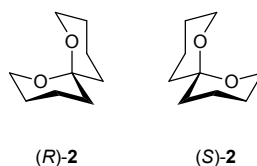


Figure 2. (*R*)-olean and (*S*)-olean **2**

It is therefore apparent that biology is sensitive to chirality and the activity of drugs will also depend on which enantiomer is used. Chiral drugs are often sold in the racemic form, with only one of the enantiomers matching the target receptor in the cell. In the late 1950s, the drug thalidomide **3** was prescribed as a sedative and anti-

emetic for pregnant women (**Figure 3**).^{4, 5} Following reports revealing a link between limb growth defects in babies and maternal usage of thalidomide, the drug was withdrawn from the market in 1961. It was subsequently found that while the (*R*)-enantiomer of **3** was beneficial, the (*S*)-enantiomer caused the teratogenic effects. As a consequence, pharmaceutical companies now test both enantiomers of a drug, and the ability to synthesise enantiomerically pure compounds is of great importance in drug production.

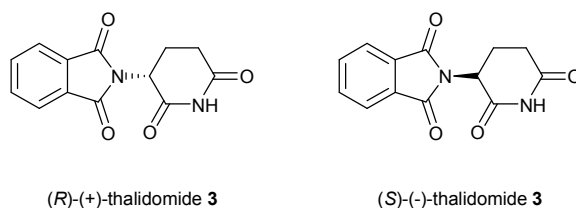


Figure 3. *Thalidomide 3*

1.2 ASYMMETRIC SYNTHESIS

There are four main methods for achieving asymmetric synthesis based on:

- The chiral pool approach
- Resolution of a racemate
- The use of chiral auxiliaries
- Asymmetric catalysis

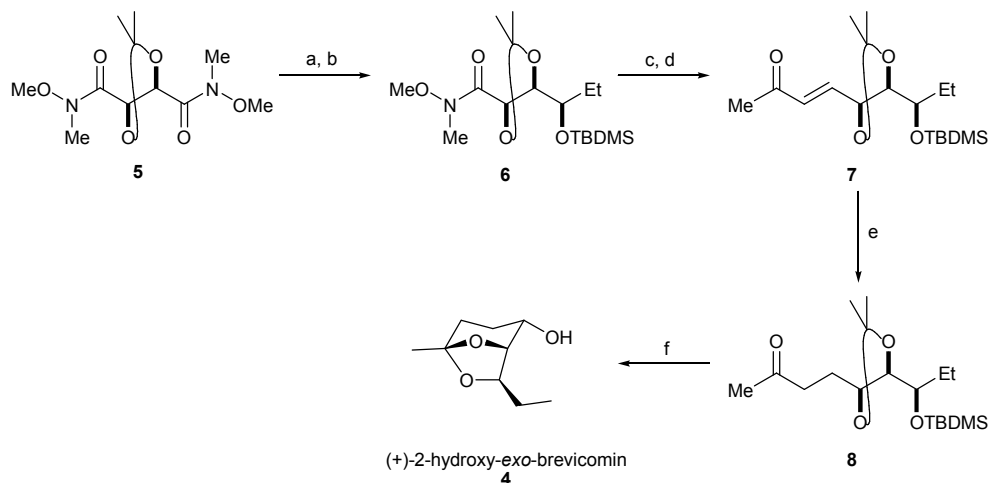
Examples of each of these approaches will now be discussed together with the relative scope and limitations of each method.

1.2.1 Chiral Pool Approach

The use of a chiral starting material, derived from a naturally occurring product, is a popular methodology, with a large number of chiral molecules having been manufactured in this way. A recent example in the literature is by Prasad and co-workers, who reported the synthesis of both enantiomers of the Western pine beetle pheromone 2-hydroxy-*exo*-brevicomine **4** from the protected bis-Weinreb amide **5**, which was derived from the naturally abundant L-(+)-tartaric acid.^{6, 7}

For (+)-2-hydroxy-*exo*-brevicomine **4**,⁶ the synthesis proceeded *via* the stereoselective addition of ethylmagnesium bromide to the bis-Weinreb amide **5** to afford the

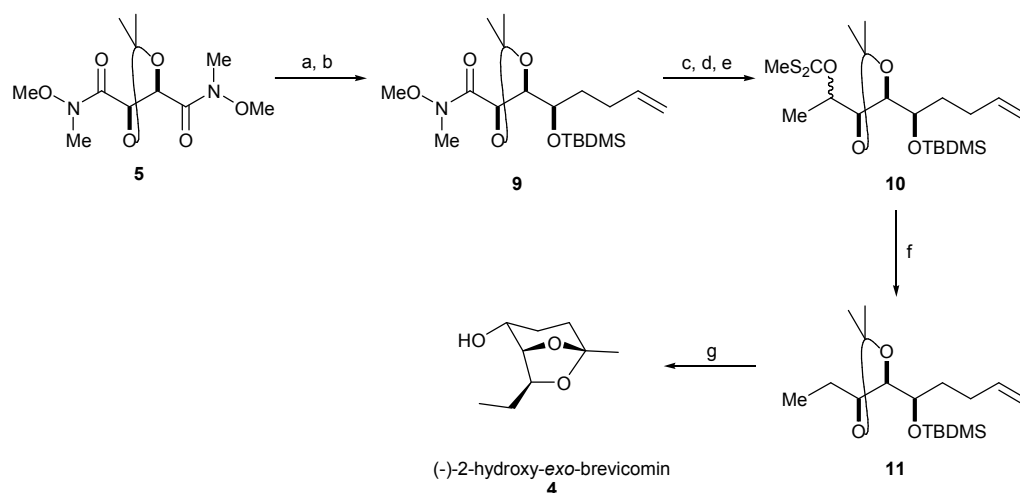
ketoamide. The highly diastereoselective reduction of the keto group furnished its corresponding (*R*)-alcohol, which was then protected as its silylether **6**. DIBAL-H reduction followed by Wittig olefination yielded the α,β -unsaturated ketone **7**, which was converted to the saturated ketone **8** by standard Pd/C hydrogenation. Simultaneous deprotection of the silyl ether and acetonide with $\text{FeCl}_3 \cdot 6\text{H}_2\text{O}$ catalysed instantaneous intramolecular ketalisation furnishing the natural product in 38% yield over all the steps (**Scheme 5**).



a) EtMgBr , THF, 0°C , 88% yield; b) (i) K-Selectride, -78°C , THF, (ii) TBDMSCl, imidazole, DMAP, DMF, 80°C , 68% yield over 2 steps; c) DIBAL-H, THF, -78°C ; d) 1-(triphenylphosphoranylidene)-2-propanone, benzene, reflux, 74% over 2 steps; e) 10% Pd/C, H_2 , MeOH, quant. yield; f) $\text{FeCl}_3 \cdot 6\text{H}_2\text{O}$, DCM, rt, 87% yield

Scheme 5. Synthesis of (+)-2-hydroxy-*exo*-brevicomine **4**

The synthesis of (-)-2-hydroxy-*exo*-brevicomine **4**⁷ proceeded *via* the controlled addition of 3-butenylmagnesium bromide to **5**, affording the ketoamide. Again stereoselective reduction of the keto group was followed by silylether protection to give silyloxy Weinreb amide **9**. Addition of MeMgCl to **9**, followed by reduction with NaBH_4 afforded a 50:50 mixture of diastereomers of the corresponding alcohol, which were converted to a mixture of xanthate esters **10** under standard conditions. These esters then underwent tributyltin hydride catalysed Barton-McCombie free radical deoxygenation to yield **11**. The desired product was obtained after **11** was subjected to a Wacker oxidation with PdCl_2 under an oxygen atmosphere in DMF, which resulted in the formation of the ketone and simultaneous deprotection of the silyl and acetonide group followed by intramolecular ketalisation, to afford the opposing (-)-enantiomer of the pheromone in a high overall yield of 35% (**Scheme 6**).



a) 3-Butenylmagnesium bromide, THF, $-15\text{ }^{\circ}\text{C}$, 90% yield; b) (i) L-Selectride, $-78\text{ }^{\circ}\text{C}$, THF, (ii) TBDMSCl, imidazole, DMAP, DMF, $80\text{ }^{\circ}\text{C}$, 78% yield over 2 steps; c) MeMgCl, THF, $0\text{ }^{\circ}\text{C}$, 98% yield; d) NaBH_4 , 96% yield; e) NaH, CS_2 , MeI, THF, reflux, 94% yield; f) AIBN, Bu_3SnH , benzene, Δ ; g) PdCl_2 , CuCl, O_2 , DMF/ H_2O , rt, 56% yield over 2 steps

Scheme 6. Synthesis of (-)-2-hydroxy-exo-brevicomin **4**

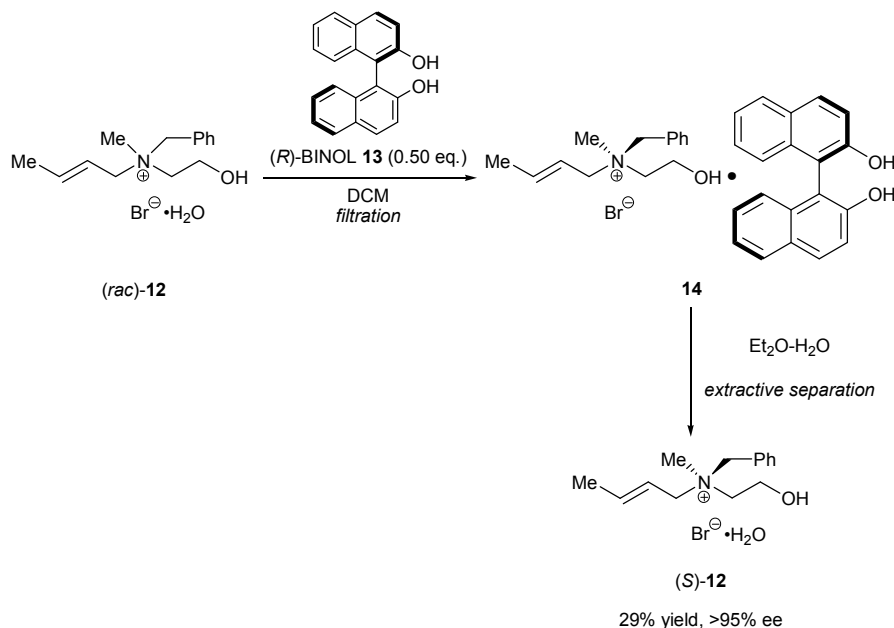
An obvious limitation with the chiral pool approach is that the desired synthetic target needs to be closely related to a natural product that is readily available; otherwise the synthetic route becomes so laborious and wasteful that it renders the method unfeasible. Another major drawback is the lack of availability of both enantiomers of many natural products, meaning that synthesis requiring the opposite enantiomer may require additional steps to invert chiral centres.

1.2.2 Resolution of Racemates

Chiral Resolving Agents

Classical resolution, where the enantiomers of a racemic mixture are separated by addition of a chiral resolving agent, is still a popular technique in asymmetric synthesis. The addition of the chiral resolving agent results in a mixture of diastereomers that can then be separated by fractional crystallisation or column chromatography. For example, Tayama *et al.* recently demonstrated that a racemic mixture of β -hydroxy-tetraalkylammonium bromide **12** could be resolved using chiral BINOL (Scheme 7).⁸ After addition of 0.50 equivalents of (*R*)-BINOL **13** to (*rac*)-**12**, the precipitate that formed (a 1:1 complex of **12** and BINOL) was filtered off. A diethyl ether-water extraction separated the two components of **14**, with the

enantioenriched β -hydroxy-tetralkylammonium bromide (*S*)-**12** (>95% ee) recovered from the aqueous phase, and (*R*)-BINOL **13** recovered from the organic phase.



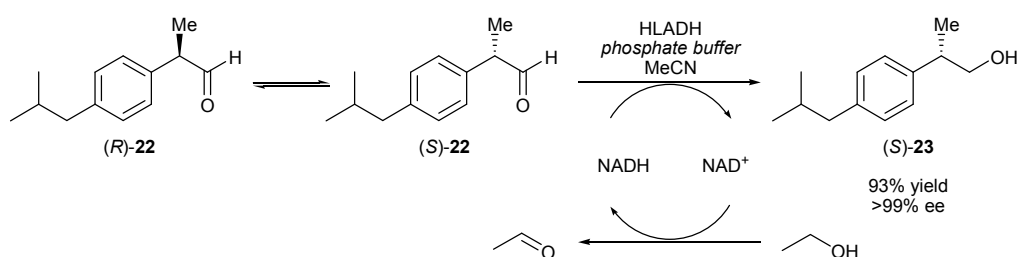
Scheme 7. Resolution of chiral β -hydroxy-tetralkylammonium bromide **12** by (*R*)-BINOL **13**

Unfortunately, the maximum theoretical yield from such a process can only ever be 50%, which means it is highly wasteful. In industrial synthesis, the disposal of such a quantity of high quality waste would be prohibitively expensive. The exception to this is when the undesired enantiomer can be re-racemised and recycled.

Kinetic Resolution

This strategy relies on the differences in rates of reaction of the two enantiomers of a racemic mixture with an enantiomerically pure reagent or catalyst. In an ideal scenario, the difference in rates is such that one of the enantiomers reacts while the other essentially remains unreacted. Again the major drawback is that the maximum theoretical yield is 50%. In 2007, Hoveyda and Snapper and co-workers demonstrated its potential, with the kinetic resolution of 1,2-diols through asymmetric silylation catalysed by dipeptide **15**.⁹ For example, reaction of racemic 1,2-diol **16** bearing a primary alcohol and tertiary carbinol proceeded with excellent regioselectivity (>98% primary silyl ether), yielding the (*S*)-silyl ether **17** in 49% yield and 91% ee with (*R*)-**16** recovered in 45% yield and >98% ee (**Scheme 8**).

representative example of enzymatic DKR uses Horse Liver Alcohol Dehydrogenase (HLADH) enzyme and nicotinamide adenine dinucleotide (NADH) as the reducing agent, to yield (2*S*)-2-(4-*iso*-butylphenyl)propanol **23** ((*S*)-ibuprofenol) from the starting racemic ibuprofenal **22** (Scheme 10).¹¹ In the process of reducing one enantiomer of aldehyde (*rac*)-**22** to the primary alcohol **23**, NADH is oxidised to NAD⁺ which results in stoichiometric consumption of the expensive cofactor. The addition of an excess of ethanol to the reaction mixture allows for the use of a catalytic amount of cofactor, which was successfully regenerated *in situ* by the same HLADH enzyme. This process yields the desired product in 93% yield and >99% ee.



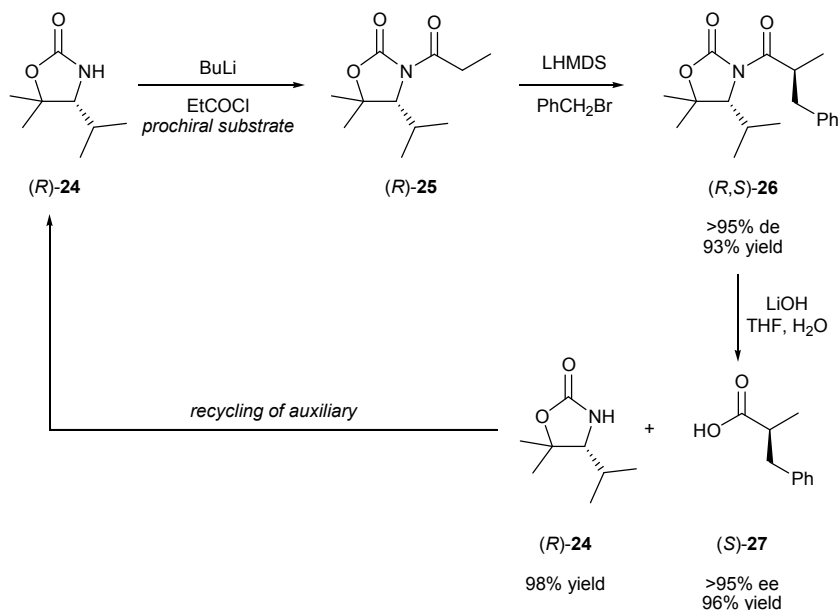
Scheme 10. Enzymatic DKR of racemic ibuprofenal **22**

However, enzymes often suffer from being highly substrate specific and sensitive to their reaction conditions. They tend only to operate in aqueous environments at specific pHs and temperatures, and any variations in these conditions can cause the enzyme to denature. As a consequence, many reactions have to be performed in biphasic solvent systems complicating the process even further.

1.2.3 Chiral Auxiliaries

A chiral auxiliary is an enantiomerically pure compound that is attached to a prochiral substrate that then influences the stereochemical course of a reaction. In most cases the auxiliary is introduced prior to the stereoselective reaction and removed afterwards. These additional synthetic steps and the cost of stoichiometric amounts of auxiliary can make this process unattractive. However, for many of these applications no enantioselective catalytic method exists.¹² The most well known chiral auxiliaries are the oxazolidin-2-ones, which were first reported by Evans in 1981,¹³ and are derived from chiral amino acids. Nowadays, many structural variations of these auxiliaries exist. For example, the SuperQuat auxiliary (*R*)-**24**,

developed by Davies *et al.*, was employed in the synthesis of the chiral α -substituted carboxylic acid (*S*)-**27** (Scheme 11).¹⁴ In the alkylation step, the enolate of **25** is coordinated to the lithium counterion and the electrophile approaches from the opposing face to the stereodirecting *iso*-propyl group of the auxiliary, exclusively forming (*R,S*)-**26** in high diastereoselectivity and yield. After cleavage of the auxiliary, carboxylic acid (*S*)-**27** is obtained in high enantiomeric excess and yield, with the auxiliary recovered for recycling.



Scheme 11. Use of chiral SuperQuat (*R*)-**24** for the synthesis of α -alkyl carboxylic acid (*S*)-**27**

1.2.4 Asymmetric Catalysis

The principles behind asymmetric catalysis are that a chiral reagent, upon coordination to the achiral substrate, modifies the course of a reaction to afford diastereomeric transition states that differ in energy. The transition state which is lower in energy is kinetically favoured, and therefore the reaction results in one of the enantiomers being formed in excess. Since the catalyst is not destroyed in this process, it can be used in substoichiometric amounts, significantly reducing the overall cost of the process. However, it is often found that catalysts are highly substrate specific, with different classes of substrate requiring development of a new catalytic system. Today, modern asymmetric catalysis can be classified into one of three main processes, namely:

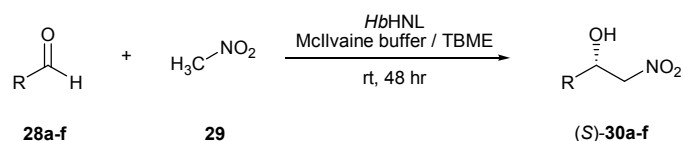
- Biocatalysis

- Organocatalysis
- Organometallic catalysis

Recent examples of asymmetric catalysis from each of these subcategories will now be discussed.

Biocatalysis

As mentioned earlier, reactions catalysed by enzymes are highly desirable as they are often considered ‘greener’ than the corresponding organometallic catalysed systems. For example, in 2007 Griengl and co-workers published the first example of an enzymatic nitroaldol (Henry) reaction (**Scheme 12**).¹⁵ In their work, the hydroxynitrile lyase from *Hevea brasiliensis* (*HbHNL*) was shown to accept nitromethane **29** as an enolate donor for reaction with various aldehydes, to yield the β -nitro alcohols **30a-f** in modest yields and high enantioselectivity (**Table 1**). The reaction was found to be broadly applicable to aromatic (entries 1-2), heteroaromatic (entries 3-4) and aliphatic aldehydes (entries 5-6).



Scheme 12. Enzyme catalysed Henry reaction of nitromethane **29** and aldehydes **28a-f**

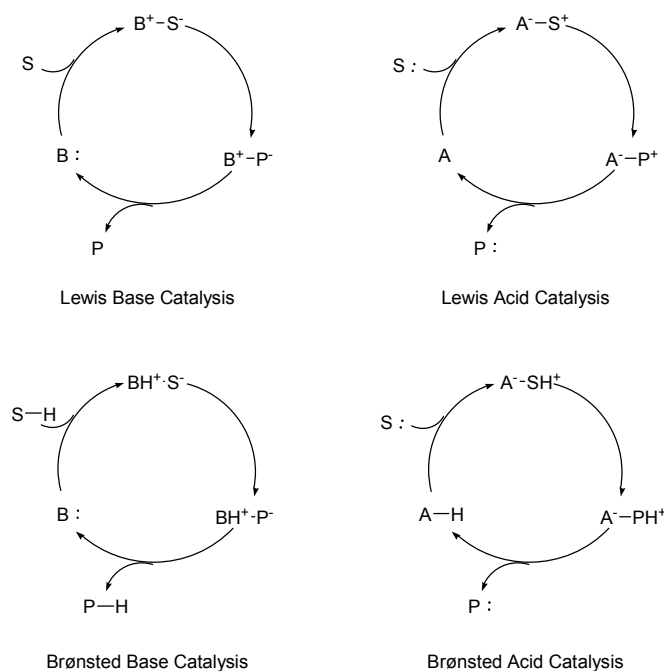
Table 1

Entry	Product	R	Yield /%	ee /%
1	30a	C ₆ H ₅	32	97
2	30b	3-Cl(C ₆ H ₄)	36	98
3	30c	2-furyl	43	88
4	30d	2-thienyl	29	98
5	30e	<i>n</i> -hexyl	34	96
6	30f	cyclohexyl	18	99

Organocatalysis

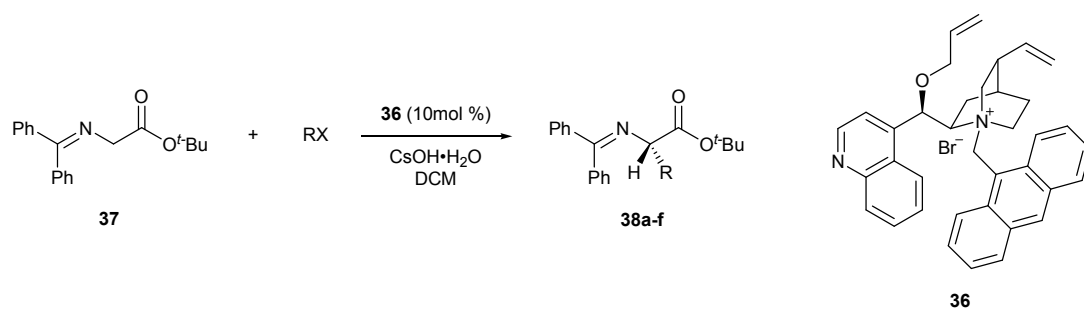
The term organocatalysis describes the acceleration of chemical reactions through the addition of a substoichiometric quantity of an organic compound.¹⁶ The interest in this field has grown quite dramatically in recent years, with the efficiency and selectivity of some of these organocatalytic reactions now approaching the standards

of established asymmetric reactions.¹⁷ Due to the vastly increasing types of organocatalysts employed in asymmetric catalysis, List and co-workers recently devised a system of categorising them by their mechanistic behaviour.¹⁸ Accordingly, the organocatalysts can be categorised as either Lewis base, Lewis acid, Brønsted base and Brønsted acid, since most organocatalysts fall into one of these categories. The simplified catalytic cycles are shown in **Scheme 13**. Lewis base catalysts (B:) work by initiating the catalytic cycle *via* nucleophilic addition to the substrate (S). The resulting complex then undergoes a reaction before the product (P) is released, allowing for the catalyst to perform further turnovers. Lewis acid catalyst (A) activate nucleophilic substrates (S:) in a similar manner. Brønsted base and acid catalytic cycles are initiated *via* partial deprotonation or protonation of the substrate, respectively.



Scheme 13. Organocatalytic cycles

The majority of organocatalysts are N-, C-, O-, P- and S-based Lewis bases, which convert the substrates into either activated nucleophiles or electrophiles. Typical reactive intermediates include iminium ions, enamines, carbenes, acyl ammonium ions or 1-, 2- or 3-ammonium enolates. An example of a Lewis base organocatalyst is the imidazolidinone **31**, which Macmillan and co-workers demonstrated to facilitate the Diels-Alder reaction between (*E*)-cinnaldehyde **32** and cyclopentadiene **33**, giving the desired Diels-Alder adducts (*2S*)-*endo*-**34** and (*2S*)-*exo*-**34** in 93% ee (ratio of *endo*-**34** to *exo*-**34** 1:1.3) (**Scheme 14**).¹⁹ The sense of asymmetric induction

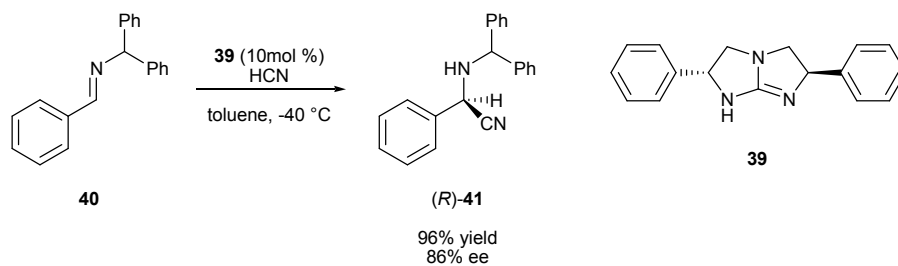


Scheme 16. Enantioselective catalytic phase transfer alkylation of **37** using Cinchona alkaloid-derived ammonium salt **36**

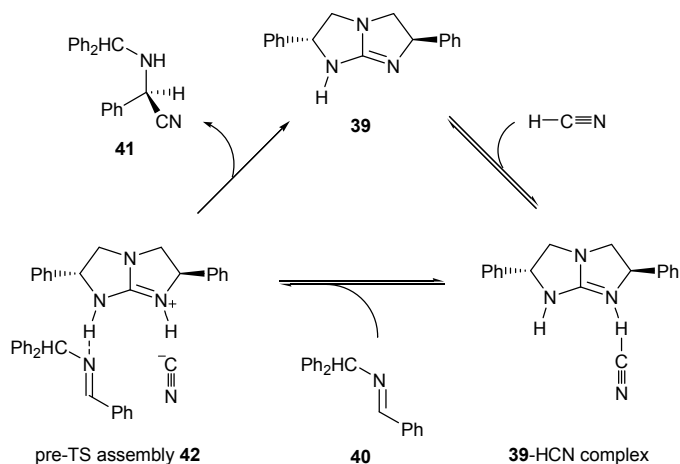
Table 2

Entry	RX	Product	Temp /°C	Time /h	Yield /%	ee /%
1	CH ₃ I	38a	-60	28	71	97
2	CH ₃ (CH ₂) ₄ CH ₂ I	38b	-60	32	79	99.5
3		38c	-60	36	75	99
4		38d	-78	22	89	97
5	PhCH ₂ Br	38e	-78	23	87	94
6	Ph ₂ CHBr	38f	-78	22	73	99.5

An example of an organic Brønsted base catalyst is the *C*₂-symmetric guanidine **39**, which was used to catalyse the addition of hydrogen cyanide to aldimine **40** to form the corresponding α -amino nitrile **41** in 96% yield and 86% ee (**Scheme 17**).²⁴ The reaction proceeds *via* interaction of the hydrogen cyanide with the nitrogen base generating a guanidinium cyanide complex, which can then serve as a hydrogen bond donor to the aldimine **40** forming the pre-transition-state termolecular assembly **42** (**Scheme 18**). Finally, attack by the cyanide ion within the ion pair on the hydrogen-bond-activated aldimine affords the Strecker product (*R*)-**41**.

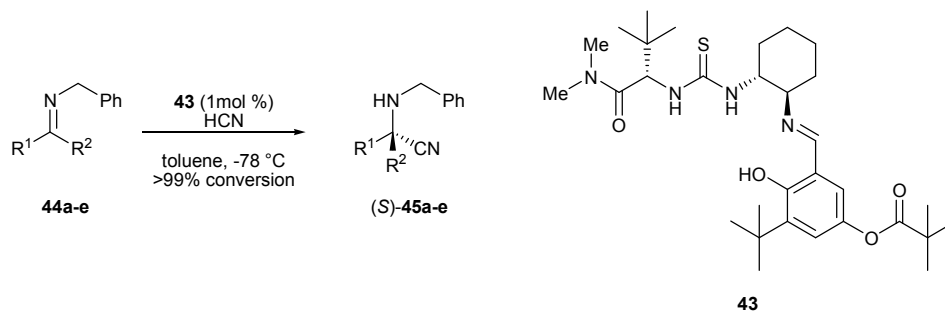


Scheme 17. Addition of hydrogen cyanide to imine **40** catalysed by *C*₂-symmetric guanidine **39**



Scheme 18. Proposed mechanism of the Strecker reaction of imine **40** catalysed by C_2 -symmetric guanidine **39**

In contrast, Jacobsen and co-workers showed that their thiourea organocatalyst **43** behaved as a Brønsted acid in the reaction of similar aldimine substrates with hydrogen cyanide, with the reaction proceeding through formation of a hydrogen bond between the imine nitrogen and the thiourea hydrogens (**Scheme 19, Table 3**).²⁵ For example, the reaction of **44e** with two equivalents of hydrogen cyanide, in the presence of 1 mol % of organocatalyst **43**, led to the formation of the corresponding α -amino nitrile (*S*)-**45e** in quantitative conversion and 99.3% ee (entry 5).



Scheme 19. Asymmetric Strecker reaction of aldimines and ketoimines **44a-e** catalysed by organocatalyst **43**

Table 3

Entry	Substrate	R ¹	R ²	ee /%
1	44a	<i>i</i> -Pr	H	97
2	44b	<i>n</i> -Pent	H	96
3	44c	<i>t</i> -Bu	H	86
4	44d	<i>t</i> -Bu	Me	99.3
5	44e	Ph	H	99.3

The use of organocatalysts in reactions has been shown to give rise to extremely high enantioselectivities. Preparative advantages are notable with the reactions generally being more tolerant of air and water. The catalysts are inexpensive and are often more stable than enzymes or other bioorganic catalysts. However, as yet, organocatalysis does not rival the scope of reactions of organometallic catalysis, or the efficiency and selectivity of enzymes.

Organometallic Catalysis

Organometallic catalysis describes the use of metal based complexes to catalyse an asymmetric process. In 2001 the Nobel Prize in Chemistry was awarded to Dr William S. Knowles, Professor Ryoji Noyori and Professor K. Barry Sharpless for “their development of catalytic asymmetric synthesis”. Knowles and Noyori received half the prize for “their work on chirally catalysed hydrogenation reactions” and Sharpless was rewarded with the other half of the prize for “his work on chirally catalysed oxidation reactions”. The pioneering work of these three chemists have had a great impact on academic research and the development of new drugs and materials and are used in many industrial syntheses of drugs and other biologically active compounds.²⁶ For example, Knowles and co-workers worked on developing an industrial synthesis of L-DOPA **49**, a drug used in the treatment of Parkinson’s disease. They showed that the cationic rhodium (III) complex, containing the chiral diphosphine ligand (*R,R*)-DiPAMP **46** (**Figure 4**), catalysed the enantioselective hydrogenation of enamide **47** to afford the protected amino acid **48** in quantitative yield and 95% ee (**Scheme 20**).²⁷ Acid hydrolysis of **48** completed the synthesis of L-DOPA **49**. This was the first industrial process to employ a chiral transition metal complex for asymmetric synthesis.

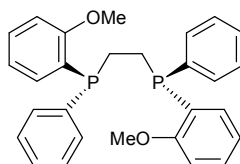
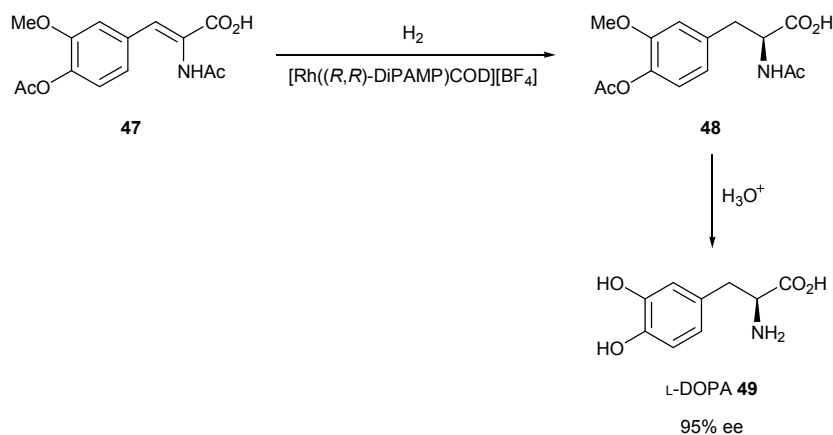


Figure 4. Chiral diphosphine ligand, (*R,R*)-DiPAMP **46**



Scheme 20. Synthesis of *L*-DOPA **49** using a rhodium complex of (*R,R*)-DiPAMP **46**

In 1980, Noyori *et al.* developed a chiral diphosphine ligand (*S*)-BINAP **50** (Figure 5), which was found to be an excellent ligand for rhodium catalysed hydrogenation reactions of enamides.²⁸ In a later publication, the authors found that ruthenium complexes of BINAP were superior in the asymmetric hydrogenation of α,β -unsaturated carboxylic acids that didn't bear an α -amino or related group.²⁹ For example, the hydrogenation of α,β -unsaturated carboxylic acid **51** in the presence a Ru(II)-BINAP complex gave the anti-inflammatory agent (*S*)-naproxen **52** in 92% yield and 97% ee (Scheme 21).

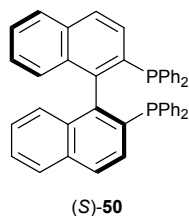
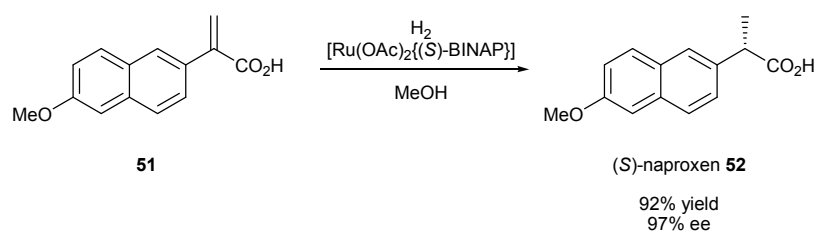


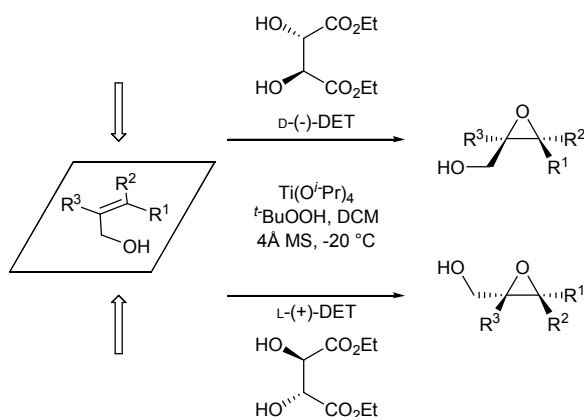
Figure 5. Chiral diphosphine ligand, (*S*)-BINAP **50**



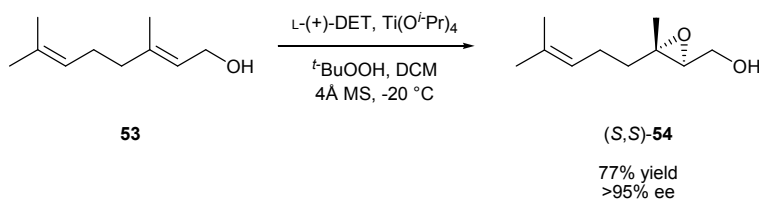
Scheme 21. Synthesis of anti-inflammatory agent (*S*)-naproxen **52** using a ruthenium complex of (*S*)-BINAP **50**

Around the same time, Sharpless *et al.* were developing catalysts for asymmetric oxidation reactions. In 1980, they reported the first practical method for asymmetric epoxidation of allylic alcohol using titanium tetra-*iso*-propoxide, *tert*-butyl hydroperoxide and diethyl tartrate (DET).³⁰ It was found that the reaction was highly

stereoselective with the selectivity totally reagent controlled: by using either (+)- or (-)-DET the corresponding enantiomer of the 2,3-epoxy alcohol can be obtained. For example, use of (-)-diethyl tartrate will direct the epoxidation to the top face of the alkene (as shown by the mnemonic in **Scheme 22**), switching to (+)-diethyl tartrate will result in the bottom face being epoxidised. **Scheme 23** shows an example of its use with geraniol **53** being epoxidised to give (*S,S*)-**54** in 77% yield and >95% ee, using the naturally occurring (+)-diethyl tartrate.³⁰



Scheme 22. Allylic epoxidation catalysed by the Sharpless titanium-tartrate complex



Scheme 23. Asymmetric epoxidation of geraniol **53** under Sharpless conditions

Throughout the literature there are many different examples of metal-ligand complexes that have been used for asymmetric organometallic catalysis, and whose efficiency is influenced by the steric and electronic demands of the chiral ligand responsible for asymmetric induction. One of the factors to consider in the design of a new class of chiral ligands is the ligand symmetry.

1.3 LIGAND SYMMETRY

While twofold rotational symmetry has been successfully employed in a large number of chiral reagents and catalysts,³¹ there is still comparatively little known about the efficiency of systems of higher rotational symmetry.³² In recent years, more and more interest has been focused on C_3 -symmetric chiral ligands and

complexes and their application in catalysis.^{33, 34} In considering how a C_3 -symmetric ligand might be advantageous in comparison to its C_2 -symmetric counterpart, it is first necessary to look at the potential architecture of such a molecule.

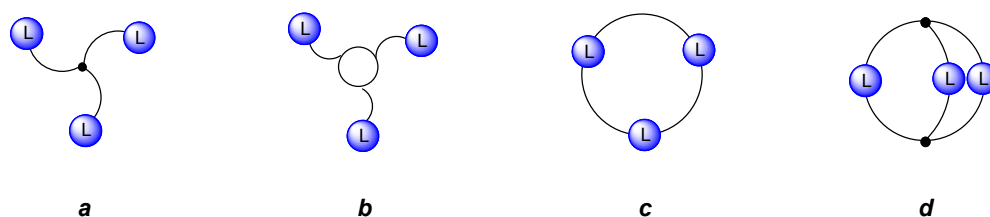


Figure 6. Topologies of structures with C_3 -symmetry

A tridentate ligand or a trifunctional molecule with C_3 -symmetry can be considered to have one of four principal topologies: acyclic (*a*), exocyclic (*b*), macrocyclic (*c*), or bicyclic (*d*).³³ In explaining the potential of such a ligand in asymmetric catalysis it is necessary to consider the effects of ligand symmetry on square planar and octahedral complexes.³⁵

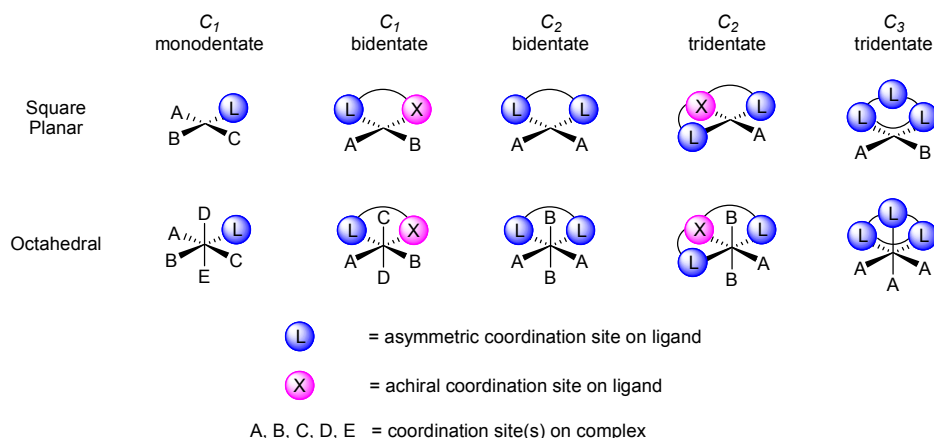


Figure 7. Symmetry and geometry in chemistry

In the simplest case, a single, monodentate chiral ligand generates a chiral catalyst in which none of the remaining coordination sites are equivalent, regardless of the complex geometry. As a result, this type of ligand, despite its simplicity of preparation, has proven difficult to utilise and obtain high levels of enantioselectivity.³⁵ The C_2 -bidentate ligand gives a favourable situation for the square planar complex, as the remaining two sites are homotopic, but the octahedral complex gives two sets of sites (A and B) which are pairwise homotopic. The C_2 -tridentate ligand leaves only one remaining vacant site in the square planar complex. In the octahedral complex there remain two diastereotopic sites (A and B) in a ratio of 2:1. The relative ease of designing a C_2 -symmetric ligand, has meant the

vast majority of ligands used in asymmetric catalysis fall into this category. Ligands such as BINOL **13** (Figure 8) have proven to be remarkably general in terms of their applicability in a wide array of synthetic transformations.³⁶

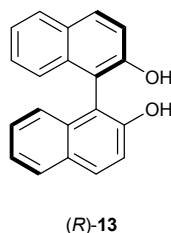


Figure 8. (R)-BINOL **13**

The situation changes with the C_3 -tridentate ligands, as they demonstrate a potential superiority over lower symmetry species in the case of octahedral complexes, where the remaining sites on the octahedral complex are homotopic. The situation is different in a square planar complex, where a bidentate, C_3 -symmetric ligand affords two inequivalent coordination sites. For reactions that proceed *via* an octahedral ligand-metal-substrate complex, C_3 -symmetric ligands have the potential to enhance stereocontrol. One drawback to consider, is the fact that ligands of this type can potentially deactivate the catalyst, by generating a metal centre that is too electron rich, due to its three donating sites.

1.4 C_3 -SYMMETRY IN CHEMISTRY

1.4.1 Applications of C_3 -Symmetric Molecules in Molecular Recognition

The ability of a C_3 -symmetric receptor (**H**) to differentiate the two enantiomers of a chiral guest molecule (**G_R** and **G_S**) is determined by the environment of the small, medium and large groups of the guest.³⁷ On first inspection of the two diastereomeric complexes (**H-G_R** and **H-G_S**), formed between the guest molecule and host, it might appear that the steric requirements of the two complexes are of equal energy (Figure 9). This would be true if the analysis were only to consider each of the substituents in the diastereomeric host-guest complexes in isolation (Figure 10). However, such a simple analysis does not take into account the chirality of the guest molecule. Instead, the order in space of the three substituents of the guest needs to be factored in. Only after consideration of all the non-identical segments of the diastereomeric

host-guest complexes $\mathbf{H-G}_R$ and $\mathbf{H-G}_S$ (Figure 11), does it become apparent that the steric requirements of the two complexes are different (one favourable, two unfavourable interactions for $\mathbf{H-G}_R$ compared to two favourable, one unfavourable for $\mathbf{H-G}_S$), with certain interactions bearing more importance than others. It is this difference in steric demands that could, in theory, lead to differentiation of the two guest molecules.

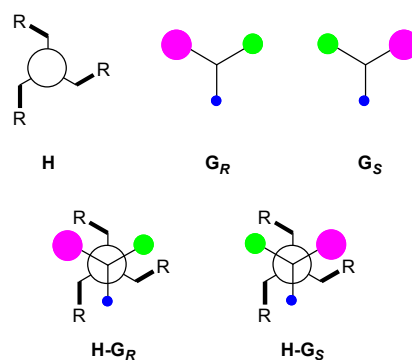


Figure 9. C_3 -symmetric host (\mathbf{H}), enantiomeric guests (\mathbf{G}_R and \mathbf{G}_S) and diastereomeric host-guest complexes. The pink, green and blue spheres represent large, medium and small substituents, respectively, in the guest

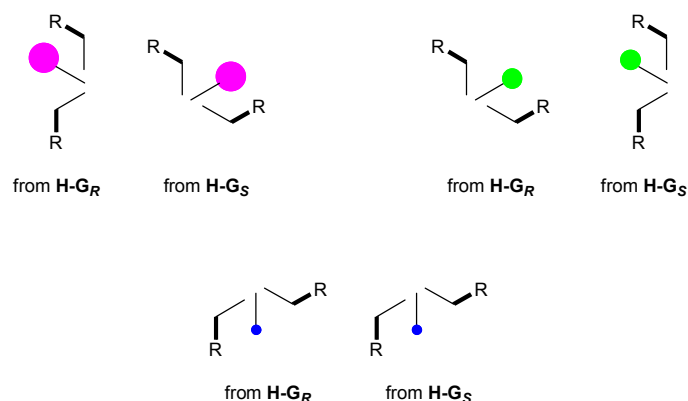


Figure 10. Isolated, isometric segments of diastereomeric host-guest complexes, $\mathbf{H-G}_R$ and $\mathbf{H-G}_S$

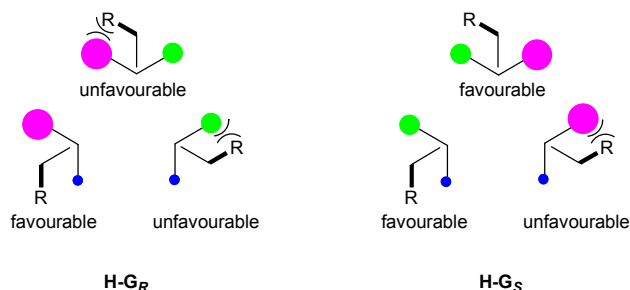
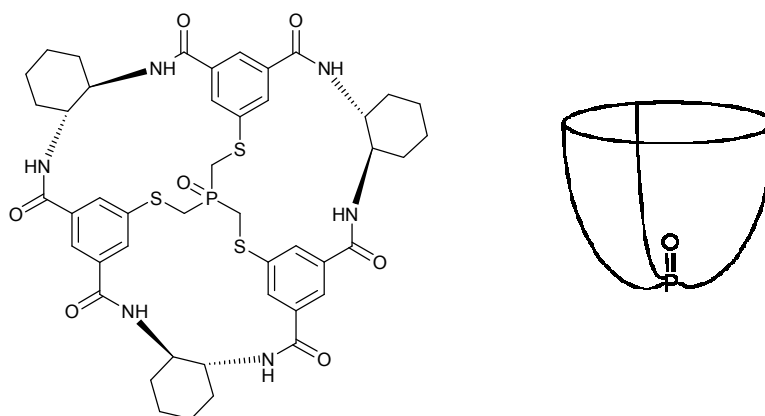


Figure 11. The non-identical segments of diastereomeric host-guest complexes, $\mathbf{H-G}_R$ and $\mathbf{H-G}_S$

The ability of C_3 -symmetric molecules to differentiate between the two enantiomers of a chiral guest molecule has been demonstrated for a number of examples in the

literature. Representative examples of recent applications of these types of receptors are briefly reviewed herein.

The synthesis of a bowl-shaped C_3 -symmetric receptor **55** with a phosphine oxide functionality in the interior of the molecular bowl was reported by Hong and co-workers (**Figure 12**).³⁸ In NMR titration experiments, the receptor exhibited good binding affinities for *N*-dodecylamide amino acids, with the D-isomer always binding preferentially (**Table 4**). *N*-Alkylamide amino acid derivatives with a lipophilic side chain showed weaker binding affinity compared with those with a hydrophilic side chain (entries 1-2 versus entries 3-9). The highest affinity was found for the asparagine (Asn) derivatives (entry 5). In comparison, glutamine (Gln) derivatives with the same H-bond donor and acceptor geometry except for an additional methylene on the side chain showed a much lower binding affinity to **55** (entry 8).



55

Figure 12. Bowl-shaped C_3 -symmetric receptor **55**

Entry	Guest ^b	K_a / M^{-1}		es
		D-isomer	L-isomer	
1	D,L-Val-NHR	400	80	83:17
2	D,L-Phe-NHR	1000	170	85:15
3	D,L-Ser-NHR	1800	1500	55:45
4	D,L-Thr-NHR	2250	1050	68:32
5	D,L-Asn-NHR	45000	12000	79:21
6	D,L-Asn-(β -NHMe)-NHR	3100	2000	61:39
7	D,L-Asp-NHR	5000	1600	76:24
8	D,L-Gln-NHR	3000	2000	60:40
9	D,L-Glu-NHR	5200	700	88:12

^a Measured by ¹H NMR titration in CDCl₃/CD₃OD (10:1, v/v) at 25 °C. ^b Guests were used as their trifluoroacetate salts; R = doceryl.

The enantiomeric recognition of α -chiral primary ammonium ions by C_3 -symmetric trisoxazoline receptor **56** was reported by Ahn *et al.* (Figure 13, Table 5).³⁹ The chiral discrimination was found to be general in the case of α -aryl substituted guests, suggesting π - π interactions were an important factor. For example, receptor **56** displayed a moderate level of enantioselectivity (71:29) between the enantiomers of α -phenylethylammonium ions (entry 1).

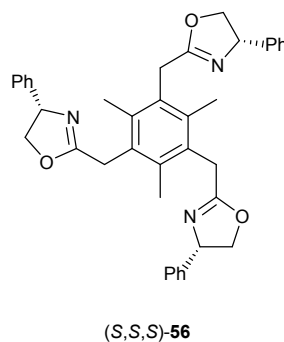
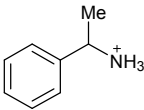
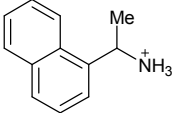
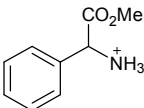
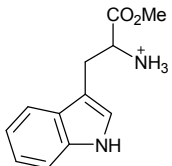
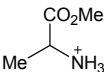
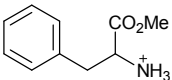


Figure 13. C_3 -symmetric trisoxazoline receptors, **56**

Table 5

Entry	Racemic ammonium guest	Enantioselectivity ^a	Extraction /% ^b
1		71(R):29(S)	82
2		70:30	99
3		78(S):22(R)	60
4		67(S):33(R)	57
5		53(S):47(R)	41
6		55(S):45(R)	36

^a Enantioselectivity of the ammonium ion extracted from excess racemic salts ($\text{RNH}_3^+\text{Cl}^-$, 10 M equiv, 0.5 M in D_2O ; 0.6 M NaPF_6) by trisoxazoline **56** (0.05 M in CDCl_3) at 25 °C. ^b Percentage of the ammonium salts extracted in CDCl_3 with respect to trisoxazoline **56**.

In a later publication, the authors showed that receptor **56** could also be used in the enantio-discrimination of β -chiral primary ammonium ions.⁴⁰ One difficulty in the recognition of β -chiral amines *via* their ammonium ions is that the β -chiral site is relatively remote from the binding site. To overcome this problem, bifurcated H-bonds were suggested to block the free rotation of β -substituents (**Figure 14**).

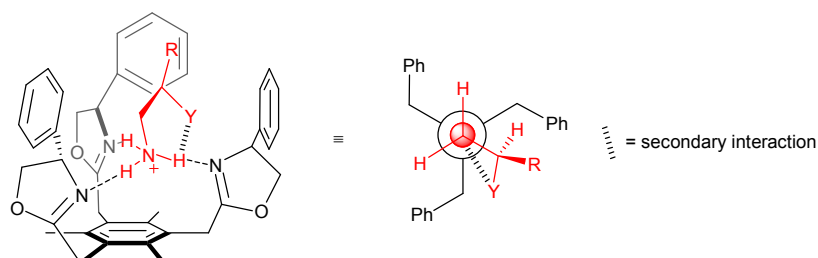
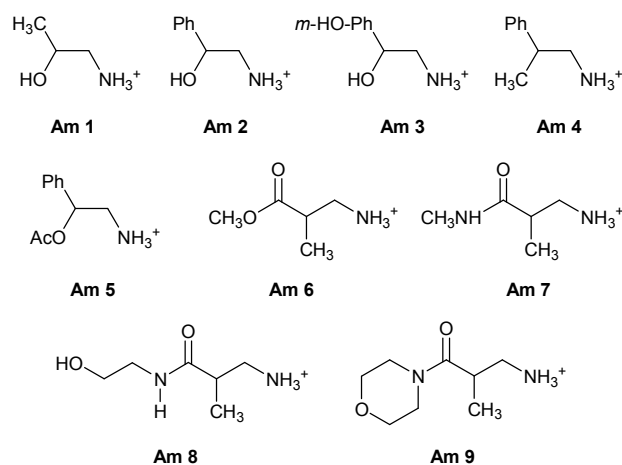


Figure 14. Diastereomeric inclusion complexes between receptor **56** and β -chiral primary ammonium ions with a secondary interaction

Guests with a β -hydroxy functionality, which can act as a hydrogen bond acceptor, were initially examined. It was found that the β -OH group plays a crucial role in the chiral discrimination, presumably by forming a bifurcated H-bond (**Table 6**, entries 1-3). In contrast, when no β -hydroxy group was present then no chiral discrimination was observed (entry 4). When the β -hydroxy group was changed to β -acetoxy and β -carbomethoxy groups, lower selectivity was observed (entries 5 and 6). With carboxamide functionalities at the β -position, higher levels of enantiodiscrimination were observed, indicating that the carboxamide functionality similarly participates in the intramolecular bifurcated H-bonding (entries 7-9).

**Table 6**

Entry	Racemic Guest	Enantioselectivity ^a	Extraction I/% ^b
1	Am 1	63:37	50
2	Am 2	75:25	60
3	Am 3	72:28	40
4	Am 4	50:50	97
5	Am 5	58:42	72
6	Am 6	58:42	71
7	Am 7	71:29	<5
8	Am 8	61:39	10
9	Am 9	83:17	<5

^a Enantioselectivity of the ammonium ion extracted from excess racemic salts (10 M equiv, 0.5 M in D₂O) by trisoxazoline **56** (0.05 M in CDCl₃) at 25 °C. ^b Percentage of the ammonium salts extracted in CDCl₃ with respect to trisoxazoline **56**.

The synthesis of the C₃-symmetric receptor (*S,S,S*)-**57**, which incorporated 1,3,5-triphenylbenzene and 1,3,5-tris(phenylethynyl)benzene platforms as the ‘floor’

and ‘ceiling’, was reported by Diederich *et al.* (**Figure 15**).⁴¹ The host-guest complexes of receptor **57** with octyl glucosides in CDCl₃, were of modest stability, with the highest association constant (K_a) of 270 M⁻¹ being reported for the complexation of **57** with octyl β -D-glucoside. The authors noted that the modest complex stabilities were probably due to the monosaccharides ‘nestling’ on the outside, rather than being incorporated inside the cavity of the receptor.

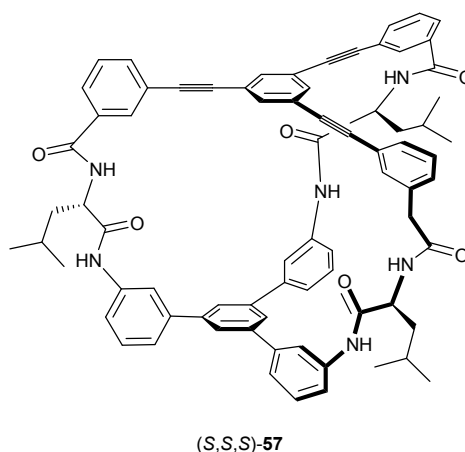


Figure 15. C_3 -symmetric receptor **57**

In 2003, Kubik and co-workers reported the synthesis of a series of C_3 -symmetric cyclic hexapeptides, **58a-d**, containing alternating L-proline and 3-aminobenzoic acid derivatives as subunits (**Figure 16**).⁴² In the presence of racemic *N,N,N*-trimethyl-1-phenylethyl ammonium salt **59**, the peptides formed diastereomeric complexes, giving well defined splittings of the guest signals in the ¹H NMR spectrum. In all cases the stability constants (K_a) were greater for the complexes of the (*R*)-enantiomer of the ammonium salt than the (*S*)-enantiomer. Peptide **58c** formed the most stable complexes with the ammonium salt, while peptide **58b** gave the best discrimination (de of 21) (**Table 7**, entries 2-3).

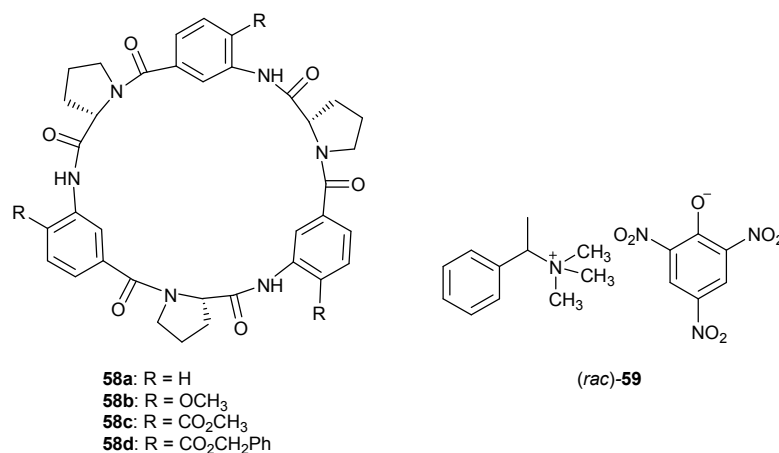


Figure 16. *C*₃-symmetric cyclic hexapeptides **58a-d**, and the picrate salt of (*rac*)-*N,N,N*-trimethyl-1-phenylethylammonium salt **59**

Table 7

Entry	Hexapeptide	<i>K_a</i>		de
		(<i>R</i>)-enantiomer	(<i>S</i>)-enantiomer	
1	58a	1580	1330	8
2	58b	1550	1030	21
3	58c	4550	3050	20
4	58d	3620	3150	7

In 2000, the novel receptor **60a**, based on a scaffold of trifunctionalised triphenylene ketals, was reported in the selective recognition of caffeine **61** and other *N*-alkylated oxopurines (**Figure 17**).⁴³ In a later publication, a series of receptors **60b-e** were screened, which were shown to give good enantiofacial discrimination of caffeine **61** (**Scheme 24, Table 8**).⁴⁴ In the variable temperature NMR spectroscopy experiments, receptor **60b** failed to show any preference for either of the diastereomeric forms (entry 1). The repulsive interaction between the *N*-7 methyl group of caffeine and the *tert*-butyl fragment of receptor **60c** meant a preference for the β -form was observed (entry 2). Host-guest complexes of **60d** and **60e** both showed a preference for the α -form, with the strongly restricted chiral coordination space of receptor **60e** leading to an excellent enantiofacial differentiation (entries 3 and 4).

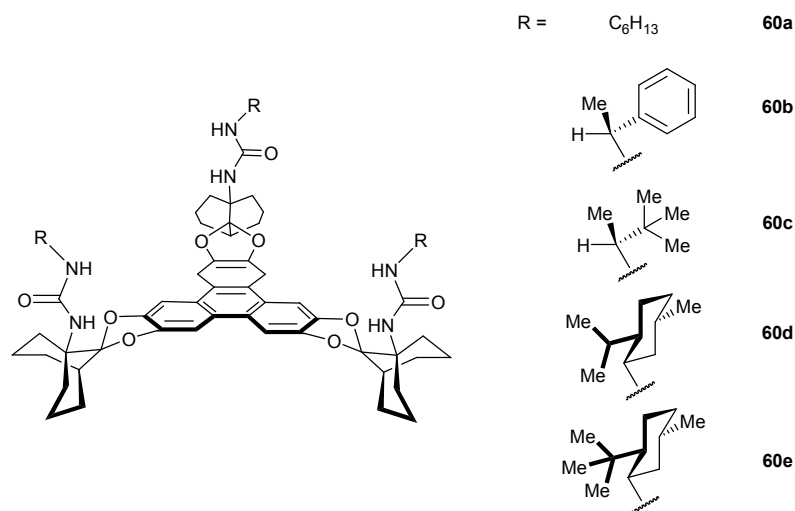
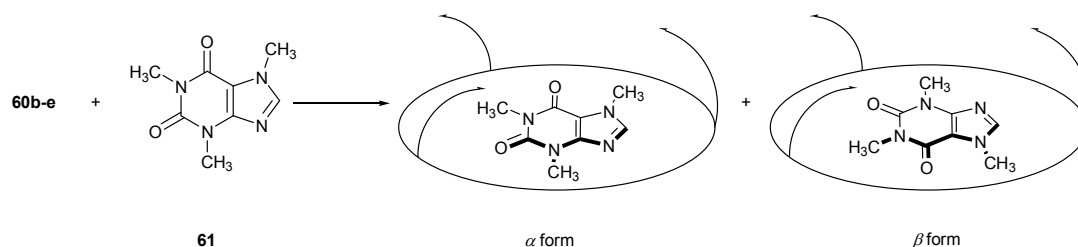


Figure 17. Artificial receptors **60a-e**



Scheme 24. Schematic representation of the enantiofacial differentiation of caffeine **61** by receptors **60b-e**, giving the two diastereomeric complexes described as the α - and β -form.

Table 8

Entry	Host-guest complex	Diastereomeric ratio ^a	Preference ^b
1	60b + 61	1:1	-
2	60c + 61	3±0.5:1	β
3	60d + 61	3.4±0.6:1 ^c	α
4	60e + 61	≥9:1 ^c	α

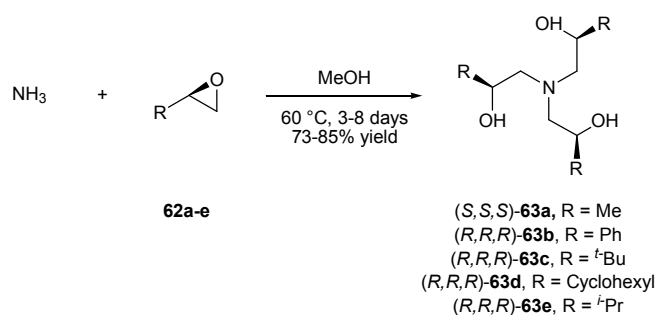
^a ¹H NMR spectroscopy experiments: [**60**] = [**61**] = 10mM, CD₂Cl₂, 193 K. Integrals for the resonance signals of NH_(distal) of the receptor and of H-8 of **61**. ^b Molecular modelling studies. ^c Difference NMR spectra with [8-D]caffeine

1.4.2 Applications of C₃-Symmetric Ligands in Catalysis

The applications of C₃-symmetric ligands and their complexes for enantioselective catalysis are reviewed herein, and are conveniently categorised according to the class of ligand used for metal complex formation.

Hydroxyl Based Ligands

In 1992, Nugent first reported the use of trialkanolamines **63a-c** as ligands in asymmetric catalysis, for the zirconium catalysed desymmetrization of *meso* epoxides with azides.⁴⁵ The ligands were synthesised from reaction of the enantiopure epoxides **62a-e** with ammonia at 60 °C in 73-85% yield (**Scheme 25**).⁴⁶ Formation of the active catalyst required sequential treatment of ligand **63a** with $Zr(O^t\text{Bu})_4$, followed by the addition of one equivalent of water to give the complex $(\mathbf{63a}\text{-Zr-OH})_2\text{-}^t\text{BuOH}$, **64**. The combination of catalyst **64** and trimethylsilyl trifluoroacetate was found to catalyse the opening of *meso* epoxides with azidosilanes in good yields and enantioselectivities with a best result of 86% yield and 93% ee for the desymmetrisation of cyclohexane oxide with azido(*iso*-propyl)dimethylsilane (**Table 9**, entry 1).

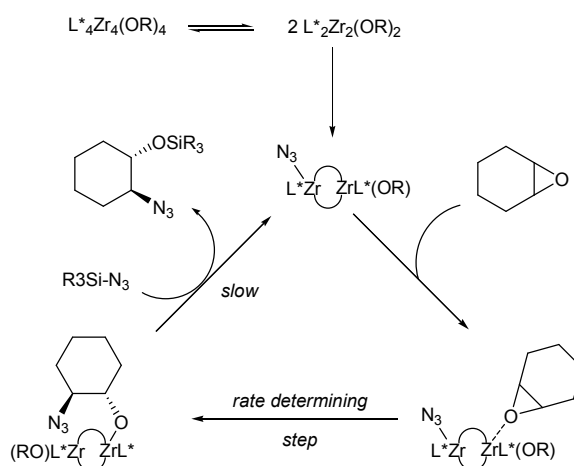


Scheme 25. Synthesis of trialkanolamines **63a-e**

Table 9

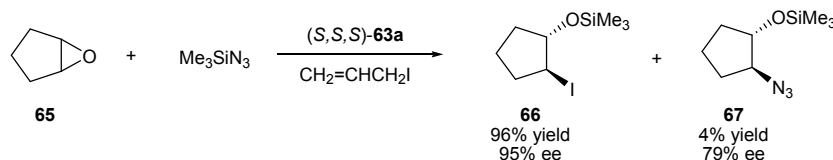
Entry	Epoxide	Azide	Temp /°C	Product	Yield /%	ee /%
1		<i>t</i> PrMe ₂ SiN ₃	0		86	93
2		<i>t</i> PrMe ₂ SiN ₃	0		59	87
3		<i>t</i> PrMe ₂ SiN ₃	25		79	89
4		<i>t</i> PrMe ₂ SiN ₃	25		64	83
5		Me ₃ SiN ₃	25		78	88

In a subsequent publication the complex was shown to exist as a mixture of interconverting dimeric and tetrameric zirconium tri-*iso*-propanolamine species.⁴⁷ The precatalytic complex was proposed to be a dimeric species, activated by exchange of an alkoxide or hydroxide ligand for an azide. The proposed catalytic cycle involved coordination of the epoxide to one metal centre, followed by intramolecular delivery of the azide from the other zirconium centre to the activated epoxide in the rate determining step (**Scheme 26**).



Scheme 26. Proposed catalytic cycle of the desymmetrisation of meso epoxides by the zirconium complex **64**

The authors hypothesised that if the azide on the zirconium atom could be replaced with another nucleophile, then the alternative nucleophile might undergo selective transfer to the epoxide as well.⁴⁸ This was proven when two equivalents of allyl iodide were added to the reaction of cyclopentene oxide **65** and azidotrimethylsilane under the same conditions as before. Here the β -iodohydrin **66** was obtained in 96% yield with only 4% of the usual azide product **67**, with **66** being formed in 95% ee (**Scheme 27**).

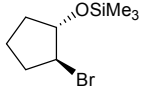
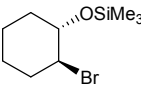
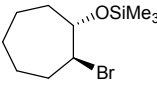
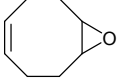
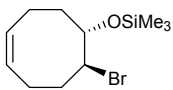
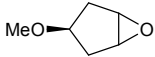
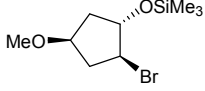
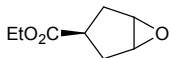
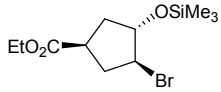


Scheme 27. The desymmetrisation of cyclopentene oxide **65** to yield β -iodohydrin **66**

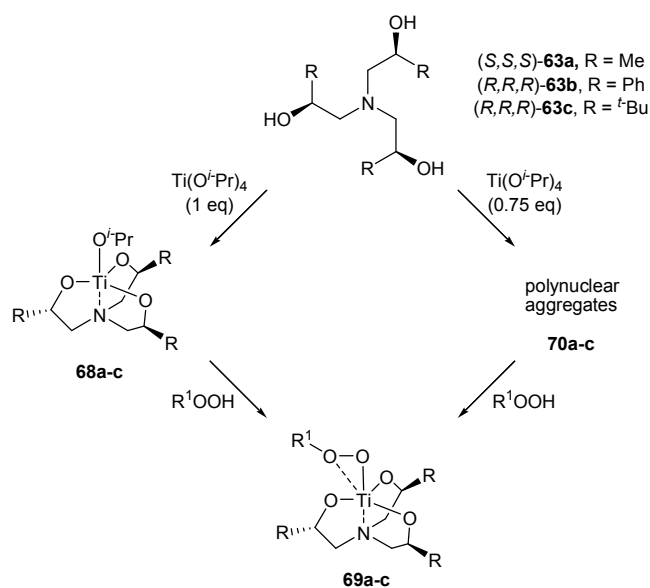
The reaction was then extended to the synthesis of protected β -bromohydrins. Large excesses of allyl bromides were required to suppress the formation of azide side products as the rate of exchange of the zirconium bound azide with bromide was

slower than had been observed with iodide. In all cases twenty equivalents of allyl bromide was sufficient to keep the yield of azide to <5%. The results are summarised in **Table 10**.

Table 10

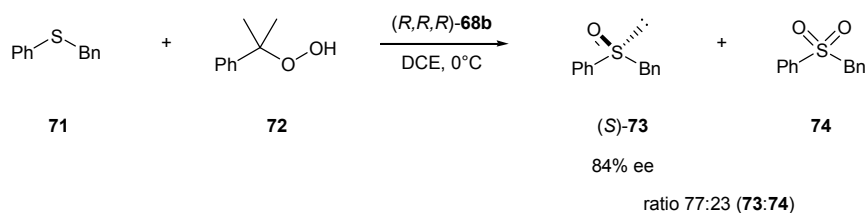
Entry	Epoxide	Product	Yield /%	ee /%
1			81	95
2			86	91
3			90	89
4			92	84
5			89	96
6			83	95

Nugent *et al.* went on to report coordination of ligands **63a-c** to titanium (IV) *iso*-propoxide, to give well defined monomeric complexes **68a-c**, with one *iso*-propoxy group retained in the titanium coordination sphere as an axial ligand.⁴⁹ Displacement of the *iso*-propoxide group by an alkyl hydroperoxide gave the corresponding monomeric peroxocomplexes **69a-c**. When ligands **63a-c** were treated with substoichiometric amounts of titanium (IV) *iso*-propoxide a mixture of discrete 2:1, 3:2 and 4:3 oligomers were produced, in which excess trialkanolamine ligands bridged multiple titanatrane units.⁵⁰ Treatment of these polynuclear aggregates **70a-c** with alkyl hydroperoxide also gave the monomeric peroxocomplexes **69a-c** (**Scheme 28**).



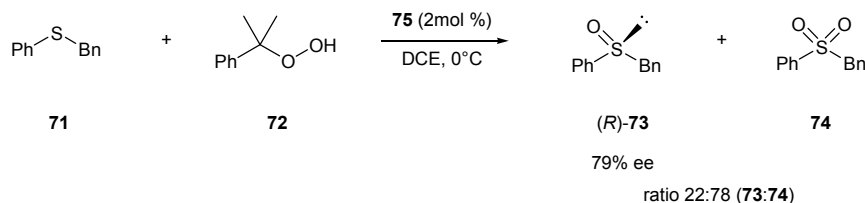
Scheme 28. Formation of the peroxocomplexes **69a-c**

The catalysts **68a-c** were screened in the oxidation of alkyl aryl sulfides with cumyl hydroperoxide (CHP) as the oxidant, with peroxocomplex **69b** proving to be the most effective. In the initial screening using methyl-*p*-tolyl sulfide as a model substrate, with 0.1 equivalent of catalyst **68b**, the (*S*)-sulfoxide was obtained in modest enantioselectivity (36%), together with the over oxidised sulfone in a ratio of 84:16 (sulfoxide:sulfone). The sulfone was found to be present in the early stages of the reaction indicating that two different asymmetric processes were involved: asymmetric oxidation of the sulfide to the sulfoxide and kinetic resolution of the resultant scalemic sulfoxide *via* oxidation to its sulfone. Fortunately, both processes were working in tandem to increase the enantioselectivity. In the asymmetric oxidation, the (*S*)-sulfoxide formed preferentially (29% ee when almost no sulfone is present), whilst in the oxidation of the sulfone the (*R*)-enantiomer reacted faster. This was proven for the kinetic resolution of racemic methyl-*p*-tolyl sulfoxide, which gave the (*S*)-enantiomer in 33% ee after 50% conversion. The best result obtained was for the oxidation of benzyl phenyl sulfide **71** with cumyl hydroperoxide (CHP) **72** in the presence of 10mol % **68b**, giving the (*S*)-sulfoxide **73** in 84% ee together with sulfone **74** in a ratio of 77:23 (**73**:**74**) (**Scheme 29**).



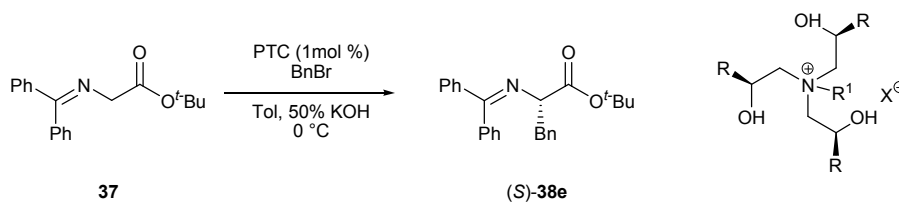
Scheme 29. Oxidation of benzyl phenyl sulfide **71** by CHP **72** catalysed by (R,R,R) -**68b**

In 1999 Nugent and co-workers showed that a partially hydrolysed zirconium catalyst bearing the same trialkanolamine **63b** also mediated the stereoselective sulfoxidation, giving higher levels of enantioselection but with the opposite enantiomer being formed compared to the Ti(IV)/**63b** system.⁵¹ The catalytic species **75**, formed by reaction of $\text{Zr}(\text{O}^t\text{-Bu})_4$ with **63b** in the presence of water, was shown to have the formula $[[\text{Zr}_2\text{63b}_2(\text{O}^t\text{-Bu})(\text{OH})]\cdot n\text{H}_2\text{O}]_m$ ($n = 3,4$). Reactions employing only 2mol % of **75**, using CHP **72** as the oxidant, (R) -sulfoxides were obtained in 79-91% ee. For example, the reaction of benzyl phenyl sulphide **71** with this new complex yielded (R) -benzyl phenyl sulfoxide **73** in 79% ee together with sulfone **74** in a ratio of 22:78 (**73:74**) (**Scheme 30**).



Scheme 30. Sulfoxidation of **71** by CHP **72** catalysed by zirconium catalyst **75**

More recently Takabe *et al.* have shown that the quaternary amine salts of **63b**, **63d** and **63e** can act as chiral phase-transfer catalysts (PTC) in the alkylation of *tert*-butyl glycinate-benzophenone Schiff base **37** to give the alkylated product (S) -**38e** in moderate yields and enantioselectivities (**Scheme 31**).⁵² The PTC derived from **63e** was found to give the best enantioselectivity. Increasing the solubility of the catalyst in toluene by using a long chain alkyl halide to form the quaternary ammonium salt or exchanging the bromide counter anion to a triflate improved the enantiomeric excess of the resultant chiral α -amino acid (**Table 11**, entries 4 and 5).



Scheme 31. Alkylation of **37** with benzyl bromide employing chiral phase-transfer catalysts **63b**, **63d** and **63e**

Table 11

Entry	PTC	R ¹	X	Time /h	Yield /%	ee /%
1	63b	Bn	Br	6	65	27
2	63d	Bn	Br	7	75	50
3	63e	Bn	Br	20	62	55
4	63e	CH ₃ (CH ₂) ₁₁ Bn	Br	10	62	57
5	63e	Bn	TfO	12	55	58

The authors proposed that selectivity was due to hydrogen bonding between the hydroxyl group on the PTC and the nitrogen of the *E*-enolate of **37**, resulting in a nine-membered transition state in which the R group sits *pseudo*-equatorial. Benzyl bromide approaches from the less hindered face (*Re* face) to afford the product **38e** with an *S* configuration (**Figure 18**).

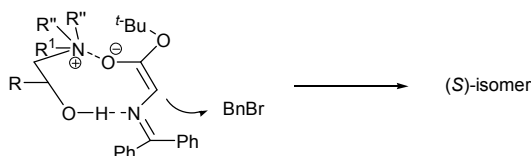
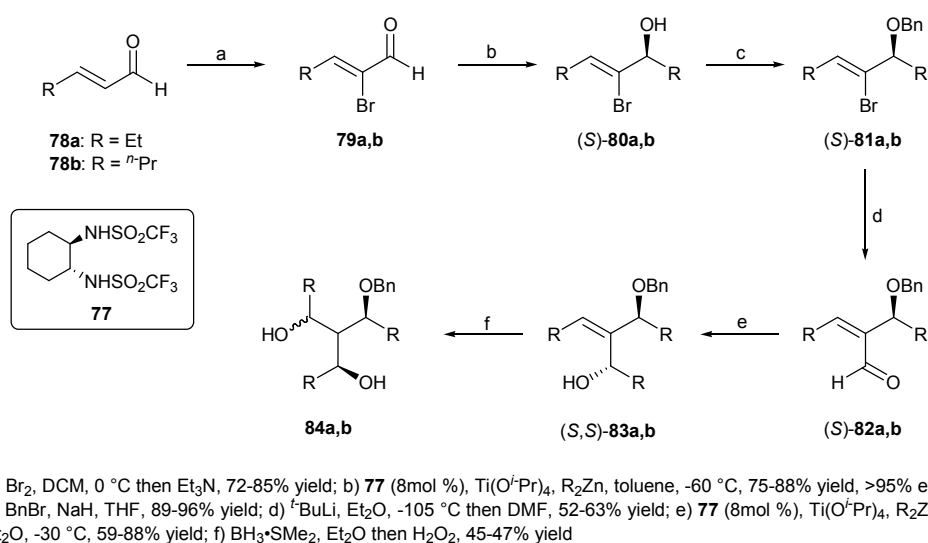


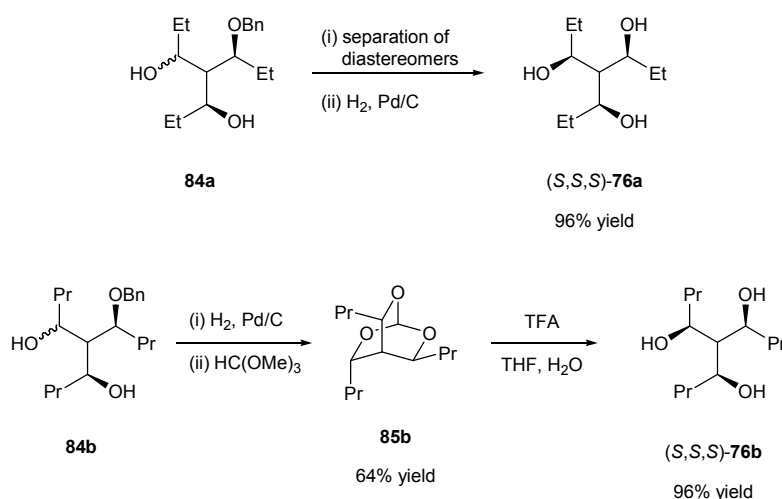
Figure 18. Proposed mechanism for enantioselectivity in the PTC

In 1997, Sundermeyer and co-workers reported the synthesis of C_3 -symmetric triols **76a** and **76b** and their coordination to titanium and vanadium alkoxides.⁵³ The synthesis of the triols started from the commercially available aldehydes **78a,b**, which were converted to their α -bromo derivatives **79a,b** by a bromination-elimination sequence. Alkylation with the appropriate dialkyl zinc in the presence of $Ti(O^iPr)_4$ and the chiral disulfonamide **77** furnished the (*S*)-alcohols **80a,b** in 75-88% yield and >95% ee. Following benzyl protection of the alcohol, giving (*S*)-**81a,b**, reaction with *tert*-butyl lithium allowed for a bromine-lithium exchange, which after quenching with excess *N,N*-dimethylformamide gave the α,β -unsaturated aldehydes **82a,b** in 52-63% yield. A second alkylation with dialkyl zinc in the

presence of **77** and $\text{Ti}(\text{O}^i\text{Pr})_4$ gave the secondary alcohols (*S,S*)-**83a,b**. The third stereocentre was introduced *via* diastereoselective hydroboration, giving the desired monobenzylated triols **84a,b** together with the undesired epimer (**Scheme 32**). In the case of triol **76a**, the desired diastereomer could be separated by flash chromatography, and following hydrogenolysis, **76a** was obtained in 96% yield. For the isolation of triol **76b**, even after debenzylation the desired diastereomer could not be separated from the other isomer. However, when treated with trimethylorthoformate only the C_3 -symmetric isomer formed the cyclic ortho ester **85b** and thus could be separated from its epimer. Following hydrolysis the desired triol **76b** was isolated in 61% yield over the two steps (**Scheme 33**).

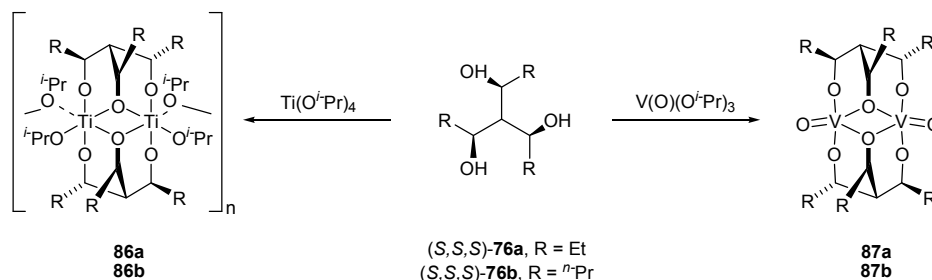


Scheme 32. Synthesis of monobenzylated triols **84a** and **84b**



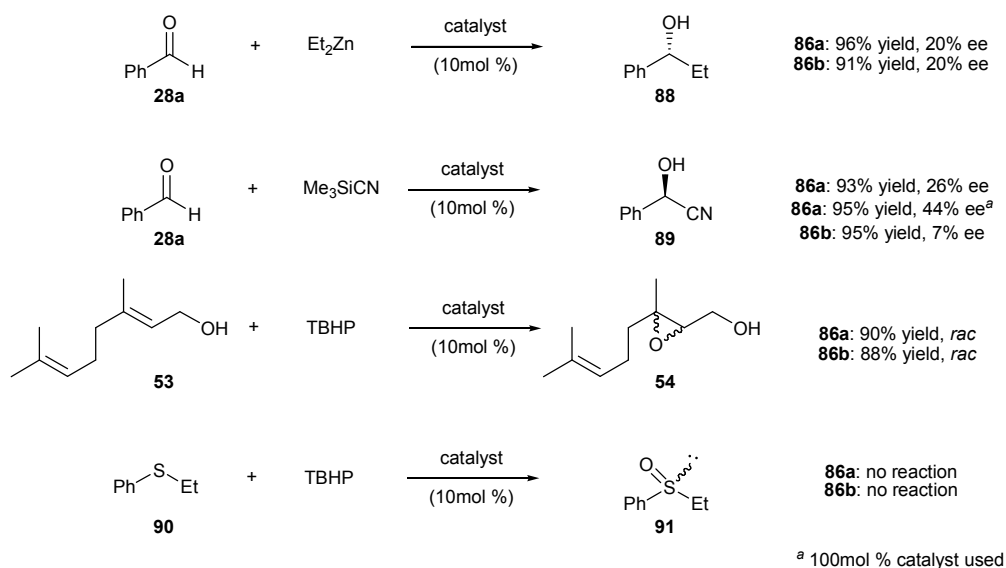
Scheme 33. Isolation of the C_3 -symmetric triol (*S,S,S*)-**76a** and (*S,S,S*)-**76b**

In reacting ligands **76a,b** with $\text{Ti}(\text{O}^i\text{Pr})_4$ only oligomers **86a** and **86b** were formed, with their conformation rapidly interconverting through bridging alkoxide intermediates on the NMR timescale. In contrast the vanadyl complexes **87a** or **87b**, obtained in good yields from transesterification reactions of $[\text{VO}(\text{O}^i\text{Pr})_3]$ with triols **76a,b**, could be isolated and characterised. They were shown to exist as a binuclear complex, where two triolato ligands bridge the two metal centres, thus destroying the C_3 -symmetry of the complex (**Scheme 34**).



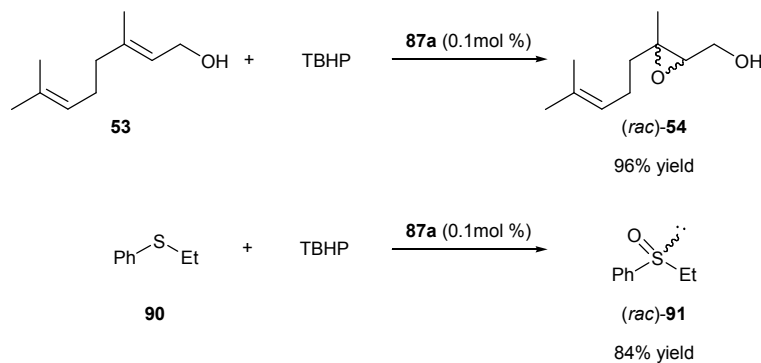
Scheme 34. C_3 -symmetric triols **76a** and **76b** and their complexes

The catalytic activity of these complexes was tested for a series of asymmetric transformations: the addition of diethyl zinc and trimethylsilyl cyanide to benzaldehyde **28a**, and the oxidation of geraniol **53** and phenyl ethyl sulfide **90** with *tert*-butyl hydroperoxide (TBHP). The titanium complexes **86a,b** showed limited stereocontrol in the addition reactions to benzaldehyde **28a**, with both catalysts giving the resulting alcohols **88** and **89** in modest enantioselectivities but good yields. The oxidation of geraniol **53** with TBHP resulted in epoxide **54** in good yields for both catalysts (90% and 88% yield for **86a** and **86b** respectively). However, no enantioselectivity was observed in either reaction. Both **86a** and **86b** failed to catalyse the oxidation of phenyl ethyl sulfide **90** (**Scheme 35**).



Scheme 35. Screening of titanium complexes **86a,b**

The screening of vanadyl complex **87a** was also attempted, but when tested in the addition reactions to benzaldehyde **28a**, no catalytic activity was observed. However, it was found that **87a** was a very efficient catalyst for oxidations using TBHP. Geraniol **53** was oxidised in the presence of 0.1mol % of **87a** resulting in the racemic product **54** in 96% yield. Similarly, the oxidation of phenyl ethyl sulfide **90** with TBHP, in the presence of 0.1mol % of **87a** gave the racemic sulfoxide (*rac*)-**91** in 84% yield (**Scheme 36**).



Scheme 36. Screening of vanadyl complex **87a**

A C_3 -symmetric triol **92** (**Figure 19**) was used in the enantioselective addition of diethyl zinc to benzaldehyde **28a** by Armstrong and co-workers.⁵⁴ The presumed complex arising from **92** and $Ti(O^iPr)_4$ gave racemic 1-phenylpropanol **88** in good yield. When an additional ten equivalents of $Ti(O^iPr)_4$ was added to the reaction mixture the resulting alcohol was obtained in 10% ee (in favour of the (*R*)-enantiomer) (**Scheme 37**).

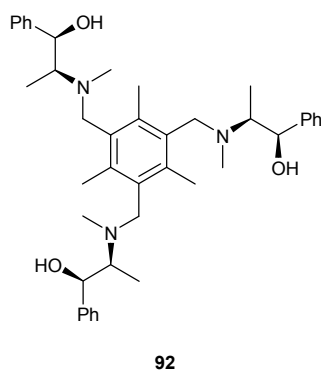
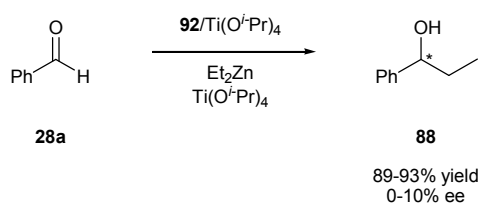
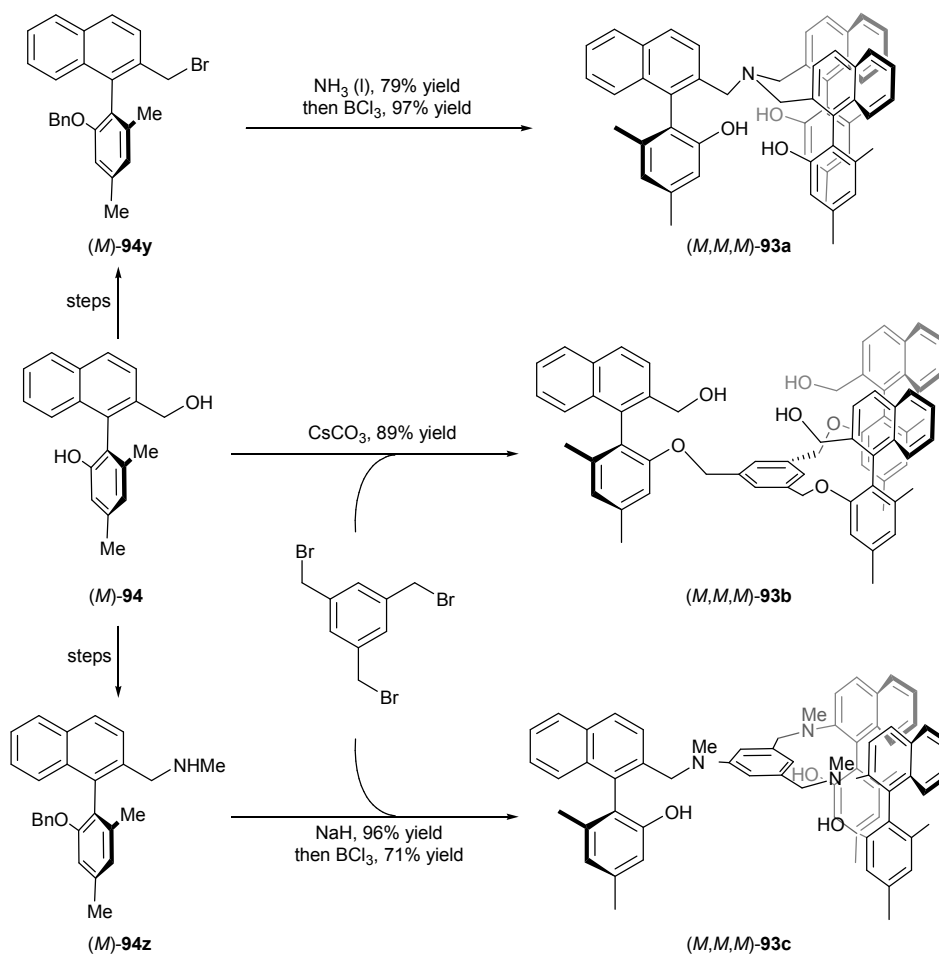


Figure 19. C_3 -symmetric triol **92**



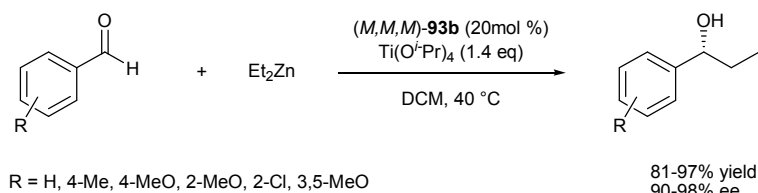
Scheme 37. Titanium catalysed addition of diethyl zinc to benzaldehyde **28a** using triol **92**

In 2003, Bringmann *et al.* reported the synthesis of a series of axially chiral C_3 -symmetric tripodal ligands (M,M,M)-**93a**, (M,M,M)-**93b** and (M,M,M)-**93c** from the same biaryl subunit (M)-**94** (Scheme 38).⁵⁵ For example, treatment of the homochiral phenyl-(2-bromomethyl)naphthalene (M)-**94y** with liquid ammonia in toluene led to the corresponding primary amine as the initial product, which was further alkylated by two more equivalents of (M)-**94y** to the tertiary amine. Following deprotection of the oxygen functional groups with boron trichloride ligand (M,M,M)-**93a** was obtained in 77% yield over the two steps.⁵⁶ Ligands (M,M,M)-**93b** and (M,M,M)-**93c**, were constructed by attaching tris(bromomethyl)benzene to the phenolic oxygen atoms on (M)-**94** or to the benzylic nitrogen of (M)-**94z** respectively. Reaction of (M)-**94** with tris(bromomethyl)benzene delivered the tripodal ligand (M,M,M)-**93b** in just a single step and 89% yield. Similarly, reaction of (M)-**94z** with tris(bromomethyl)benzene, followed by deprotection with boron trichloride gave (M,M,M)-**93c** in 68% yield over the two steps.⁵⁵



Scheme 38. Synthesis of axially chiral C_3 -symmetric ligands (M,M,M)-93a, (M,M,M)-93b and (M,M,M)-93c

The ligands were initially screened for the enantioselective addition of diethyl zinc to benzaldehyde, with (M,M,M)-93a catalysing the reaction with a moderate enantiomeric excess of 56%. Further optimisation investigated the addition of $\text{Ti}(\text{O}^i\text{Pr})_4$ to form titanium complexes of (M,M,M)-93b and (M,M,M)-93c *in situ*. (Previous studies had shown that the titanium complex of (M,M,M)-93a was unstable, indicating that the binding cavity was too small to accommodate titanium).⁵⁶ Under these conditions only (M,M,M)-93b catalysed the reaction, with 0.2 equivalents of ligand 93b, 1 equivalent of diethyl zinc and 1.4 equivalents of $\text{Ti}(\text{O}^i\text{Pr})_4$, resulting in (*R*)-ethylcarbinols in excellent yields (81-97%) and 90-98% ee (Scheme 39).



Scheme 39. Enantioselective additions of diethylzinc to aromatic aldehydes catalysed by *(M,M,M)*-**93b**

A series of tris(β -hydroxy amide) ligands **95a-d** were used in the catalytic asymmetric alkynylation of aldehydes.⁵⁷ In initial screening of the enantioselective addition of phenylacetylene to benzaldehyde, it was found that the use of diethyl zinc and $\text{Ti}(\text{O}^i\text{Pr})_4$, ligands **95a**, **95b** and **95d** gave the corresponding (*R*)-propargyl alcohol in <20% ee. Promisingly ligand **95c** gave the (*S*)-enantiomer in 85% yield and 78% ee. By fine-tuning the proportion of **95c**: $\text{Ti}(\text{O}^i\text{Pr})_4$ to a ratio of 1:7, the result was improved to give the (*S*)-propargyl alcohol in 84% yield and 87% ee. The application of these metal complexes to other substituted benzaldehydes shows it tolerated both electron-withdrawing and electron-donating groups to give products in high yields and enantioselectivities (**Scheme 40**).

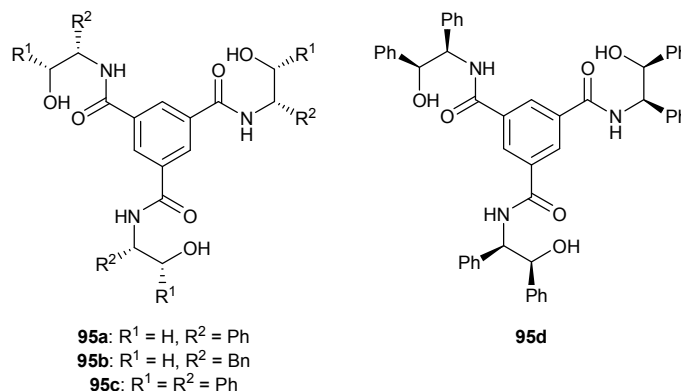
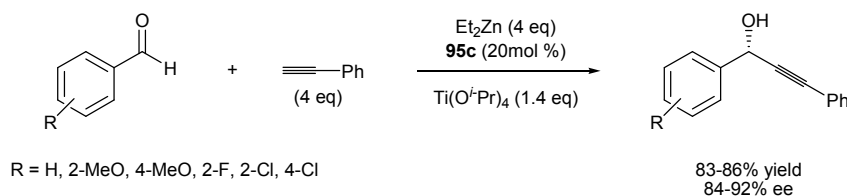


Figure 20. C_3 -symmetric tris(β -hydroxy amide) ligands **95a-d**



Scheme 40. Enantioselective addition of phenylacetylene to aldehydes catalysed by **95c**

In later publications, application of the structurally related ligands tris(β -hydroxy amide) **95e** and tris(β -hydroxy phosphoramidate) **95f** (**Figure 21**) to the enantioselective borane reduction of prochiral ketones was reported.^{58, 59} Both

proved efficient in the reduction of electron-deficient and electron-rich ketones, furnishing chiral alcohols in high yields and high ees (**Scheme 41**, **Table 12**). **95f** had the added advantage of being recoverable from the reaction mixture (>70% yield by crystallisation), and could be recycled *in situ*, with no loss of activity or selectivity after eight iterative additions of ketone and borane.

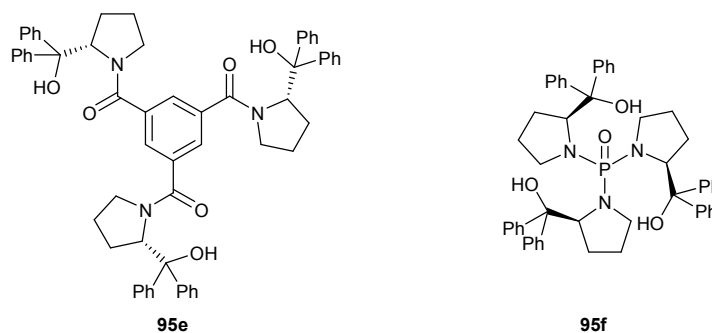
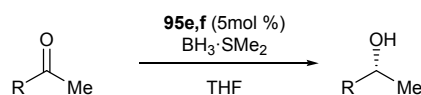


Figure 21. *C*₃-symmetric tris(β -hydroxy amide) ligand **95e** and tris(β -hydroxy phosphoramidate) ligand **95f**



Scheme 41. Enantioselective borane reduction of ketones catalysed by **95e** and **95f**

Table 12

Entry	R	95e ^a		95f ^b	
		Yield /%	ee /%	Yield /%	ee /%
1	Ph	96	94	94	95
2	4-F(C ₆ H ₅)	94	97	95	95
3	4-Br(C ₆ H ₅)	93	96	96	95
4	4-MeO(C ₆ H ₅)	90	91	92	93
5	4-NO ₂ (C ₆ H ₅)	94	97	95	98
6	3,5-NO ₂ (C ₆ H ₄)	94	74	94	95
7	2-Naphthyl	94	95	94	94

^a Reaction run at 50 °C; ^b Reaction run at 45 °C

The authors proposed a transition state for the reaction of **95f**, in which one borane atom is associated with the three oxygens of the hydroxyl groups, with another borane interacting with the phosphoramidate oxygen atom facilitating hydride attack at the *Re* face of the prochiral ketone, to yield an alcohol with an *R* configuration (**Figure 22**).

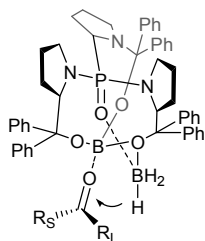


Figure 22. Proposed transition state for borane reduction by **95f**

Phosphoramidate Based Ligands

In 1992, Tolman *et al.* first reported application of the C_3 -symmetric polypyrazole ligand **96** in the copper catalysed cyclopropanation of styrene **99** by ethyldiazoacetate **100** (Scheme 42).⁶⁰ The ligand series was later expanded to include the structurally related tris(pyrazolyl)phosphine oxide ligand **97** and the tris(pyrazolyl)hydroborate ligand **98** (Figure 23).⁶¹ Of the three, the copper complex of **98** produced the best result, giving *cis*-(1*R*,2*S*) cyclopropane **101** in 85% ee and *trans*-(1*R*,2*R*) cyclopropane **101** in 81% ee in a *cis:trans* ratio of 60:40 (Table 13, entry 4).

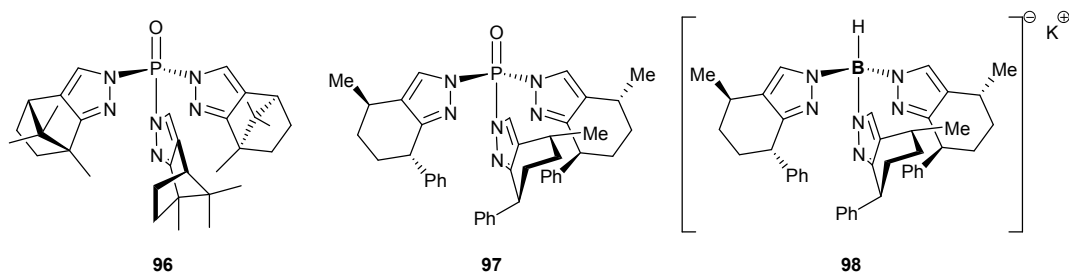
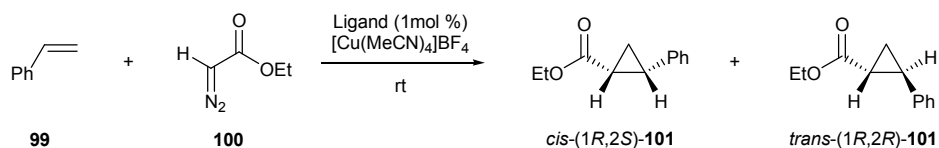


Figure 23. C_3 -symmetric polypyrazole ligands **96-98**



Scheme 42. Copper catalysed cyclopropanation of styrene **99** by ethyldiazoacetate **100**

Table 13

Entry	Ligand	Yield /%	<i>cis:trans</i> ratio	ee /%	
				<i>cis</i> -101	<i>trans</i> -101
1	96	52	56:44	51	31
2 ^a	96	48	67:33	60	40
3	97	51	35:65	24	36
4	98	46	60:40	85	81

^a Reaction performed at -78 °C.

In 1993, Wills and co-workers reported the synthesis of a novel C_3 -symmetric catalyst **102** containing an phosphoramidate structural unit for the asymmetric reduction of ketones, using borane as the reductant (**Figure 24, Scheme 43**).⁶² With a catalyst loading of 10mol %, acetophenone **103** was reduced to give the (*S*)-alcohol **104** in 70% yield and 20% ee after only 1 hour at room temperature.

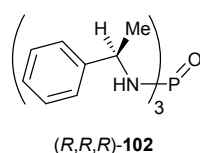
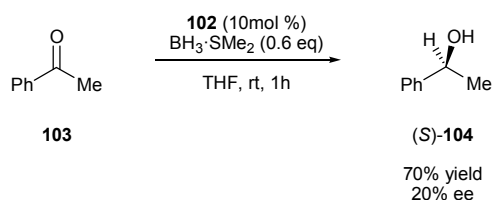


Figure 24. C_3 -symmetric catalyst **102** containing an $N-P=O$ structural unit



Scheme 43. Borane reduction of acetophenone **103** with chiral catalyst (*R,R,R*)-**102**

Nitrogen Based Ligands

In 2000, Bolm *et al.* reported application of a dinuclear manganese(III) complex **106** bearing a novel proline derived C_3 -symmetric trispyrrolidine-1,4,7-triazacyclononane (TP-TACN, **105, Figure 25**), for the enantioselective epoxidation of styrenes.⁶³ For example, reaction of styrene **99** and hydrogen peroxide, in the presence of 2mol % of catalyst **106**, gave the (*S*)-epoxide **107** in 28% conversion and 24% ee after 2 hours. Extending the reaction time to 4 hours increased the conversion (ca. 88%) but reduced the enantioselectivity to 15% ee (**Scheme 44**).

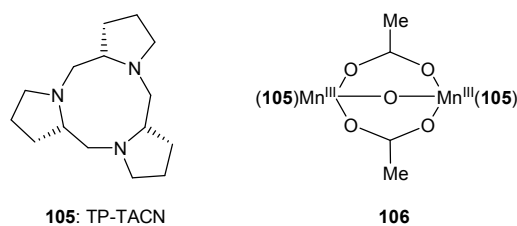
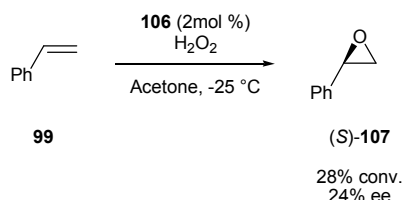


Figure 25. TP-TACN **105** and its dinuclear manganese complex **106**



Scheme 44. Enantioselective epoxidation of styrene **99** by dinuclear manganese complex **106**

A series of C_3 -symmetric receptors, **108a-c** (Figure 26), based around a hexasubstituted benzene scaffold were synthesised in the labs of Anslyn and co-workers.⁶⁴ These were tested for the asymmetric alkylation of the enolate of 2-acetylcyclohexanone **110** with benzyl bromide. Use of a [2.2.1] cryptand **109** was necessary to separate the enolate from the sodium counterion and promote binding of the enolate to the receptor. In the benzylation reaction, both **108a** and **108b** gave low enantioselectivities (10% ee and 20% ee respectively), with the best result obtained using **108c**, furnishing the alkylated product **111** in 40% yield and 42% ee (Scheme 45).

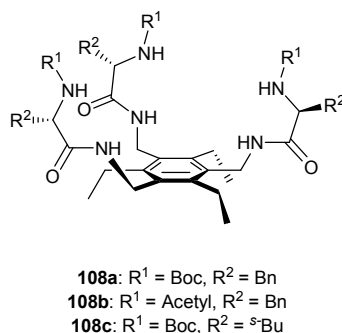
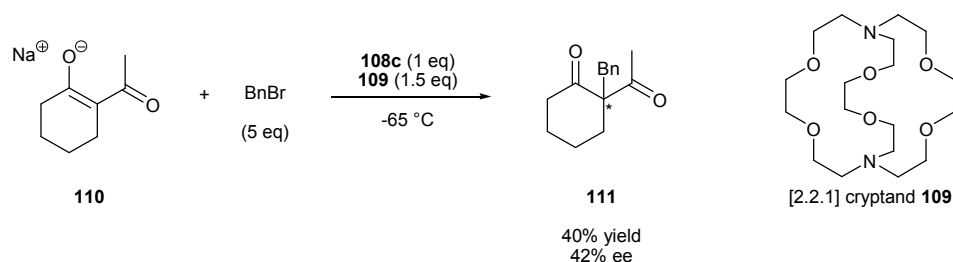


Figure 26. Receptors **108a-c**



Scheme 45. Enantioselective benzylation of the enolate **110** by **108c**

The use of zirconium alkyl complexes **112a** and **112b** (Figure 27) as catalysts for the stereoselective addition of a methyl group to aryl aldehydes and ketones was reported by Gade *et al.* (Scheme 46).^{32, 65}

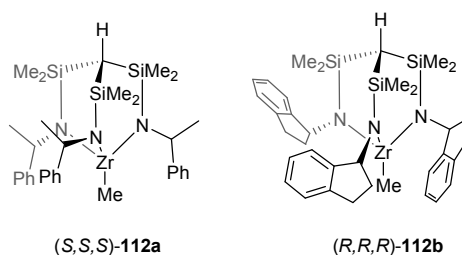
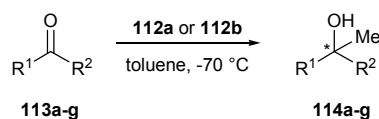


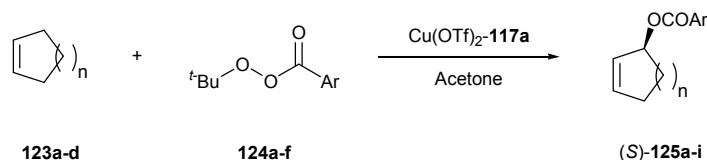
Figure 27. Zirconium complexes **112a** and **112b**

The reaction of (*S,S,S*)-**112a** with aryl ketones was found to give the corresponding (*S*)-alcohols with the best result being obtained for propiophenone **113c** of 40% ee (Table 14, entries 1-3). In contrast, the conversion of aryl aldehydes with **112a** gave the secondary alcohols (entries 4-7), with much higher levels of stereoselectivity, with 2-naphthaldehyde **113g** giving the corresponding (*S*)-alcohol **114g** in 80% ee (entry 7). Reaction of (*R,R,R*)-**112b** with 2-naphthaldehyde gave (*R*)-**114g** in 82% ee (entry 8).



Scheme 46. Stereoselective addition of a methyl group to aryl ketones **113a-c** and aryl aldehydes **113d-g**

The first application of amine based trisoxazolines **117a** and **117b** (**Figure 28**) for the copper catalysed enantioselective allylic oxidation of cyclic alkenes was reported in 1995 by Katsuki *et al.* (**Scheme 50**).⁶⁸ For example, the complex resulting from trisoxazoline (*S*)-**117a** and Cu(OTf)₂ catalysed the allylic oxidation reaction of cyclopentene **123a** with *tert*-butyl perbenzoate **124a** giving (*S*)-2-cyclopentenyl benzoate **125a**, in 74% ee and 68% yield. In contrast when ligand (*S*)-**117b** was used, the asymmetric induction observed was much lower (23% ee). The enantioselectivity could be increased to 88% by performing the reaction at -20 °C; however the yield was only 11% after 111 hours (**Table 15**, entry 2). Oxidation of other cycloalkenes, cyclohexene **123b** and cyclooctene **123d**, gave the corresponding products in 54-69% ee, with only the oxidation of cycloheptene **123c** showing a poor enantioselectivity of 14% ee (**Table 15**, entries 3 to 6). In a subsequent report the influence of the aryl substituent of peroxy esters on enantioselectivity for the oxidation of cyclopentene **123a** using ligand (*R*)-**117a** was examined (**Table 15**, entries 7 to 12).⁷⁰ The use of *meta*- or *para*-substituents did not influence the selectivity, though introduction of a *para*-nitro group strongly retarded the reaction (entries 7 to 9). The presence of an *ortho*-methyl substituent gave the best result (91% ee when performed at -20 °C), while an *ortho*-chloro substituent decreased enantioselectivity whilst increasing the yield of the reaction (entries 10 to 12).



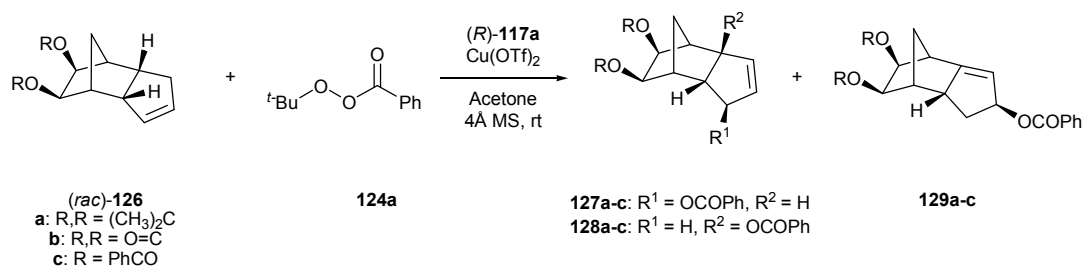
Scheme 50. Enantioselective allylic oxidation of cycloalkenes

Table 15

Entry	Product	n	Ar	Temp /°C	Time /h	Yield /%	ee /%
1	125a	1	Ph	rt	40	68	74
2	125a	1	Ph	-20	111	11	88
3	125b	2	Ph	rt	48	11	56
4	125b	2	Ph	-20	670	10	69
5	125c	3	Ph	rt	90	34	14
6	125d	4	Ph	rt	90	18	54
7	125e	1	4-MeO(C ₆ H ₄)	rt	17	55 ^a	68
8	125f	1	4-NO ₂ (C ₆ H ₄)	rt	17	- ^a	-
9	125g	1	3-Me(C ₆ H ₄)	rt	17	61 ^a	65
10	125g	1	2-Me(C ₆ H ₄)	rt	17	16 ^a	83
11	125h	1	2-Me(C ₆ H ₄)	-20	190	5 ^a	91
12	125i	1	2-Cl(C ₆ H ₄)	rt	17	70 ^a	74

^a Reaction performed in the presence of 4Å molecular sieves

The authors were able demonstrate the application of this reaction in the oxidative functionalisation of racemic dioxygenated dicyclopentadiene derivatives (*rac*)-**126a-c**.⁷¹ The reaction of **126** in the presence of *tert*-butyl peroxybenzoate **124a** and Cu(OTf)₂-**117a** provides a mixture of isomers **127**, **128** and **129** (Scheme 51). The results are summarised in Table 16, with the best result using substrate **126b** with isomer **127a** obtained in 87% ee.

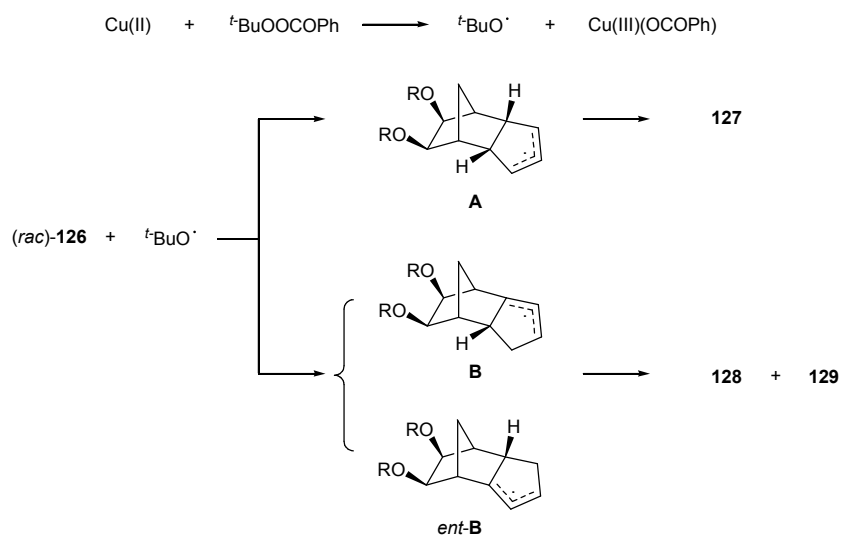


Scheme 51. Oxidative functionalisation of dioxygenated dicyclopentadienes **126a-c**

Table 16

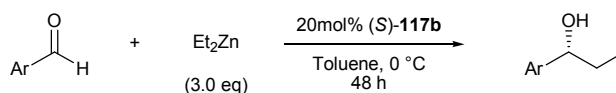
Entry	Substrate	Time /h	Regioselectivity (127:128:129)	Yield /%	ee /% (127:128:129)
1	126a	69	6.0:5.9:1	78	80, 12, 42
2	126b	144	3.8:3.6:1	57	87, 22, 69
3	126c	132	3.2:3.2:1	69	59, 7, 17

The Kharash-Sosnovsky reaction has been proposed to start with the copper catalysed reductive cleavage of the O-O bond of the peroxy ester and subsequent hydrogen atom abstraction by the resulting *tert*-butoxy radical (**Scheme 52**). Abstraction of hydrogen at the methylene carbon provides a *meso*-allyl radical **A**, with abstraction at the methine carbon giving racemic allyl radicals (**B** and *ent*-**B**). After ligation of the resulting allyl radical to the copper carboxylate, it is the face selectivity that determines the enantioselectivity of **127** from the *meso*-allyl radical **A**. The efficiency of the catalyst to differentiate between **B** and *ent*-**B** to give **128** and **129** was not as good, as demonstrated by the observed ees.



Scheme 52. Proposed reaction pathway of the reaction of **126**

The efficiency of trisoxazoline (*S*)-**117b** in the enantioselective addition of diethyl zinc to aldehydes was demonstrated by Chan and co-workers.⁶⁹ Use of 20mol % of **117b** in the presence of diethylzinc gave the alcohols in good yield (81-95%) and up to 90% ee (**Scheme 53**).

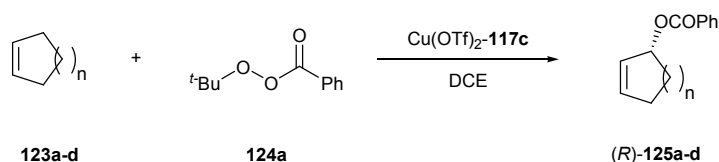


Ar = C₆H₅, 2-MeO(C₆H₄), 1-Naphthyl,
2-Naphthyl, 9-Phenanthrenyl

81-95% yield, 72-90% ee (*R*)

Scheme 53. Addition of diethylzinc to aldehydes catalysed by (*S*)-**117b**

In 2000, Katsuki *et al.* went on to expand the ligand series to include (*R*)-**117c**, where the central nitrogen was replaced by a carbon methine (**Figure 28**).⁷² In the allylic oxidation of cycloalkenes, under similar conditions as before, the products were now obtained in better yields and ees across all ring sizes (**Scheme 54**, **Table 17**). It is noteworthy that when compared to ligand (*R*)-**117a**, the allylic alcohol products now had an *R* configuration even though both ligands bear the same chirality in the oxazoline units.



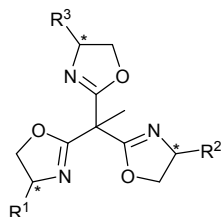
Scheme 54. Copper(II) catalysed enantioselective allylic oxidation of cycloalkenes with *tert*-butyl peroxybenzoate **124a**

Table 17

Entry	Product	n	Temp /°C	Time /h	Yield /%	ee /%
1	125a	1	0	48	73	85
2	125a	1	-20	200	46	89
3	125b	2	0	48	80	82
4	125b	2	-20	200	50	86
5	125c	3	0	48	64	88
6	125c	3	-20	200	13	92
7	125d	4	rt	48	24	81
8	125d	4	0	200	25	85

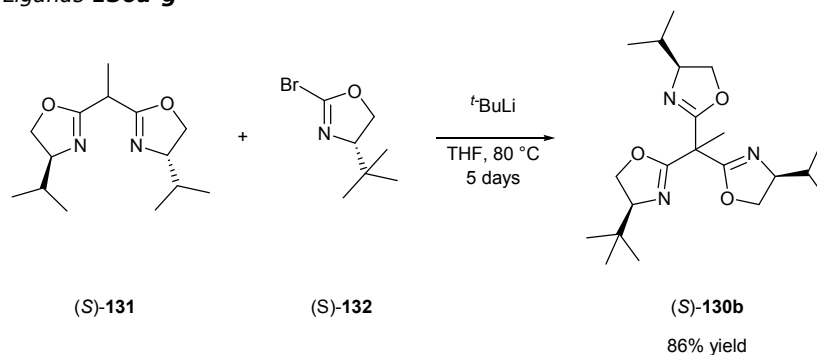
A series of structurally related 1,1,1-tris(oxazoliny)ethane derivatives were synthesised in the labs of Gade and co-workers (**Figure 29**).⁷³ The modular approach to the synthesis of such ligands, not only allowed for the conventional symmetrically substituted derivatives (eg, 1,1,1-tris[2-((*S*)-4-*iso*-propyl)oxazoliny]ethane **130a**) but also tripods of mixed substitution patterns (eg, **130b,c**). For example, the synthesis

of (*S*)-**130b** was achieved by coupling of bisoxazoline (*S*)-**131** with 2-bromooxazoline (*S*)-**132** to afford the trisoxazoline in 88% yield (**Scheme 55**).



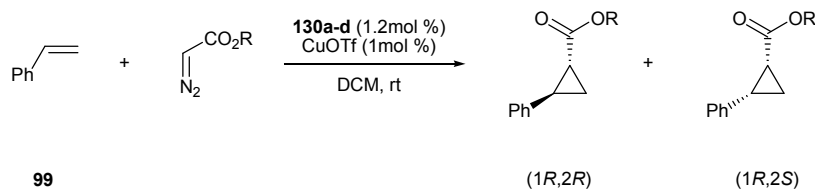
(*S*)-**130a**: R¹ = R² = R³ = *i*-Pr
 (*S*)-**130b**: R¹ = *t*-Bu, R² = R³ = *i*-Pr
 (*S*)-**130c**: R¹ = *i*-Pr, R² = R³ = *t*-Bu
 (*S*)-**130d**: R¹ = R² = R³ = *t*-Bu
 (*R*)-**130e**: R¹ = R² = R³ = Ph
 (*S*)-**130f**: R¹ = R² = R³ = Bn
 (4*R*,5*S*)-**130g**: R¹ = R² = R³ = Ind

Figure 29. Ligands **130a-g**



Scheme 55. Synthesis of ligand (*S*)-**130b**

Ligands **130a-d** were screened in the copper(I)-catalysed asymmetric cyclopropanation of styrene **99** with *tert*-butyl and ethyl diazoacetate (**Scheme 56**).⁷³ The strong preference for the *trans* diastereomer is similar to results obtained for bisoxazoline ligands. Of the four, mixed tripod ligand **130c** was found to give the best results: 85% ee for the *cis* diastereomer in the reaction with *tert*-butyl diazoacetate and 86% ee for the *trans* diastereomer in the reaction with ethyl diazoacetate (**Table 18**, entry 3).

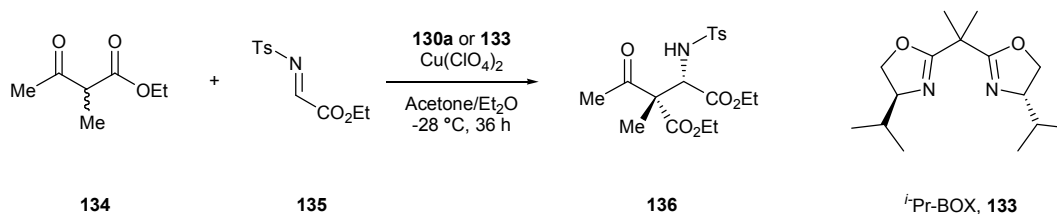


Scheme 56. Copper(I) catalysed cyclopropanation of styrene **99** with *tert*-butyl and ethyl diazoacetate

Table 18

Entry	Ligand	R = <i>tert</i> -Bu			R = Et		
		<i>cis:trans</i>	<i>cis</i> ee /%	<i>trans</i> ee /%	<i>cis:trans</i>	<i>cis</i> ee /%	<i>trans</i> ee /%
1	130a	22:78	70	65	29:71	64	67
2	130b	22:78	72	66	29:71	72	78
3	130c	23:77	85	81	31:69	81	86
4	130d	19:81	73	70	31:69	68	70

In a subsequent publication, the authors reported a direct comparison of the enhanced efficiency of *t*-Pr-trisox ligand **130a** compared to its analogous *t*-Pr-BOX ligand **133**.⁷⁴ The comparison was made for the copper(II)-catalysed enantioselective Mannich reaction of ethyl 2-methylacetoacetate **134** with *N*-tosyl- α -imino methyl ester **135** at different catalyst loadings. With 10mol % of **130a** the product **136** was obtained in 84% yield and 90% ee. At lower catalyst loadings the enantioselectivity remained unchanged (at 0.01mol% the product was isolated in 36% yield and 90% ee). In contrast, using 10mol % of *t*-Pr-BOX ligand **133** under the same reaction conditions gave the Mannich product in 84% yield and 84% ee, dropping to 35% yield and 66% ee using 0.01mol % of catalyst (**Scheme 57**, **Table 19**).

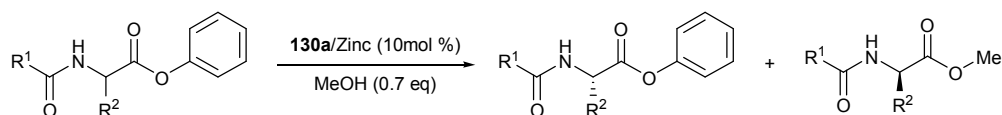


Scheme 57. Copper(II) catalysed enantioselective Mannich reaction of ethyl 2-methylacetoacetate **134** with *N*-tosyl- α -imino methyl ester **135**

Table 19

Entry	Catalyst loading /mol %	<i>t</i> -Pr-BOX 133		<i>t</i> -Pr-trisox 130a	
		Yield /%	ee /%	Yield /%	ee /%
1	10	84	84	84	90
2	1	70	84	75	89
3	0.1	56	80	59	91
4	0.01	35	66	36	90

The complex formed by reaction of trisoxazoline (**S**)-**130a** and $\text{Zn}(\text{OTf})_2$ was found to give modest enantioselectivity for the kinetic resolution of various phenyl ester derivatives of *N*-protected amino acids by transesterification with methanol (**Scheme 58**).⁷⁵ The catalyst gave a selectivity factor (*S*) of between 1.3 and 2.0 for the various substrates. Changing from a zinc triflate complex to an acetate complex improved the selectivity factor (*S*), but the trifluoroacetate complex gave the best results (up to *S* = 5.1, **Table 20**, entry 3).



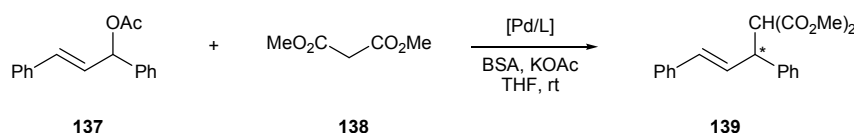
Scheme 58. Kinetic resolution of phenyl ester derivatives of *N*-protected amino acids

Table 20

Entry	Substrate		Selectivity factor (<i>S</i>) ^a		
	R ¹	R ²	Zn(OTf) ₂	Zn(OAc) ₂	Zn(OCOCF ₃) ₂
1	Ph	Ph	1.8	3.5	3.8
2	Ph	Me	1.3	2.7	3.0
3	Me	Me	2.0	4.5	5.1
4	Me	Bn	1.8	2.6	4.3

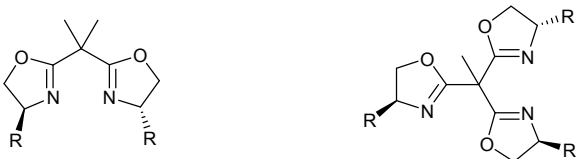
^a Selectivity factor *S* = (rate of the fast-reacting enantiomer)/(rate of the slow-reacting enantiomer)

The use of trisoxazolines **130a,e-g** in the palladium-catalysed asymmetric allylic alkylation was reported by Gade *et al.*⁷⁶ The complexation of trisoxazolines with palladium(II) species gave a structure where the ligand adopted a bidentate coordination, with the third oxazoline unit not coordinated. The trisoxazoline-Pd(II) complexes formed between **130a,e-g** and $[\{\text{PdCl}(\eta^3\text{-C}_3\text{H}_5)\}_2]$ were tested in the allylic alkylation of 1,3-diphenyl-prop-2-enyl acetate **137**, with dimethyl malonate **138** as the nucleophile (in the presence of *N,O*-bis(trimethylsilyl)acetamide (BSA)) (**Scheme 59**, **Table 21**).



Scheme 59. Palladium catalysed allylic alkylation of 1,3-diphenylprop-2-enyl acetate **137**

Table 21

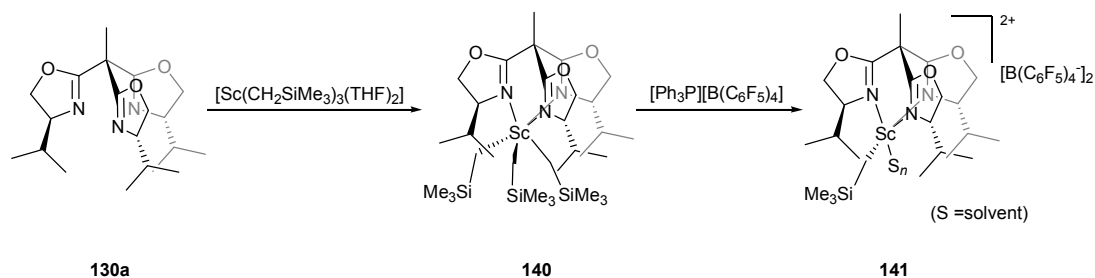


Entry	R	Yield /%	ee /%	TOF /h ⁻¹	Yield /%	ee /%	TOF /h ⁻¹
1	(S)- ^t Pr (130a)	89	89 (S)	1.35	90	95 (S)	5.02
2	(R)-Ph (130e)	7	72 (R)	0.05	28	88 (R)	0.2
3	(S)-Bn (130f)	88	83 (S)	0.91	92	88 (S)	3.73
4	(4 <i>R</i> ,5 <i>S</i>)-Ind (130g)	13	93 (R)	0.19	95	98 (R)	12.2

As a comparison the corresponding bisoxazolines ligands were also studied under the same reaction conditions. For example, use of ^tPr-BOX ligand gave the product in 89% yield and 89% ee after 3 days, whereas ^tPr-trisoxazoline gave an ee of 95% and 90% yield (**Table 21**, entry 1). A similar pattern emerged, with other trisoxazolines giving better enantioselectivities compared to their bisoxazoline analogues (entries 2-4). The trisoxazolines also enhanced the rate of reaction, as shown by their superior turn-over frequencies (TOFs). The reason for this is not clear, but could be due to the presence of an additional donating group inducing the formation of the Pd(0) species, both in the initial generation of the active species as well as in the product/substrate exchange at the end of the catalytic cycle.

In 2005, Gade and co-workers reported the use of trisoxazoline **130a** as a ligand for lanthanide based catalysts in the stereoselective polymerisation of α -olefins.⁷⁷ The trialkyl complex **140**, [Sc(**130a**)(CH₂SiMe₃)₃] could be converted to the active catalyst species **141** by reacting with two equivalents of trityl tetrakis(pentafluorophenyl)borate (**Scheme 60**). The polymerisation of 1-hexene using **141** at 21 °C proved to be highly exothermic, with a high activity of 36200 kg mol⁻¹ h⁻¹ (**Table 22**, entry 1). However, at this temperature the tacticity of the poly(1-hexene) was relatively low and GPC analysis of the polymer indicated a bimodal mass distribution ($M_w/M_n = 2.22$) suggesting thermal degradation of the molecular catalyst. At a temperature of -30 °C, polymerisation was more controlled, producing highly isotactic polymer (mmmm = 90%) with a very narrow monomodal

molecular-mass distribution ($M_w = 750\,000$ and PDI = 1.18) suggesting the catalyst displayed living-type behaviour (entry 4).



Scheme 60. Formation the Sc complex **140** and its conversion into the dicationic catalyst **141**

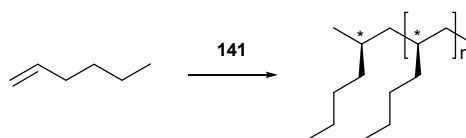
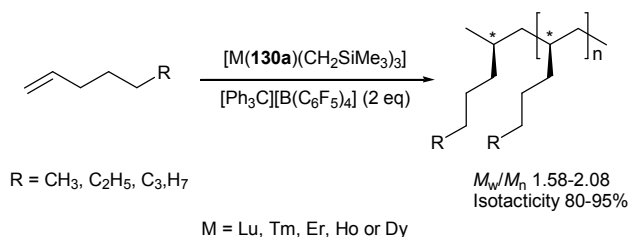


Table 22

Entry	Temp /°C	Time /min	Activity /kg mol ⁻¹ h ⁻¹	M_w	PDI (M_w/M_n)
1	21	0.5	36230	227 000	2.22
2	0	1	13080	354 000	2.36
3	-20	1.5	7600	552 000	1.87
4	-30	3	2030	750 000	1.18

The authors also reported the use of identical lanthanide complexes $[M(130a)(CH_2SiMe_3)_3]$ where $M = Lu, Tm, Er, Ho$ and Dy in the polymerisation of α -olefins.^{78, 79} Polymerisation of 1-hexene, 1-heptene and 1-octene at $-5\text{ }^\circ\text{C}$ all gave polyolefins with M_w/M_n values between 1.58 and 2.08 and isotacticities of 80-95%. The activities of the catalysts were much lower than the scandium catalyst (typically around $150\text{-}30\text{ kg mol}^{-1}\text{ h}^{-1}$) and the activity decreased with increasing chain length (activity order 1-hexene > 1-heptene > 1-octene).



Scheme 61. Polymerisation of α -olefins with organolanthanide complexes

The structurally related benzene based tripodal oxazolines, **142a-c** (**Figure 30**), were found to catalyse the enantioselective Michael addition of the potassium enolate of methyl phenylacetate **143** to methyl acrylate **144**.⁸⁰ The results showed that the *t*-Bu ligand **142b** provided a highly crowded environment around the potassium ion giving the highest enantioselectivity (82% ee) (**Scheme 62**).

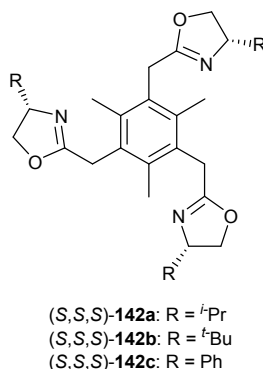
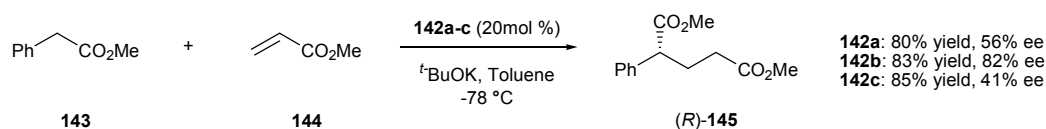


Figure 30. Benzene-based tripodal oxazolines **142a-c**



Scheme 62. Enantioselective Michael addition catalysed by **142**-*t*-BuOK complexes

In 2000, Bolm *et al.* reported the synthesis of the trisoxazolines **146a-d** mounted on the rigid backbone of a cyclohexane ring (**Figure 31**).⁸¹ These ligands were screened in both the diethyl zinc addition to benzaldehyde and the allylic oxidation of cyclopentene.

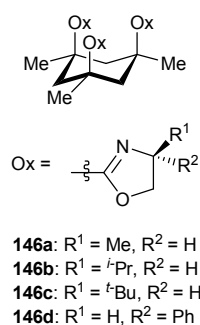
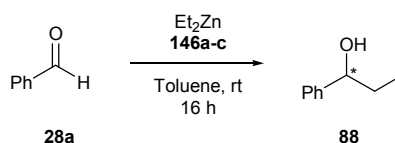


Figure 31. Chiral trisoxazolines **146a-d**

The use of trisoxazolines **146a-c** in the diethyl zinc addition to benzaldehyde **28a** gave the alcohol **88** in moderate enantioselectivities (33-43% ee) (**Scheme 63**, **Table 23**). Interestingly ligands **146a** and **146b** resulted in predominately

(*R*)-1-phenylpropanol **88**, whilst with ligand **146c** the (*S*)-enantiomer predominated. No explanation was offered for this change in selectivity.

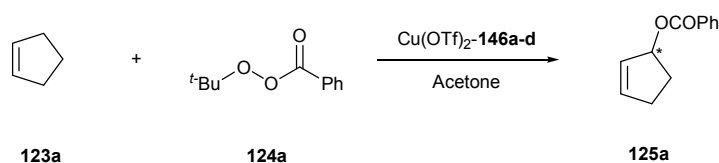


Scheme 63. Addition of diethyl zinc to benzaldehyde catalysed by trisoxazolines **146a-c**

Table 23

Entry	Ligand	Yield /%	ee /%	Configuration
1	146a	75	36	<i>R</i>
2	146b	46	43	<i>R</i>
3	146c	75	33	<i>S</i>

The copper catalysed allylic oxidation of cyclopentene **123a** with *tert*-butyl perbenzoate **124a** using ligand **146a-d** gave the product **125a** in poor to moderate ees. As with the previous amine trisoxazoline systems (*vide supra*), molecular sieves were found to enhance the reaction rate. Use of ligands **146a-c**, derived from the (*S*)-amino alcohol, gave the (*R*)-product, with **146d** giving the (*S*)-enantiomer. At -20 °C the reaction proceeded slowly to give the product in poor yields and moderate ees. Raising the temperature to 4 °C improved the yield but enantioselectivity remained low. For example use of ligand **146d** at -20 °C gave **125a** in 31% yield and 48% ee after 92 hours, while at 4 °C, **125a** was obtained in 94% yield and 45% ee after 40 hours (**Table 24**, entries 5 and 6).

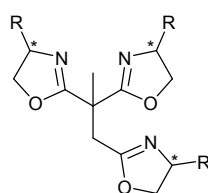


Scheme 64. Copper(II) catalysed allylic oxidation of cyclopentene **123a** with *tert*-butyl perbenzoate **124a**

Table 24

Entry	Ligand	Temp /°C	Time /h	Yield /%	ee /%	Config.
1	146a	-20	92	29	49	<i>R</i>
2	146b	-20	252	17	43	<i>R</i>
3	146b	4	40	51	31	<i>R</i>
4	146c	-20	92	12	3	<i>R</i>
5	146d	-20	92	31	48	<i>S</i>
6	146d	4	40	94	45	<i>S</i>

More recently, the use of pseudo- C_3 -symmetric trisoxazolines **147a-c** (Figure 32) in the copper catalysed Friedel-Crafts alkylation of indoles was reported by Tang and co-workers (Scheme 65).⁸² The ligands differ from the 1,1,1-tris(oxazoliny)ethane ligands of Gade and co-workers since one of the three sidearms contains a methylene group between the oxazoline ring and the central carbon.

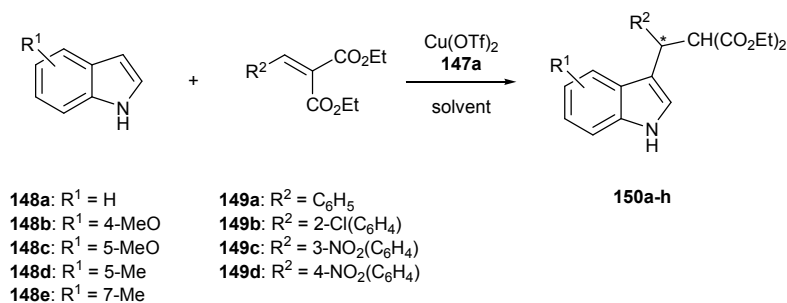


(*S*)-**147a**: R = *t*-Pr
 (*S*)-**147b**: R = *s*-Bu
 (*R*)-**147c**: R = Ph

Figure 32. Pseudo- C_3 -symmetric trisoxazolines **147a-c**

Screening of complexes $\text{Cu}(\text{OTf})_2 \cdot \mathbf{147a-c}$ in the Michael-type addition of 2-benzylidene diethylmalonate **149a** ($\text{R}^2 = \text{C}_6\text{H}_5$) to indole **148a** ($\text{R}^1 = \text{H}$) revealed **147a** to be a superior ligand. With *iso*-butanol as the solvent the (*S*)-product **150a** could be obtained in 99% yield and 94% ee, whereas using 1,1,2,2-tetrachloroethanol (TTCE) as a solvent gave an inversion in configuration to give (*R*)-**150a** in 86% yield and 80% ee (Table 25, entry 1). The scope of the reaction was shown to be tolerant to a number of arylidene malonates (entries 2-4) with the indole ester products **150b-d** obtained in high yields and ees with either *iso*-butanol (conditions A, 83-97% ee) or TTCE (conditions B, 81-89% ee) as the reaction solvent. Substitutions on the indole ring were shown to have little effect on enantioselectivity in the cases where *iso*-butanol was the solvent ((*S*)-products **150e-h** obtained in 89-98% ee). A more pronounced effect was seen with TTCE as

the solvent, with (*R*)-products obtained in 56 to 73% ee (entries 5-8). A reason for this observation was not given.



Scheme 65. Copper(II) catalyzed Friedel-Crafts alkylation of indoles **148a-e** with alkylidene malonates **149a-d**

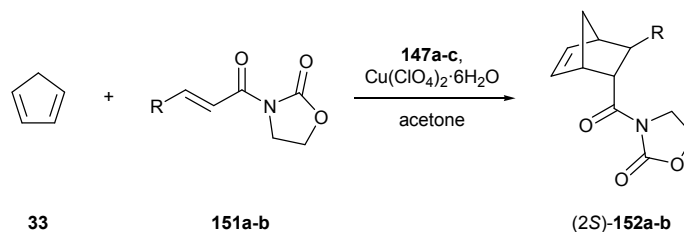
Table 25

Entry	Product	R ¹	R ²	Conditions A		Conditions B	
				Yield /%	(<i>S</i>)-150 ee /%	Yield /%	(<i>R</i>)-150 ee /%
1	150a	H	C ₆ H ₅	99	94	86	80
2	150b	H	2-Cl(C ₆ H ₄)	93	97	99	85
3	150c	H	3-NO ₂ (C ₆ H ₄)	99	83	99	89
4	150d	H	4-NO ₂ (C ₆ H ₄)	99	91	99	81
5	150e	4-MeO	C ₆ H ₅	99	98	90	61
6	150f	5-MeO	C ₆ H ₅	79	94	67	60
7	150g	5-Me	C ₆ H ₅	89	95	75	73
8	150h	7-Me	C ₆ H ₅	82	89	90	56

Conditions A: Cu(OTf)₂ (10mol %), **147a** (11-12mol %), *iso*-butanol, -20 °C. Conditions B: Cu(OTf)₂ (10mol %), **147a** (6.7mol %), TTCE, 0 °C.

The screening of pseudo-*C*₃-symmetric trisoxazolines **147a-c** in the copper catalyzed enantioselective Diels-Alder reaction has also been reported.⁸³ Initially the copper(II) complexes of ligands **147a-c** and Cu(ClO₄)₂·6H₂O were screened in the reaction of cyclopentadiene **33** with *N*-acryloyl-2-oxazolidinone **151a** (Table 26, entries 1-3). The reactions were performed under an air atmosphere at -20 °C in acetone, giving the (*2S*)-*endo*-product **152a** in high yields (99% with all three ligands) and high diastereoselectivity (*exo:endo* ratio between 7:93 and 12:88). Out of the three ligands screened, **147b** gave the best enantioselectivity for the *endo* product which was obtained in 75% ee (entry 2). Lowering the temperature to -45 °C improved the ee of the *endo* product to 80% without affecting the yield (entry 4). Conducting the

reaction at $-78\text{ }^{\circ}\text{C}$ resulted in an improved 82% ee, but the yield fell to 20% due to the poor solubility of **151a** at this temperature (entry 5). Reaction with the less reactive β -methyl dienophile **151b** went to completion after 48 hours at $0\text{ }^{\circ}\text{C}$, with product **152b** obtained in 90% and 74% ee (*endo* product). At $-20\text{ }^{\circ}\text{C}$, the yield fell to 21% but enantioselectivity improved to 81% ee (entries 6-7).

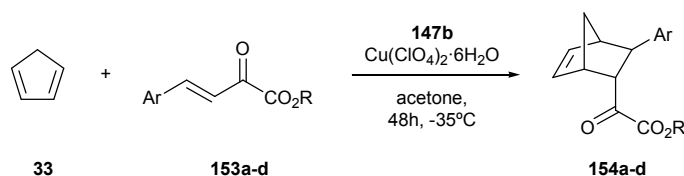


Scheme 66. Copper(II) catalysed Diels-Alder reaction between cyclopentadiene **33** and 2-oxazolidinones **151a-b**

Table 26

Entry	Ligand	Product	R	Temp /°C	Time /h	Yield /%	exo:endo	ee /%
1	147a	152a	H	-20	3	99	8:92	67
2	147b	152a	H	-20	3	99	7:93	75
3	147c	152a	H	-20	3	99	12:88	41
4	147b	152a	H	-45	6	99	4:96	80
5	147b	152a	H	-78	24	20	4:96	82
6	147b	152b	Me	0	48	90	19:81	74
7	147b	152b	Me	-20	48	21	10:90	81

The Diels-Alder reaction between cyclopentadiene **33** and ketoesters **153a-d** was also conducted (**Scheme 67**, **Table 27**). These proceeded with good enantioselectivities (up to 71% ee) and good yields (47-82%). The best result was with ketoester **153a** and cyclopentadiene **33**, affording the *endo* product **154a** in 64% yield and 71% ee (*exo:endo* ratio of 3:97) (entry 1).



Scheme 67. Copper(II) catalysed Diels-Alder reaction between cyclopentadiene **33** and ketoesters **153a-d**

Table 27

Entry	Product	Ar	R	Yield /%	exo:endo	ee /%
1	154a	Ph	Me	64	3:97	71
2	154b	Ph	Et	82	3:97	64
3	154c	Ph	Bn	47	3:97	62
4	154d	4-Br(C ₆ H ₄)	Me	56	nd ^a	nd ^a

^a Not determined; diastereomer and enantiomers could not be resolved.

The authors proposed a transition state based on a distorted octahedral geometry at the copper centre to account for the stereochemistry observed (**Figure 33**). In this model the *Si* face of *N*-acryloyl-2-oxazolidinone is blocked by the *iso*-butyl substituent on the ligand, so the diene attack is favoured from the *Re* face, thus affording the (*S*)-enantiomers.

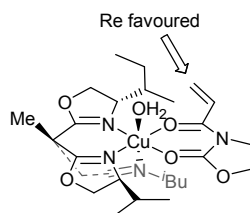
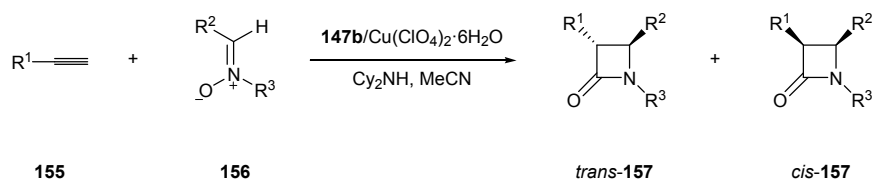


Figure 33. Proposed transition state

The use of trisoxazoline **147b** in the asymmetric synthesis of β -lactams *via* the copper-catalysed Kinugasa reaction of nitrones and terminal alkynes has also been reported (**Scheme 68, Table 28**).⁸⁴ Initial screening revealed that a combination of the copper(II) salt, Cu(ClO₄)₂·6H₂O with **147b**, and dicyclohexylamine gave optimal yields, diastereoselectivity and enantioselectivity. Under these conditions a variety of structurally different nitrones and alkynes were examined. The electronic character of the aromatic group on the nitrogen atom of the nitron (R^3) affected both the yields and stereoselectivity. Electron-rich aromatic groups increased the enantioselectivity but gave lower yields (entries 1-3), whilst electron-deficient groups gave better yields but lower ees (entries 4-5). Changes in the electronic properties of aromatic group on the carbon atom (R^2) had little effect on the enantioselectivity (entries 6-8), however with a α -furyl moiety the best enantiomeric excess was obtained (85%) but with poorest diastereoselectivity (*cis:trans* ratio 2:1) (entry 9). The reaction proved sensitive to changes in the R^1 group of the alkyne with trimethylsilyl acetylene not reacting and 1-cyclohexenyl acetylene affording a *cis*

product in 72% ee and high dr of 13:1 (entries 10-11). Ethyl propiolate reacted with an inversion in diastereoselectivity with the *trans* stereoisomer obtained as the major product (*cis:trans* ratio 1:5) in moderate ee (48%) (entry 12).



Scheme 68. Kinugasa reaction of alkynes **155** and nitrones **156** to give *trans*- and *cis*-lactams **157**

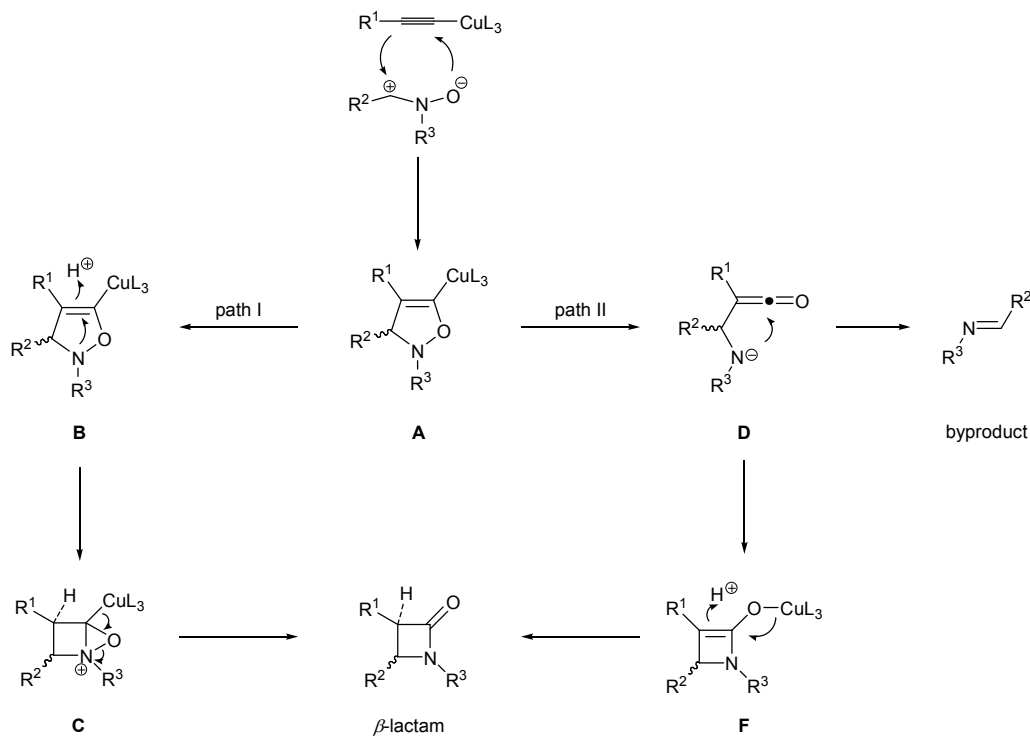
Table 28

Entry	R ¹	R ²	R ³	Lactam	Yield /%	<i>cis:trans</i>	<i>cis</i> - 157 ee /%
1	Ph	Ph	Ph	157a	56	15:1	82
2	Ph	Ph	4-Me(C ₆ H ₄)	157b	36	19:1	82
3	Ph	Ph	4-MeO(C ₆ H ₄)	157c	36	31:1	84
4	Ph	Ph	4-Br(C ₆ H ₄)	157d	70	13:1	74
5	Ph	Ph	4-EtO ₂ C(C ₆ H ₄)	157e	98	10:1	70
6	Ph	4-Me(C ₆ H ₄)	Ph	157f	50	18:1	82
7	Ph	4-MeO(C ₆ H ₄)	Ph	157g	58	18:1	83
8	Ph	4-CF ₃ (C ₆ H ₄)	Ph	157h	75	14:1	82
9	Ph	α -furyl	Ph	157i	56	2:1	85
10	1-cyclohexenyl	Ph	Ph	157j	33	13:1	72
11	Me ₃ Si	Ph	Ph	157k	nr	-	-
12	EtO ₂ C	Ph	Ph	157l	45	1:5	48 ^a

^a ee of the *trans* enantiomer

In the literature, the Kinugasa reaction is proposed to proceed via a [3+2] cycloaddition reaction to give **A**, followed by a rearrangement (**B** to **C**) to give the β -lactam (**Scheme 69**, path I).⁸⁵⁻⁸⁷ Following the observation that an imine was forming as a by-product in the reactions and that the nitrones with *N*-bound electron-withdrawing substituents gave better yields than those with *N*-bound electron-rich substituents (**Table 28**, entries 4-5 versus entries 1-3), the authors proposed another possible mechanism. In their proposed pathway, cycloaddition adduct **A** decomposes into an intermediate ketene **D**, followed by an intramolecular

nucleophilic cyclisation to give enolate **F**, as in the Staudinger reaction. Enolate **F** is then protonated to afford the β -lactam (**Scheme 69**, path II). They proposed that nitrones with *N*-bound electron-withdrawing substituents stabilised intermediate **D** and prevented its decomposition into the corresponding imine.



Scheme 69. Proposed mechanisms of the Kinugasa reaction

To help explain the stereochemical outcome of the reactions, the authors proposed a model to account for the enantioselectivity. Owing to the steric hindrance between the nitron and *iso*-propyl group, cuprous phenylacetylide approaches the *si*-face of the nitron to afford the (4*S*)-enantiomer of the β -lactam (**Figure 34**).

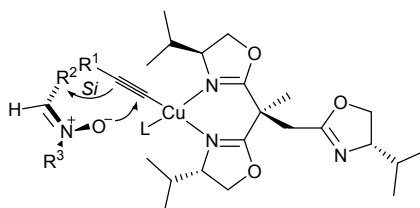


Figure 34. Proposed stereochemical model

Phosphorus Containing Ligands

In 1991, Burk *et al.* reported the development of novel C_3 -symmetric tripodal phosphines **158** and **159** (**Figure 35**) from the enantiomerically pure phenylphospholane (*S,S*)-**160**.⁸⁸ The synthesis of phospholane **160** is outlined in **Scheme 70**. Initially β -keto ester **161** was enantioselectively reduced to the

corresponding β -hydroxy ester **162** in 100% conversion and >99% ee. Following hydrolysis with aqueous potassium hydroxide, (*R*)-3-hydroxybutyric acid **163** was subjected to an electrochemical Kolbe-coupling procedure, which provided the enantiomerically pure 1,4-diol (*R,R*)-**164** in 47% yield over the three steps. After conversion of (*R,R*)-**164** to the bismesylate (*R,R*)-**165**, reaction with $\text{Li}_2\text{PPh}\cdot\text{THF}$ led to ring closure and afforded the desired phenyl phospholane (*S,S*)-**160** in 67% yield over the two steps.

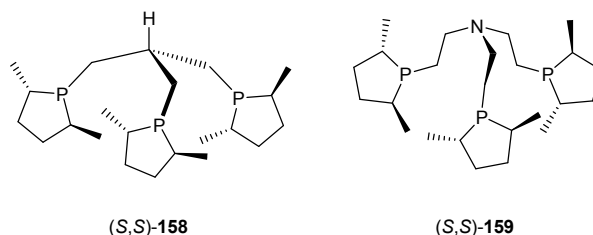
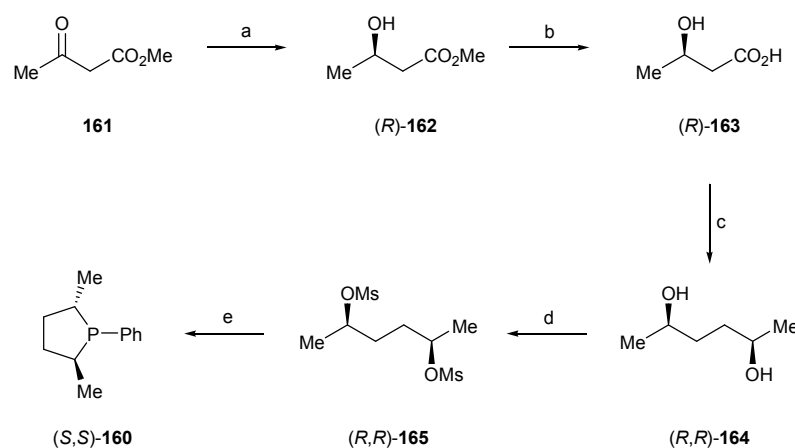


Figure 35. Chiral phosphines **158** and **159**

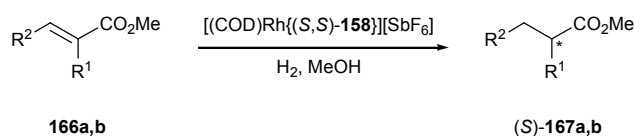


a) $[\text{Ru}((R)\text{-BINAP})]$ cat., MeOH, DCM, rt, 100% conv., >99% ee; b) KOH, H_2O , EtOH, 97% yield; c) electrochemical Kolbe coupling, NaOMe, MeOH, 48% yield; d) MsCl, Et_3N , DCM, 0 °C, 88% yield; e) $\text{Li}_2\text{PPh}\cdot\text{THF}$, THF, -78 °C, 76% yield

Scheme 70. Synthesis of (*S,S*)-2,5-dimethyl-1-phenylphospholane **160**

Ligands (*S,S*)-**158** and (*S,S*)-**159** were examined in rhodium-catalysed asymmetric hydrogenation reactions (**Scheme 71**). When screened for the hydrogenation of methyl acetamidocinnamate **166a**, (*S,S*)-**158** resulted in formation of the (*S*)-product in 89% ee after 3 days at 50 °C (**Table 29**, entry 1). In contrast, (*S,S*)-**159** failed to catalyse the reaction. Attempts to increase the rate of the hydrogenation by increasing the reaction temperature 65 °C were successful, but to the detriment of the selectivity, with the product obtained in 40% ee (entry 2). The hydrogenation of

dimethyl itaconate **166b** proceeded to give the product in 94% ee after 20 hours (entry 3).



Scheme 71. Rhodium catalysed asymmetric hydrogenation by chiral phosphine ligands **158**

Table 29

Entry	Product	R ¹	R ²	Time /h	Temp /°C	ee /%
1	167a	NHCOMe	Ph	72	50	89
2	167a	NHCOMe	Ph	48	65	40
3	167b	CH ₂ CO ₂ Me	H	20	50	94

The use of *C*₃-symmetric monodentate triarylphosphines **168a-c**, **169a-c** and **170a-c** has been reported in the palladium catalysed asymmetric allylation reactions (**Figure 36**, **Scheme 72**).^{89, 90} Three ligand-types were screened in four reactions (reactions a-d) and the best results for each class of ligand are reported for each transformation. Ligands **168-169** were found to give the highest enantioselectivities for the reactions of cyclic substrates (up to 82% ee, reactions a and b) which compare favourably with previously reported results, but do not match the best obtained for either substrate category.^{91, 92} However, the reaction involving 1,3-diphenylpropenyl acetate gave the substitution product with relatively poor selectivity (up to 32% ee, reactions c and d) compared with previously reported systems that gave selectivities of 99% or more.⁹³

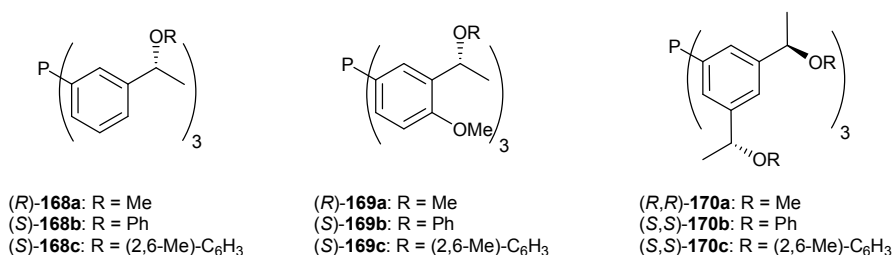
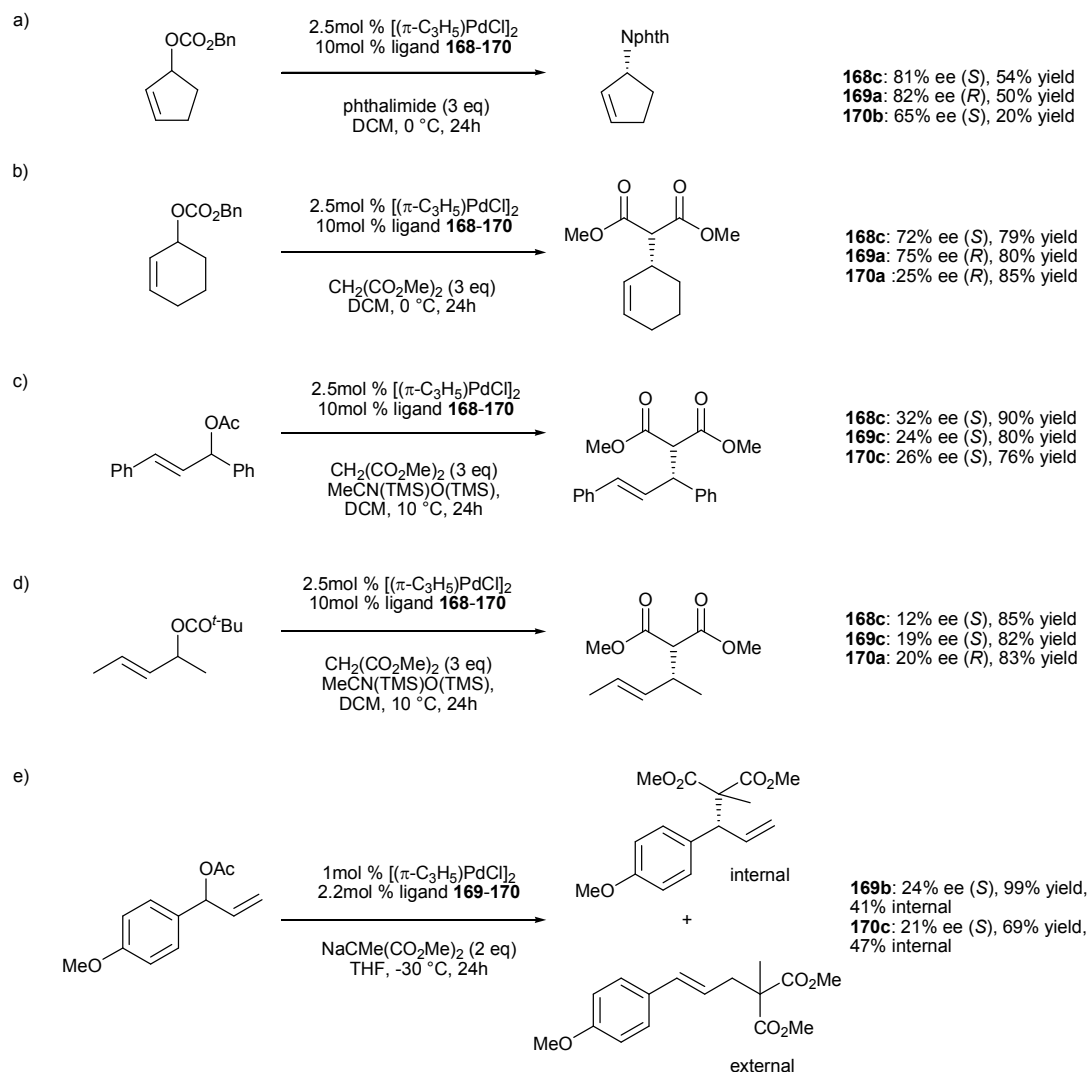


Figure 36. *C*₃-symmetric monodentate triarylphosphines **168a-c**, **169a-c** and **170a-c**

Best results for each class of ligand

**Scheme 72.** Range of transformations catalysed by ligands **168a-c**, **169a-c** and **170a-c**

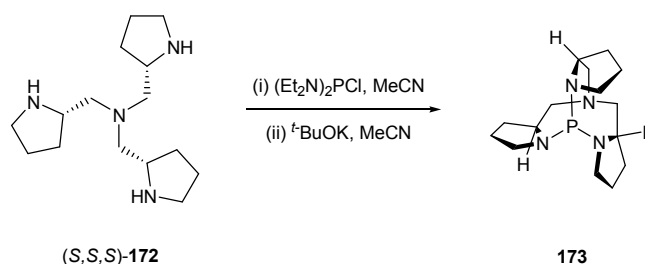
The more sterically demanding ligands (**169a-c** and **170a-c**) were also screened in transformation e. The regioselectivity of the allylation is controlled by the *trans*-directing effect of the phosphine, which can lead to high regioselectivity in favour of the internal isomer. The best regioselectivity was achieved using ligand **170c** (47:53 ratio of internal:external regioisomer), however, the enantiomeric excess was a disappointing 21% which is well below a previously reported system of Hayashi *et al.* that achieved 87% ee (90:10 ratio of internal:external regioisomer).⁹⁴

The application of a previously reported C_3 -symmetric phosphate⁹⁵ in the rhodium-catalysed asymmetric hydrosilylation of acetophenone **103** was reported by Pizzano *et al.* (**Figure 37**, **Scheme 73**).⁹⁶ After initial screening the optimal rhodium source was found to be the ethylene dimer $[\text{RhCl}(\text{C}_2\text{H}_4)_2]_2$. When the reaction was

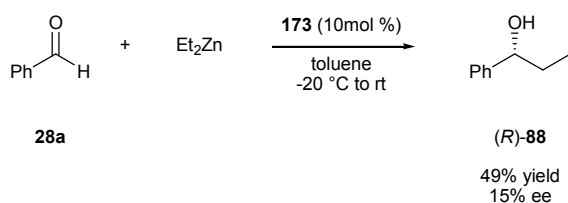
Table 30

Entry	Catalyst precursor	Ligand (L)	Conversion /%	ee /%
1	$\frac{1}{2}[\text{RhCl}(\text{C}_2\text{H}_4)_2]_2 + \text{L}$	171a	92	7
2	$\frac{1}{2}[\text{RhCl}(\text{C}_2\text{H}_4)_2]_2 + 2\text{L}$	171a	96	41
3		171b	92	52
4	$\frac{1}{2}[\text{RhCl}(\text{C}_2\text{H}_4)_2]_2 + 3\text{L}$	171a	89	51
5		171b	94	58
6	$\frac{1}{2}[\text{RhCl}(\text{C}_2\text{H}_4)_2]_2 + 4\text{L}$	171a	83	28
7	$\frac{1}{2}[\text{RhCl}(\text{C}_2\text{H}_4)_2]_2 + 5\text{L}$	171a	79	26

Yamamoto and co-workers reported the first synthesis of chiral C_3 -symmetric triamidoamine **172** and its use in the one-pot synthesis of the corresponding chiral protetraazaphosphatrane **173** (Scheme 74).⁹⁷ Protetraazaphosphatrane **173**, was shown to catalyse the silylation of benzyl alcohol, however, no asymmetric induction was observed for the attempted resolution of (*rac*)-1-phenylethanol **88**. In the reaction of diethylzinc and benzaldehyde **23a**, catalyst **173** gave the (*R*)-alcohol **88** in a moderate yield of 49% and low enantioselectivity of 15% (Scheme 75).



Scheme 74. Synthesis of chiral C_3 -symmetric protetraazaphosphatrane **173** from triamidoamine **172**



Scheme 75. Addition of diethyl zinc to benzaldehyde **28a** catalysed by protetraazaphosphatrane **173**

The use of chiral tripodal ligands, (*S,S,S*)-TRISPHOS **174a** and related (*R,R,S*)-TRISPHOS **174b**, in the rhodium-catalysed asymmetric hydrosilylation of acetophenone **103** was reported by Pastor *et al.* (**Figure 38, Scheme 76**).^{98, 99} The investigation focused on the use of dimeric, monomeric and cationic rhodium(I) catalyst precursors. For example, the combination of (*S,S,S*)-TRISPHOS **174a** with chloro(1,5-cyclooctadiene)rhodium(I) dimer (ratio Rh:P-ligand, 1:1) gave (*R*)-*sec*-phenethyl alcohol **104** in 38% yield and 81% ee (**Table 31**, entry 1). When the ratio of Rh:P-ligand was increased to 2:3, stereocontrol fell to 75% ee (entry 3). Using the monomeric Rh(I) species [(NBD)RhAcAc] also saw a drop in selectivity to 58% ee (entry 4). The cationic Rh(I) species [(NBD)Rh(ClO₄)] gave the best result with the product obtained in 65% yield and 81% ee (entry 5). Switching to the non *C*₃-symmetric (*R,R,S*)-TRISPHOS **174b** gave the (*R*)-alcohol in 5% ee, suggesting the stereocentre and stereoaxis in the enantioselective transition state were mismatched (entry 2).

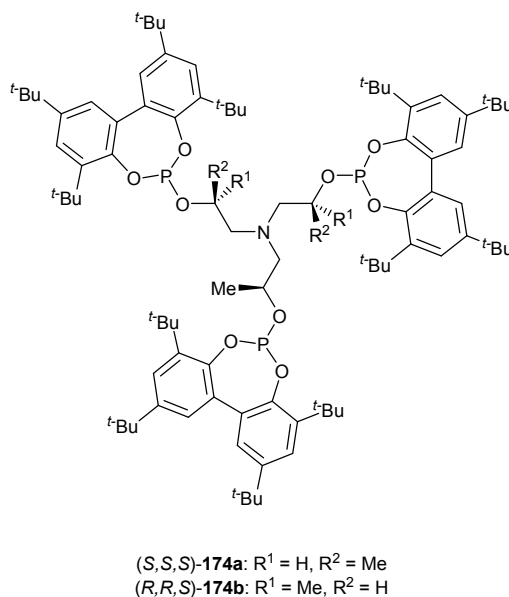
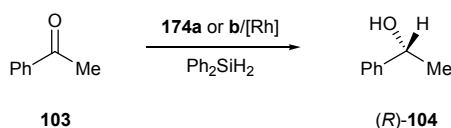


Figure 38. Tripodal phosphites, (*S,S,S*)-TRISPHOS **174a** and (*R,R,S*)-TRISPHOS **174b**



Scheme 76. Rhodium catalysed asymmetric hydrosilylation of acetophenone **103** with (*S,S,S*)-TRISPHOS **174a** and (*R,R,S*)-TRISPHOS **174b** ligands

Table 31

Entry	Catalyst precursor	Ligand	Yield /%	ee /%
1	$\frac{1}{2}[(\text{COD})\text{RhCl}]_2 + \text{L}$	174a	38	81
2		174b	NR ^a	5
3	$\frac{1}{3}[(\text{COD})\text{RhCl}]_2 + \text{L}$	174a	53	75
4	$[(\text{NBD})\text{RhAcAc}] + \text{L}$	174a	67	58
5	$[(\text{NBD})\text{Rh}(\text{ClO}_4)] + \text{L}$	174a	65	81

^a Not Reported

The synthesis of a chiral C_3 -symmetric phosphine oxide tripodal cobalt complex $\text{Na}[\text{CpCo}\{\text{PO}(\text{S-BINOL})_3\}]$, **Na(175)**, from $\text{Na}[\text{PO}(\text{S-BINOL})_3]$ and $[\text{CpCo}(\text{CO})\text{I}_2]$ was accomplished by Leung and co-workers (**Figure 39**).¹⁰⁰ The **Cu(175)** complex, prepared *in situ* from $[\text{Cu}(\text{MeCN})_4][\text{BF}_4]$ and **Na(175)**, was screened for the aziridination of substituted styrenes with $\text{PhI}=\text{NTs}$ (**Scheme 77**). The reaction of styrene, in the presence of 5 mol % of **Cu(175)**, gave (*R*)-styrene aziridine in 85% yield and 41% ee (**Table 32**, entry 1). It was found that the enantioselectivity was enhanced by electron-withdrawing substituents. For example, the reaction of 4-chlorostyrene gave the product in 61% ee, whereas the product from the reaction of 4-methylstyrene had an ee of 27% (entries 3 and 5).

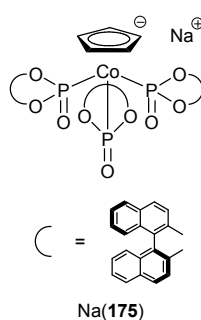
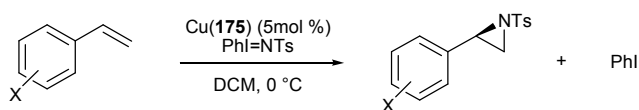
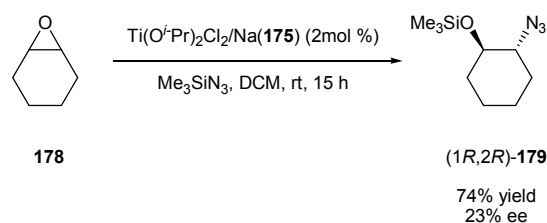
**Figure 39.** C_3 -symmetric tripodal ligand **Na(175)****Scheme 77.** Aziridination of substituted styrenes with $\text{PhI}=\text{NTs}$ catalysed by **Cu(175)** complex

Table 32

Entry	Product	X	Yield /%	ee /%
1	177a	H	85	41
2	177b	4-F	82	32
3	177c	4-Cl	82	61
4	177d	4-Br	67	41
5	177e	4-Me	77	34
6	177f	3-Cl	87	27
7	177g	2-Cl	trace	nd ^a

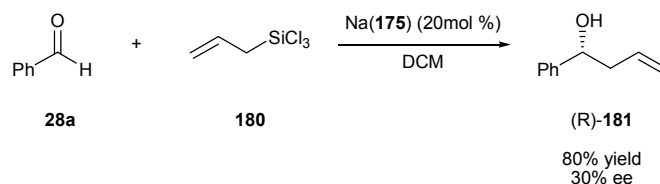
^a Not determined

Na(**175**) was also screened in the catalytic ring opening of cyclohexene oxide **178** by trimethylsilyl azide. It was found that Na(**175**), in conjunction with $\text{Ti}(\text{O}^i\text{Pr})_2\text{Cl}_2$, was an active catalyst giving 2-azido-1-((trimethylsilyl)-oxy)cyclohexane **179** in 74% and 23% ee (1*R*,2*R*) (**Scheme 78**).



Scheme 78. Enantioselective ring opening of cyclohexene oxide **178** catalysed by Na(**175**)

The use of Na(**175**) in the allylation of benzaldehyde **28a** with allyltrichlorosilane **180** was also investigated. Thus, treatment of benzaldehyde **28a** with allyltrichlorosilane in the presence of 20mol % of Na(**175**) afforded the (*R*)-homoallylic alcohol, 4-phenyl-1-buten-4-ol **181** in 80% yield and 30% ee (**Scheme 79**).



Scheme 79. Allylation of benzaldehyde **28a** catalysed by Na(**175**)

1.5 CONCLUSION

Whilst the field of C_3 -symmetry in chemistry is relatively new there are already some promising results that have been obtained. However, in the area of enantioselective catalysis, the vast majority of C_3 -symmetric ligands and complexes have yet to match their C_2 -symmetric counterparts in terms of yield and stereocontrol for comparable transformations.

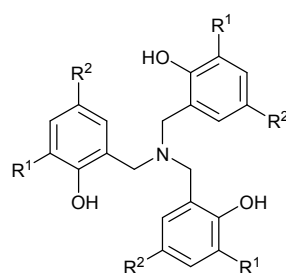
Chapter 2: Results and Discussion I

2 Results and Discussion I

2.1 AMINE TRIS(PHENOLATE) LIGANDS

2.1.1 Introduction

Triphenolamines, of the type shown in **Figure 40**, have been known for a long time, with the hydrochloride salt of **182a** first appearing in the literature in 1922.¹⁰¹ The synthesis of such a compound, in this case **182b**, was later reported in 1949 by Hultzsch.¹⁰² However, it was not until 1998 that the potential of these compounds as coordinating ligands was first realised, with **182a** used to make the iron (III) complex **183**.¹⁰³ In subsequent years, the complexation behaviour of these ligands, have been reported for a wide variety of metals (including Ti(IV),¹⁰⁴⁻¹¹⁵ Zr(IV),^{115, 116} In(III),¹¹⁷ Ga(III),¹¹⁷ Ta(V),¹¹⁸⁻¹²⁰ V(V),¹²¹ Al(III),¹²² and Ge(IV)¹²³) and main group elements (Si(IV),¹²⁴⁻¹²⁶ and P(V)¹²⁷). Examples of these appear in **Figure 41**.



182a: R¹ = R² = H
182b: R¹ = R² = Me
182c: R¹ = R² = ^tBu
182d: R¹ = ^tBu, R² = Me

Figure 40. Amine tris(phenolate) ligands **182a-d**

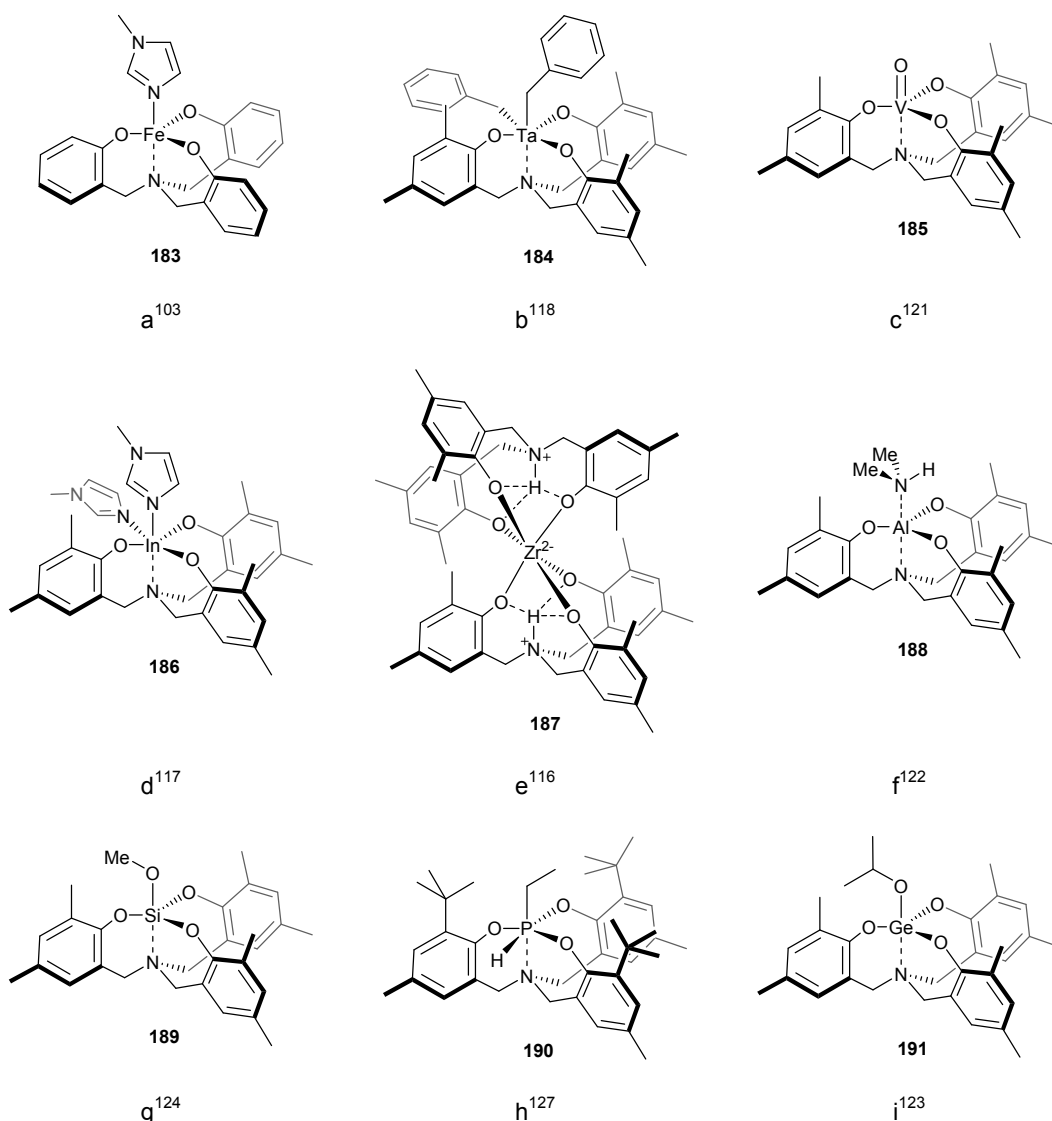
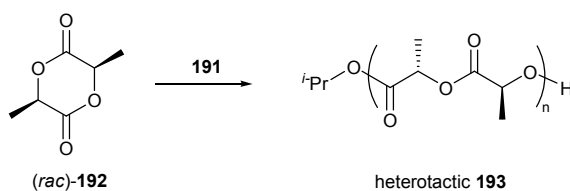


Figure 41. Representative examples of complexes of amine tris(phenolate) ligands

The catalytic potential of complexes of this type have been demonstrated by Davidson and co-workers, with the germanium alkoxide **191** showing good activity for the solvent-free ring-opening polymerisation (ROP) of (*rac*)-lactide **192**, to provide the highly heterotactic polylactide (**Scheme 80, Table 33**).¹²³ Treatment of racemic lactide (*rac*)-**192** with germanium complex **191** at 130 °C for 24 hours resulted in polylactide **193** in a 70% yield with a polydispersity index (PDI) of 1.19 (entry 3). Interestingly, analysis of the microstructure of the isolated polymers revealed a strong heterotactic bias in all cases (the probability of heterotactic enchainment, $P_r = 0.78-0.82$).



Scheme 80. Solvent-free ring-opening polymerisation of (*rac*)-lactide **192** catalysed by germanium alkoxide **191**

Table 33

Entry	M / I	Yield /%	M_n	PDI	P_r^a
1	200	71	17700	1.15	0.78
2	300	85	35700	1.15	0.79
3	600	70	52100	1.19	0.82

^a P_r is the probability of heterotactic enchainment calculated by analysis of the homonuclear decoupled ^1H NMR spectra

2.1.2 Titanium Complexes of Amine Tris(phenolate) Ligands and their Applications in Catalysis

The most studied of all amine tris(phenolate) complexes are the complexes based around a titanium centre (**Figure 42**), with a number of reports on the catalytic activity of these racemic complexes. For example, complexes **196a-b** demonstrate high activity and appreciable selectivity in the polymerisation of styrene **99**, to give syndiotactic polystyrene **198** (**Scheme 81**).¹¹² The results are summarised in **Table 34**, which reveals that **196a** displayed reasonable catalytic activity and was slightly more reactive than **196b** under comparable conditions (entries 1 and 5). When the reaction was run with a ratio of methylaluminoxane (MAO):Ti of 2000:1 at 50 °C, **196a** showed reasonably high activity (3.1×10^6) and excellent stereoselectivity (98.1%) (entry 2). This is comparable to the (η^5 -indenyl)TiCl₃/MAO and CpTi(OCH₂CH₂)₃N/MMAO catalytic systems of Rausch¹²⁸ and Do¹²⁹, which showed activities and stereospecificities of 3.7×10^7 and 98.1%, and ca. $2\text{--}4 \times 10^7$ and 98-99% respectively. At higher reaction temperatures **196a** showed a loss of stereocontrol, down to only 68% when run at 90 °C (entries 3 and 4).

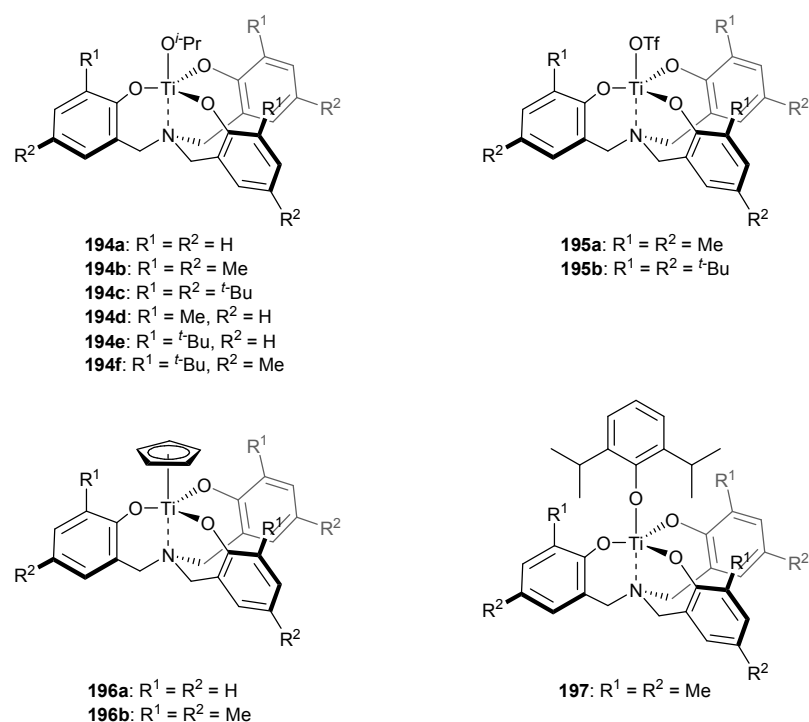
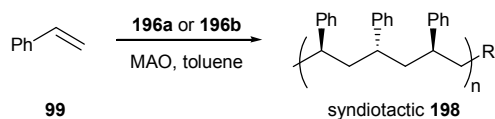


Figure 42. Titanium based amine tris(phenolate) complexes **194-197**



Scheme 81. Polymerisation of styrene **99** catalysed by titanium complexes **196a** and **196b**

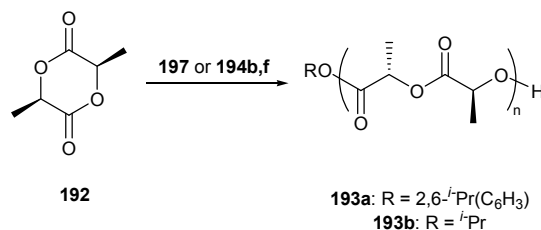
Table 34^a

Entry	Catalyst ^b	MAO/196	Temp /°C	Yield 198 /g	Activity (× 10 ⁶) ^c	% sPS
1	196a	500	50	0.374	1.38	82.4
2	196a	2000	50	0.837	3.09	98.1
3	196a	500	80	1.075	3.90	91.5
4	196a	500	90	0.383	1.40	68.1
5	196b	2000	50	0.202	0.98	50.5
6	196b	1000	80	0.382	1.85	84.8

^a 22mmol of styrene **99** used in all runs; ^b Concentration of catalysts in the reactions: [**196a**] = 1.24 nM and [**196b**] = 0.94 nM; ^c units are (g PS)/(mol of Ti)(mol of styrene)(h)

The use of the titanium complex **197** for the polymerisation of lactides was reported by Verkade and co-workers (**Scheme 82, Table 35**).¹⁰⁹ Treatment of racemic lactide (*rac*)-**192** with **197** at 130 °C for 24 hours resulted in atactic polylactide **193a** in 68%

yield with a PDI of 1.43 (entry 1). When chiral lactide (*R,R*)-**192** was employed, isotactic polylactide **193a** was obtained in 69% yield and PDI of 1.51 (entry 2). In a later publication, the authors showed that complexes **194b,f** displayed similar activities in the same polymerisation reaction (entries 3-6).¹¹³



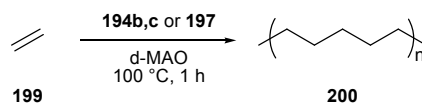
Scheme 82. Ring opening polymerisation of lactide **192** catalysed by titanium complexes **194b,f** and **197**

Table 35^a

Entry	Catalyst	Lactide	Time /h	g polymer	Yield /%	M_w^b	M_n^c	PDI ^d
1	197	(<i>rac</i>)- 192	24	1.35	68	23 000	16 000	1.43
2		(<i>R,R</i>)- 192	24	1.38	69	29 300	19 000	1.51
3	194b	(<i>rac</i>)- 192	4	1.06	53	51 400	38 000	1.35
4		(<i>R,R</i>)- 192	4	1.10	55	76 100	52 000	1.46
5	194f	(<i>rac</i>)- 192	14	0.48	24	43 400	36 200	1.44
6		(<i>R,R</i>)- 192	14	0.52	26	38 450	28 400	1.35

^a Reaction conditions: **192** (2g), **192**/Ti = 300, 130 °C; ^b The weight average molecular weight; ^c The number average molecular weight; ^d PDI = M_w/M_n

Titanium complexes **194b-c** and **197** were also shown to display high catalytic activities in the polymerisation of ethylene **199** (Scheme 83, Table 36).¹⁰⁸ Both **194b** and **194c** showed good catalytic activities at 100 °C in toluene (entries 1 and 2), with even higher catalytic activities for **194b** obtained when the reaction was run in *n*-octane (entry 4). Performing the reaction at 120 °C, gave a further increase in the activity (entry 5). In all cases the resultant polymer was shown to be linear, with low polydispersity indexes (PDI) of 1.5-2.2, suggesting that the polymerisation proceeds in a single-site manner.



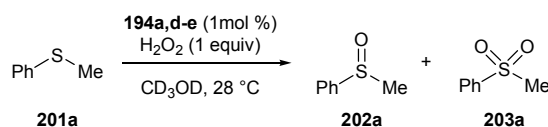
Scheme 83. Titanium catalysed polymerisation of ethylene **199**

Table 36^a

Entry	Catalyst	Solvent	Yield /mg	Activity ^b	<i>M_w</i>	PDI
1	194b	toluene	76.1	761	28 400	2.2
2	194c	toluene	185.1	1850	9100	1.5
3	197	toluene	68.1	680	nd ^c	nd ^c
4	194b	<i>n</i> -octane	161.9	1620	8000	1.6
5 ^d	194b	<i>n</i> -octane	229	2290	10 200	1.6

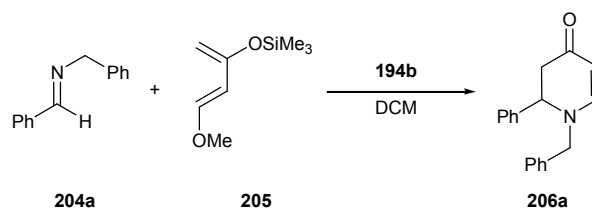
^a Reaction conditions: Catalyst (0.1 μmol), solvent (30 mL), **199** (8 atm), 100 mL scale autoclave, d-MAO (prepared by removing AlMe₃ and toluene from commercially available MAO), molar ratio of d-MAO/Ti = 40 000; ^b Units are (kg-polyethylene)/(mol-Ti)(h); ^c Not determined; ^d Reaction run at 120°C

Very recently, Licini *et al.* have reported the use of titanium *iso*-propoxide complexes **194a,d-e** in the oxidation of sulfides with aqueous hydrogen peroxide.¹⁰⁷ In an initial screening, all three complexes catalysed the oxidation of thioanisole **201a** to the corresponding sulfoxide **202a** and sulfone **203a** in high yields, good selectivities, and short reaction times (30-60 min) (Table 37). The most active complex, **194d** afforded a turnover frequency (TOF) of 1700 h⁻¹ (entry 2), followed by **194a** then **194e**. However, whilst **194e** gave the slowest reaction (entry 3), it gave the best selectivity (**202a:203a** of 98:2) and also did not decompose in solution under turnover conditions. A series of arylalkyl and dialkyl sulfides were also surveyed under these reaction conditions (Scheme 85), and these are summarised in Table 38. The reaction proved to be quite general, even tolerating the introduction of an electron-donating group on the aryl ring, without any detrimental effect on the yield or selectivity (entry 4). However, introduction of an electron-withdrawing group (a nitro group) led to a decreased yield and a decrease in selectivity for sulfoxide formation (85:15) (entry 5).



Scheme 84. Oxidation of thioanisole **201a** with hydrogen peroxide, catalysed by titanium *iso*-propoxide complexes **194a,d-e**

amounts of **194b** (10mol %) gave the desired dihydropyridinone **206a** in only 30% conversion and 12% isolated yield (entry 3).

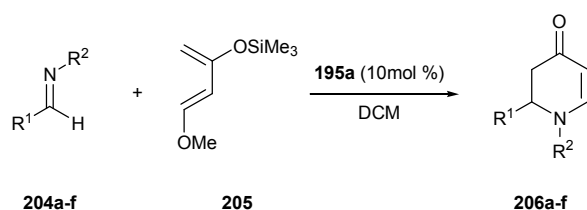


Scheme 86. Aza-Diels Alder reaction catalysed by **194b**

Table 39

Entry	Catalyst loading /mol %	Time /h	Conversion /%	Yield /%
1	100	2	62	40
2	100	21	72	32
3	10	48	30	12

In an attempt to improve the reactivity of complex **194b**, the *iso*-propoxide ligand was replaced with the more weakly coordinating axial triflate ligand, to give complex **195a**. After optimisation it was found that with 10mol % of **195a** and three equivalents of diene, *N*-benzyl-2,3-dihydro-2-phenyl-1H-pyridin-4-one **206a** could be obtained in 100% conversion and 73% isolated yield after only 45 minutes (**Scheme 87**, **Table 40**, entry 1). The scope of this reaction was investigated, with a number of imines (**204b-f**) tested. All reacted to give the corresponding 2,3-dihydropyridin-4-ones **206b-f** in good yields (100% conversions uniformly obtained) and reaction times of less than 80 minutes in all cases (entries 2-6).¹⁰⁶



Scheme 87. Aza-Diels Alder reaction between imines **204a-f** and Danishefsky's diene **205**, catalysed by **195a**

Table 40

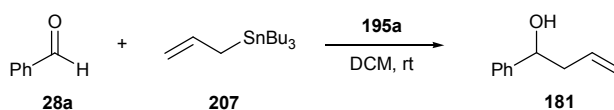
Entry	Product	R ¹	R ²	Time /min	Isolated Yield /%
1	206a	Ph	Bn	45	73
2	206b	2-naphthyl	Bn	40	71
3	206c	3,5-MeO(C ₆ H ₃)	Bn	70	60
4	206d	cyclohexyl	Bn	45	56
5	206e	Ph	^t Pr	60	72
6	206f	Ph	3,5-MeO(C ₆ H ₃)CH ₂	80	62

The success of titanium complex **195a** in catalysing the *aza*-Diels Alder reaction led to the screening of **195a** in a variety of other transformations, namely:

- Allylation of benzaldehyde
- Diethylzinc addition to benzaldehyde
- A conventional Diels Alder reaction
- An aldol reaction

Allylation of Benzaldehyde catalysed by **195a**

The allylation of benzaldehyde **28a** with allyltributyltin **207**, in the presence of **195a**, was also attempted (Scheme 88, Table 41). When 50mol % of the catalyst was employed, the reaction went to completion after only 30 minutes, with 1-phenylbut-3-en-1-ol **181** obtained in 75% yield (entry 1). Furthermore, when the catalyst loading was dropped to only 5mol % the product **181** was obtained in 64% yield after 4 hours (entry 2).



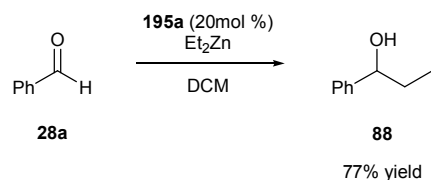
Scheme 88. Allylation of benzaldehyde **28a** with allyltributyltin **207** catalysed by **195a**

Table 41

Entry	Catalyst loading /mol %	Time	Isolated yield /%
1	50	30 min	75
2	5	4 h	64

Diethylzinc Addition to Benzaldehyde catalysed by 195a

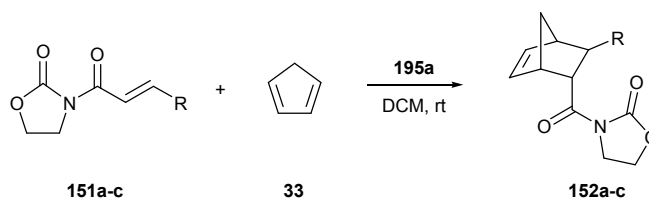
The addition of diethylzinc to benzaldehyde **28a** was also investigated. Treatment of a solution of **195a** with diethyl zinc at room temperature followed by benzaldehyde **28a** at 0 °C resulted in the formation of the crude product after 6 hours. Following column chromatography, 1-phenyl propanol **88** was isolated in 77% yield (**Scheme 89**).



Scheme 89. Diethylzinc addition to benzaldehyde **28a** catalysed by **195a**

Conventional Diels Alder Reaction catalysed by 195a

Initially, the conventional Diels Alder between *N*-acryloyloxazolidin-2-one **151a** and cyclopentadiene **33** was investigated (**Scheme 90**, **Table 42**). It was discovered that in the presence of only 5mol % of catalyst **195a**, 3-(bicyclo[2.2.1]hept-2-enecarbonyl) oxazolidin-2-one **152a** was obtained in 81% yield with an *endo:exo* selectivity of >97:3 (entry 1). However, application of these optimised conditions to other *N*-acryloyloxazolidin-2-ones **151b** and **151c** gave the desired products in substantially lower yields. Instead, conditions had to be optimised for each dienophile. For example, with (*E*)-*N*-but-2-enoyloxazolidin-2-one **151b** and cyclopentadiene **33**, a catalyst loading of 20mol % was found to give the product **152b** in 87% yield and 87:13 diastereoselectivity (entry 2). In comparison, *N*-((*E*)-3-phenyl-acryloyl)oxazolidin-2-one **151c** required one equivalent of catalyst and a reaction time of 6 hours to achieve 100% conversion, with the desired product **152c** isolated in 81% yield (entry 3).



Scheme 90. Diels Alder between *N*-acryloyl-oxazolidin-2-ones **151a-c** and cyclopentadiene **33** catalysed by **195a**

Table 42

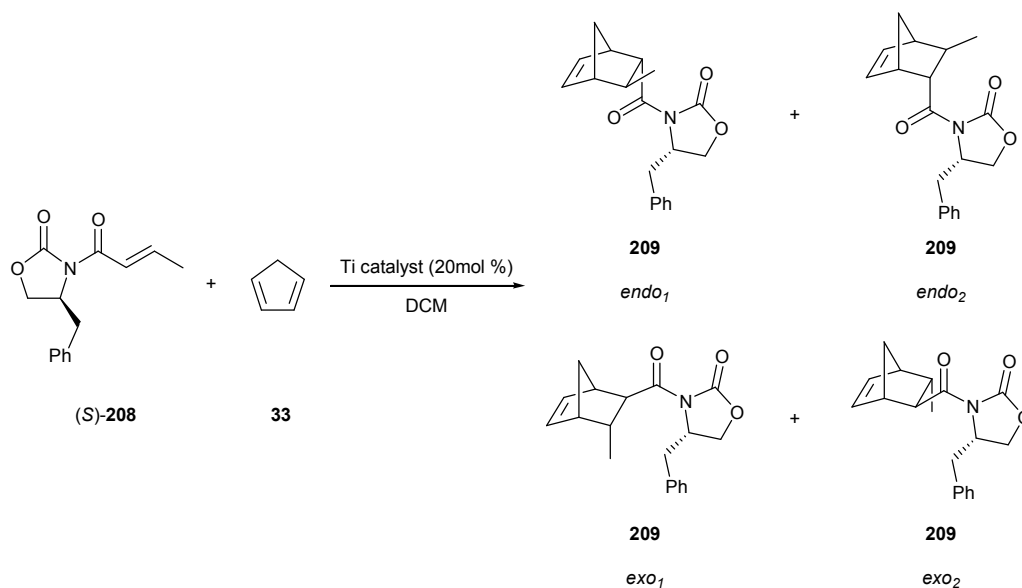
Entry	Product	R	Catalyst /mol %	Time /h	Yield /%	endo:exo
1	152a	H	5	0.5	81	>97:3
2	152b	Me	20	3	87	87:13
3	152c	Ph	100	6	81	84:16

Following the good diastereoselectivities obtained with *N*-acryloyloxazolidin-2-ones **151a-c**, the chiral Diels Alder reaction between dienophile (*S*)-**208** and cyclopentadiene **33** was also investigated in the hope that a higher diastereoselectivity would be induced (Scheme 91, Table 43).

Initially, the reaction was performed in the presence of chlorotitanium tri-*iso*-propoxide and the titanium complex generated *in situ* from 2,4-dimethylphenol and titanium (IV) chloride, to give a benchmark against which the performance of complex **195a** could be compared. The reaction catalysed by chlorotitanium tri-*is*-propoxide gave the product **209** in 84% yield and an *endo:exo* ratio of 79:21. Analysis of the product revealed that a total of three diastereoisomers were observed in a ratio of 77:21:2 (*endo*₁:*exo*₁:*endo*₂), with the major product being the *endo* product, which was obtained in 96% de (Table 43, entry 1). The catalyst derived from TiCl₄ and 2,4-dimethylphenol was found to be more reactive, affording the bicyclic product **209** in 74% yield after only 2 hours, although with a lower *endo:exo* ratio (72:28). This time four diastereomers were observed in a ratio of 70:16:2:12 (*endo*₁:*exo*₁:*endo*₂:*exo*₂), with the major *endo* product obtained in 93% de (entry 2). The presence of the fourth diastereomer (*exo*₂) implied that the flexible orientation of the phenolate ligands may have an effect on the coordination sphere around the titanium, and therefore the diastereoselectivity.

In comparison, when (*S*)-4-benzyl-*N*-but-enoyloxazolidin-2-one **208** was treated cyclopentadiene **33**, in the presence of 20mol % of catalyst **195a**, the bicyclic product **209** was obtained in an excellent 97% yield after 3 hours (Table 43, entry 3). Analysis of the product revealed that the major product had been obtained in an improved *endo:exo* ratio of 89:11. Only three diastereomers were observed in a ratio 88:11:1 (*endo*₁:*exo*₁:*endo*₂), which indicated that there was an improved interaction between the rigid phenolate framework of **195a** and the titanium's coordination

sphere when compared to the tris(2,4-dimethylphenolate) titanium complex formed *in situ* (entry 3 compared to entry 2).



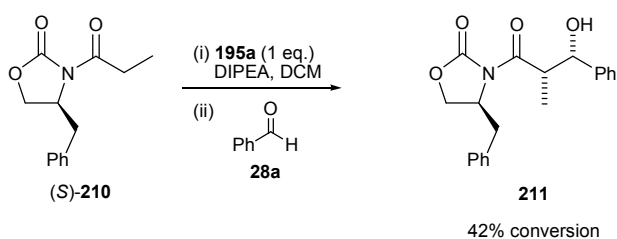
Scheme 91. Diels Alder reaction between (*S*)-4-benzyl-*N*-but-2-enoyloxazolidin-2-one **208** and cyclopentadiene **33**

Table 43

Entry	Catalyst	Time /h	Yield /%	endo:exo	endo-209 de /%
1	TiCl(O ^{<i>i</i>} Pr) ₃	24	84	79:21	96
2	2,4-Me(C ₆ H ₃)OH TiCl ₄	2	74	72:28	93
3	195a	3	97	89:11	98

Aldol Reaction catalysed by **195a**

The aldol reaction between the titanium enolate of (*S*)-**210**, generated *via* treatment of (*S*)-4-benzyl-3-propionyl-oxazolidin-2-one **210** with DIPEA and one equivalent of **195a**, with benzaldehyde **28a** was performed. After 24 hours the desired *syn*-product **211** was obtained in 42% conversion.



Scheme 92. Aldol reaction catalysed by **195a**

Given the number of organic transformations that titanium complexes of amine tris(phenolate) ligands have successfully shown to catalyse, the synthesis of a chiral triphenolate ligand was decided to be attempted.

2.2 DESIGN OF A CHIRAL AMINE TRIS(PHENOLATE) LIGAND

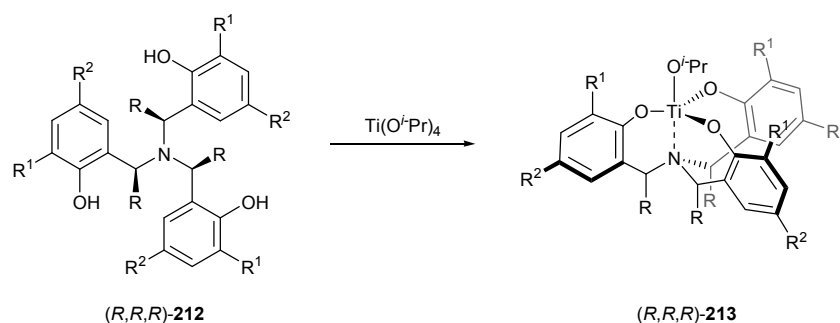
It has been shown that complexation of the achiral amine tris(phenolate) ligand to a five-coordinate metal centre gives rise to a racemic mixture of (*P*)- and (*M*)-enantiomers, owing to the propeller-like chirality of the complex formed (**Figure 43**). In the case of the titanium complexes, the barrier to invert is quite high and can be visualised on the NMR time-scale. For the titanium complexes **194b** and **194c**, the barrier for inversion was found to be $\Delta G^\ddagger_{(350\text{ K})} = 65.7\text{ kJ mol}^{-1}$ for **194b**, and $\Delta G^\ddagger_{(386\text{ K})} = 74.4\text{ kJ mol}^{-1}$ for the bulkier **194c**.¹⁰⁴ Given the relatively small difference in activation energy between two ligands that differ so much in steric bulk it was proposed that concerted inversion of the three aryl rings was responsible for the high barrier of inversion for these complexes.¹⁰⁴



Figure 43. (*P*)- and (*M*)-enantiomers of a five-coordinate metal complex of tetradentate ligand **182**

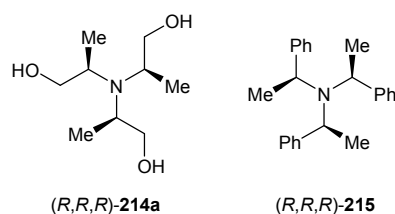
2.2.1 Novel C_3 -Symmetric Amine Tris(phenolate) Ligands

It was therefore proposed that if a chiral C_3 -symmetric version of amine tris(phenolate) ligand, such as (*R,R,R*)-**212**, could be synthesised then this would result in chiral metal complexes with a locked propeller-like conformation due to its R groups adopting a pseudoaxial conformation. Furthermore, locking of the propeller-like chirality on the underside of the complex would result in its point chirality being effectively relayed into the coordination sphere of the metal centre, through the *ortho*-substituents (R^1) of the phenolate rings (**Scheme 93**).



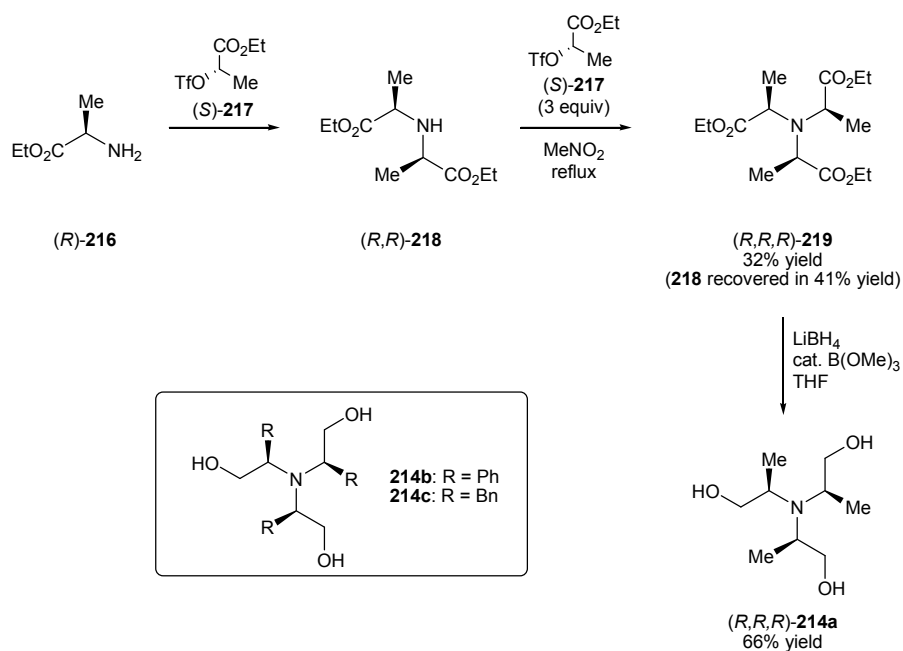
Scheme 93. Proposed formation of C_3 -symmetric complex (R,R,R) -**213**

The preparation of a ligand such as (R,R,R) -**212**, in particular the stereoselective formation of the three benzylic centres, would be difficult without recourse to a lengthy multi-step synthesis. Only a few examples of the synthesis of C_3 -symmetrical amines with chiral centres adjacent to the nitrogen atom are known. Two such examples are the homochiral triethanolamine (R,R,R) -**214a** of Van Vranken and co-workers,¹³¹ and (R,R,R) -tris(α -methylbenzyl)amine **215** of Wyatt and co-workers.¹³²



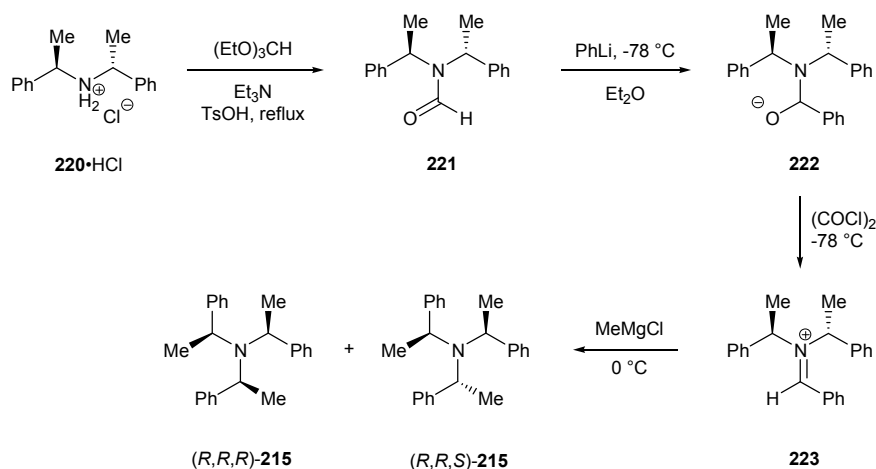
Scheme 94. Triethanolamine (R,R,R) -**214a** and (R,R,R) -tris(α -methylbenzyl)amine **215**

The synthesis of triethanolamine (R,R,R) -**214a** was accomplished in 3 steps from (R)-alanine ethyl ester **216** via bisalkylation with the triflate ester of (S)-ethyl lactate **217** (Scheme 95).¹³¹ Whilst the first alkylation proceeded smoothly, the second alkylation was much slower. Reaction of the dialkylamine (R,R) -**218** with three equivalents of (S)-**217** in refluxing nitromethane gave triamine **219** in 32% yield. The triester **219** was reduced to **214a** using lithium borohydride with 10mol % of trimethylborate in 66% yield. Overall triethanolamine (R,R,R) -**214a** was obtained in 21% yield from **216**. However, attempts to synthesise the corresponding triphenyl and tribenzyl analogues, **214b** and **214c**, were unsuccessful due to a competing elimination reaction in the alkylation step.



Scheme 95. Synthesis of triethanolamine (R,R,R) -**214a**

Wyatt and co-workers synthesis of (R,R,R) -tris(α -methylbenzyl)amine **215** started from the commercially available C_2 -symmetric amine **220** (**Scheme 96**).¹³² Initially **220** was converted into its formamide **221** *via* treatment with trimethyl orthoformate. Addition of phenyl lithium gave **222**, which was then converted into the presumed iminium species **223** with oxalyl chloride. After addition of MeMgCl, the amine (R,R,R) -**215** was obtained together with its diastereomer (R,R,S) -**215** in a 4:1 ratio in favour of the C_3 -symmetrical amine. The desired amine proved to be remarkably crystalline, making the separation from the mixture with the C_1 -symmetric diastereomer relatively facile. With this protocol, (R,R,R) -tris(α -methylbenzyl)amine **215** was obtained in an overall yield of 70% from **220**.

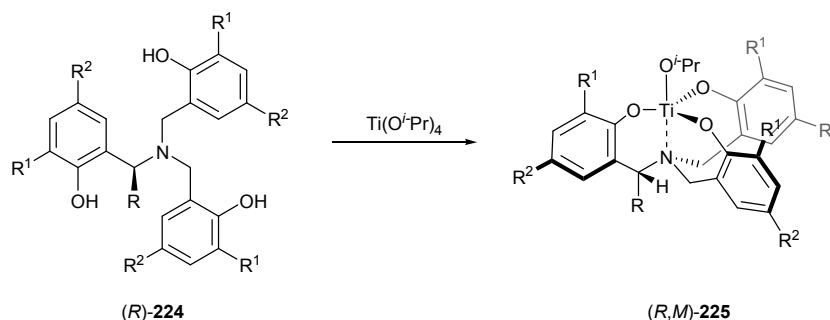


Scheme 96. Synthesis of (R,R,R) -tris(α -methylbenzyl)amine **215**

Whilst both these syntheses are impressive, they both produce relatively unfunctionalised compounds when compared to a C_3 -symmetric amine tris(phenolate) ligand such as (*R,R,R*)-**212**. Also both approaches rely on the use of commercially available chiral starting materials, something which would not be available for the synthesis of (*R,R,R*)-**212**.

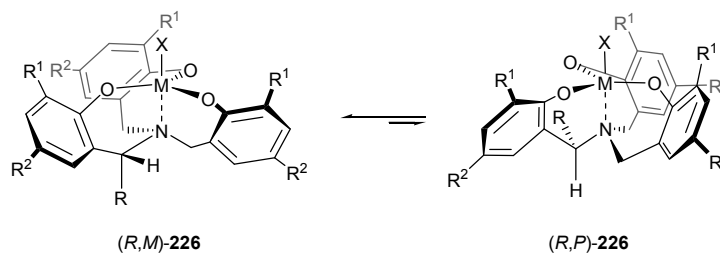
2.2.2 Pseudo- C_3 -Symmetric Ligands

Given the potential difficulties faced synthesising the C_3 -symmetric amine tris(phenolate) ligand, an alternative target was required, one in which the desired ligand could be obtained in as few a steps as possible. Consequently, it was proposed that a pseudo- C_3 -symmetric ligand such as (*R*)-**224**, which possesses only a single stereogenic centre on one of the benzylic arms, would serve equally well to control the propeller chirality of a metal derived complex (**Scheme 97**).



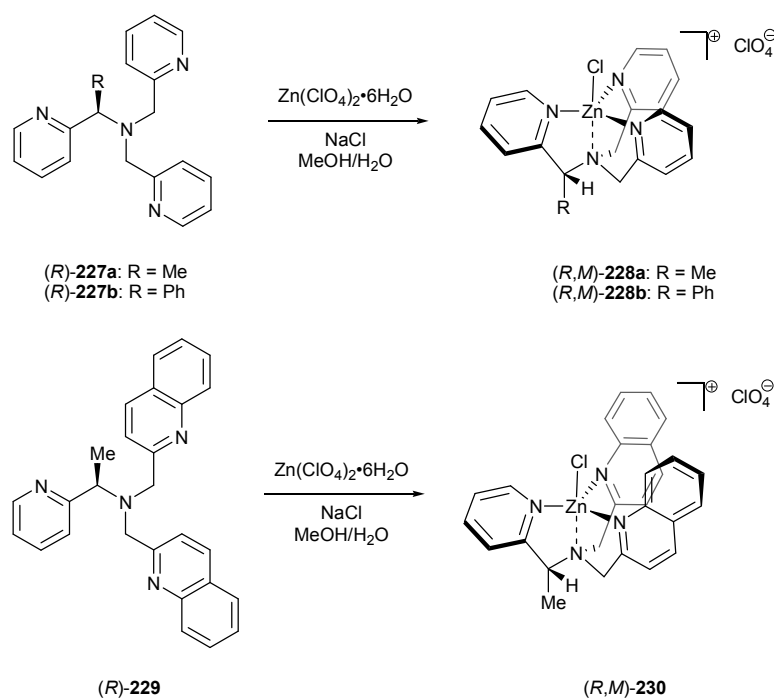
Scheme 97. Proposed formation of pseudo- C_3 -symmetric complex (*R,M*)-**225**

The complexation of amine tris(phenolate) ligand (*R*)-**224** to a five coordinate metal centre would result in a chiral metal central (*R,M*)-**226** whose helical chirality would be controlled by its stereogenic α -group adopting a pseudoaxial conformation. This diastereoisomer would occur preferentially because formation of the corresponding diastereoisomer (*R,P*)-**226** would be disfavoured by *syn*-pentane-like interactions between the pseudoequatorial α -group and its proximal aryl ring (**Scheme 98**).



Scheme 98. (*R,M*)-**226** and (*R,P*)-**226** diastereoisomers of a five-coordinate metal complex of tetradentate ligand (*R*)-**224**

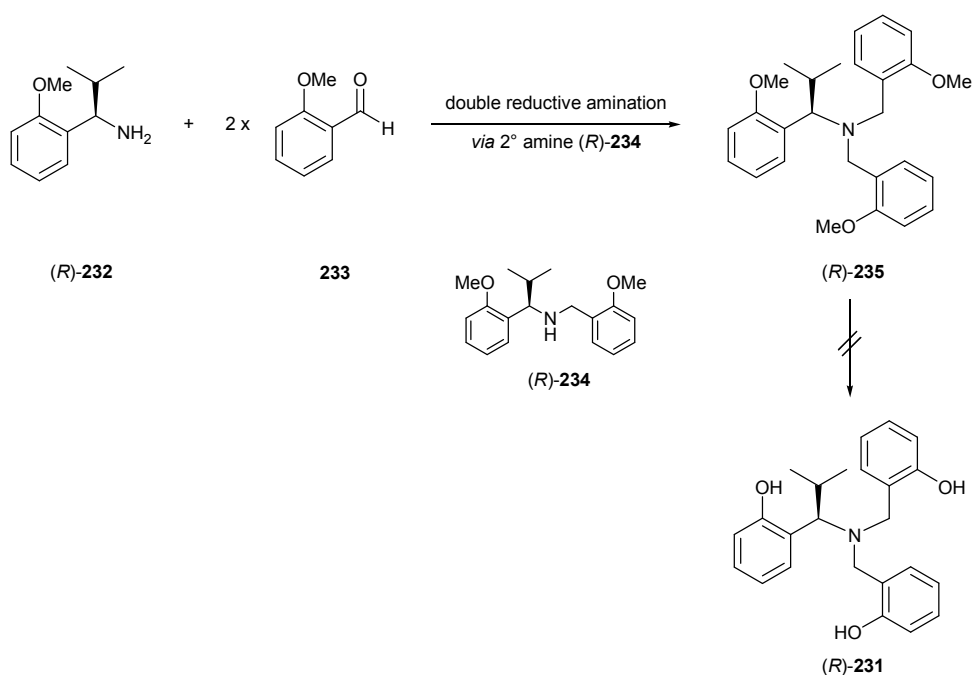
Although examples of this type of conformational control are rare, precedent did exist for control of helical chirality using point chirality within metal-ligand complexes. For example, the use of a single stereogenic centre to dictate the propeller-type chirality metal complexes had been demonstrated previously by Canary *et al.*^{133, 134} The authors showed that when a series of chiral pyridyl ligands **227a-b** and **229** were coordinated to zinc(II) the resultant penta-coordinate complex was found to have a distorted trigonal bipyramidal geometry with the pyridyl nitrogens coordinated in the equatorial positions and the tertiary amine nitrogen in an axial position (**Scheme 99**). Furthermore, it was shown that the α -substituent controlled the propeller-like twist of all three pyridyl rings, by occupying the lowest energy pseudo-axial conformer. It was shown that use of the (*R*)-enantiomer formed a complex exclusively with *M*-symmetry. Similarly, the use of the (*S*)-enantiomer delivered a complex with *P*-symmetry. The authors found that the magnitude of the tilt (as defined by the angle between the planes containing the pyridine rings and the N_{am}-Zn-Cl axis in the crystal structures) ranged between 8.3° for complex **228a**, to 12.3° for complex **228b** and 15.9° for complex **230**, although the authors proposed that much of the difference in magnitude was probably due to crystal packing forces rather than the steric differences between the complexes. To date these complexes have not been applied as catalysts for asymmetric transformations.



Scheme 99. Formation of zinc complexes **228a-b** and **230** from the corresponding pseudo- C_3 -symmetric amines **227a-b** and **229**

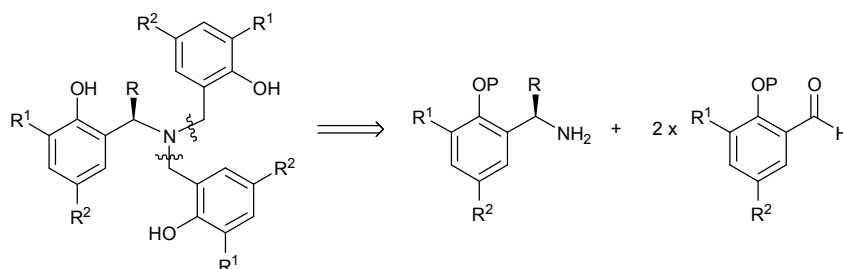
2.3 PREVIOUS WORK WITHIN THE GROUP-ATTEMPTED SYNTHESIS OF CHIRAL LIGAND (R)-231

An attempted synthesis of pseudo- C_3 -symmetric ligand (R)-**231** was first carried out by a former member of the SDB group.¹³⁰ Initial work focussed on the synthesis of ligand (R)-**231**, which bears no *ortho* or *para* substituents on the phenolate moiety, due to the commercial availability of the key starting material 2-methoxybenzaldehyde **233**. The attempted synthesis is highlighted in **Scheme 100**. The chiral ligand precursor (R)-**235** was successfully synthesised from the chiral primary amine (R)-**232** via a double reductive amination strategy with the secondary amine (R)-**234** as the intermediate. However, cleavage of the methyl aryl ethers of (R)-**235** proved unsuccessful, with numerous different demethylation strategies employed. Under most conditions screened, competitive cleavage of the benzylic C-N bond was observed.



Scheme 100. Attempted synthesis of chiral ligand (*R*)-**231**

Since the work in synthesising the ligand precursor (*R*)-**235** had been shown to be robust, it was decided that any new strategy to generate chiral ligands like (*R*)-**231** should follow a similar route with the selection of a more suitable protecting group being the only alteration required (**Scheme 101**).

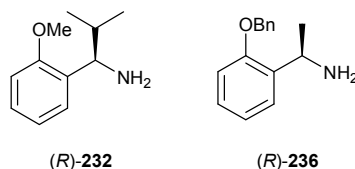


Scheme 101. Retro-synthesis analysis of pseudo- C_3 -symmetric amine

It was considered that a benzyl protecting group might be a more suitable protecting group because like methyl ethers, benzyl ethers are robust and stable to a wide range of aqueous acidic and basic conditions, and are not readily attacked by metal hydride reducing agents or mild oxidising agents.¹³⁵ However, unlike methyl ethers they can be easily deprotected under relatively mild hydrogenolysis conditions, thus avoiding the problems encountered with Lewis acids.

2.4 WORK TOWARDS THE SYNTHESIS OF (*R*)-232 AND (*R*)-236

Initially, as an introduction into the chemistry, work was focussed towards the synthesis of chiral primary amine (*R*)-232 and the related benzyl protected amine (*R*)-236 (Scheme 102). This was to ensure that the introduction of the benzyl protecting group would not impede the synthesis of the chiral amines.

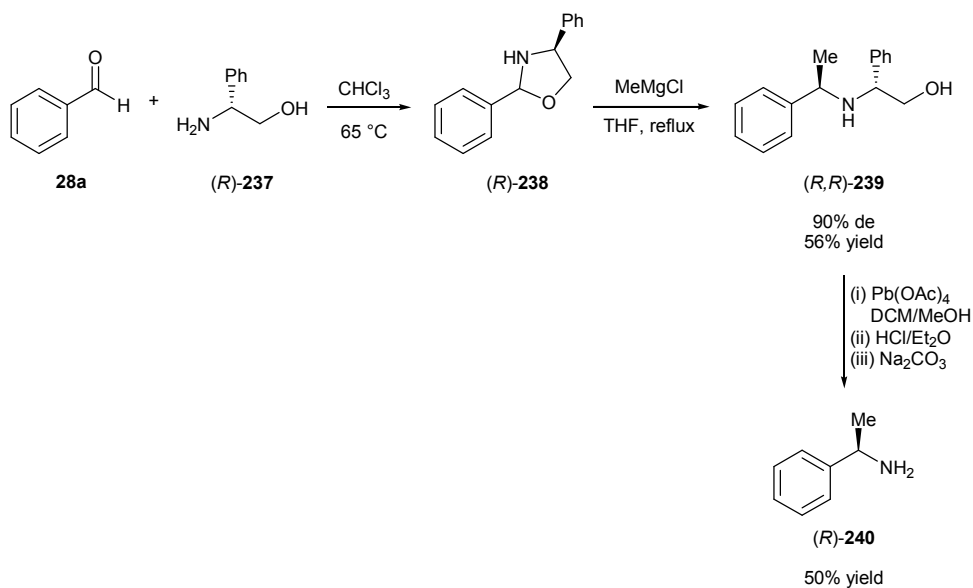


Scheme 102. Chiral primary amines (*R*)-232 and (*R*)-236

Given the previous efforts within the group, it was envisioned that the synthesis of primary amine (*R*)-232 and (*R*)-236 could be achieved by a diastereoselective alkylation of chiral imine precursors

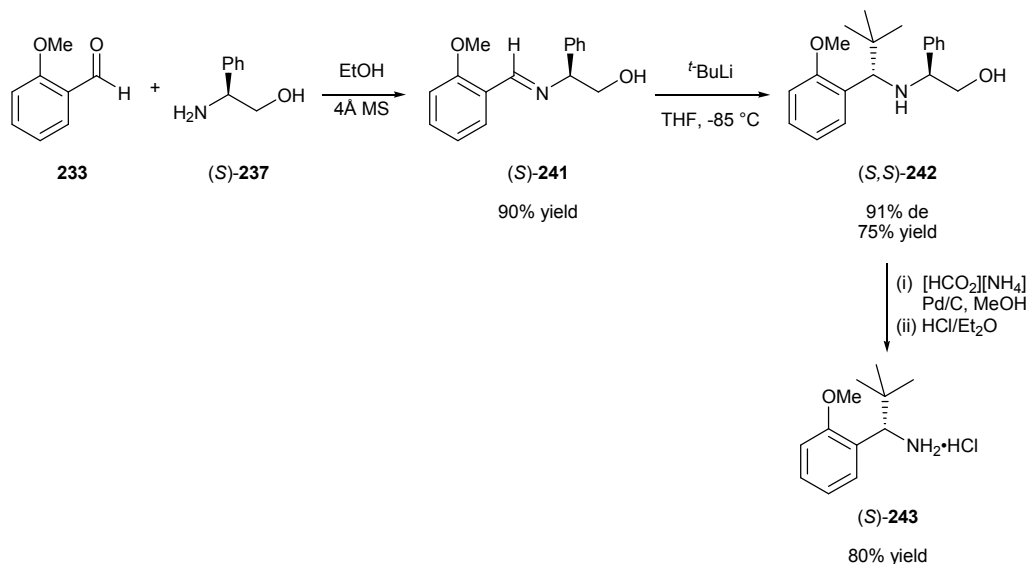
2.4.1 Literature Precedent

In the literature there are a number of reports of the synthesis of chiral amines using (*S*)- and (*R*)-2-amino-2-phenylethanol **237** as a chiral auxiliary.¹³⁶⁻¹⁴¹ For example in 1991, Pridgen *et al.* showed that addition of methyl magnesium chloride to the oxazolidine **238**, formed by condensation of benzaldehyde **28a** and (*R*)-2-amino-2-phenylethanol **237**, gave (*R,R*)-**239** in 56% yield and 90% de.¹⁴¹ This was then deprotected using lead (IV) acetate, followed by acid hydrolysis to give primary amine (*R*)-**240** in 50% yield (Scheme 103).



Scheme 103. Addition of methyl magnesium chloride to oxazolidine **(R)-238**

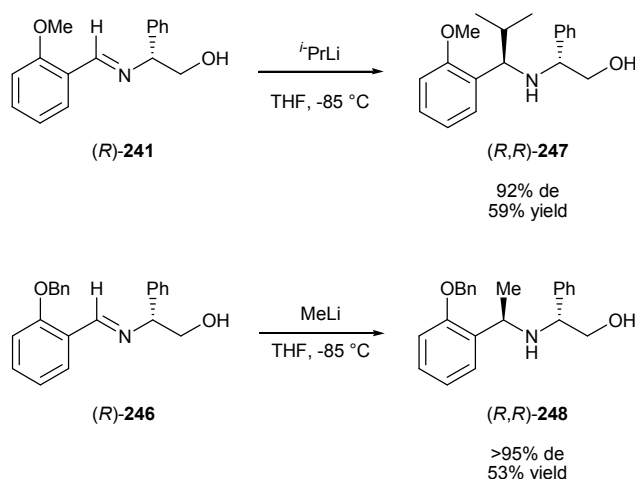
In 2000, Kündig and co-workers showed that the structurally related chiral amine **(S)-243** could be obtained in a similar manner (**Scheme 104**).¹³⁹ This involved formation of imine **(S)-241** from **(S)-2-amino-2-phenylethanol 237** and 2-methoxybenzaldehyde **233**, followed by addition of *tert*-butyl lithium at $-85\text{ }^\circ\text{C}$ to yield the secondary amine **(S,S)-242** in 91% de and 75% yield after chromatography. This time cleavage was achieved with palladium on carbon and ammonium formate giving amine **(S)-243** in 80% yield.



Scheme 104. Addition of *tert*-butyl lithium to chiral imine **(S)-241**

2.4.4 Addition of Alkyl Lithium to Imines (*R*)-**241** and (*R*)-**246**

Since both *iso*-propyl lithium and methyl lithium were available in the laboratory it was decided to test both in the addition to imines (*R*)-**241** and (*R*)-**246**, with *iso*-propyl lithium added to (*R*)-**241** and methyl lithium added to (*R*)-**246**. For imine (*R*)-**241**, after addition of an excess of *iso*-propyl lithium the reaction was stirred at -85 °C for 6 hours before being allowed to slowly warm to room temperature overnight. After column chromatography, the product (*R*)-2-((*R*)-1-(2-methoxyphenyl)-2-methylpropylamino)-2-phenylethanol **247** was isolated in 92% de and 59% yield. The structure of the product was confirmed by ¹H NMR spectroscopy, which indicated the presence of the *iso*-propyl group, with two doublets at $\delta = 1.13$ ppm and $\delta = 0.73$ ppm corresponding to the methyl groups and a multiplet at $\delta = 2.00$ ppm for the methine proton. It is noteworthy that the two diastereotopic methyl groups are split by 0.40 ppm indicating that the compound has a relatively rigid structure with one of the methyl groups shielded by the anisotropic effect of one of the aryl groups. Following a similar protocol for the addition of methyl lithium to imine (*R*)-**246** the product (*R,R*)-**248** could be obtained in 53% yield. The presence of the methyl group was indicated by the doublet at $\delta = 1.23$ ppm. The diastereomeric excess was determined to be >95% with no signals corresponding to the minor diastereomer observed when the ¹H NMR was run in either CDCl₃ or C₆D₆.



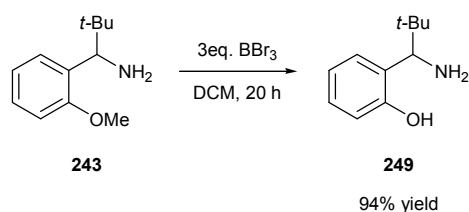
Scheme 107. Addition of *iso*-propyl lithium and methyl lithium to imines (*R*)-**241** and (*R*)-**246**

Having demonstrated that the presence of the benzyl group did not have any detrimental effect on addition of alkyl lithium to the chiral imine (*R*)-**246**, it was

decided to turn efforts towards the synthesis of a ligand bearing an *ortho* substituent on the phenolate ring. As mentioned earlier, in order for there to be effective transfer of the propeller-like chirality of a propeller ligand within a metal complex there needs to be an *ortho* substituent on the aryl ring. However, before attempting synthesis of this type of ligand it was decided to test the relative ease of deprotection of each protecting group of the secondary amines (*R,R*)-**247** and (*R,R*)-**248**.

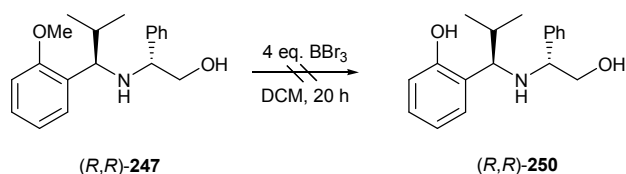
2.4.5 Attempted Cleavage of Methyl Aryl Ether of Amine (*R,R*)-**247**

In 2000, Kündig *et al.* reported the cleavage of methyl aryl ether **243** using boron tribromide in dichloromethane to give amine **249** in 94% yield after 20 hours (**Scheme 108**).¹³⁹ As a consequence it was decided to test these conditions on amine (*R,R*)-**247**.



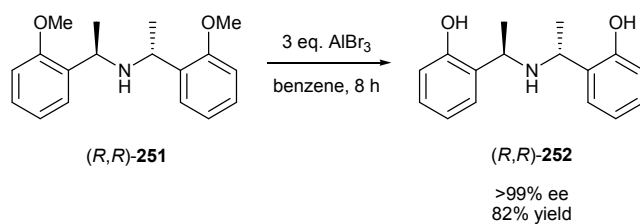
Scheme 108. Demethylation of amine **243** using boron tribromide

Following treatment of amine (*R,R*)-**247** with boron tribromide for 20 hours the reaction was worked up and the crude product was analysed by ¹H NMR spectroscopy. This revealed that no product had formed, with only the starting amine (*R,R*)-**247** present in the mixture (**Scheme 109**).



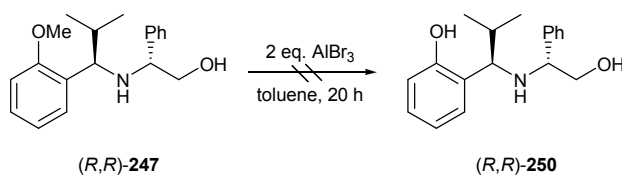
Scheme 109. Attempted demethylation of amine (*R,R*)-**247** with boron tribromide

Similarly, in another publication Kündig and co-workers had reported demethylation of the secondary amine (*R,R*)-**251** using aluminium tribromide in benzene, to give the product (*R,R*)-**252** in 82% yield and >99% ee after eight hours (**Scheme 110**).¹⁴² The authors had noted that the use of boron tribromide in this transformation resulted in the competitive cleavage of the benzylic C-N bond.



Scheme 110. Demethylation of amine (R,R) -**251** using aluminium tribromide

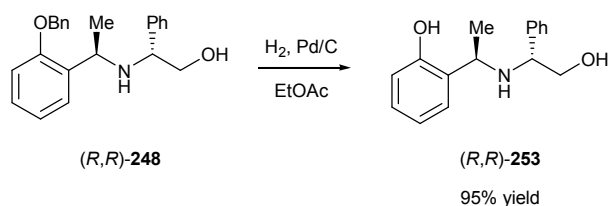
In an attempt to apply these conditions, secondary amine (R,R) -**247** was treated with two equivalents of aluminium tribromide in toluene for 20 hours. Disappointingly, under these conditions again no product was formed with only starting amine (R,R) -**247** recovered (**Scheme 111**).



Scheme 111. Attempted demethylation of amine (R,R) -**247** with aluminium tribromide

2.4.6 Successful Cleavage of Benzyl Aryl Ether of Amine (R,R) -**248**

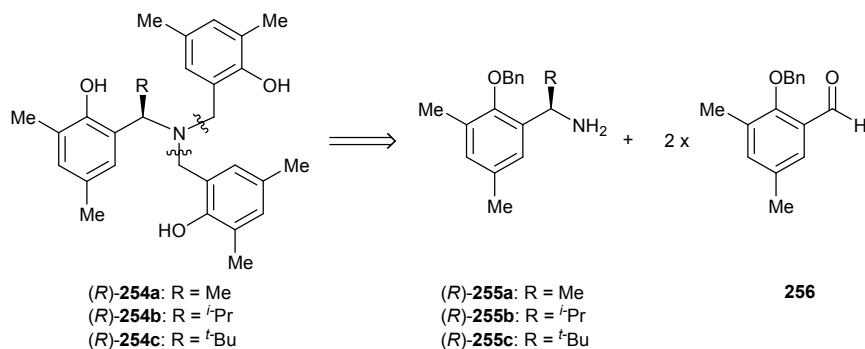
Given the lack of success at cleaving the methyl aryl ether of secondary amine (R,R) -**247**, attention was instead turned to the analogous benzyl protected amine (R,R) -**248**. Cleavage of the benzyl group was achieved by hydrogenolysis; amine (R,R) -**248** together with 10% palladium on carbon in ethyl acetate were stirred vigorously under one atmosphere of hydrogen for 24 hours, after which time the desired product (R,R) -**253** was isolated in 95% yield (**Scheme 112**). Analysis by ^1H NMR spectroscopy showed that the benzylic protons in the starting material (which appeared as doublets at $\delta = 4.46$ ppm and $\delta = 4.40$ ppm) were no longer present in the product. High resolution mass spectrometry identified the molecular mass of $[\text{M}+\text{H}]^+$ as 258.1491 ($\text{C}_{16}\text{H}_{20}\text{NO}_2$ requires 258.1489). In the low resolution spectrum there were signals at 258 for the molecular ion and at 138 corresponding to the molecular ion with loss of the 2-phenylethanol unit.



Scheme 112. Cleavage of benzyl protecting group on amine (R,R)-248

2.5 SYNTHESIS OF CHIRAL AMINES (R)-255A-C

Having determined that benzyl ethers would be a suitable protecting group, the focus of the project was directed towards the synthesis of the chiral ligands (R)-254a-c, which possessed *ortho*- and *para*-methyl groups on the aryl rings (Scheme 113). Whilst an α -methyl group at the benzylic position had been shown to be sufficiently sterically encumbering to control the gait of the propeller in 5-membered zinc complexes of Canary *et al.* (see Section 2.2.2) it was uncertain if this would be the case in our 6-member metalocycles. Therefore a series of ligands with different α -substituents would need to be synthesised. Given the commercial availability of solutions of methyl lithium, *iso*-propyl lithium and *tert*-butyl lithium and the steric differences that these groups would provide, the synthesis of the primary amines (R)-255a-c was undertaken.

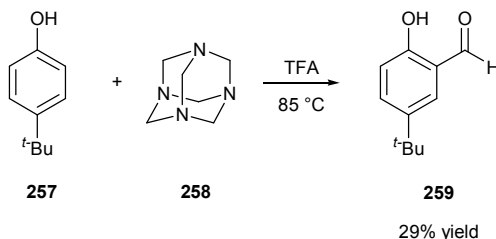


Scheme 113. Retrosynthetic analysis of ligands (R)-254a-c

2.5.1 Preparation of Aldehyde 261

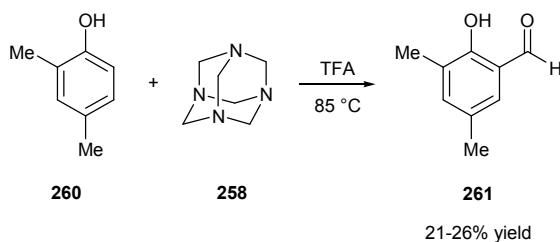
In order to synthesis chiral ligands (R)-255a-c it was necessary to prepare 2-hydroxy-3,5-dimethylbenzaldehyde 256 from commercially available 2,4-dimethylphenol 260. The method chosen was a modification of the Duff reaction reported by Svenstrup and co-workers in 1998.¹⁴³ They had shown that monoformylation of 4-*tert*-butylphenol 257 could be achieved using one equivalent

of hexamethylenetetramine **258** in refluxing trifluoroacetic acid to give 4-*tert*-butyl-2-hydroxybenzaldehyde **259** in 29% yield. Whilst the yield of this transformation was modest, the relative inexpense of the starting materials meant scale-up of this method should produce sufficient quantities of the desired aldehyde.



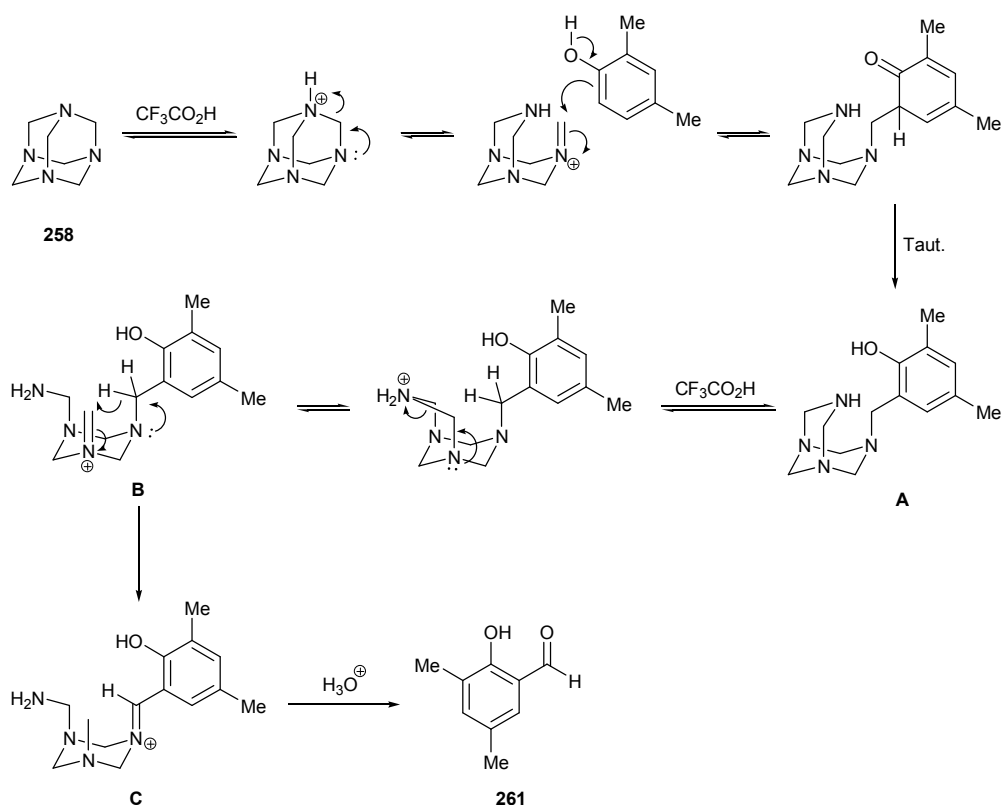
Scheme 114. Monoformylation of 4-*tert*-butylphenol **257** with hexamethylenetetramine **258** in TFA

Thus, the reaction of 2,4-dimethylphenol **260** under these conditions yielded 2-hydroxy-3,5-dimethylbenzaldehyde **261** in 21-26% yield. With this reaction it was easily possible to synthesise *ca.* 2-3 grams of aldehyde at a time.



Scheme 115. Synthesis of 2-hydroxy-3,5-dimethylbenzaldehyde **261** from 2,4-dimethylphenol **260**

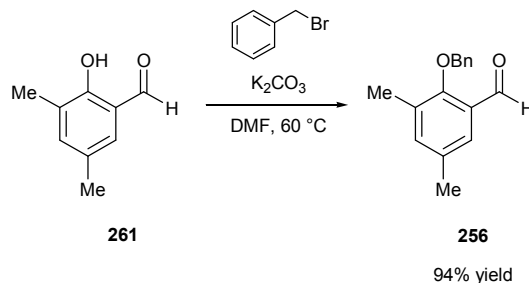
A proposed mechanism of the Duff reaction under these conditions is shown in **Scheme 116**.¹⁴⁴ Initially, hexamethylenetetramine **258** is protonated and then decomposes to form the iminium species. 2,4-Dimethylphenol then adds to the iminium ion followed by tautomerisation, resulting in aryl amine **A**. A similar protonation/decomposition of aryl amine **A** forms the iminium species **B**. The iminium ion abstracts a hydrogen from the aryl amine moiety in **B** to form iminium species **C**. Acid hydrolysis of this releases the product **261**.



Scheme 116. Proposed mechanism of the modified Duff reaction

2.5.2 Synthesis of Benzyl Protected Aldehyde **256**

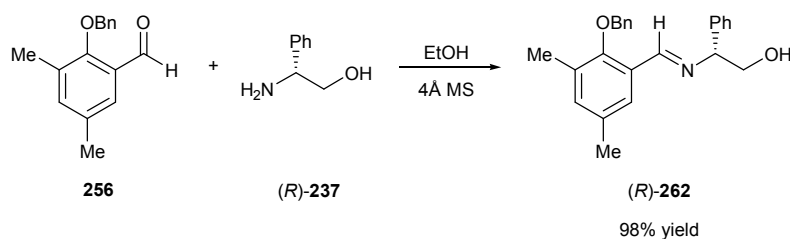
The conversion of 2-hydroxy-3,5-dimethylbenzaldehyde **261** to 2-(benzyloxy)-3,5-dimethylbenzaldehyde **256** was accomplished by reacting **261** with one equivalent of benzyl bromide and excess potassium carbonate in *N,N*-dimethylformamide at 60 °C for 24 hours. The desired product was isolated in 94% yield and its structure was confirmed by analysis of the ^1H NMR spectrum with the benzylic protons appearing as a singlet at $\delta = 4.94$ ppm.



Scheme 117. Formation of aldehyde **256**

2.5.3 Formation of Imine (*R*)-**262**

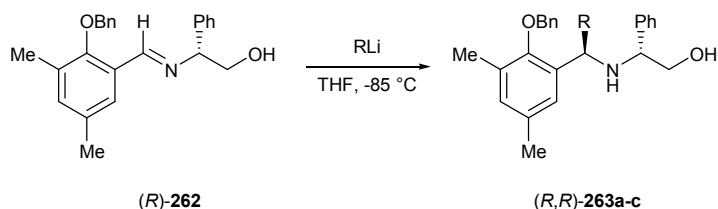
The formation of imine (*R*)-**262** from the dehydration of 2-(benzyloxy)-3,5-dimethylbenzaldehyde **256** with (*R*)-2-amino-2-phenylethanol **237** proceeded in 98% yield. The imine (*R*)-**262** was detected by the presence of a singlet at $\delta = 8.64$ ppm in its ^1H NMR spectrum.



Scheme 118. Formation of the imine (*R*)-**262** from the reaction of aldehyde **256** and (*R*)-2-amino-2-phenylethanol **237**

2.5.4 Diastereoselective Addition of Alkyl Lithium to Imine (*R*)-**262**

The addition of methyl lithium, *iso*-propyl lithium and *tert*-butyl lithium to imine (*R*)-**262** gave the corresponding amines (*R,R*)-**263a-c** (Scheme 119, Table 44). For both the addition of methyl lithium and *iso*-propyl lithium the product was isolated in good diastereomeric excess (94% and 91% de respectively, entries 1 and 2). However for the addition of *tert*-butyl lithium the diastereomeric excess of the isolated product dropped to 85%, which was not improved after repeated purification by column chromatography (entry 3). Given the lower de of amine **263c** it was decided not to take this substrate on through further synthesis.



Scheme 119. Diastereoselective addition of alkyl lithium to imine (*R*)-**262**

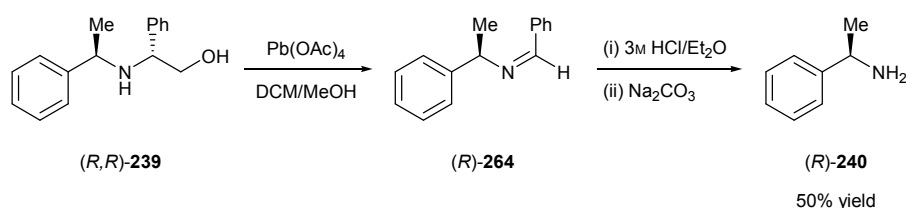
Table 44

Entry	R	Product	Yield /%	de ^a /%
1	Me	263a	49	94
2	^t Pr	263b	60	91
3	^t Bu	263c	55	85

^a Diastereomeric excess of products after column chromatography

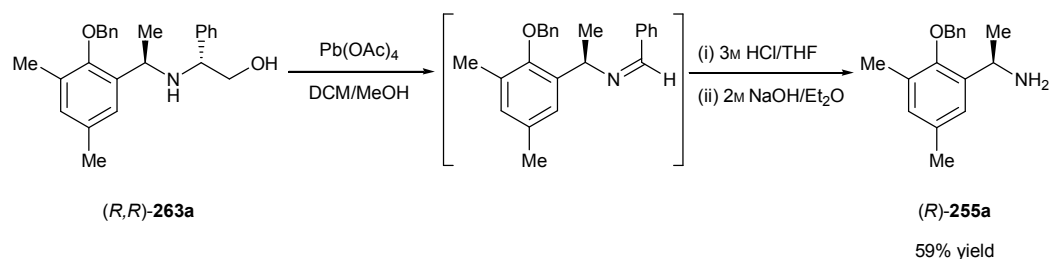
2.5.5 Oxidative Cleavage of Amines (*R,R*)-**263a** and (*R,R*)-**263b**

The cleavage of the 2-phenyl ethanol auxiliary with lead (IV) acetate had been shown to be an efficient and effective method to deliver chiral primary amines. For example, Pridgen and co-workers had shown that lead (IV) acetate followed by acid hydrolysis was successful in the deprotection of α -amino alcohol (*R,R*)-**239**.¹⁴¹ Treatment of (*R,R*)-**239** with lead (IV) acetate for 10 minutes, lead to the formation of imine (*R*)-**264**, which was immediately hydrolysed, without further purification, with 3M hydrochloric acid to yield (*R*)-1-phenylethylamine **240** in 50% yield (Scheme 120).



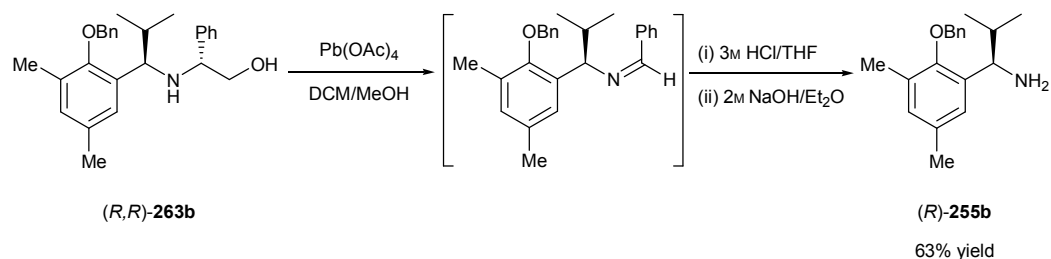
Scheme 120. Deprotection of (*R,R*)-**239** using lead (IV) acetate

The application of these conditions to secondary amine (*R,R*)-**263a**, resulted in the formation of amine (*R*)-**255a** in 59% yield. Its structure was confirmed by ¹H NMR spectroscopy which showed an absence of signals relating to the 2-phenyl ethanol auxiliary or the imine formed after the first step. Analysis of the IR spectrum revealed there to be two absorptances at 3367 and 3299 cm⁻¹ corresponding to the two primary amine N-H stretches.



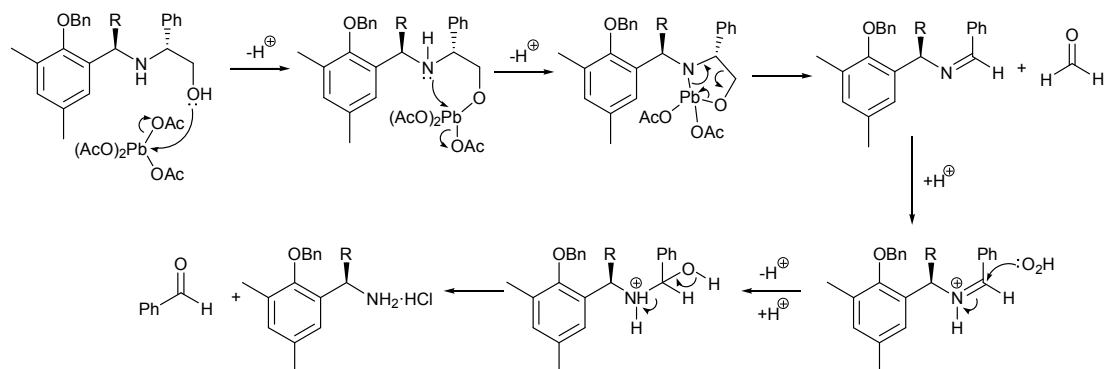
Scheme 121. Deprotection of amine (*R,R*)-**263a** using lead (IV) acetate

Similarly for amine (*R,R*)-**263b** treatment with lead (IV) acetate followed by acid hydrolysis yielded the amine (*R*)-**255b** in 63% yield. The ^1H NMR spectrum confirmed its structure, with the two methyl groups of the *iso*-propyl unit appearing as doublets at $\delta = 1.03$ ppm and $\delta = 0.83$ ppm. Again analysis of the IR spectrum confirmed the presence of the amine functionality with two stretch absorptances at 3376 and 3310 cm^{-1} .



Scheme 122. Deprotection of amine (*R,R*)-**263b** using lead (IV) acetate

The mechanism of the oxidative cleavage of α -amino alcohols **263a-b** is shown in **Scheme 123**. Initially, the lead (IV) acetate chelates to the alcohol and amine to form a 5-member cyclic intermediate which then undergoes elimination to afford the desired imine and formaldehyde. The imine is then hydrolysed by the hydrochloric acid to liberate the amine (as the hydrochloride salt) and benzaldehyde.

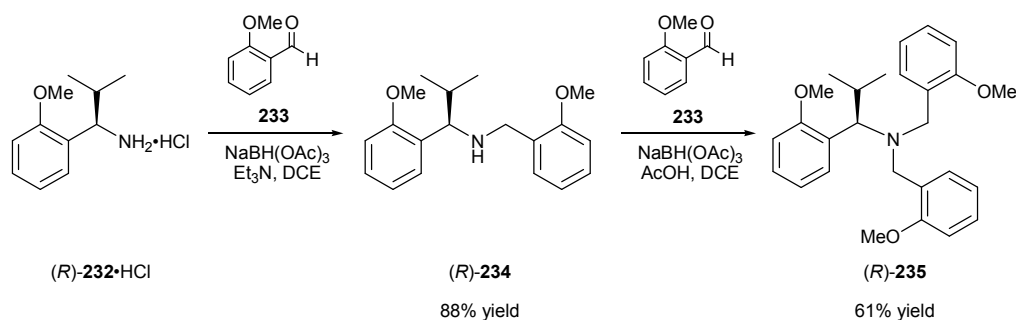


Scheme 123. Mechanism of the oxidative cleavage of α -amino alcohol (*R,R*)-**263a** or (*R,R*)-**263b** with lead (IV) acetate

2.6 SYNTHESIS OF CHIRAL LIGAND (R)-254A

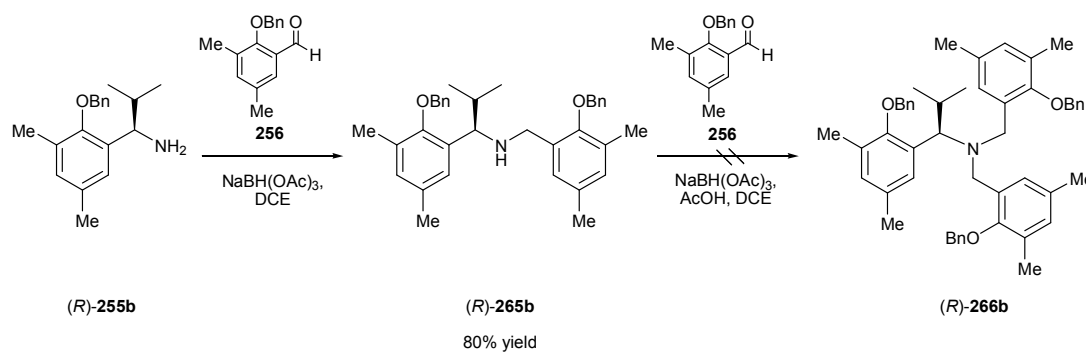
2.6.1 Attempted Formation of Amine (R)-266b via a Two Step Reductive Amination

Previous work within the SDB group had shown that tertiary amine (R)-235 could be synthesised from the primary amine (R)-232 via a two step reductive amination protocol. Treatment of amine (R)-232·HCl with triethylamine yielded the free base *in situ*, followed by addition of one equivalent of 2-methoxybenzaldehyde **233** and 1.4 equivalents of sodium triacetoxyborohydride. This afforded secondary amine (R)-234 in 88% yield. The secondary amine was then further treated with 2-methoxybenzaldehyde and triacetoxyborohydride, in the presence of a catalytic amount of acetic acid, to yield tertiary amine (R)-235 in 61% yield.



Scheme 124. Formation of tertiary amine (R)-235 from primary amine (R)-232·HCl

It was therefore decided to apply these conditions to the synthesis of ligand (R)-266b using primary amine (R)-255b. Thus, amine (R)-255b was treated with 1 equivalent of 2-(benzyloxy)-3,5-dimethylbenzaldehyde **256** and 1.4 equivalents of triacetoxyborohydride (**Scheme 125**). After column chromatography the secondary amine (R)-265b was isolated in 80% yield. The product was identified by the presence of a singlet corresponding to the newly formed benzylic methylene group at $\delta = 3.72$ ppm.

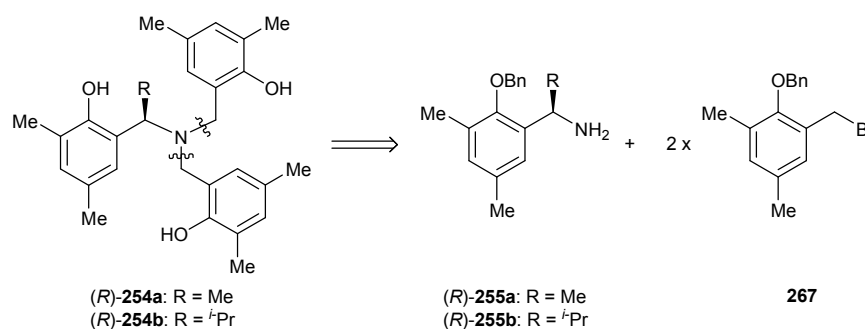


Scheme 125. Reductive amination of amine (R)-255b

In an attempt to form the tertiary amine (R)-266b, secondary amine (R)-265b was further treated with aldehyde 256 and sodium triacetoxyborohydride with a catalytic amount of acetic acid added. However, these conditions were found to be ineffective with no tertiary amine formed after 48 hours, with only the competing reaction involving the reduction of the aldehyde predominating, albeit very slowly.

2.6.2 Alternative Strategy for the Synthesis of Amines (R)-254a and (R)-254b

Since the reductive amination approach proved unsuccessful to produce the tertiary amine (R)-254b an alternative strategy was required. One alternative was a potential bisalkylation strategy, where the primary amine (R)-255a,b was reacted with two equivalents of a benzyl bromide analogue of 2-(benzyloxy)-3,5-dimethylbenzaldehyde 267.

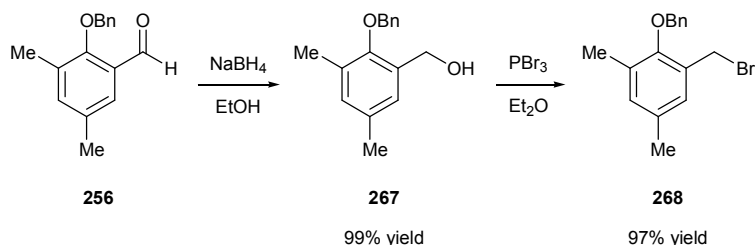


Scheme 126. Retrosynthesis analysis of ligands (R)-254a and (R)-254b

2.6.3 Preparation of Benzyl Bromide 267

The benzyl bromide 267 could be synthesised in very high yields from 2-(benzyloxy)-3,5-dimethylbenzaldehyde 256 via the alcohol 268. Thus, aldehyde 256 was treated with 1.4 equivalents of sodium borohydride in ethanol to yield

(2-benzyloxy)-3,5-dimethylphenyl)methanol **268** in 99% after 4 hours. The product was identified by ^1H NMR spectroscopy by the absence of the aldehyde resonance seen in the starting material and from the singlet at $\delta = 4.62$ ppm corresponding to the newly formed methylene group.

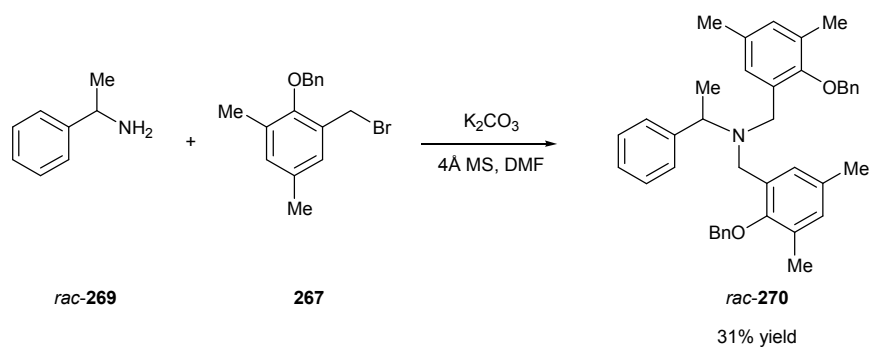


Scheme 127. Formation of benzyl bromide **267** from aldehyde **256**

The benzyl bromide **267** could be easily prepared from the benzyl alcohol **268** by reacting with 1.1 equivalents of phosphorus tribromide. The product was isolated in 97% yield with no further purification required. Overall the benzyl bromide **267** was obtained from the aldehyde **256** in 96% yield over the two steps and could be prepared on a multi-gram scale.

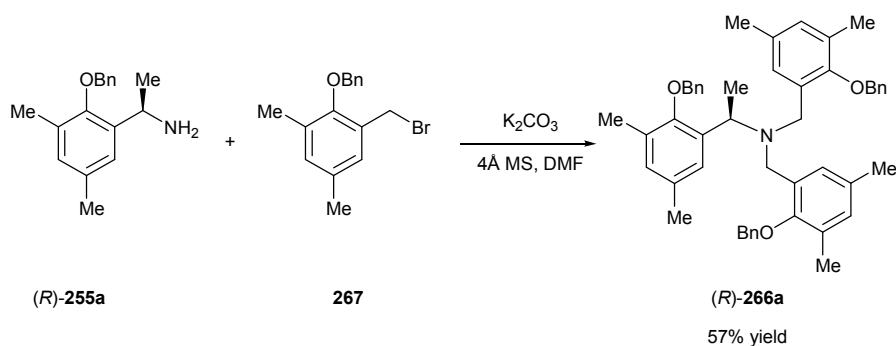
2.6.4 Formation of Amines (*R*)-**266a** and (*R*)-**266b** via a Bisbenzylation Reaction

It was decided to test the bisbenzylation protocol on a model system of α -methylbenzylamine **269** and bromide **267**, before using any precious chiral amine. Thus, a solution of racemic α -methylbenzylamine **269** in DMF was treated with two equivalents of benzyl bromide **267** and potassium carbonate. Pleasingly, after 20 hours, analysis of the crude product by ^1H NMR spectroscopy revealed that the desired tertiary amine had been formed together with the secondary amine in a ratio of *ca.* 3:1. The desired tertiary amine was isolated after column chromatography in 31% yield. Its structure was confirmed by resonances at $\delta = 3.79$ ppm and $\delta = 3.53$ ppm corresponding to the new benzylic methylene protons group which were equivalent to four protons.



Scheme 128. Bisbenzylation tested on model substrate **269**

For the bisbenzylation of (*R*)-**255a** with two equivalents of bromide **267**, the progress of the reaction was monitored by TLC. It was found that an additional 0.5 equivalents of bromide **267** and a reaction time of 48 hours were required to get the reaction to go to completion. After column chromatography the tertiary amine (*R*)-**266a** was isolated in 57% yield (**Scheme 129**). The structure of the product was confirmed by ¹H NMR spectroscopy, with two resonances corresponding to the new benzylic methylene group ($\delta = 3.72$ ppm and $\delta = 3.61$ ppm) which were equivalent to four protons (**Figure 44**). Four sets of singlets were observed for the *ortho*- and *para*-methyl groups at $\delta = 2.18$ ppm (equivalent to 3 protons), $\delta = 2.17$ ppm (6 protons), $\delta = 2.14$ ppm (3 protons) and $\delta = 2.10$ ppm (6 protons).



Scheme 129. Formation of tertiary amine (*R*)-**266a**

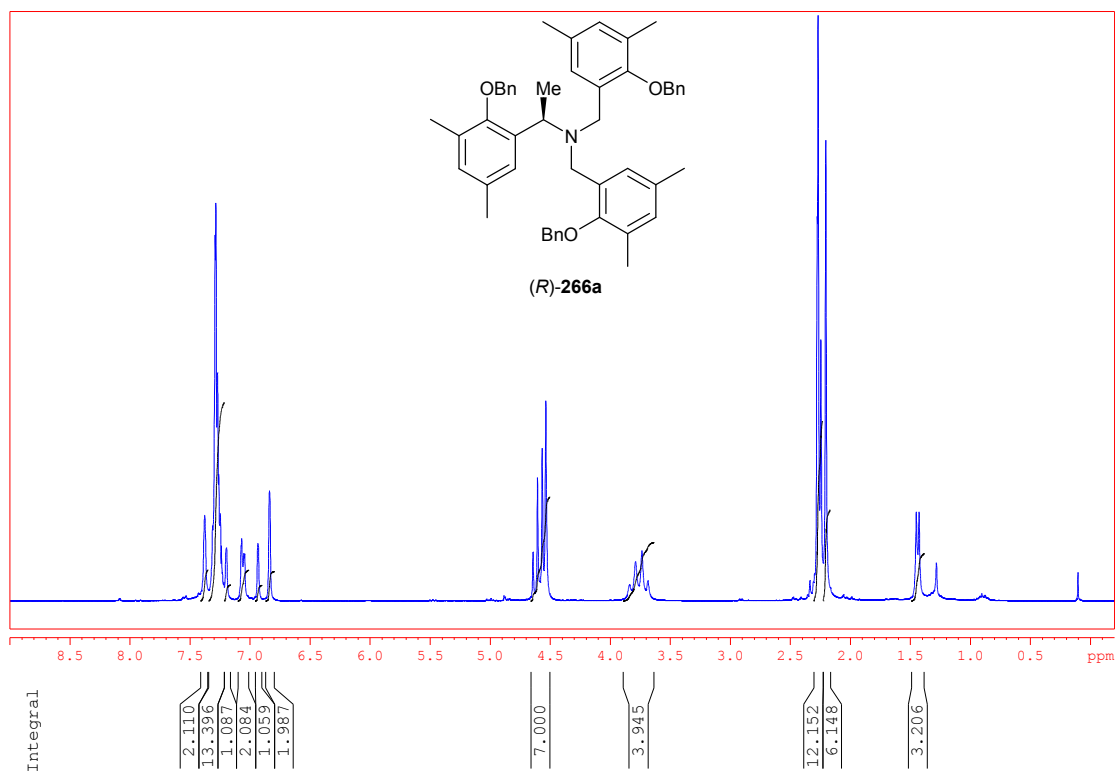
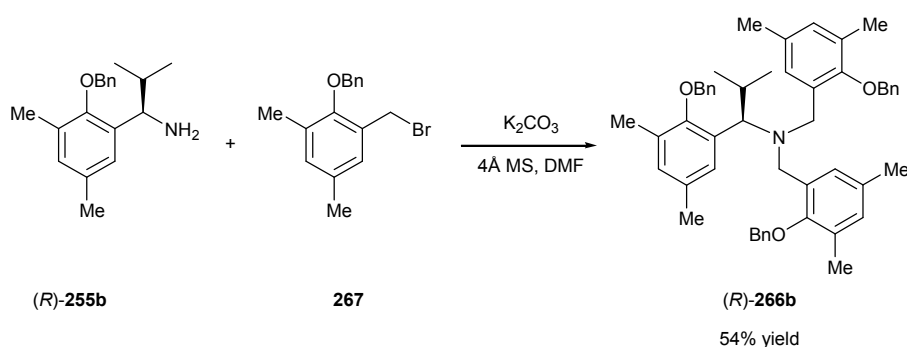


Figure 44. ^1H NMR (CDCl_3) of the tertiary amine (R)-266a

Similarly for the formation (R)-266b, primary amine (R)-255b was reacted with a total of 2.5 equivalents of bromide **267** over 48 hours to yield the tertiary amine in 54% yield (Scheme 130). Analysis of the ^1H NMR spectrum showed resonances at $\delta = 3.70$ ppm and $\delta = 3.56$ ppm corresponding to the new benzylic methylene protons group (Figure 45).



Scheme 130. Formation of tertiary amine (R)-266b

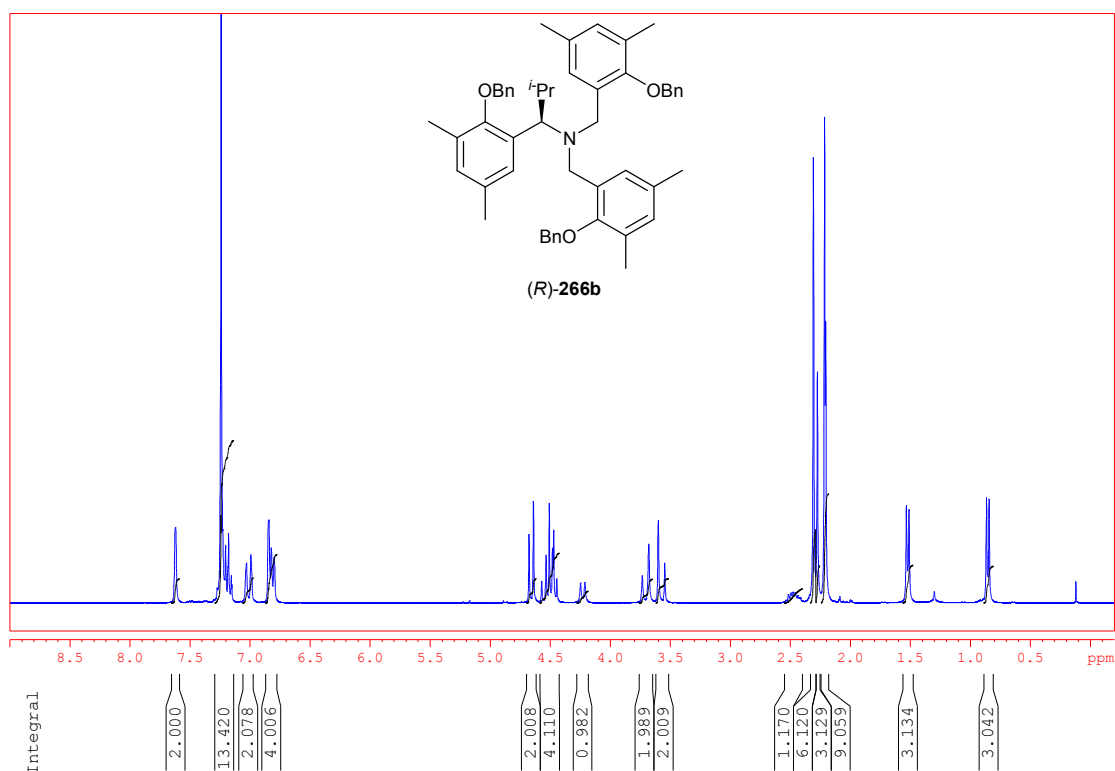
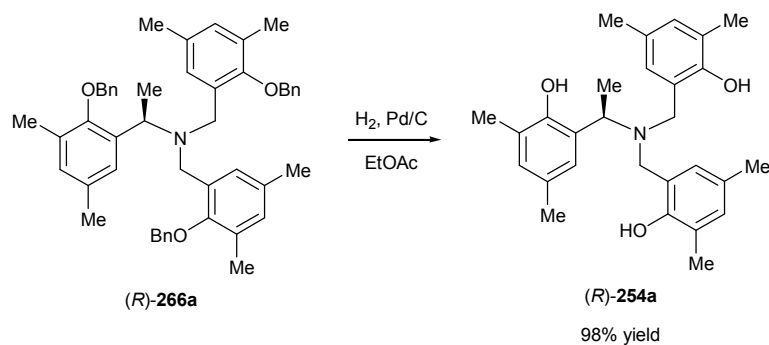


Figure 45. ^1H NMR (CDCl_3) of the tertiary amine (*R*)-**266b**

2.6.5 Deprotection of Tertiary Amines (*R*)-**266a** and (*R*)-**266b**

The hydrogenation of amine (*R*)-**266a** with 10% palladium on carbon in ethyl acetate under one atmosphere of hydrogen proceeded smoothly to deliver the chiral ligand, (*R*)-*N,N*-bis(2-(hydroxy)-3,5-dimethylbenzyl)-1-(2-(hydroxy)-3,5-dimethylphenyl) ethylamine **254a** in 98% yield (**Scheme 131**). The chiral ligand was identified by the presence of two resonances in the ^1H NMR spectrum corresponding to the benzylic methylene group ($\delta = 3.87$ ppm and $\delta = 3.51$ ppm) which were now equivalent to four protons (**Figure 46**). The methine proton adjacent to the chiral methyl group appeared as a quartet at $\delta = 4.34$ ppm. The three phenolic protons were observed as a broad singlet at $\delta = 4.49$ ppm. High resolution mass spectrometry identified the molecular mass of $[\text{M}+\text{H}]^+$ as 434.2693 ($\text{C}_{28}\text{H}_{36}\text{NO}_3$ requires 434.2690). In the low resolution spectrum there were signals at 434 for the molecular ion and at 286 corresponding to the molecular ion with loss of the chiral arm.



Scheme 131. Hydrogenolysis of tertiary amine (R) -**266a** to give chiral ligand (R) -**254a**

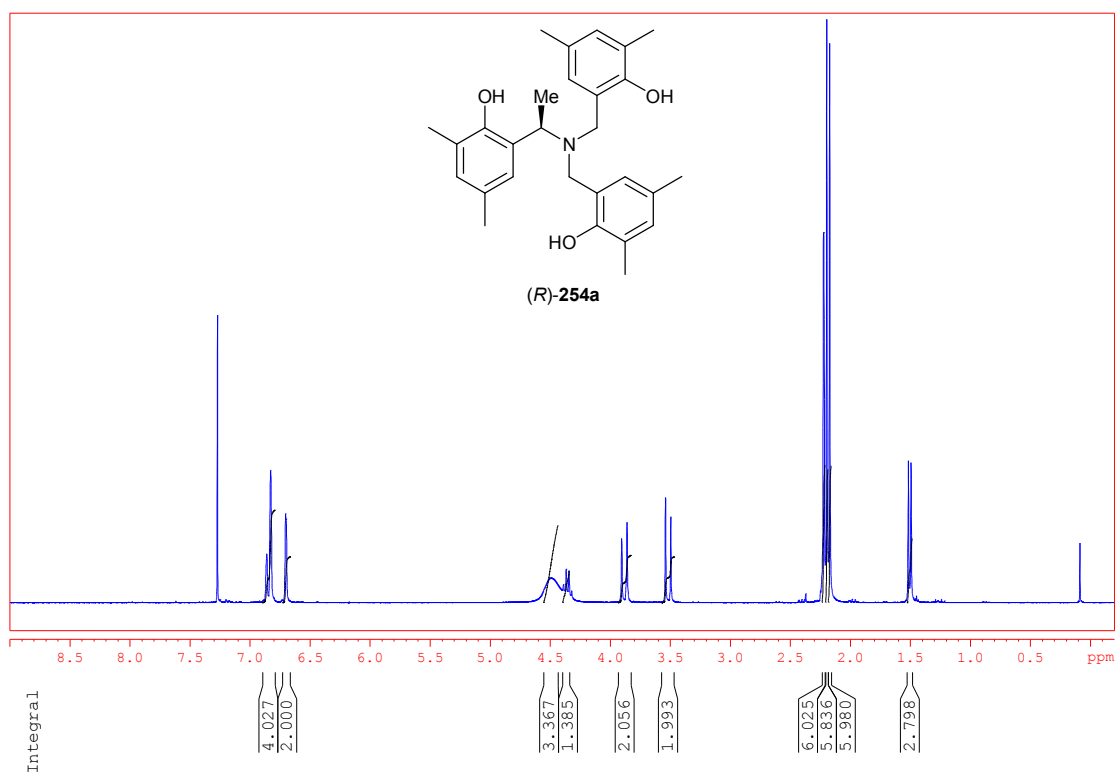
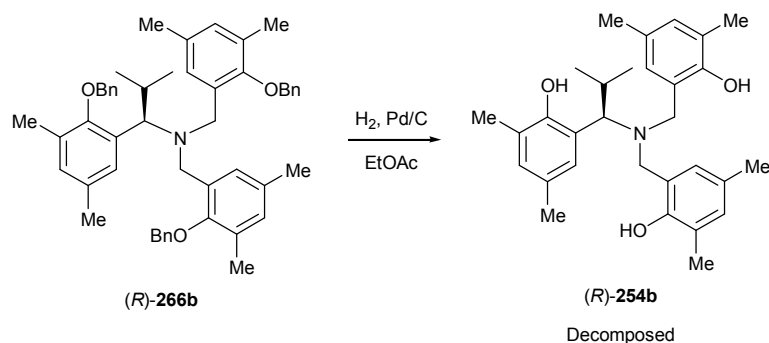


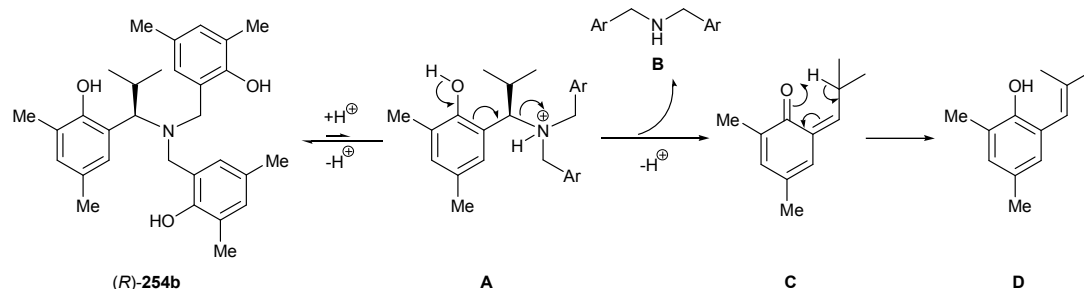
Figure 46. ^1H NMR (CDCl_3) spectrum of chiral ligand (R) -**254a**

In an attempt to isolate the chiral ligand (R) -**254b**, tertiary amine (R) -**266b** was subjected to the same hydrogenation conditions. Unfortunately, whilst the benzyl groups were successfully cleaved as shown by the ^1H NMR spectrum of the crude product, a number of other products were also observed (**Scheme 132**). Even after repeated attempts at the reaction and numerous attempts to purify the crude mixture by column chromatography the desired product (R) -**254b** could never be isolated.



Scheme 132. Attempted formation of chiral ligand (*R*)-254b

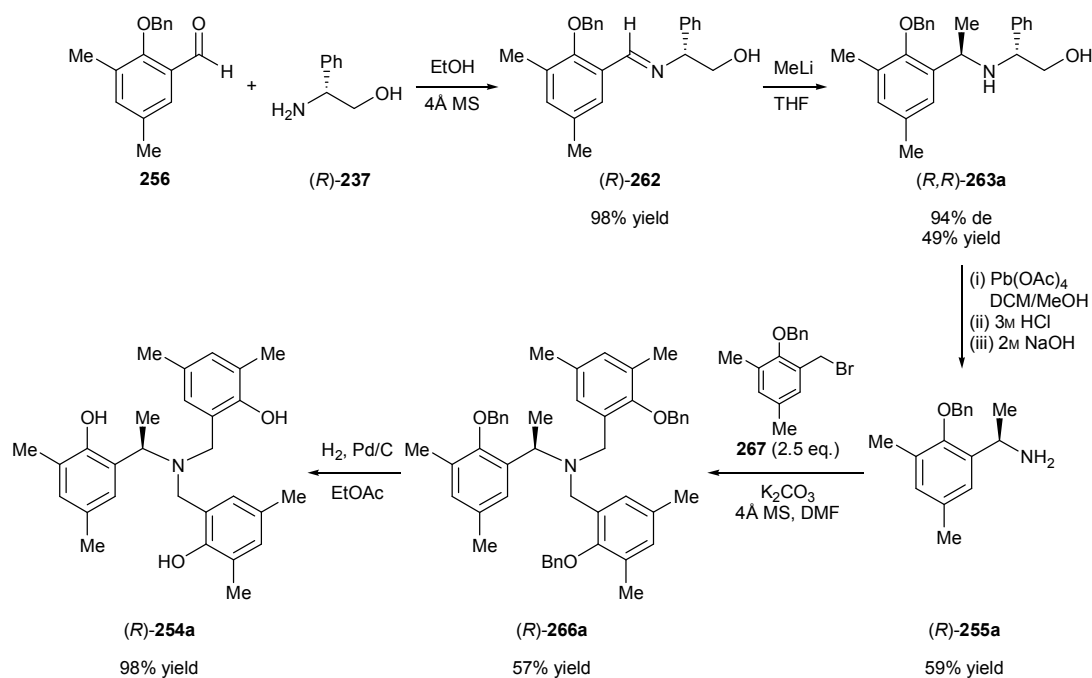
A number of observations suggested that the chiral ligand was unstable and readily decomposed. Monitoring the hydrogenation reaction by TLC showed that it went from the one spot of starting material to one spot of assumed product. After filtration of the reaction solution through Celite[®] and concentration under reduced pressure, another TLC was run which showed that many products were now present, which was confirmed by ¹H NMR analysis. Similarly, in an attempt to purify the crude product by flash chromatography, the spot relating to the product could be isolated. However after concentration of those fractions any subsequent TLC of the isolated product appeared identical to a pre-column sample. A possible mechanism for this decomposition is shown in **Scheme 133**. Following protonation of the ligand (*R*)-254b (possibly by the phenolic proton of another ligand) to give the quaternary ammonium ion **A**, secondary amine **B** is eliminated to give intermediate **C**. Following rearrangement of intermediate **C**, alkene **D** is formed. The reason this process occurs with ligand (*R*)-254b and not ligand (*R*)-254a could be due to the increase in steric strain the *iso*-propyl group introduces to the protonated ligand (*R*)-254b compared with the corresponding protonated form of ligand (*R*)-254a.



Scheme 133. Possible mechanism for the decomposition of ligand (*R*)-254b

2.7 CONCLUSION

The chiral ligand (*R*)-**254a** was synthesised *via* the protocol described in **Scheme 134**. The synthesis involved asymmetric addition to imine (*R*)-**262** followed by deprotection of amine (*R,R*)-**263a** with lead (IV) acetate. Bisbenzylation of primary amine (*R*)-**255a** with the benzyl bromide **267** lead to tertiary amine (*R*)-**266a**. The chiral ligand (*R*)-**254a** was obtained following deprotection by hydrogenolysis. The chiral ligand was synthesised in 16% overall yield.



Scheme 134. Overall synthesis of ligand (*R*)-**254a**

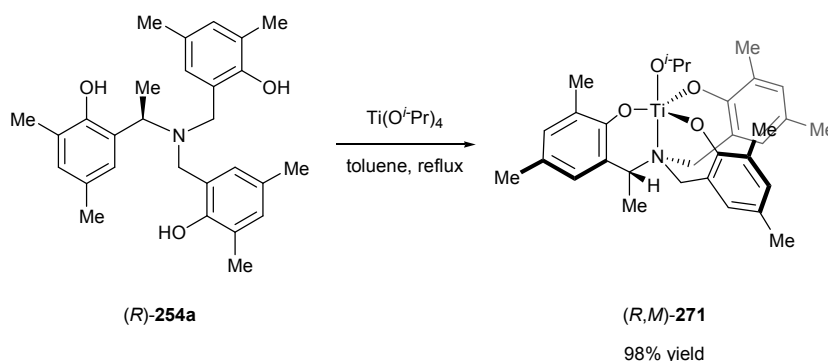
Chapter 3:

Results and Discussion II

3 Results and Discussion II

3.1 FORMATION OF TITANIUM TRIS(PHENOLATE) *ISO*-PROPOXIDE COMPLEX (*R,M*)-271²

Having successfully synthesised the pseudo-*C*₃-symmetric ligand (*R*)-**254a**, attention was then turned to coordinating it to titanium (IV) *iso*-propoxide. The treatment of ligand (*R*)-**254a** in toluene with titanium (IV) *iso*-propoxide followed by removal of the solvent gave the crude product as an orange/red solid. Initial attempts at isolating (*R,M*)-**271** proved unsuccessful with complex mixtures of products obtained, further attempts at purifying by recrystallisation also being unsuccessful. Eventually a small amount of reasonably pure product was obtained without the need for further purification (Scheme 135).



Scheme 135. Coordination of pseudo-*C*₃-symmetric ligand (*R*)-**254a** to $Ti(O^iPr)_4$, giving rise to titanium tris(phenolate) complex (*R,M*)-**271**

The structure of the complex was analysed spectroscopically, with the *iso*-propoxide ligand showing a doublet at $\delta = 1.53$ ppm and a septet at $\delta = 5.24$ ppm in the ¹H NMR spectrum (Figure 47). Most notably, the resonances corresponding to the benzylic protons of the tripodal ligand were now much more complex than when compared to the corresponding parent amine tris(phenolate) titanium *iso*-propoxide (*rac*)-**194b**.^{104, 130} In the ¹H NMR spectrum of (*rac*)-**194b** the diastereotopic benzylic protons appeared as two broad doublets at $\delta = 2.75$ ppm and $\delta = 3.89$ ppm. In comparison, the five benzylic protons of the tripodal ligand in (*R,M*)-**271** now appeared as a quartet and four doublets (two partially overlapped) between $\delta = 4.06$ ppm and $\delta = 3.07$ ppm (Figure 48). These signals were ascribed to the three

² This work was conducted in collaboration with Miss Carly J. Gilfillan

pseudoequatorial benzylic protons (appearing as a quartet at $\delta = 4.00$ ppm, and two doublets at $\delta = 3.74$ ppm and $\delta = 3.54$ ppm) and two pseudoaxial benzylic protons (appearing between $\delta = 3.22$ and 3.07 ppm). This indicated that the proposed chiral relay strategy was successful in controlling the propeller-like conformation of the ligand.

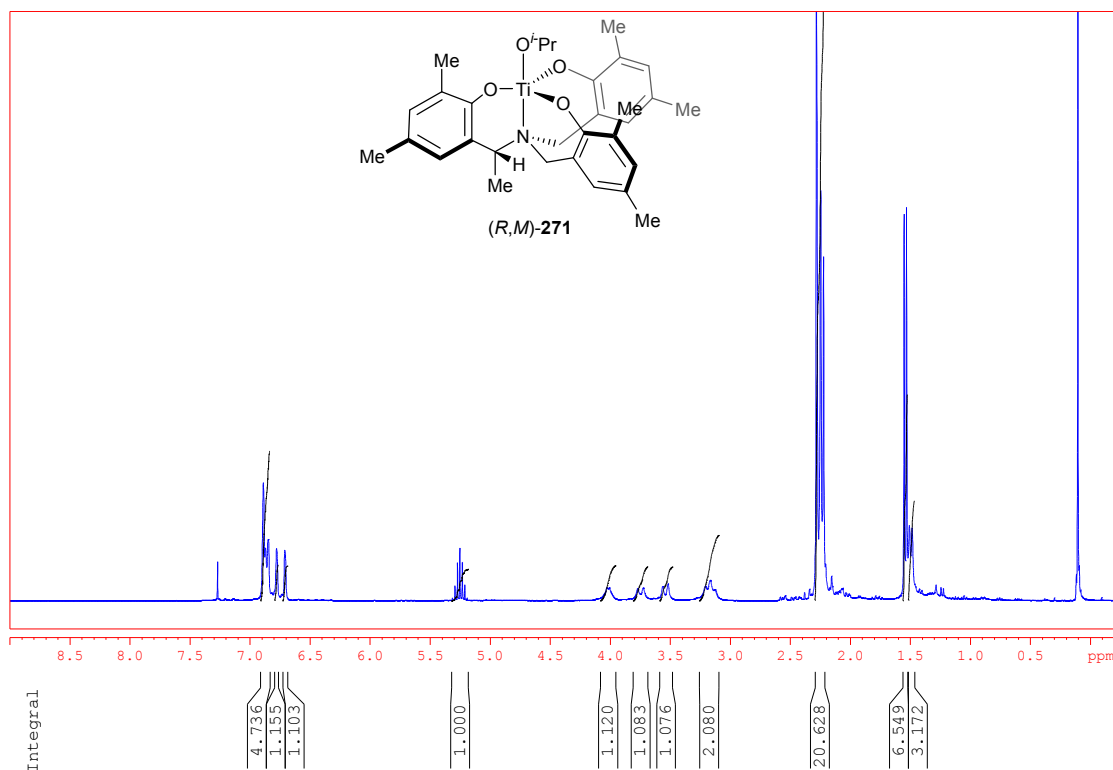


Figure 47. ^1H NMR (CDCl_3) spectrum of titanium complex (*R,M*)-**271**

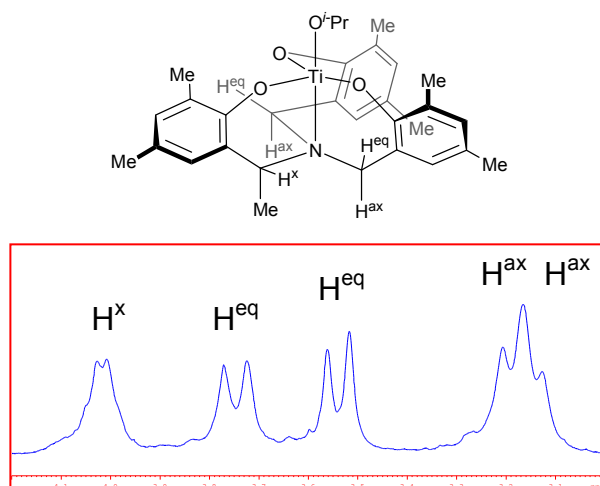


Figure 48. Expansion of ^1H NMR of titanium complex (*R,M*)-**271** showing the benzylic region

In an attempt to obtain a crystalline sample of (*R,M*)-**271** a solution of the complex in hexane was allowed to stand for two weeks, after which time, crystals that were

suitable for X-ray analysis were obtained. It was found that these contained both the complex *(R,M)*-**271** co-crystallised with a partially hydrolysed trimetallic amine tris(phenolate)-oxo-alkoxide complex (**Figure 49**). In the crystal, there was no intermolecular interaction between these two components. For *(R,M)*-**271**, the crystal structure agreed with what had been observed in the solution phase, with the configuration of the C(1) (*R*)-stereocentre serving to lock the axial chirality of the complex into the (*M*)-isomer such that the α -methyl group occupies its predicted pseudoaxial orientation. In the solid state this is disordered over the three possible sites. Most of the key structural parameters are similar to those observed for *(rac)*-**194b**,^{104, 130} with the bonds between the titanium atom and the three phenolate oxygen atoms in *(R,M)*-**271** being of similar lengths [Ti-O(phenolate) distances (Å): Ti(1)-O(1) 1.841(6), Ti(1)-O(2) 1.844(6), Ti(1)-O(3) 1.853(6)]. The bond angles between the three phenolate oxygens are also similar to one another [bond angles between phenolate oxygen atoms (°): O(1)-Ti(1)-O(2) 116.4(3), O(2)-Ti(1)-O(3) 118.3(3), O(3)-Ti(1)-O(1) 119.9(3)]. The axial sites of the trigonal bipyramidal titanium centre were occupied by the apical nitrogen and the monodentate *iso*-propoxide anion, with a Ti-N bond length of 2.411(7) Å and a Ti-O^{*i*}Pr distance of 1.763(6) Å, and a bond angle between N(1)-Ti(1)-O(4) of 178.3(3)°. This is compared to a Ti-N bond length of 2.303(2) Å and a Ti-O^{*i*}Pr distance of 1.774(2) Å found in the crystal structure of *(rac)*-**194b**. In both cases the titanium atom sits the same distance above the plane of the three equatorial phenolate oxygen atoms [the distance of the Ti atom above the plane of the three phenolate O atoms is 0.2497(16) Å for *(R,M)*-**271** and 0.247(1) Å for *(rac)*-**194b**]. The observed differences in Ti-N bond lengths means there is a reduction in the tilt of the aryl rings (as defined by the average angle between the aryloxide planes and the Ti-N bond vector) from 15° for *(rac)*-**194b** to 4° for *(R,M)*-**271**.

The second component within the structure consisted of a trimetallic adduct of two *(R,M)*-**271** bridged by a Ti(O)(O^{*i*}Pr)₂ fragment, which presumably resulted from the incomplete reaction and slow hydrolysis of *(R,M)*-**271**. Both Ti(2) and Ti(3) are six-coordinate via the μ^3 -oxo atom, O(13) of the central unit and one arm of each tripodal ligand bridged to the central Ti centre. This binding mode caused one arm of the tripodal ligand to ‘flip’ thereby reducing the symmetry of the system. This was observed with unequal angles between the three phenolate oxygens and each

titanium centre [bond angles between phenolate oxygen atoms ($^{\circ}$): O(6)-Ti(2)-O(7) 162.7(19), O(5)-Ti(2)-O(7) 90.6(2), O(6)-Ti(2)-O(5) 98.0(2) and O(11)-Ti(3)-O(10) 161.7(19), O(9)-Ti(3)-O(10) 90.3(19), O(11)-Ti(3)-O(9) 99.0(2)].

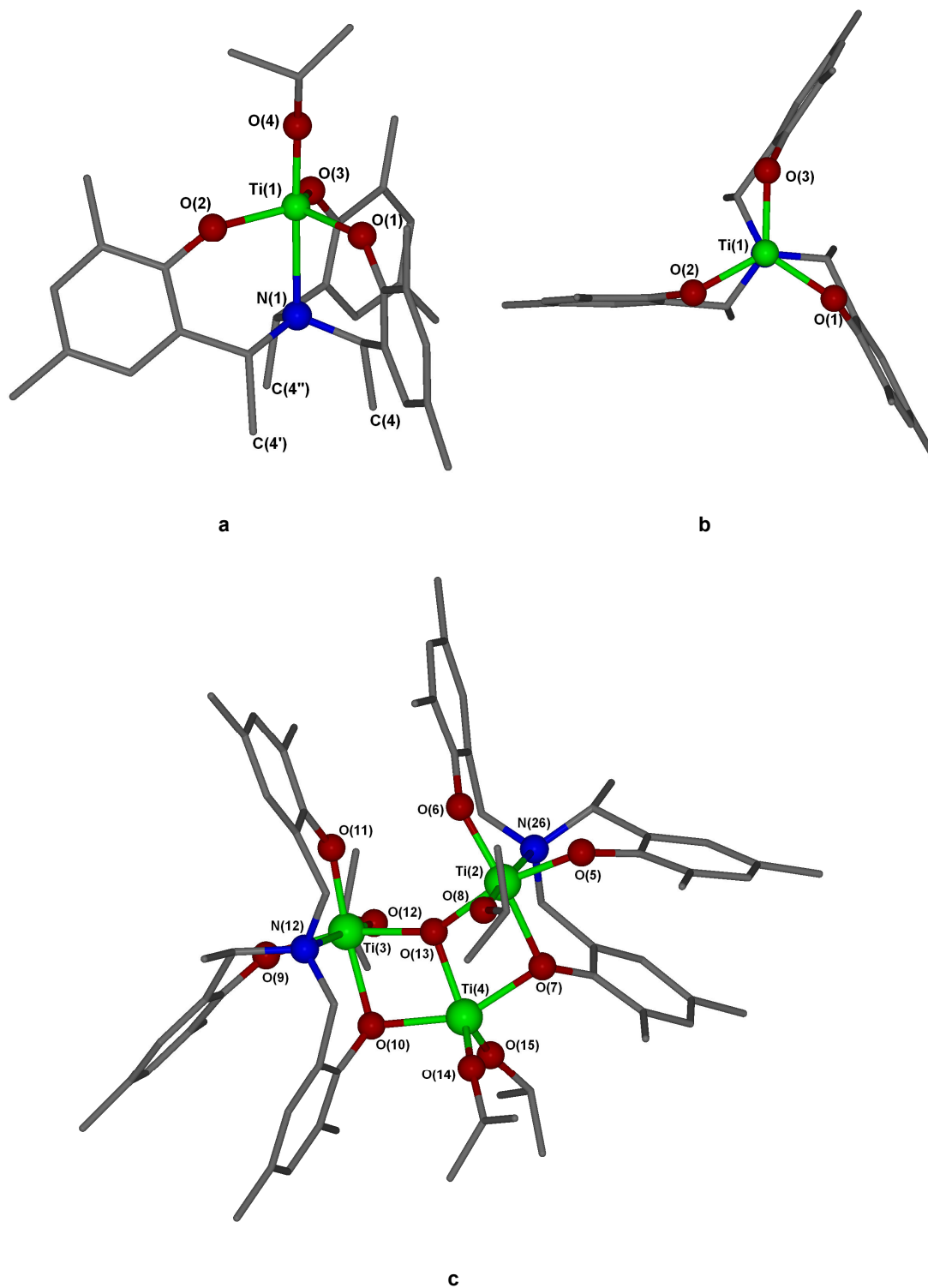
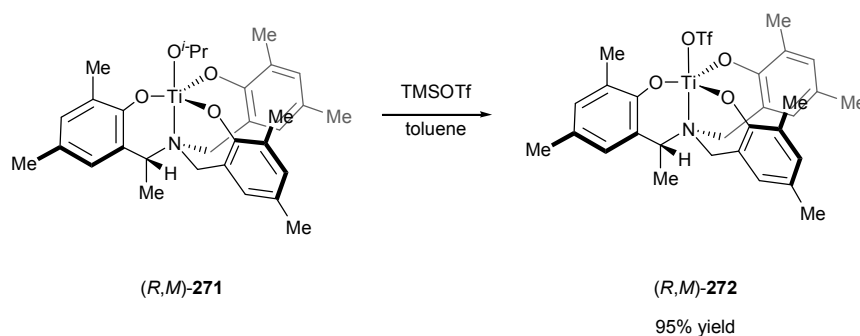


Figure 49. Side and top views of the X-ray crystal structure of (R,M)-271 (a and b) and the co-crystallised trimetallic amine (trisphenolate)-oxo-alkoxide complex (c)

3.2 FORMATION OF TITANIUM TRIS(PHENOLATE) TRIFLATE COMPLEX (*R,M*)-272³

The titanium tris(phenolate) *iso*-propoxide complex (*R,M*)-271 was converted to the corresponding titanium tris(phenolate) triflate complex (*R,M*)-272 by treatment with trimethylsilyltriflate (**Scheme 136**). The structure of the complex was analysed by ¹H NMR with the resonances corresponding to the *iso*-propoxide ligand of (*R,M*)-271 no longer present (**Figure 50**). The signals for the benzylic protons of the tripodal ligand again appeared as a quartet and four doublets (two partially overlapped) between $\delta = 4.17$ ppm and $\delta = 3.30$ ppm. As before, the quartet at $\delta = 4.11$ ppm was ascribed to the pseudoequatorial methine benzylic proton adjacent to the methyl substituent. The two doublets at $\delta = 3.88$ ppm and $\delta = 3.67$ ppm were due to the other two pseudoequatorial benzylic protons. The resonances for the two pseudoaxial benzylic protons were observed between $\delta = 3.49$ ppm and $\delta = 3.30$ ppm. A doublet at $\delta = 1.60$ ppm corresponded to the pseudoaxial methyl substituent. The *ortho*- and *para*-methyl groups on the aryl rings appeared as singlets at $\delta = 2.29$, 2.26, 2.24, 2.24, 2.23 and 2.21 ppm. In the ¹³C NMR spectrum there were signals at $\delta = 55.1$, 54.3 and 51.3 ppm which corresponded to the three benzylic carbons. High resolution mass spectrometry identified the molecular mass of [M]⁺ as 627.1375 (C₂₉H₃₂F₃NO₆STi requires 627.1376).



Scheme 136. Formation of titanium tris(phenolate) triflate complex (*R,M*)-272

³ This work was conducted in collaboration with Miss Carly J. Gilfillan

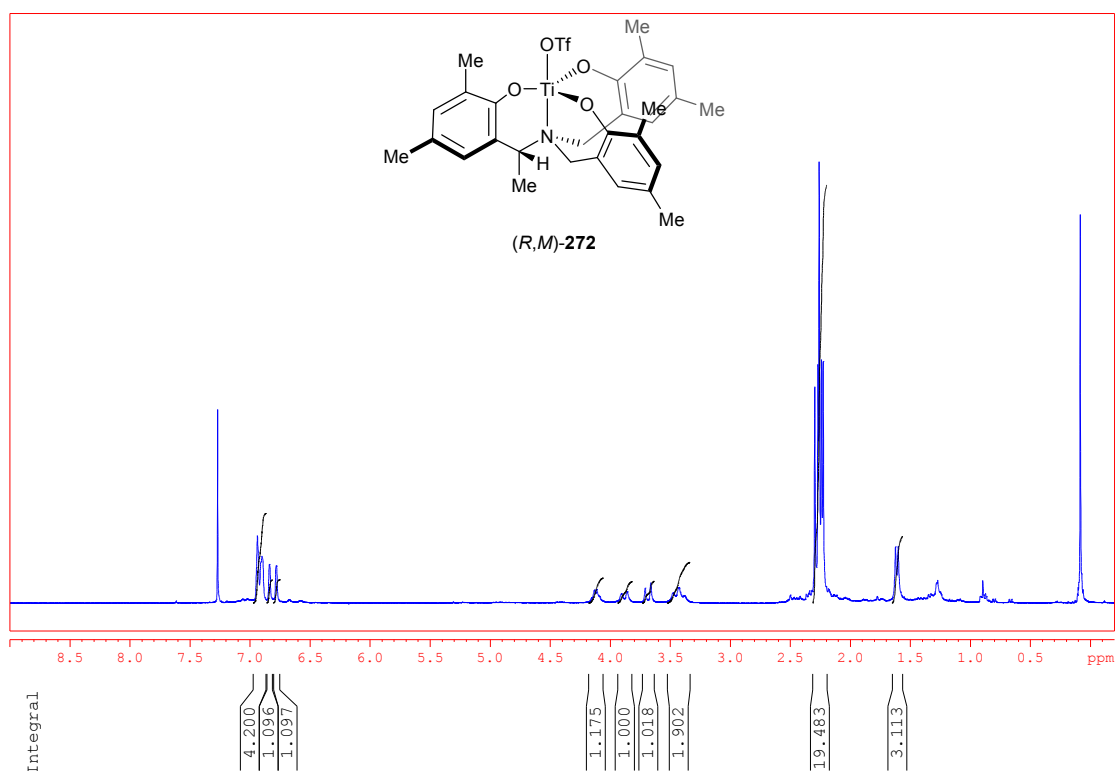


Figure 50. ^1H NMR (CDCl_3) spectrum of titanium complex (R,M) -**272**

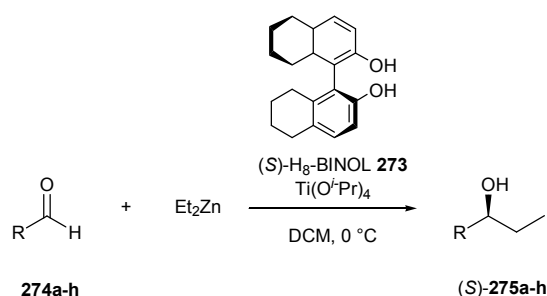
3.3 INITIAL SCREENING OF THE CHIRAL TITANIUM COMPLEXES OF (R,M) -**271** AND (R,M) -**272**

Having prepared a small quantity of both (R,M) -**271** and (R,M) -**272**, the next goal was to screen these complexes in a number of organic transformations. Therefore, it was decided to screen reactions where the corresponding racemic titanium catalyst (rac) -**195a** had shown appreciable activity.

3.3.1 Diethyl Zinc Addition to Benzaldehyde

In 1997, Chan and co-workers reported the enantioselective addition of diethyl zinc to aromatic aldehydes catalysed by (S) - H_8 -BINOL **273** and titanium (IV) *iso*-propoxide (**Scheme 137**).¹⁴⁵ With a 7:1 ratio of titanium (IV) *iso*-propoxide to (S) - H_8 -BINOL **273**, the addition of diethyl zinc was found to give the desired products in excellent conversion and enantioselectivity (up to 98% ee) after 5 hours at 0 °C. For example, the addition of diethyl zinc to benzaldehyde **274a** resulted in (S) -1-phenylpropan-1-ol **275a** in 100% conversion and 98% ee (**Table 45**, entry 1). A lower enantioselectivity was observed with 2-bromobenzaldehyde (85% ee),

possibly due to the steric hindrance that the ortho-substituent exerted upon coordination to the metal (entry 2). The introduction of an electron-withdrawing group (-NO₂) at the meta-position also resulted in a decreased enantioselectivity for the product (88% ee, entry 4). Excellent enantioselectivities were also obtained for 1-naphthaldehyde **274g** and 2-naphthaldehyde **274h** (98% ee and 95% ee, entries 7 and 8 respectively).



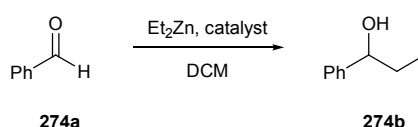
Scheme 137. Enantioselective addition of diethyl zinc to aromatic aldehydes catalysed by (S)-H₈-BINOL **273** and Ti(O^{*i*}Pr)₄

Table 45

Entry	Product	R	Conversion /%	ee /%
1	275a	C ₆ H ₅	100	98
2	275b	2-Br(C ₆ H ₄)	98	85
3	275c	3-MeO(C ₆ H ₄)	100	96
4	275d	3-NO ₂ (C ₆ H ₄)	100	88
5	275e	4-Cl(C ₆ H ₄)	89	97
6	275f	4-MeO(C ₆ H ₄)	99	97
7	275g	1-Naphthyl	100	98
8	275h	2-Naphthyl	100	95

Given the number of reports on the enantioselective addition of diethyl zinc to aromatic aldehydes by complexes of titanium,¹⁴⁶ it was decided to screen both the racemic titanium *iso*-propoxide complex (*rac*)-**194b** and the chiral titanium complex (*R,M*)-**271** in this transformation (**Scheme 138, Table 46**). Treatment of a solution of (*rac*)-**194b** with diethyl zinc at room temperature followed by benzaldehyde **274a** at 0 °C resulted in the crude product. Analysis of the ¹H NMR spectrum of the crude product revealed that the reaction had gone to 54% conversion (entry 1). Column chromatography afforded the product 1-phenyl propanol **275a** as a yellow oil in 29% yield. Repeating the reaction with (*R,M*)-**271** afforded the product in 45% conversion

and 20% yield (entry 2). The enantioselectivity of this product was determined by chiral HPLC analysis to be 0% ee. Given the low conversions obtained with these two catalysts, it was decided to run a reaction under identical conditions but without the addition of either of the complexes to ensure that these were indeed showing catalytic activity. Under these conditions the alcohol product was formed in trace amounts (entry 3).



Scheme 138. Diethyl zinc addition to benzaldehyde **274a**

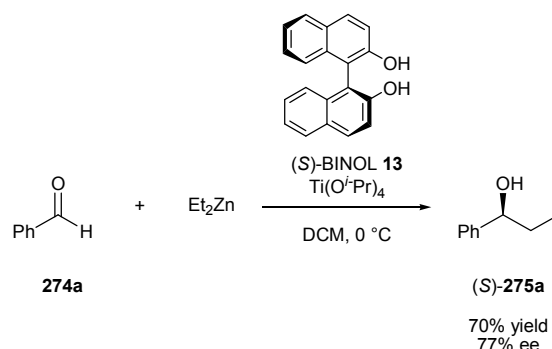
Table 46

Entry	Catalyst	Conversion /%	Isolated yield /%	ee /%
1	(<i>rac</i>)- 194b (20mol %)	54	29	0
2	(<i>R,M</i>)- 271 (20mol %)	45	20	0
3	none	trace	-	-
4	(<i>R</i>)- 254a (20mol %)	trace	-	-
5	(<i>R,M</i>)- 272 (20mol %)	57	32	0

The reaction was also attempted with just the chiral ligand (*R*)-**254a** as the catalyst. However, analysis of the crude reaction mixture by ¹H NMR once again revealed that almost no product was present (entry 4). Finally, the chiral titanium triflate complex (*R,M*)-**272** was also screened in the transformation. The product was obtained in 57% conversion and 32% isolated yield (entry 5). Again analysis of the alcohol product showed it to be racemic.

As a comparison, the addition of diethyl zinc to benzaldehyde **274a** was performed with (*S*)-BINOL **13** and titanium (IV) *iso*-propoxide as reported by Chan and co-workers.¹⁴⁷ Thus, treatment of a solution of 20mol % of BINOL and 140mol % of titanium (IV) *iso*-propoxide in dichloromethane with diethyl zinc followed by benzaldehyde gave the crude product in 86% conversion (**Scheme 139**). Following purification by column chromatography the product **275a** was isolated in 70% yield. Analysis by chiral HPLC showed the enantiomeric excess to be 77% in favour of the (*S*)-enantiomer. Whilst this result is somewhat lower than was reported by Chan and

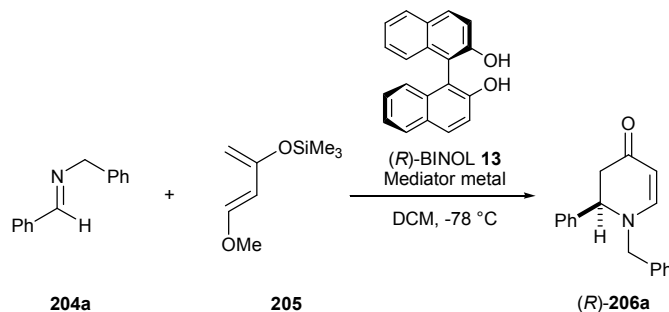
co-workers (100% conversion, 92% ee),¹⁴⁷ it does compare favourably to results reported by Nakai *et al.*,¹⁴⁸ that under similar conditions they obtained the product in 98% yield and 84% ee.



Scheme 139. Addition of diethyl zinc to benzaldehyde **274a** catalysed by (*S*)-BINOL **13** and $\text{Ti}(\text{O}^i\text{Pr})_4$

3.3.2 Aza-Diels Alder Reaction

In 1993, Yamamoto *et al.* reported the enantioselective aza-Diels Alder reaction of benzylidenebenzylamine **204a** with Danishefsky's diene **205** catalysed by metal complexes of (*R*)-BINOL **13** to give *N*-benzyl-2,3-dihydro-2-phenyl-4-pyridinone **206a** (Scheme 140).¹⁴⁹ Initial screening with various metal sources revealed that whilst complexes of aluminium and titanium did catalyse the reaction, use of borane with BINOL gave a superior yield and enantioselectivity (Table 47, entries 1-3). Using dimethyl zinc as a metal source failed to catalyse the reaction with no product obtained (entry 4). The use of trimethyl borate and triphenyl borate also mediated the transformation, with the bulkier aryloxy reagent giving the best result, with the product isolated in 75% yield and 82% ee (entries 5 and 6).

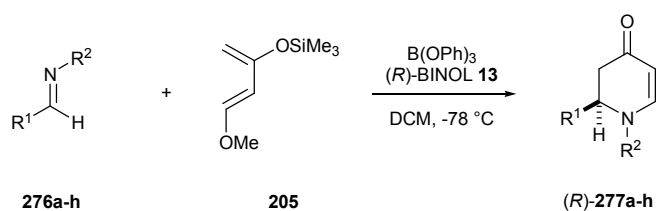


Scheme 140. Asymmetric aza-Diels Alder reaction mediated by various metal complexes of (*R*)-BINOL **13**

Table 47

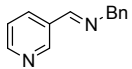
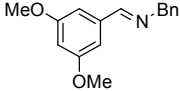
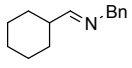
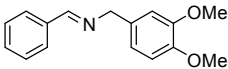
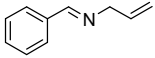
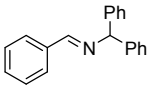
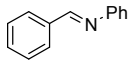
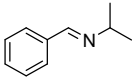
Entry	Mediator metal	Yield /%	ee /%
1	BH ₃	62	72
2	TiCl ₂ (O ^{<i>i</i>} Pr) ₂	20	17
3	Me ₃ Al	15	12
4	Me ₂ Zn	0	-
5	B(OMe) ₃	42	72
6	B(OPh) ₃	75	82

The authors went on to screen a range of imines in the reaction with the chiral complex formed from triphenyl borate and (*R*)-BINOL acting as the catalyst (**Scheme 141**). The reaction was tolerant to a range of imines, with both aromatic and non-aromatic groups tolerated at the R¹ position (**Table 48**, entries 1-3). Generally, a benzyl type substituent at the R² position gave better enantioselectivity (entries 4-8).

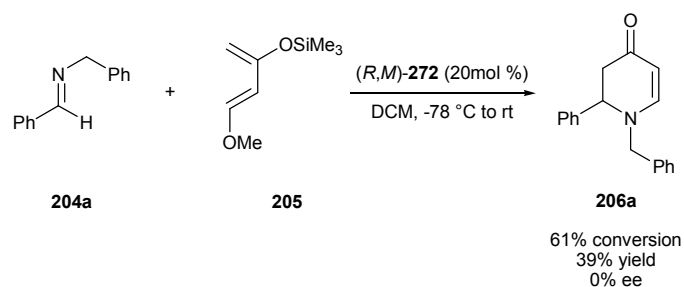


Scheme 141. Asymmetric aza-Diels Alder reaction of imines **276a-h** with Danishefsky's diene **205**

Table 48

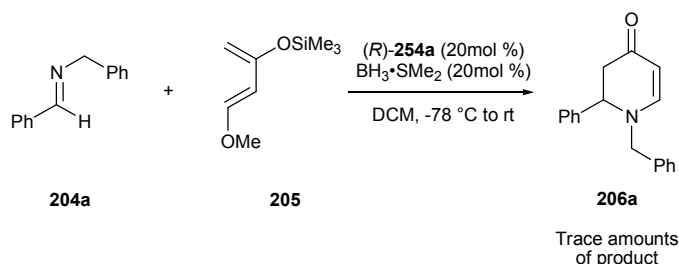
Entry	Imine	Product	Yield /%	ee /%
1		277a	71	90
2		277b	89	74
3		277c	45	76
4		277d	73	85
5		277e	97	70
6		277f	0	-
7		277g	77	24
8		277h	13	4

Given the success of the amine tris(phenolate) titanium triflate complex (*rac*)-**195a** in catalysing this transformation to afford racemic pyridones, it was decided to test the corresponding chiral titanium triflate complex (*R,M*)-**272**. Thus, to a solution of *N*-benzylidenebenzylamine **204a** and titanium complex (*R,M*)-**272** in dichloromethane at -78 °C was added three equivalents of Danishefsky's diene **205** (Scheme 142). Analysis of the crude reaction mixture revealed that the reaction had proceeded to give the dihydropyridinone product **206a** in 61% conversion. After purification by column chromatography the product was isolated as a yellow oil in 39% yield. The structure of the dihydropyridone **206a** was confirmed by ¹H NMR spectroscopy with doublets at $\delta = 4.32$ ppm and $\delta = 4.09$ ppm corresponding to the diastereotopic benzylic protons. Similarly the resonances of the two diastereotopic protons adjacent to the carbonyl appeared as a doublets of doublets at $\delta = 2.82$ ppm and $\delta = 2.65$ ppm. Analysis of the product by chiral HPLC showed that the product had formed in 0% ee.



Scheme 142. Aza-Diels Alder between *N*-benzylidenebenzylamine **204a** and Danishefsky's diene **205** catalysed by (*R,M*)-**272**

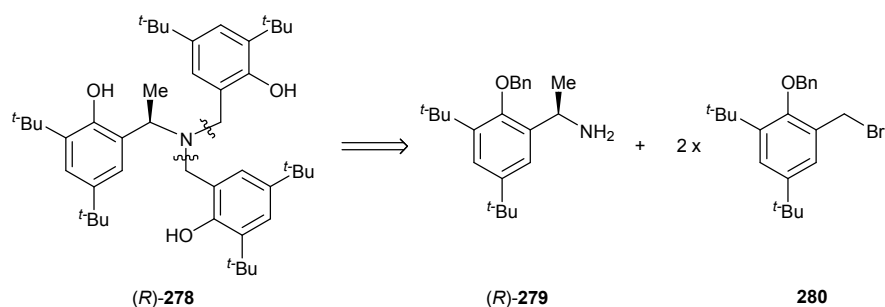
In analogy to the work of Yamamoto and co-workers,¹⁴⁹ the reaction was also attempted using the chiral ligand (*R*)-**254a** and borane as the metal source. The reaction was performed by adding the imine **204a** and Danishefsky's diene **205** to a solution of containing the borane and ligand (*R*)-**254a**. Disappointingly, analysis of the crude reaction mixture revealed that only trace amounts of product had formed (**Scheme 143**).



Scheme 143. Attempted aza-Diels Alder between *N*-benzylidenebenzylamine **204a** and Danishefsky's diene **205** catalysed by borane dimethyl sulfide and chiral ligand (*R*)-**254a**

3.4 SYNTHESIS OF CHIRAL LIGAND (*R*)-278

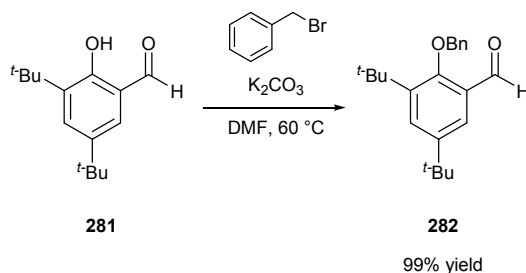
Given that the complex derived from the dimethyl substituted ligand (*R*)-**254a** had not shown any enantioselectivity in the initial screening it was decided that the synthesis of the analogous di-*tert*-butyl substituted ligand would be undertaken. It was hoped that the introduction of these bulkier substituents at the *ortho* position would improve the relay of the chirality of the complex to the upper hemisphere where coordination of a substrate would occur. It was planned that the synthesis of the chiral ligand (*R*)-**278**, which has *tert*-butyl groups at the *ortho* and *para* positions of the aryl ring, would follow a similar strategy to the synthesis of the ligand (*R*)-**254a** (**Scheme 144**). Therefore, in order to synthesise the chiral ligand, it was first necessary to produce the chiral primary amine (*R*)-**279** via the diastereoselective addition of methyl lithium to its corresponding imine.



Scheme 144. Retrosynthetic analysis of ligand (R)-278

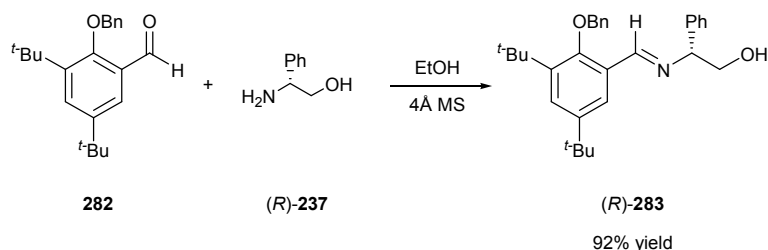
3.4.1 Synthesis of Aldehyde **282** and Imine (R)-283

The benzyl protection of commercially available 3,5-di-*tert*-butyl-2-hydroxybenzaldehyde **281** was achieved by reacting with benzyl bromide in the presence of potassium carbonate in *N,N*-dimethylformamide (Scheme 145). The product 2-(benzyloxy)-3,5-di-*tert*-butylbenzaldehyde **282** was isolated in 99% yield with its structure confirmed by the resonance at $\delta = 5.08$ ppm in the ^1H NMR spectrum corresponding to the benzylic methylene group.



Scheme 145. Formation of aldehyde **282**

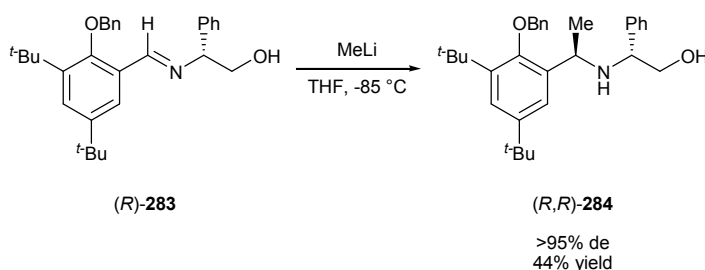
The imine (R)-**283**, formed from the reaction of aldehyde **282** with (R)-2-amino-2-phenylethanol **237**, proceeded to give the desired imine (R)-**283** in 92% yield (Scheme 146). The presence of a singlet ($\delta = 8.73$ ppm) in the ^1H NMR spectrum corresponded to the methine proton of the imine moiety. An absorption at 1632 cm^{-1} in the infrared spectrum was also observed which corresponds to the imine stretch.



Scheme 146. Formation of imine (R)-283

3.4.2 Diastereoselective Addition of Methyl Lithium to Imine (*R*)-**283**

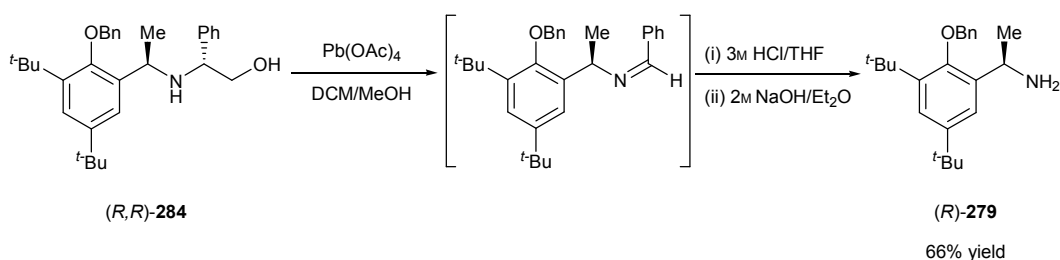
For the addition to imine (*R*)-**283**, methyl lithium was added to a solution of (*R*)-**283** at -85 °C. After column chromatography the product (*R*)-2-((*R*)-1-(2-(benzyloxy)-3,5-di-*tert*-butylphenyl)ethylamino)-2-phenylethanol **284** was isolated in a diastereomeric excess of >95% and a yield of 44%. The presence of the methyl group was indicated by the doublet at $\delta = 1.46$ ppm in the ^1H NMR spectrum. High resolution mass spectrometry identified the molecular mass of $[\text{M}+\text{H}]^+$ as 460.3209 ($\text{C}_{31}\text{H}_{42}\text{NO}_2$ requires 460.3210).



Scheme 147. Diastereoselective addition of methyl lithium to imine (*R*)-**284**

3.4.3 Oxidative Cleavage of Amine (*R,R*)-**284**

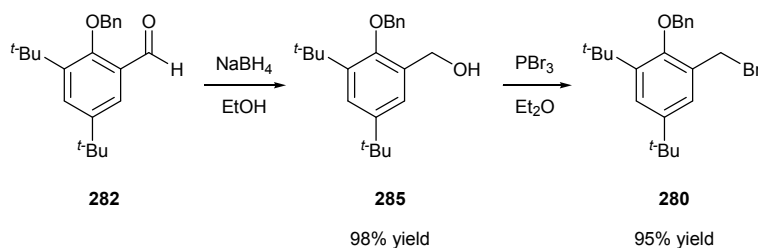
The cleavage of the 2-phenyl ethanol auxiliary from amine (*R,R*)-**284** with lead (IV) acetate following the conditions of Pridgen and co-workers, gave the desired primary amine (*R*)-**279** in 66% yield (**Scheme 148**). Its structure was confirmed by ^1H NMR spectroscopy which showed an absence of signals relating to the 2-phenyl ethanol auxiliary or the imine formed after the first step. Analysis of the IR spectrum revealed there to be two absorptions at 3379 and 3305 cm^{-1} corresponding to the two primary amine N-H stretches.



Scheme 148. Deprotection of amine (*R,R*)-**284** using lead (IV) acetate

3.4.4 Preparation of Benzyl Bromide **280**

The benzyl bromide **280** was prepared from the aldehyde **282** via the corresponding alcohol **285**. Thus, aldehyde **280** was treated with 1.4 equivalents of sodium borohydride in ethanol to yield (2-(benzyloxy)-3,5-di-*tert*-butylphenyl)methanol **285** in 98% after 4 hours (**Scheme 149**). The structure of the product was confirmed by ^1H NMR spectroscopy, with a resonance observed at $\delta = 4.81$ ppm corresponding to the newly formed methylene benzylic protons.

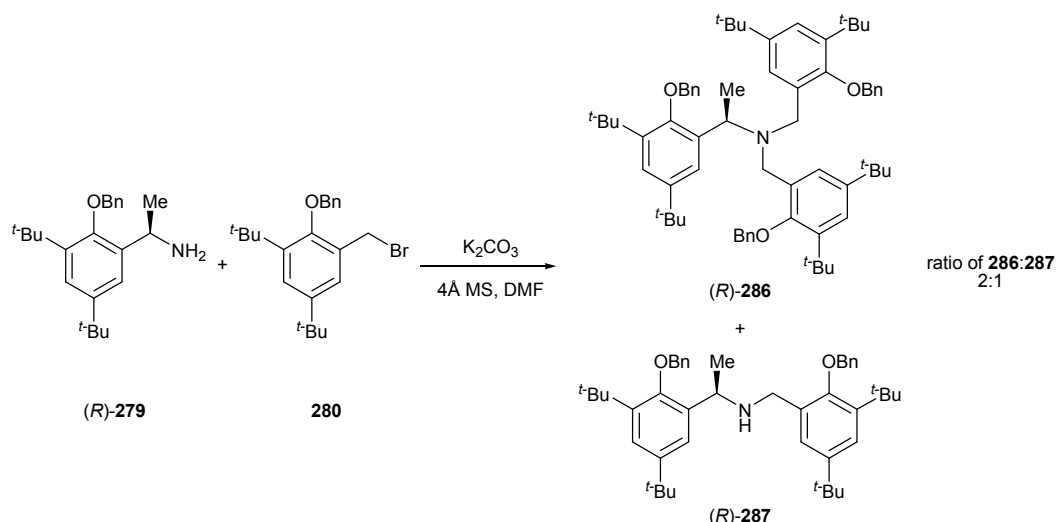


Scheme 149. Formation of the benzyl bromide **280**

The alcohol **285** was converted to the bromide **280** by treatment with phosphorus tribromide. The product was isolated in 95% yield without the need for further purification. The ^1H NMR spectrum showed the resonance relating to the methylene benzylic protons was now observed at $\delta = 4.62$ ppm. The benzyl bromide **280** was obtained in 93% overall yield from the aldehyde **282**.

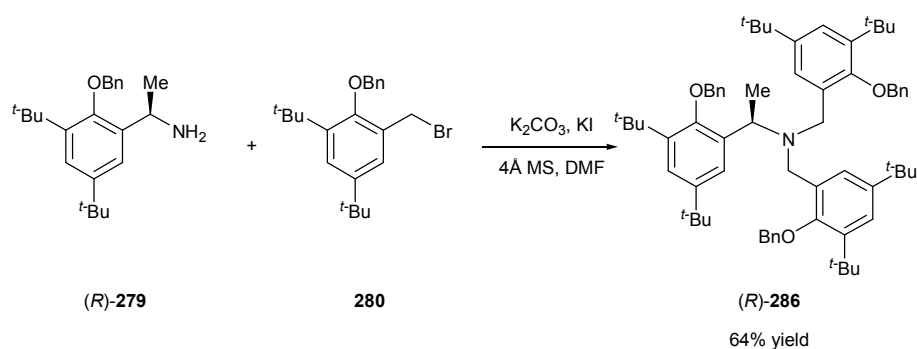
3.4.5 Formation of the tertiary amine (*R*)-**286**

Following the conditions that had successfully given the tertiary amines (*R*)-**266a** and (*R*)-**266b** (See Section 2.6.4), amine (*R*)-**279** was reacted with 2.5 equivalents of benzyl bromide **280** in the presence of potassium carbonate for 48 hours. After this time, analysis of the crude mixture by ^1H NMR analysis revealed that the reaction had not gone to completion, with both the tertiary amine (*R*)-**286** and the secondary amine (*R*)-**287** present in a ratio of *ca.* 2:1 (**Scheme 150**). It was reasoned that the increased steric bulk that the *tert*-butyl groups provided was to account for the incomplete reaction.



Scheme 150. Formation of tertiary and secondary amines (R)-**286** and (R)-**287**

It was found that the reaction of amine (R)-**279** with 3.5 equivalents of bromide **280** and five equivalents of potassium carbonate in the presence of one equivalent of potassium iodide was needed to force the reaction to completion (**Scheme 151**). The presence of the potassium iodide presumably allowed for a Finkelstein reaction to occur, where an equilibrium exchange of the benzylic bromide with the iodide was initiated. After 48 hours under these conditions no secondary amine was observed by analysis of the crude reaction mixture by TLC or 1H NMR spectroscopy. Following purification by column chromatography the desired tertiary amine (R)-**286** was isolated in 64% yield. The 1H NMR spectrum confirmed its structure with two resonances ($\delta = 3.75$ ppm and $\delta = 3.62$ ppm) corresponding to the two new benzylic methylene protons (**Figure 51**). Four sets of singlets were observed for the *ortho*- and *para-tert*-butyl groups at $\delta = 1.28$ ppm (equivalent to 18 protons), $\delta = 1.26$ ppm (9 protons), $\delta = 1.19$ ppm (9 protons) and $\delta = 1.18$ ppm (18 protons). High resolution mass spectrometry identified the molecular mass of $[M+H]^+$ as 956.6921 ($C_{67}H_{90}NO_3$ requires 956.6915). In the low resolution spectrum there were signals at 957 for the molecular ion and at 649 corresponding to the molecular ion with loss of one of the non-chiral arms.



Scheme 151. Formation of tertiary amine (*R*)-**286**

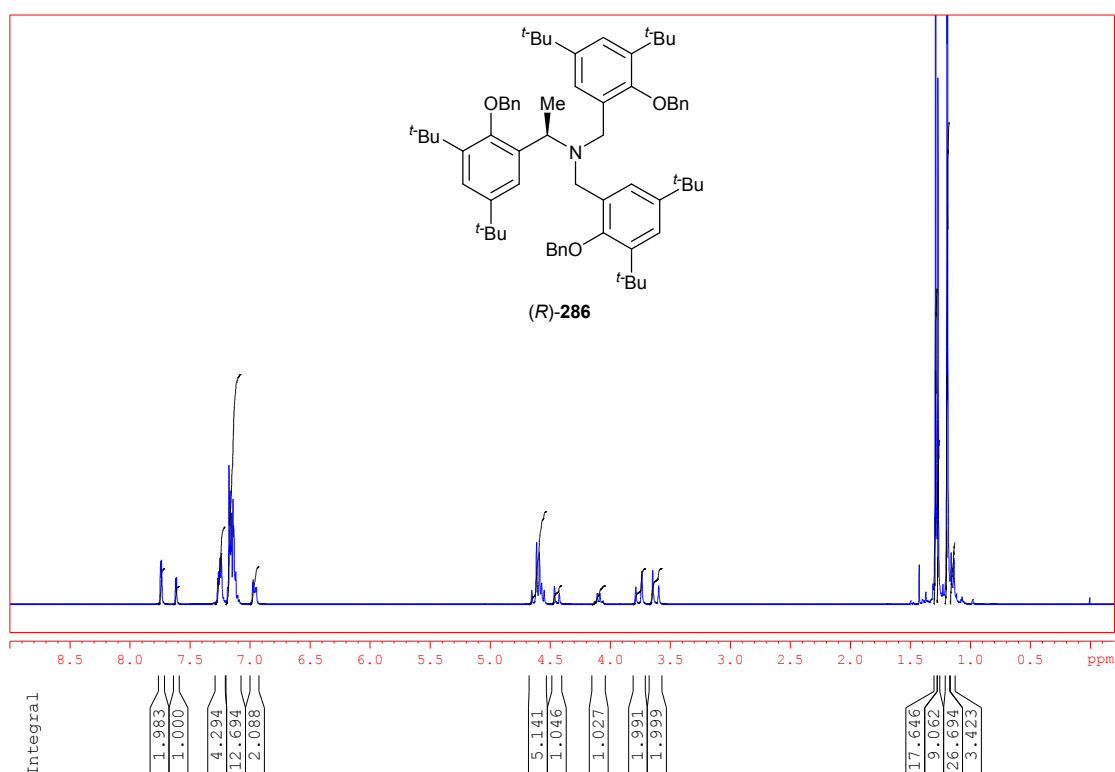
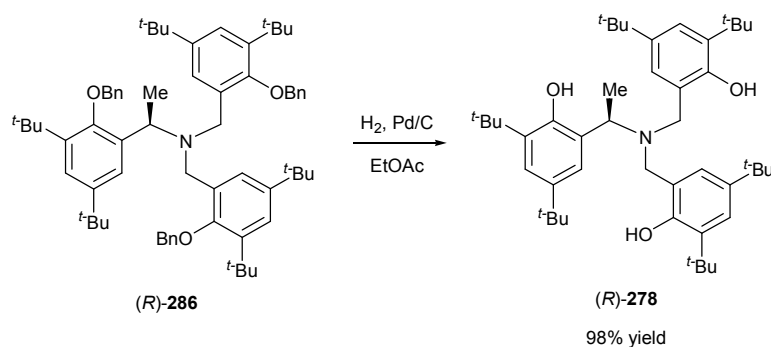


Figure 51. ^1H NMR (CDCl_3) spectrum of tertiary amine (*R*)-**286**

3.4.6 Deprotection of Tertiary Amine (*R*)-**286**

The cleavage of the benzyl protecting groups on amine (*R*)-**286**, was performed under the same conditions as before, with (*R*)-**286** stirred with 10% palladium on carbon in ethyl acetate under one atmosphere of hydrogen to give (*R*)-*N,N*-bis(2-(hydroxy)-3,5-di-*tert*-butylbenzyl)-1-(2-(hydroxy)-3,5-di-*tert*-butylphenyl)ethylamine **278** in 98% yield (**Scheme 152**). Its structure was confirmed by ^1H NMR spectroscopy with two resonances corresponding to the benzylic methylene group observed at $\delta = 3.93$ ppm and $\delta = 3.49$ ppm which were equivalent to two protons each (**Figure 52**). The methine proton adjacent to the chiral methyl group appeared

as a quartet at $\delta = 4.28$ ppm. The three phenolic protons were observed as broad singlet at $\delta = 6.59$ ppm. High resolution mass spectrometry identified the molecular mass of $[M+H]^+$ as 686.5509 ($C_{46}H_{72}NO_3$ requires 686.5507). In the low resolution spectrum there were signals at 686 for the molecular ion and at 454 corresponding to the molecular ion with loss of the chiral arm.



Scheme 152. Cleavage of the benzyl protecting groups of **(R)-286**

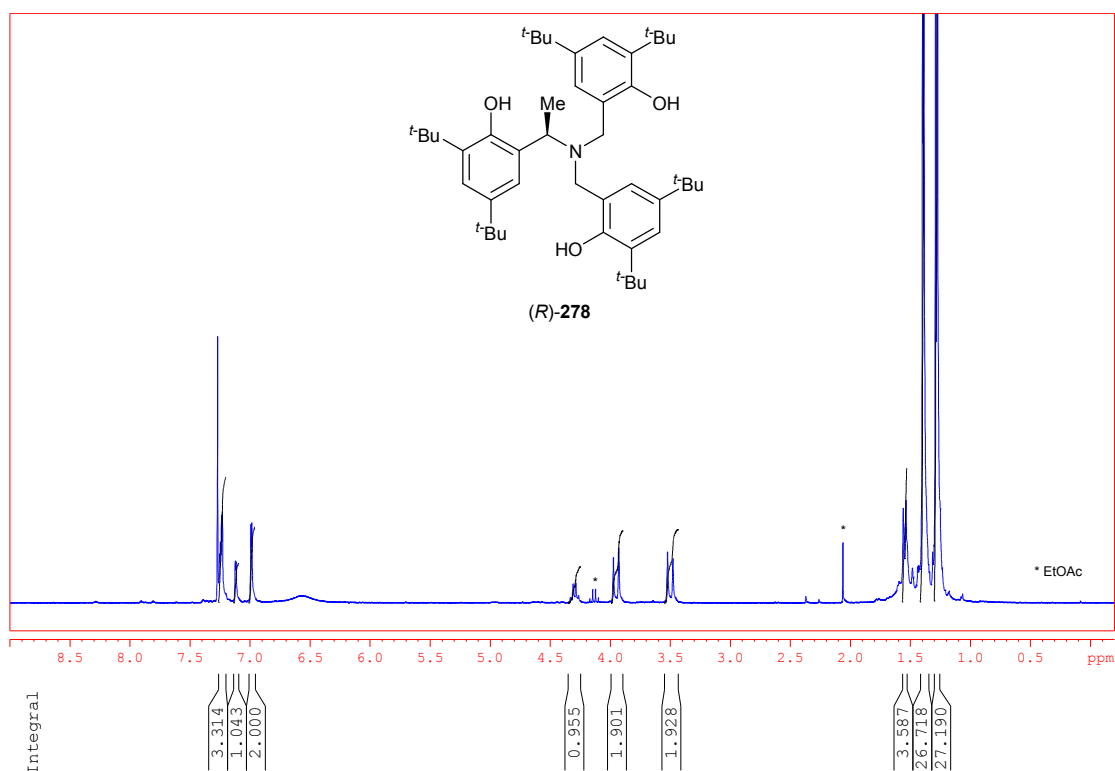
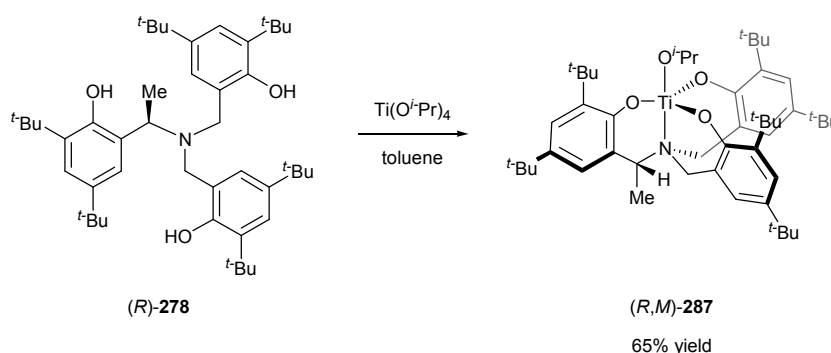


Figure 52. ^1H NMR (CDCl_3) spectrum of chiral ligand **(R)-278**

3.5 FORMATION OF TITANIUM COMPLEX (*R,M*)-287⁴

The reaction of ligand (*R*)-278 in toluene with titanium (IV) *iso*-propoxide followed by removal of the solvent gave the crude titanium *iso*-propoxide complex. After recrystallisation from hexane, the analytically pure complex (*R,M*)-287 was obtained as yellow crystals in 65% yield (**Scheme 153**). Analysis of its structure by ¹H NMR spectroscopy revealed a quartet and four AB doublets (two partially overlapped) between $\delta = 4.05$ ppm and $\delta = 3.10$ ppm (**Figure 53**). These resonances are similar to the ones that were observed for the *ortho*- and *para*-methyl substituted complex (*R,M*)-271 (*vide supra*). The signals were assigned to the two pseudoaxial and three pseudoequatorial benzylic protons of the ligand, with NOE spectroscopy establishing close proximity between the methyl protons and the two inequivalent pseudoaxial benzylic protons (**Figure 54**). Similarly the aromatic methine protons were also inequivalent with all six appearing as singlets between $\delta = 7.24$ ppm and $\delta = 6.93$ ppm. These observations are consistent with the predicted pseudoaxial orientation of the α -methyl group implying that in solution the complex exists as (*R,M*)-287.



Scheme 153. Formation of titanium tris(phenolate) *iso*-propoxide complex (*R,M*)-287

⁴ This work was conducted in collaboration with Dr. Matthew D. Jones

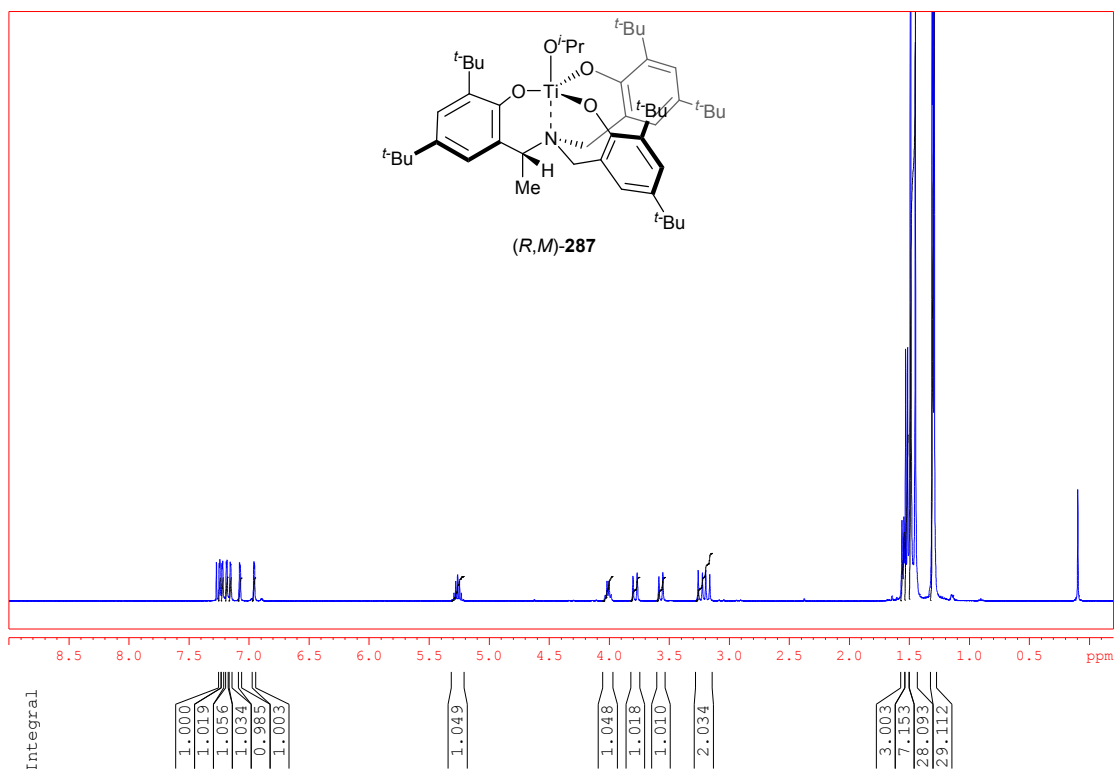


Figure 53. ^1H NMR (CDCl_3) spectrum of titanium complex (R,M) -**287**

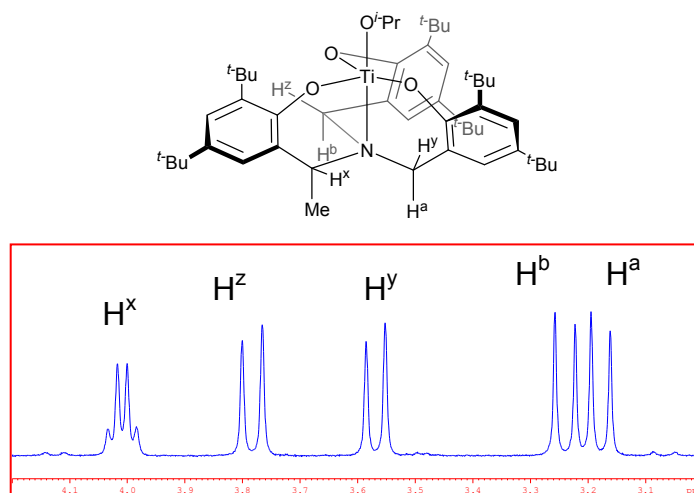


Figure 54. Expansion of ^1H NMR of titanium complex (R,M) -**287** showing the benzylic region

Following recrystallisation from hexane, an X-ray crystal structure of (R,M) -**287** was obtained and was consistent with the structure inferred in solution by ^1H NMR spectroscopy (**Figure 55**). The trigonal bipyramidal titanium centre is shown to be sitting centrally with all three phenolate oxygens being of similar lengths [Ti-O(phenolate) distances (\AA): Ti(1)-O(2) 1.786(2), Ti(1)-O(3) 1.836(2), Ti(1)-O(4) 1.848(2)]. Similarly the bond angles between the three phenolate oxygens are also similar to one another [bond angles between phenolate oxygen atoms ($^\circ$):

O(3)-Ti(1)-O(2) 116.4(10), O(3)-Ti(1)-O(4) 118.2(10), O(2)-Ti(1)-O(4) 120.6(10)]. The axial sites of the trigonal bipyramidal titanium centre are occupied by the apical nitrogen and the monodentate *iso*-propoxide anion, with a Ti-N bond length of 2.351(2) Å and a Ti-O^{*i*}Pr distance of 1.786(2) Å, and a bond angle between N(1)-Ti(1)-O(1) of 179.5(9)°. This is compared to a Ti-N bond length of 2.334(5) Å and a Ti-O^{*i*}Pr distance of 1.778(4) Å found in the crystal structure of (*rac*)-**194c**. In (*R,M*)-**287**, the titanium lies 0.2364(6) Å above the plane defined by the three oxygen atoms of the phenolate rings. The tilt of the aryl rings (as defined by the average angle between the aryloxy planes and the Ti-N bond vector) is 11°. This observed tilt of the aryl rings was greater than with (*R,M*)-**271** (the complex formed from the dimethyl substituted ligand (*R*)-**254a**), which had a tilt of 4°.

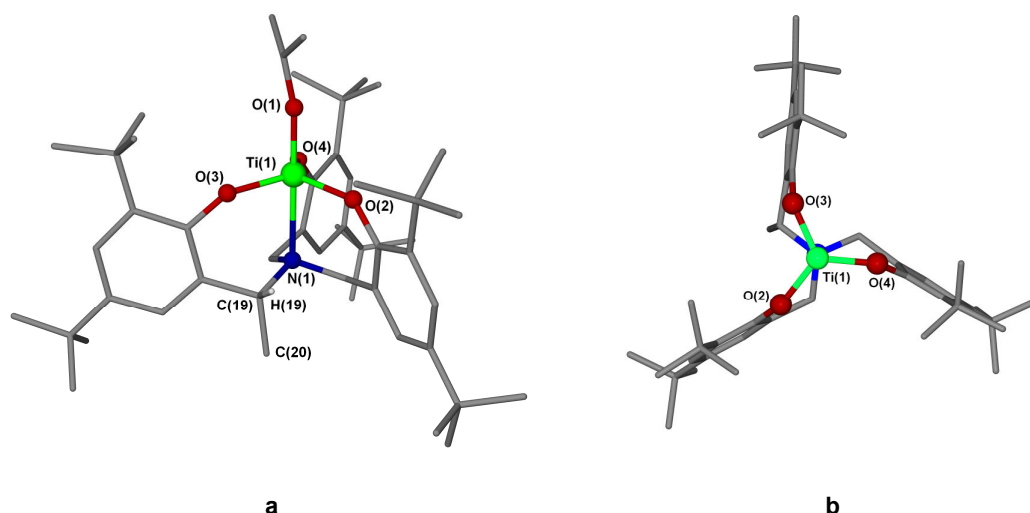


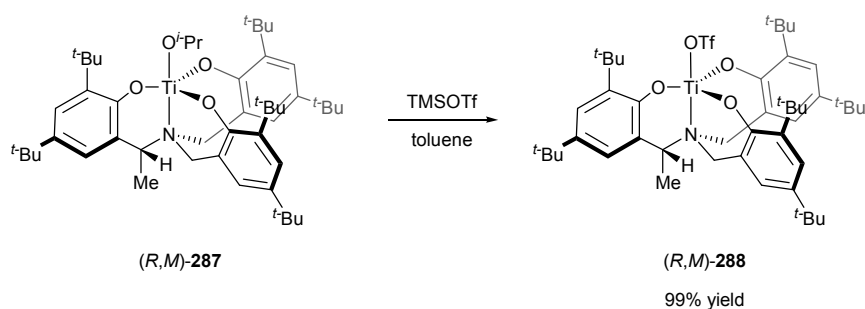
Figure 55. Side and top views (**a** and **b**) of the X ray crystal structure of (*R,M*)-**287**

3.6 FORMATION OF TITANIUM COMPLEX (*R,M*)-**288**⁵

Conversion of the titanium tris(phenolate) *iso*-propoxide complex (*R,M*)-**287** to the corresponding titanium tris(phenolate) triflate complex (*R,M*)-**288** was accomplished by treating (*R,M*)-**287** with trimethylsilyltriflate. The ¹H NMR spectrum of the product was similar to that of the starting complex. Notably the signals corresponding to the *iso*-propoxide ligand were no longer present. Again the signals for the benzylic protons of the tripodal ligand appeared as a quartet and four doublets

⁵ This work was conducted in collaboration with Dr. Matthew D. Jones

(two partially overlapped) between $\delta = 4.15$ ppm and $\delta = 3.40$ ppm. As before, the quartet at $\delta = 4.13$ ppm was assigned to the pseudoequatorial methine benzylic proton adjacent to the methyl substituent. The two doublets at $\delta = 3.93$ ppm and $\delta = 3.72$ ppm were due to the other two pseudoequatorial benzylic protons. The two pseudoaxial benzylic protons were observed as two partially overlapped doublets between $\delta = 3.53$ ppm and $\delta = 3.42$ ppm. A doublet at $\delta = 1.69$ ppm corresponded to the pseudoaxial α -methyl substituent. The *ortho*- and *para*-*tert*-butyl groups on the aryl rings appeared as singlets at $\delta = 1.45, 1.43, 1.40, 1.31, 1.30$ and 1.29 ppm. In the ^{13}C NMR spectrum there were signals at $\delta = 55.3, 54.7$ and 51.8 ppm which corresponded to the three benzylic carbons. High resolution mass spectrometry identified the molecular mass of $[\text{M}]^+$ as 879.4188 ($\text{C}_{47}\text{H}_{68}\text{F}_3\text{NO}_6\text{STi}$ requires 879.4193).



Scheme 154. Formation of titanium tris(phenolate) triflate complex (*R,M*)-**288**

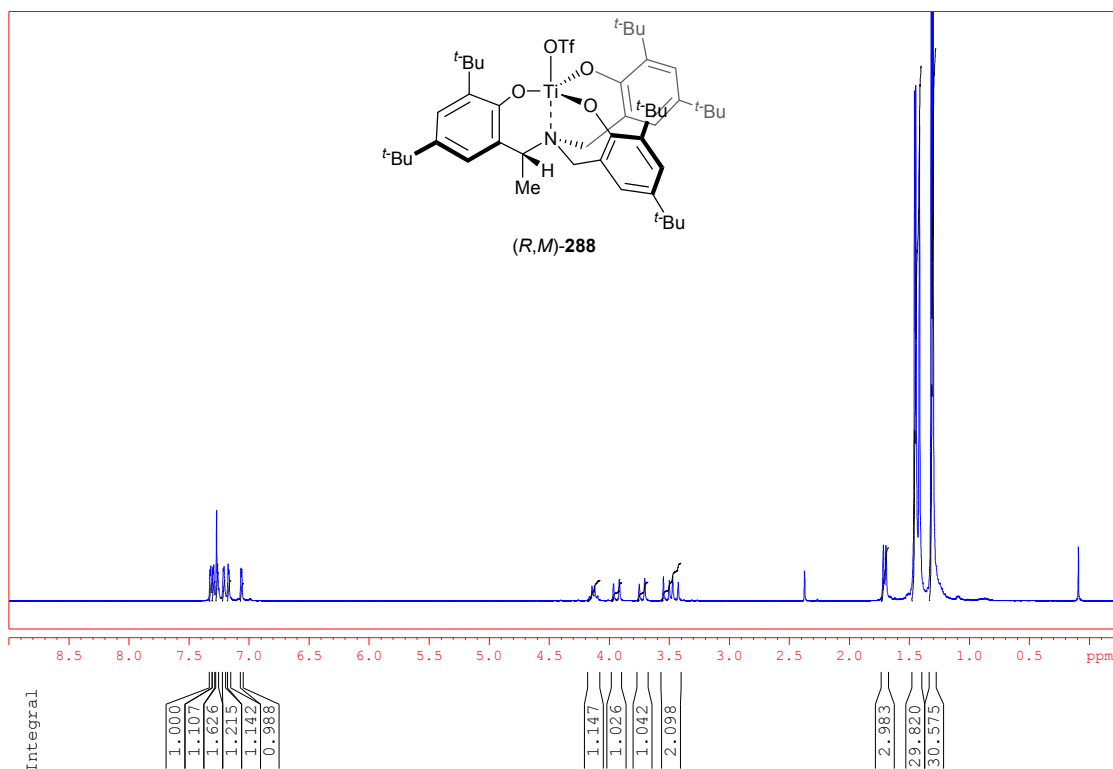
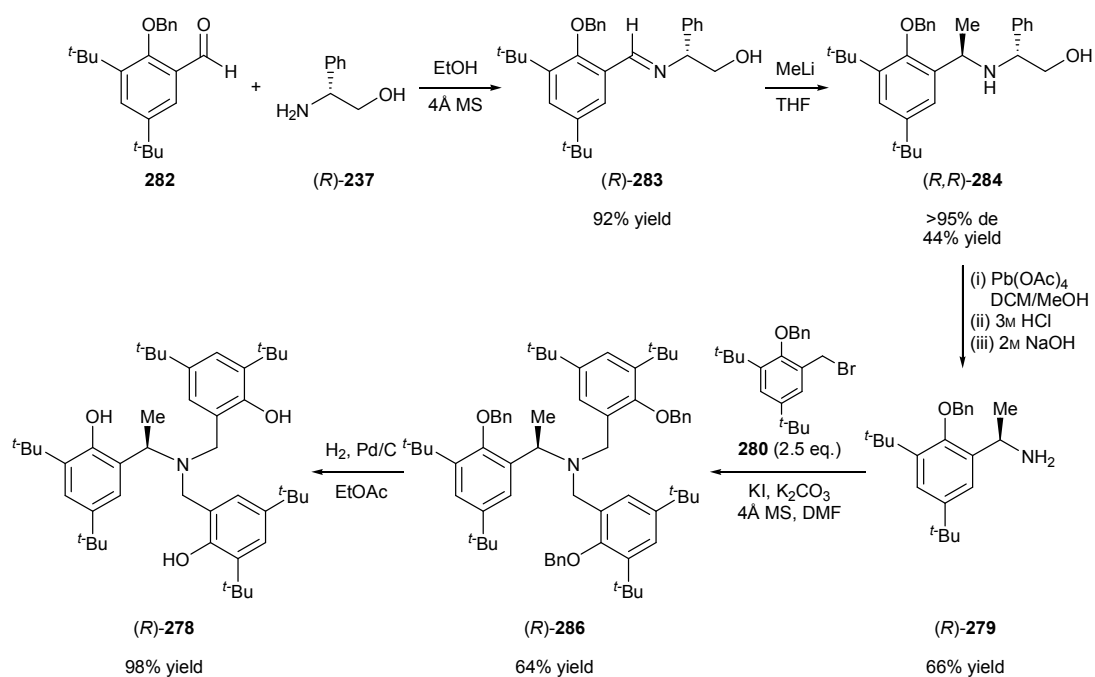


Figure 56. ^1H NMR (CDCl_3) spectrum of titanium complex (R,M) -**288**

3.7 CONCLUSION

The chiral ligand (R) -**254a** was successfully coordinated to titanium tetra-*iso*-propoxide to give titanium tris(phenolate) *iso*-propoxide complex (R,M) -**271**, which was also converted to the corresponding titanium tris(phenolate) triflate complex (R,M) -**272** by treatment with trimethylsilyltriflate. Both these complexes showed that the α -methyl substituent was successful in controlling the gait of the propeller-like conformation of the ligand. Disappointingly, both complexes failed to induce any stereocontrol in the addition of diethyl zinc to benzaldehyde **274a** or in the aza-Diels Alder reaction of *N*-benzylidenebenzylamine **204a** and Danishefsky's diene **205**. Consequently, the synthesis of the analogous di-*tert*-butyl substituted ligand (R) -**278** was completed *via* the protocol described in **Scheme 155**. As with the synthesis of (R) -**254a**, the synthesis involved asymmetric addition to imine (R) -**283** followed by deprotection of amine (R,R) -**284** with lead (IV) acetate. The ligand precursor (R) -**286** was obtained by bisalkylation of the primary amine (R) -**279** by the benzyl bromide **280**. The synthesis of the chiral ligand (R) -**278** was completed by hydrogenolytic deprotection of (R) -**286**, with the synthesis completed in 17% overall yield.



Scheme 155. Overall synthesis of chiral ligand *(R)*-**278**

As before, the coordination of ligand *(R)*-**278** to titanium (IV) *iso*-propoxide gave the titanium tris(phenolate) *iso*-propoxide complex *(R,M)*-**287**. Conversion of *(R,M)*-**287** to its titanium tris(phenolate) triflate complex *(R,M)*-**288** was accomplished by treatment with trimethylsilyltriflate. With both these complexes synthesised, the screening of these in other organic transformations was then conducted.

Chapter 4:

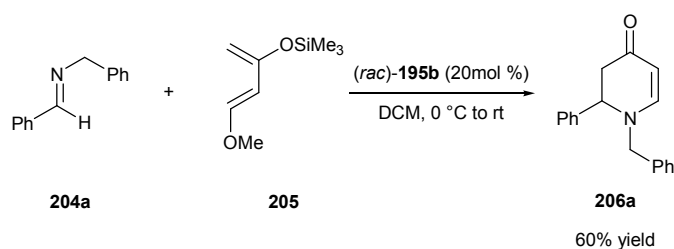
Results and Discussion III

4 Results and Discussion III

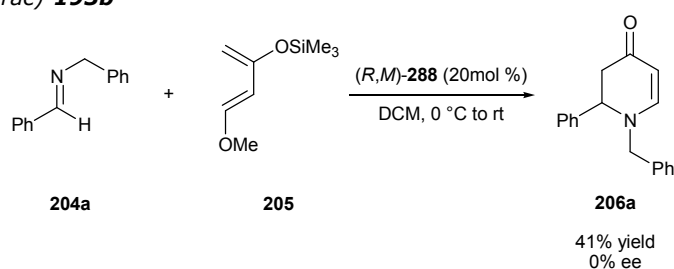
Having successfully synthesised a significant amount of the chiral titanium complex (*R,M*)-**288** the next step was to screen the complex as a possible catalyst in a number of organic transformations.

4.1 AZA-DIELS ALDER REACTION

As had been shown in the previous chapter (see Section 3.3.2), the 2,4-dimethylphenol derived ligand-titanium complex (*R,M*)-**272** had been shown to catalyse the aza-Diels Alder reaction between *N*-benzylidenebenzylamine **204a** and Danishefsky's diene **205** to give the dihydropyridinone product **206a** in 39% yield. It was decided to screen the racemic titanium triflate complex (*rac*)-**195b** alongside the chiral titanium triflate complex (*R,M*)-**288** in this reaction for comparison. Thus, to a solution of the imine **204a** and catalyst (either (*rac*)-**195b** or (*R,M*)-**288**) in dichloromethane was added three equivalents of Danishefsky's diene **205**. Both reactions were conducted at 0 °C and allowed to warm to room temperature overnight. After purification, the product was isolated from each of the crude mixtures in 60% yield and 41% yield respectively. Chiral HPLC analysis of the product **206a** obtained with catalyst (*R,M*)-**288** revealed it was racemic.



Scheme 156. Aza-Diels Alder between *N*-benzylidenebenzylamine **204a** and Danishefsky's diene **205** catalysed by (*rac*)-**195b**



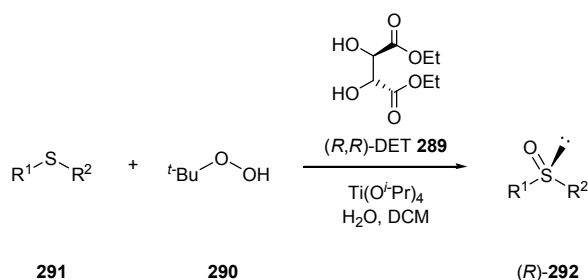
Scheme 157. Aza-Diels Alder between *N*-benzylidenebenzylamine **204a** and Danishefsky's diene **205** catalysed by (*R,M*)-**288**

4.2 SULFOXIDATION REACTION

Given that the chiral titanium complexes (*R,M*)-**287** and (*R,M*)-**288** went on to give promising results in the enantioselective oxidation of sulfides, there now follows a brief literature review on the titanium-catalysed asymmetric sulfoxidation reaction.

4.2.1 Titanium-Catalysed Asymmetric Oxidation of Sulfides

In 1984, two groups independently reported the enantioselective oxidation of unsymmetrical sulfides mediated by chiral titanium complexes.^{150, 151} Both protocols used titanium (IV) *iso*-propoxide and (*R,R*)-diethyl tartrate **289** in catalytic systems based upon the Sharpless reagent for asymmetric epoxidation of allylic alcohols. Kagan and co-workers found that employing the standard Sharpless conditions of titanium (IV) *iso*-propoxide, (*R,R*)-diethyl tartrate **289** and *tert*-butyl hydroperoxide **290** (in a ratio of 1:1:2) in the oxidation of methyl-*p*-tolyl sulfide **291a** yielded only the racemic sulfoxide product **292a** in 41% yield together with the over-oxidised sulfone product **293a** in 17% yield. However, the combination of titanium (IV) *iso*-propoxide, (*R,R*)-diethyl tartrate **289**, *tert*-butyl hydroperoxide **290** and water in a ratio of 1:2:2:1 gave (*R*)-methyl-*p*-tolyl sulfoxide **292a** in 90% yield and 91% ee (**Table 49**, entry 1).¹⁵² Under these conditions sulfone formation was negligible. A number of other aryl methyl sulfides were reacted to give the corresponding (*R*)-sulfoxides in 58-88% yields and 77-90% ee (entries 2 to 5). The variation of the alkyl moiety in aryl alkyl sulfides **291f-h** gave the products with much lower enantioselectivities (7-24% ee), when compared with the analogous aryl methyl sulfides (entries 6 and 7 versus entry 1 and entry 8 versus entry 3). The asymmetric oxidation of alkyl methyl sulfides **292i-j** was also possible under these conditions, giving the desired products in moderate enantioselectivities (entries 9 and 10).

**Scheme 158.** Asymmetric oxidation of sulfides **291** to sulfoxides (R)-**292****Table 49**

Entry	Sulfide	R ¹	R ²	Reaction conditions ^a	Yield /%	ee /%
1	291a	4-Me(C ₆ H ₄)	Me	-20 °C, 4 h ^b	90	91
2	291b	4-Br(C ₆ H ₄)	Me	-20 °C, 4 h	70	80
3	291c	2-naphthyl	Me	-20 °C, 4 h	88	90
4	291d	4-MeO(C ₆ H ₄)	Me	-21 °C, 15 h	58	86
5	291e	4-NO ₂ (C ₆ H ₄)	Me	-20 °C, 60 h	63	77
6	291f	4-Me(C ₆ H ₄)	<i>n</i> -Bu	-20 °C, 3 h ^b	75	20
7	291g	4-Me(C ₆ H ₄)	Bn	-20 °C, 12 h ^b	40	7
8	291h	2-naphthyl	<i>n</i> -Pr	-21 °C, 12 h	78	24
9	291i	cyclohexyl	Me	-21 °C, 18 h	67	54
10	291j	<i>t</i> -Bu	Me	-21 °C, 22 h	72	53

^a Reaction conditions: Ti(O^{*i*}Pr)₄ (100mol %), (R,R)-DET **289** (100mol %), TBHP **290** (110mol %) and H₂O (100mol %). ^b Reaction conditions as in ^a but with 200mol % of TBHP **290**

Similarly, Modena and co-workers reported the asymmetric oxidation of sulfides **291** using titanium (IV) *iso*-propoxide, (R,R)-diethyl tartrate **289** and *tert*-butyl hydroperoxide **290** in a ratio of 1:4:2.¹⁵⁰ The (R)-sulfoxides **292** were obtained in 41-99% yield and 14-88% ee. The enantiomeric excess obtained in the oxidation of methyl-*p*-tolyl sulfide **291a** (88%) was similar to that obtained by Kagan's system (91% ee).¹⁵²

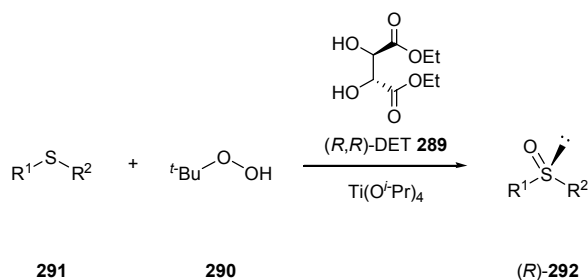
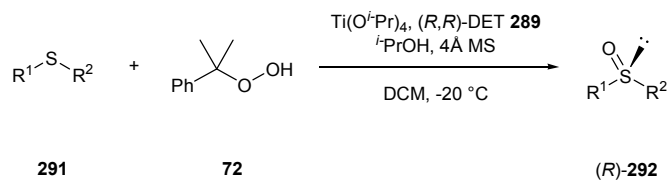
**Scheme 159.** Asymmetric oxidation of sulfides **291** to the corresponding (R)-sulfoxides **292**

Table 50

Entry	Sulfide	R ¹	R ²	Reaction conditions ^a	Yield /%	ee /%
1	291a	4-Me(C ₆ H ₄)	Me	toluene -20 °C, 24 h	46	65
2	291a	4-Me(C ₆ H ₄)	Me	1,2-dichloroethane -20 °C, 14 h	60	88
3	291k	Ph	^t Bu	toluene -20 °C, 30 h	99	35
4	291l	4-Cl(C ₆ H ₄)	CH ₂ CH ₂ OH	toluene -20 °C, 24 h	41	14
5	291m	Bn	Me	DCM -77 °C, 24 h	70	46

^a Reaction conditions: Ti(O^{*i*}Pr)₄ (100mol %), (*R,R*)-DET **289** (400mol %), TBHP **290** (200mol %).

In 1996, Kagan and co-workers discovered that the addition of 4 mol equivalence of *iso*-propanol to the Modena system gave a complex that could be used in catalytic quantities.¹⁵³ In the oxidation of methyl-*p*-tolyl sulfide **291a** by cumyl hydroperoxide **72**, the use of 10mol % of a combination of Ti(O^{*i*}Pr)₄/*(R,R)*-DET/^{*i*}PrOH (1:4:4) was found to give (*R*)-methyl-*p*-tolyl sulfoxide **292a** in 77% yield and 96% ee (entry 1). The reaction required the presence of 4Å molecular sieves. A number of other aryl methyl sulfides reacted to give the corresponding (*R*)-sulfoxides with >90% ee (entries 2-4). The oxidation of benzyl methyl sulfide **292o** proceeded in 90% ee (entry 5). Also (*R*)-methyl-*n*-octyl sulfoxide **292p** could be formed in moderate enantiomeric excess (71% ee, entry 6), however, this is lower than was obtained with the stoichiometric procedure (85% ee).¹⁵²

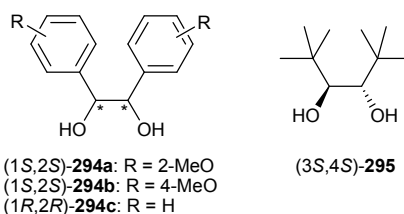
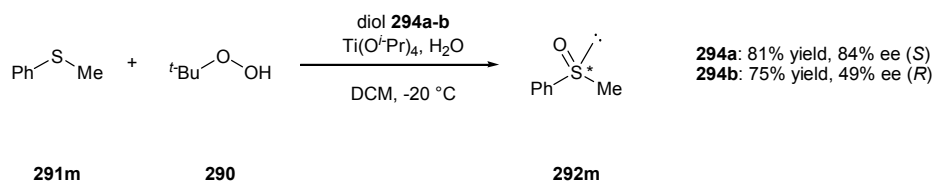


Scheme 160. Catalytic asymmetric sulfoxidation of sulfides **291**

Table 51

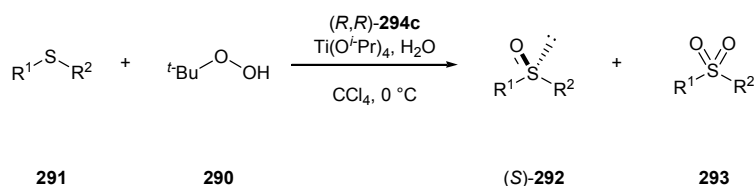
Entry	Sulfide	R ¹	R ²	Yield /%	ee /%
1	291a	4-Me(C ₆ H ₄)	Me	77	96
2	291m	Ph	Me	81	91
3	291d	4-MeO(C ₆ H ₄)	Me	73	92
4	291n	4-Me(C ₆ H ₄)	Et	68	78
5	291o	Bn	Me	72	90
6	291p	<i>n</i> -Octyl	Me	69	71

In 1989 Yamamoto *et al.* reported the application of both 1,2-bis(2-methoxyphenyl)ethane-1,2-diol **294a** and 1,2-bis(4-methoxyphenyl)ethane-1,2-diol **294b** in the titanium catalysed oxidation of thioanisole **291m** (Figure 57, Scheme 161).¹⁵⁴ The reaction was performed in the presence of stoichiometric amounts of Ti(O^{*i*}-Pr)₄/diol/H₂O (1:2:1) giving the (*S*)-sulfoxide product **292m** in 81% yield and 84% ee when diol **294a** was used. Interestingly, use of diol **294b** under identical reaction conditions gave an inversion in the stereochemistry, with (*R*)-sulfoxide **292m** obtained in 75% yield and 49% ee.

Figure 57. Chiral 1,2-diols **294a-c** and **295**Scheme 161. Titanium catalysed oxidation of phenyl methyl sulfide **291m**

The use of the complex formed from titanium (IV) *iso*-propoxide, (*R,R*)-diphenylethane-1,2-diol **294c** and water in the asymmetric oxidation of aryl alkyl and aryl benzyl sulfides was reported by Rosini and co-workers (Scheme 162, Table 52).^{155, 156} Optimum reaction conditions were 5mol % of a combination of Ti(O^{*i*}-Pr)₄/*(R,R)*-**293c**/H₂O (1:2:20), together with two equivalence of *tert*-butyl hydroperoxide **290** (70% in water) in CCl₄ for two hours. Under these conditions

(*S*)-methyl-*p*-tolyl sulfoxide **292a** was obtained in 62% yield and 80% ee, together with the undesired sulfone **293a** in 8% yield (entry 1). It was found that extending the reaction time resulted in the decomposition of the diol together with an increase in the formation of sulfone, without raising the yield or enantiomeric excess of the sulfoxide product. A number of sulfides were screened, with the oxidation of aryl benzyl sulfides **291g**, **291q** and **291r** giving the best results, delivering the (*S*)-sulfoxide in 92-99% ee (entries 4-6).



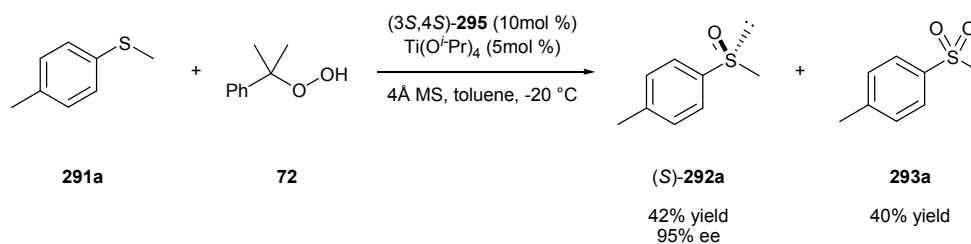
Scheme 162. Asymmetric oxidation of sulfides **291** giving (*S*)-sulfoxides **292**

Table 52

Entry	Sulfide	R ¹	R ²	Yield sulfoxide /% ^a	ee /%
1	291a	4-Me(C ₆ H ₄)	Me	62	80
2	291c	2-naphthyl	Me	65	73
3	291d	4-MeO(C ₆ H ₄)	Me	55	69
4	291g	4-Me(C ₆ H ₄)	Bn	65	98
5	291q	Ph	Bn	73	99
6	291r	4-MeO(C ₆ H ₄)	Bn	60	92

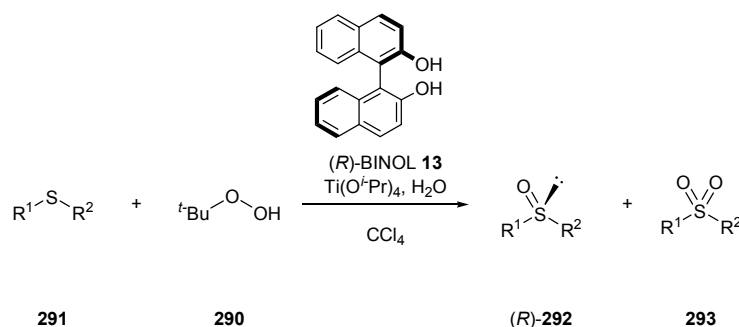
^a Yield of corresponding sulfoxide <10%.

The synthesis and application of (3*S*,4*S*)-2,2,5,5-tetramethyl-3,4-hexanediol **295** in the titanium catalysed sulfoxidation reaction was reported by Imamoto and co-workers.¹⁵⁷ The reaction of methyl-*p*-tolyl sulfide **291a** with cumyl hydroperoxide **72**, in the presence of the titanium complex prepared *in situ* from Ti(O^{*i*}Pr)₄ and **295**, yielded the (*S*)-sulfoxide **292a** in 42% yield and 95% ee together with the sulfone **293a** in 40% yield (**Scheme 163**). Kinetic studies revealed that following the asymmetric oxidation of the initial sulfide there was a kinetic resolution of the sulfoxide. These two processes worked in a cooperative fashion to enhance the enantioselectivity, since preferential oxidation of the (*R*)-sulfoxide to sulfone took place.



Scheme 163. Asymmetric oxidation of methyl-*p*-tolyl sulfide **291a**

In 1992 Uemura *et al.* first reported that (*R*)-BINOL **13** could be used in conjunction with titanium (IV) *iso*-propoxide in the oxidation of methyl-*p*-tolyl sulfide **291a** (Scheme 164).¹⁵⁸ The use of 10mol % of a combination of Ti(O^{*i*}Pr)₄/*R*-BINOL **13**/H₂O (1:2:20) in toluene at -20 °C, together with *tert*-butyl hydroperoxide **290**, delivered the (*R*)-sulfoxide **292a** in 88% yield and 73% ee. In a later publication the scope of their catalytic system was explored.¹⁵⁹ It was found that running the reaction at room temperature in carbon tetrachloride with 2.5mol % of the catalyst together with 70% aqueous *tert*-butyl hydroperoxide **290** gave (*R*)-methyl-*p*-tolyl sulfoxide **292a** in 44% yield and 96% ee (Table 53, entry 1). It was found that the high enantioselectivity was due to the simultaneous kinetic resolution of the sulfoxide formed in the initial step. It was estimated that (*R*)-methyl-*p*-tolyl sulfoxide was formed in only 50% ee through the enantioselective oxidation of the starting sulfide. The screening of other aryl methyl sulfides also gave the corresponding sulfoxides in high enantioselectivity (entries 2 and 3). However the reaction of methyl-*n*-octyl sulfide **291p** proceeded to give the (*R*)-sulfoxide **292p** in only 64% yield and 69% ee (entry 4).



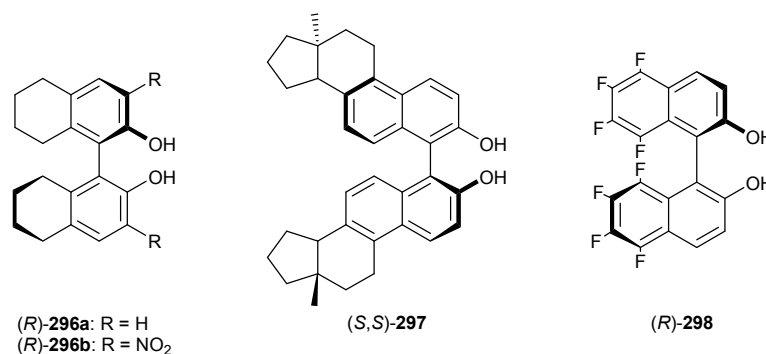
Scheme 164. Use of (*R*)-BINOL **13** in the enantioselective oxidation of sulfides **291**

Table 53^a

Entry	Sulfide	R ¹	R ²	Temp /°C	Time /h	Yield sulfoxide /%	ee /%
1	291a	4-Me(C ₆ H ₄)	Me	25	9	44	96
2	291b	4-Br(C ₆ H ₄)	Me	25	10	39	96
3	291m	Ph	Me	25	9	28	96
4 ^b	291p	<i>n</i> -octyl	Me	0	31	64	69

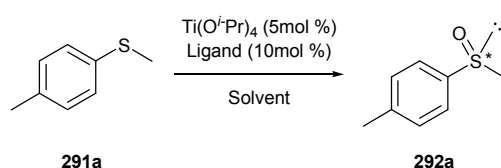
^aReaction conditions: (*R*)-BINOL **13** (5mol %), Ti(O^{*i*}Pr)₄ (2.5mol %) and H₂O (50mol %); ^bReaction conditions: (*R*)-BINOL **13** (20mol %), Ti(O^{*i*}Pr)₄ (10mol %) and H₂O (200mol %).

A number of other BINOL analogues have also been utilised in the titanium catalysed sulfoxidation reaction, including the octahydro- and dinitrooctahydro-derivatives **296a** and **296b**, the steroid-derived BINOL derivative **297** and the octafluoro-derivative **298** (Figure 58). For example, Reetz and co-workers compared the efficiency of both octahydrobinaphthol (*R*)-**296a** and 3,3'-dinitrooctahydrobinaphthol (*R*)-**296b** in the oxidation of methyl-*p*-tolyl sulfide **291a** under similar conditions employed by Uemura (5mol % of titanium (IV) *iso*-propoxide and 10mol % of ligand together with two equivalents of both water and cumene hydroperoxide **72**) (Scheme 165).¹⁶⁰ Performing the reaction in toluene at 0 °C with ligand (*R*)-**296a** yielded the (*R*)-sulfoxide product **292a** in 10% ee (Table 54, entry 1). In comparison, use of dinitrooctahydro-derivative (*R*)-**296b** in CCl₄ led to the preferential formation of the (*S*)-sulfoxide **292a** in 52% yield and 86% ee (entry 2). The reason for the reversal of enantioselectivity of the reaction when switching from ligand (*R*)-**296a** and (*R*)-**296b** was not reported.

Figure 58. BINOL derivatives **296a-b**, **297** and **298**

In 1999, Bolm *et al.* reported the use of the previously reported BINOL analogue (*S,S*)-**297** prepared from equilenine. In the reaction of methyl-*p*-tolyl sulfide **291a** with *tert*-butyl hydroperoxide **290** (1.1 equivalents) in THF, in the presence of water

(3 equivalents) the (*S*)-sulfoxide product **292a** was obtained in 63% yield and 86% ee (**Table 54**, entry 3).¹⁶¹ Similarly, the use of the octafluoro-binaphthol (*R*)-**298** in the sulfoxidation of methyl-*p*-tolyl sulfide **291a** was reported by Yudin and co-workers.¹⁶² They found that reaction of the sulfide with cumene hydroperoxide **72** (1.2 equivalents) in chloroform gave the (*S*)-sulfoxide product **292a** in 55% yield and 80% ee (entry 4). The preference for the formation of (*S*)-sulfoxide product is in contrast to the work of Uemura and co-workers who showed that use of (*R*)-BINOL **13** led to the formation of the (*R*)-sulfoxide (*vide supra*).^{158, 159} The authors speculated that the change in enantioselectivity was as a result of differences in aggregation of the catalytically active species.

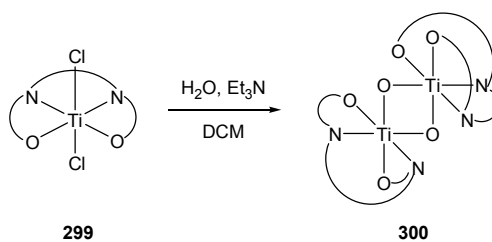
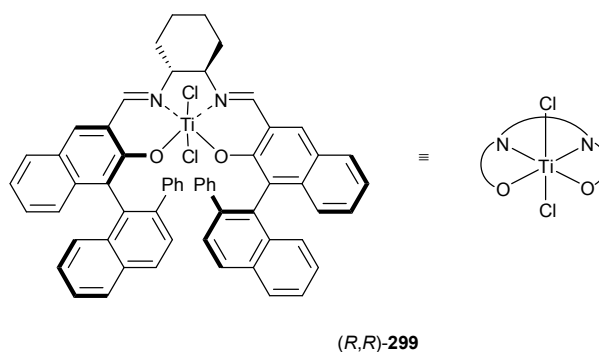


Scheme 165. Catalytic asymmetric sulfoxidation using BINOL derivatives **296a-b**, **297** and **298**

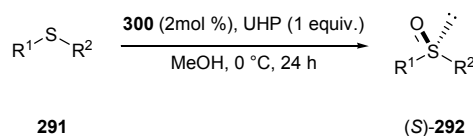
Table 54

Entry	Ligand	Conditions	Solvent	Temp /°C	Yield sulfoxide /%	ee /%	Ref
1	296a	H ₂ O (2 eq.)	Toluene	0	NR	10 (<i>R</i>)	160
2	296b	CHP (2 eq.)	CCl ₄		52	86 (<i>S</i>)	
3	297	H ₂ O (3 eq.) TBHP (1.1 eq.)	THF	0	63	86 (<i>S</i>)	161
4	298	H ₂ O (2 eq.) CHP (1.2 eq.)	CHCl ₃	rt	55	80 (<i>S</i>)	162

The use of (*R,R*)-di- μ -oxo-titanium(salen) complex **300** in the asymmetric oxidation of various sulfides with urea hydrogen peroxide was reported by Katsuki *et al.*^{163, 164} The di- μ -oxo species **300** was prepared from reaction of the parent (salen)titanium (IV) complex (*R,R*)-**299** with water in the presence of triethylamine (**Scheme 166**). The reaction of methyl aryl sulfides, **291a**, **291b** and **291e**, with one equivalent of urea hydrogen peroxide in the presence of 2mol % of **300** yielded the corresponding (*S*)-sulfoxides in 78-93% yield and 92-96% ee (**Scheme 167**, **Table 55**, entries 1-3). Similarly, oxidation of benzyl methyl sulfide **291o** and ethyl phenyl sulfide **291s** gave the desired products in 72% and 91% yield respectively, with an enantioselectivity 93% in both cases (entries 4 and 5).



Scheme 166. Formation of (*R,R*)-di- μ -oxo Ti(*salen*) **300** catalyst from (*salen*)titanium (IV) complex (*R,R*)-**299**



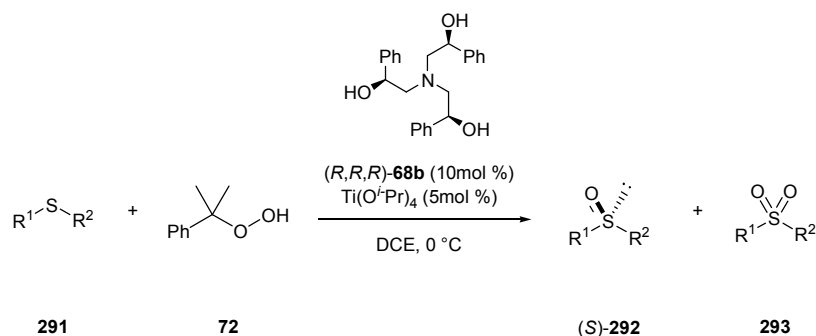
Scheme 167. Asymmetric sulfoxidation of sulfides **291** with urea hydrogen peroxide catalysed by (*R,R*)-di- μ -oxo Ti(*salen*) **300**

Table 55

Entry	Sulfide	R ¹	R ²	Yield I%	ee I%
1	291a	4-MeO(C ₆ H ₄)	Me	78	96
2	291b	4-Br(C ₆ H ₄)	Me	93	96
3	291e	4-NO ₂ (C ₆ H ₄)	Me	92	92
4	291o	Bn	Me	72	93
5	291s	Ph	Et	91	93

The use of the *C*₃-symmetric chiral trialkanolamine (*R,R,R*)-**68b** in the titanium catalysed sulfoxidation has also been reported.⁴⁹ In this work, Licini and co-workers found employing 5mol % of titanium (IV) *iso*-propoxide and 10mol % of ligand **68b** with one equivalent of cumyl hydroperoxide **72** in 1,2-dichloroethane gave the desired (*S*)-sulfoxide product together with the over-oxidised sulfone product (**Scheme 168**). For example, reaction of methyl-*p*-tolyl sulfide **291a** yielded (*S*)-methyl-*p*-tolyl sulfoxide **292a** in 45% ee and methyl-*p*-tolyl sulfone **293a** in a

ratio of 62:38 (**292:293**) (**Table 56**, entry 1). Kinetic studies revealed that methyl-*p*-tolyl sulfone **293a** is formed from the outset of the reaction and that the two different asymmetric processes involved, the asymmetric oxidation of the sulfide to the sulfoxide and the kinetic resolution *via* oxidation of the sulfoxide to sulfone, worked in tandem to improve the enantioselectivity of the sulfoxide product. It was shown that the (*S*)-sulfoxide **292a** was formed in 29% ee when almost no sulfone was present. The screening of other aryl methyl sulfides showed that the electronic effect of the aryl substituents had a significant effect on the enantioselectivity with the electron withdrawing *para*-nitro substituted sulfide **291e** giving the corresponding (*S*)-sulfoxide **292e** in only 15% ee (entry 4). The best result was obtained with benzyl phenyl sulfide **291q** with the sulfoxide (*S*)-**292q** obtained in 84% ee and a ratio of sulfoxide to sulfone of 77:23 (entry 7).



Scheme 168. Titanium catalyzed asymmetric oxidation of sulfides **291** using trialkanolamine (*R,R,R*)-**68b**

Table 56

Entry	Sulfide	R ¹	R ²	Yield /%	292:293	ee /%
1	291a	4-Me(C ₆ H ₄)	Me	98	62:38	45
2	291c	2-Naphthyl	Me	86	60:40	38
3	291d	4-MeO(C ₆ H ₄)	Me	94	68:32	41
4	291e	4-NO ₂ (C ₆ H ₄)	Me	88	26:74	15
5	291n	4-Me(C ₆ H ₄)	Et	99	64:36	38
6	291k	Ph	<i>t</i> -Bu	98	60:40	60
7	291q	Ph	Bn	94	77:23	84

Summary

This brief review on titanium-catalysed oxidations of sulfides has shown that a variety of conditions were employed with the different catalytic systems. The most

common organic peroxides used in these reactions appear to be *tert*-butyl hydroperoxide **290** or cumene hydroperoxide **72**, with reactions that were conducted in aqueous media using hydrogen peroxide or urea hydrogen peroxide. Where organic peroxides were employed as the oxidant, reactions typically performed best in chlorinated solvents, such as dichloromethane, 1,2-dichloroethane and carbon tetrachloride, or non-chlorinated solvents, such as toluene and benzene. Typical reaction temperatures ranged from -77 °C to room temperature, with a number of catalytic systems working optimally at *ca.* -20 °C. For some of the catalytic systems additives such as water, alcohols or molecular sieves were also found to improve the efficiency of the reaction.

4.3 SULFOXIDATION REACTION CATALYSED BY (RAC)-195B, (R,M)-287 AND (R,M)-288

It was decided that before any initial investigations into the screening of titanium complexes (R,M)-**287** and (R,M)-**288** were conducted, the screening of the parent titanium complex (rac)-**195b** would first be performed (**Figure 59**). As a starting point, benzyl phenyl sulfide **291q** was chosen as a model substrate due to its commercial availability. But before any screening reactions could commence, it was first necessary to prepare an authentic sample of benzyl phenyl sulfoxide **292q** for comparison.

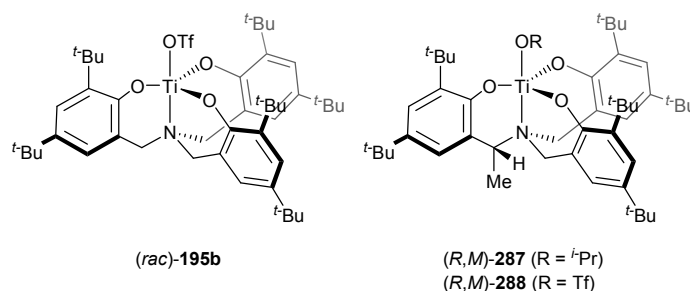
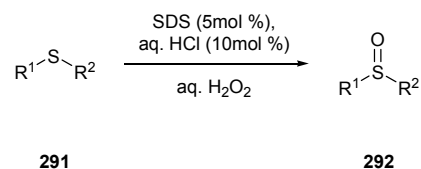


Figure 59. Titanium complexes (*rac*)-**195b**, (*R,M*)-**287** and (*R,M*)-**287**

4.3.1 Synthesis of Racemic Benzyl Phenyl Sulfoxide (*rac*)-**292q**

A search through the literature for the oxidation of sulfides to their racemic sulfoxides revealed a number synthetic procedures were available. However, a recent protocol that used aqueous hydrogen peroxide and sodium dodecyl sulphate to

oxidise sulfides to sulfoxides, in the absence of any organic co-solvent and under metal-free conditions, was chosen to do this. Firouzabadi and co-workers showed that dodecyl hydrogen sulphate, generated *in situ* from protonation of the dodecyl sulphate anion, catalysed the oxidation of sulfides **291** to their corresponding sulfoxides **292** in high yields (**Scheme 169**, **Table 57**).¹⁶⁵

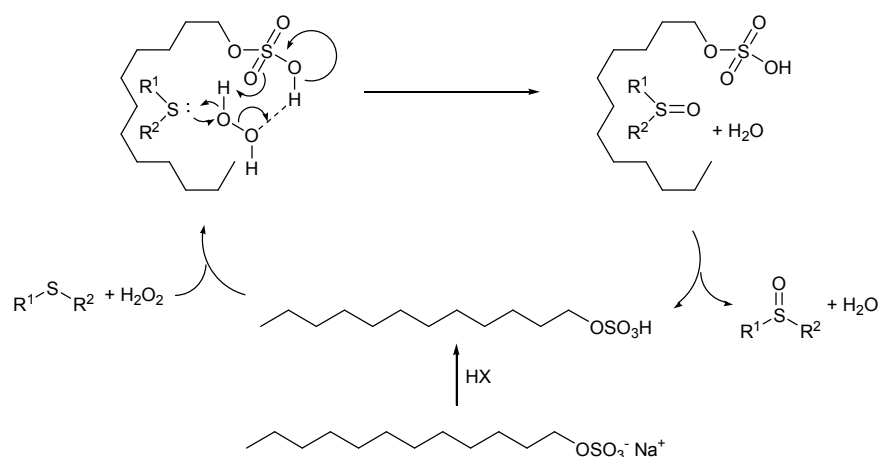


Scheme 169. Oxidation of sulfides **291** to sulfoxides **292** by hydrogen peroxide catalysed by sodium dodecyl sulphate

Table 57

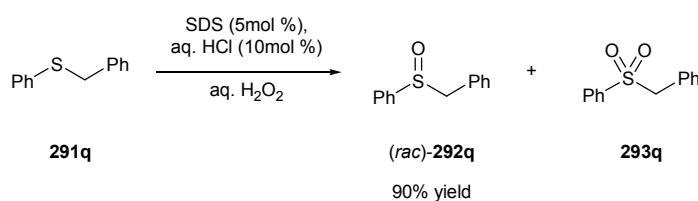
Entry	Sulfide	R ¹	R ²	Time /min	Yield /%
1	291m	Ph	Me	5	92
2	291q	Ph	Bn	5 h	91
3	291t	<i>n</i> -Bu	<i>n</i> -Bu	5	88
4	291u	CH ₂ =CHCH ₂ -	-CH ₂ CH=CH ₂	5	85
5	291v	Bn	-CH ₂ CH ₂ OH	10	93
6	291w	Ph	-CH ₂ CH ₂ C(O)CH ₃	10	90
7	291x	Ph	-CH ₂ CH ₂ CN	10	92

The authors proposed that the reaction proceeds by proton transfer from the strong acid to the dodecyl sulphate anion to form dodecyl hydrogen sulphate (**Scheme 170**). This *in situ* generated Brønsted acid surfactant shows dual activity. Firstly, the non-polar tail wraps round the sulfide molecule which also acts to bring the peroxide molecule close to the sulphur atom. After this process, the reaction proceeds *via* activation of hydrogen peroxide by hydrogen bonding between R-OSO₃H and H₂O₂ in the vicinity of the sulphur atom.



Scheme 170. Proposed catalytic role of *in situ* generated dodecyl hydrogen sulphate, for the activation of hydrogen peroxide by ROSO_3H and solubilisation of the lipophilic organic sulfide by its hydrocarbon tail

This method was applied to the synthesis of benzyl phenyl sulfoxide (*rac*)-**292q**. Thus, benzyl phenyl sulfide **291q** was treated with four equivalents of aqueous hydrogen peroxide, in the presence of sodium dodecyl sulphate and aqueous hydrochloric acid, until all the starting sulfide had been consumed (as determined by TLC). Analysis of the crude product by ^1H NMR spectroscopy showed that the major product to form was the sulfoxide **292q** together with a small quantity of the sulfone **293q** (ratio of **292**:**293** was 95:5). Following purification by column chromatography, the desired racemic sulfoxide **292q** was obtained in 90% yield. Its structure was confirmed by comparison of its ^1H NMR spectrum with the literature, with the two benzylic protons appearing as doublets at $\delta = 4.02$ and 3.93 ppm (**Scheme 171**).¹⁶⁶

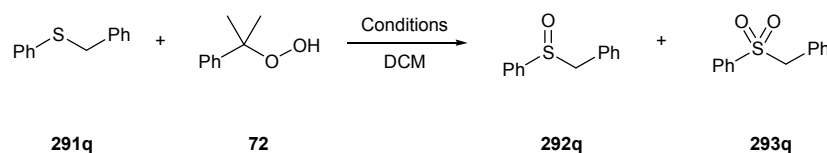


Scheme 171. Oxidation of benzyl phenyl sulfide **291q** to benzyl phenyl sulfoxide **292q** by hydrogen peroxide in the presence of dodecyl hydrogen sulphate

4.3.2 Screening of (*rac*)-**195b** in the Oxidation of Benzyl Phenyl Sulfide **291q**

For screening of the parent titanium complex (*rac*)-**195b**, the reactions were performed in dichloromethane since this had proven to be one of the best solvent systems for a number of other titanium-based catalysts (*vide supra*). Similarly, the

oxidant chosen to be used in this screening was cumene hydroperoxide **72**. The reaction was first run with 10mol % of (*rac*)-**195b** and one equivalent of cumene hydroperoxide **72** at -30 °C (**Scheme 172**, **Table 58**). After twenty-four hours the reaction was worked up and the crude reaction mixture was analysed by ¹H NMR spectroscopy. This revealed that the desired product, benzyl phenyl sulfoxide **292q**, had been obtained in only 16% conversion (entry 2). Increasing the number of equivalents of cumene hydroperoxide **72** to two gave the product in an improved conversion of 29% (entry 3). In both of these reactions no over-oxidation of the sulfoxide **292q** to the sulfone **293q** was observed. When the reaction was run with two equivalents of cumene hydroperoxide without any catalyst present, the sulfoxide product was observed in less than 5% conversion without any sulfone present (entry 1). This indicated that the titanium complex (*rac*)-**195b** was catalysing the reaction. Running the reaction at room temperature for 24 hours, in the presence of 10mol % of catalyst and two equivalents of cumene hydroperoxide, increased the conversion to 61%, however analysis of the crude reaction mixture revealed that both the sulfoxide **292q** and sulfone **293q** were present in a ratio of 93:7 in favour of the sulfoxide (entry 4).



Scheme 172. Screening of titanium catalyst (*rac*)-**195b** in the oxidation of benzyl phenyl sulfide **291q** with cumene hydroperoxide **72**

Table 58

Entry	Catalyst	Conditions	Temp /°C	Conversion /%	Ratio 292:293
1	none	CHP 72 (2 eq.)	-30	<5	no sulfone
2	(<i>rac</i>)- 195b (10mol %)	CHP 72 (1 eq.)	-30	16	no sulfone
3	(<i>rac</i>)- 195b (10mol %)	CHP 72 (2 eq.)	-30	29	no sulfone
4	(<i>rac</i>)- 195b (10mol %)	CHP 72 (2 eq.)	rt	61	93:7

4.3.3 Screening of (*R,M*)-**287** and (*R,M*)-**288** in the Oxidation of Benzyl Phenyl Sulfide **291q**

Following the success of the parent racemic amine tris(phenolate) titanium complex (*rac*)-**195b** in the sulfoxidation reaction, the screening of the chiral titanium complexes (*R,M*)-**287** and (*R,M*)-**288** in the same reaction was then investigated (Scheme 173, Table 59). The reactions were therefore repeated under the same conditions as before, with the oxidation of benzyl phenyl sulfide **291q** by cumene hydroperoxide **72** conducted in dichloromethane at -30 °C. Thus, to a solution of the sulfide and 10mol % of the titanium triflate complex (*R,M*)-**288** was added two equivalents of the oxidant. After twenty-four hours the reaction was worked up and the crude product was analysed by ¹H NMR spectroscopy, which revealed that all of the starting material had been consumed. Furthermore, it showed that both benzyl phenyl sulfoxide **292q** together with the over-oxidised product, sulfone **293q**, had formed in a ratio of 85:15 in favour of the desired sulfoxide. Following purification *via* column chromatography, the sulfoxide product **292q** was isolated in 74% yield. Analysis of the sulfoxide by chiral HPLC showed the product had formed in 23% ee (entry 1). Based on the order of elution of the enantiomers on the HPLC and also by comparison of the optical rotation of the product with the literature, the major enantiomer was determined to be the (*R*)-enantiomer.^{167, 168}

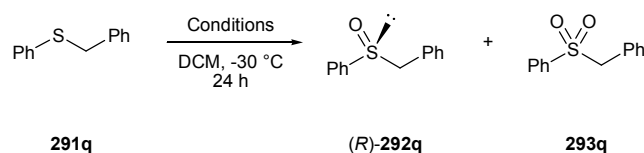
When the reaction was repeated with the titanium *iso*-propoxide complex (*R,M*)-**287**, the reaction went to only 63% conversion after twenty-four hours. The ratio of sulfoxide **292q** to sulfone **293q** was found to be 90:10, and following purification (*R*)-benzyl phenyl sulfoxide was isolated in 46% yield and 18% ee (entry 2). Given the superior reactivity and enantioselectivity that the titanium triflate complex (*R,M*)-**288** had given in comparison to (*R,M*)-**287**, all further reactions were conducted with this catalyst.

Another aspect of this reaction to explore was the choice of oxidant, and for this reason the reaction was repeated under the same conditions, with two equivalents of *tert*-butyl hydroperoxide **290** in place of cumene hydroperoxide **72**. Under these conditions sulfoxide **292q** formed in 25% conversion with only traces of sulfone

293q present. Following isolation of sulfoxide **292q** (16% yield), the enantiomeric excess was found to be only 3% ee (entry 3).

In an attempt to improve the selectivity obtained in the first reaction, where 10mol % of (*R,M*)-**288** and two equivalents of cumene hydroperoxide **72** were employed, the reaction was repeated but with the temperature maintained at -78 °C. After ten hours at this temperature, the reaction was continued at -30 °C for the remaining fourteen hours. Following work-up, analysis of the crude product by ¹H NMR spectroscopy showed that the reaction had again gone to 100% conversion, but that the ratio of sulfoxide **292q** to sulfone **293q** had now improved to 91:9 (from 85:15, entry 1). Disappointingly, the enantioselectivity of the reaction had not improved with the sulfoxide isolated also having 23% ee (entry 4).

When the reaction was run with only 5mol % of catalyst the reaction went to only 25% conversion after the twenty-four hours (entry 5). Repeating the reaction with a catalyst loading of 50mol %, gave a 90% conversion after only eighteen hours, with a ratio of sulfoxide **292q** to sulfone **293q** of 91:9. HPLC analysis showed the sulfoxide had formed in only 10% ee (entry 6). When the sulfide was reacted with only one equivalent of cumene hydroperoxide **72**, the reaction went to only 54% conversion, with the sulfoxide formed in 8% ee (entry 7).



Scheme 173. Screening of titanium catalysts (*R,M*)-**287** and (*R,M*)-**288** in the oxidation of benzyl phenyl sulfide **291q**

Table 59

Entry	Catalyst	Oxidant	Conversion /%	Ratio 292:293	Yield of 292 /%	ee /%
1	(<i>R,M</i>)- 288 (10mol %)	CHP 72 (2 eq.)	100	85:15	74	23
2	(<i>R,M</i>)- 287 (10mol %)	CHP 72 (2 eq.)	63	90:10	46	18
3	(<i>R,M</i>)- 288 (10mol %)	TBHP 290 (2 eq.)	25	trace sulfone	16	3
4	(<i>R,M</i>)- 288 (10mol %)	CHP 72 (2 eq.)	100 ^a	91:9	80	23
5	(<i>R,M</i>)- 288 (5mol %)	CHP 72 (2 eq.)	25	no sulfone	-	-
6	(<i>R,M</i>)- 288 (50mol %)	CHP 72 (2 eq.)	90 ^b	91:9	-	10
7	(<i>R,M</i>)- 288 (10mol %)	CHP 72 (1 eq.)	54	97:3	28	8

^a Reaction run at -78 °C for 10 hours, then -30 °C for 14 hours; ^b Reaction run for 18 hours

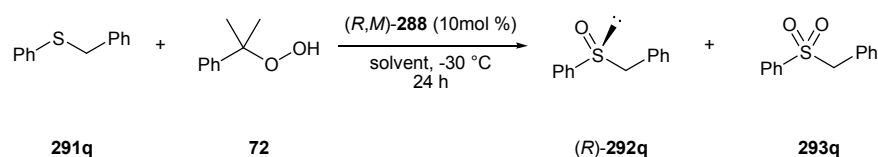
4.3.4 Solvent Screen in the Oxidation of Benzyl Phenyl Sulfide **291q** Catalysed by (*R,M*)-**288**

Since the reaction had shown to proceed in good yield in dichloromethane, the screening of different solvents in the oxidation benzyl phenyl sulfide **291q** with cumene hydroperoxide **72** was also explored (**Scheme 174**, **Table 60**). Given that other chlorinated solvents had also been employed in other catalytic systems in the literature (see Section 4.2.1), the reaction was repeated using 1,2-dichloroethane as the solvent system. Under these conditions the reaction went to 100% conversion, with both the sulfoxide **292q** and the sulfone **293q** present in the crude reaction mixture, in a ratio of 86:14 (entry 2). Following purification the (*R*)-sulfoxide **292q** was obtained in 65% yield and 23% ee, which was almost identical to the result obtained with dichloromethane as the solvent (entry 1).

When the reaction was repeated with acetonitrile as the solvent, the reaction went to only 70% conversion, with the sulfoxide **292q** the predominant product present (with a ratio of sulfoxide to sulfone of 94:6). After purification, the sulfoxide (*R*)-**292q** was isolated in 60% yield and 9% ee (entry 3). The reaction was then attempted using toluene as the solvent and this time the reaction went to completion. The ratio

of sulfoxide to sulfone was 89:11 in favour of the sulfoxide. (*R*)-Benzyl phenyl sulfoxide **292q** was isolated in 78% yield and 37% ee (entry 4), which was a significant improvement on the reaction in dichloromethane (entry 1).

Finally, two reactions were attempted in benzene and hexane. However, since benzene freezes at *ca.* 5 °C, it was necessary to add the minimum amount of dichloromethane to the reaction, in order to achieve homogeneity. At a ratio of benzene to dichloromethane of 2:1 this was obtained. For the reaction in hexane, the addition of dichloromethane was required to dissolve the catalyst, such that the reaction was run in a mixed solvent system of hexane and dichloromethane at a ratio of 5:1. Both these reactions were shown to go to 100% conversion after twenty-four hours, but both reactions showed that a significant amount of over-oxidation to the sulfone **293q** had occurred (ratio **292:293** 65:35 and 59:41 respectively). Significantly, the isolated benzyl phenyl sulfoxide from both of these reactions was shown to have a much lower enantiomeric excess than in previous reactions, with only a 7% ee obtained in both cases (entries 5 and 6, compared to the 37% ee obtained using toluene, entry 4).



Scheme 174. Solvent screening in the oxidation of benzyl phenyl sulfide **291q** with cumene hydroperoxide **72** in the presence of (*R,M*)-**288**

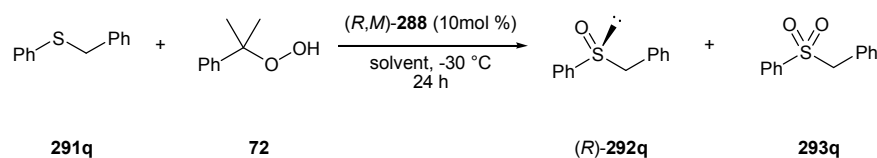
Table 60

Entry	Solvent	Conversion / %	Ratio 292:293	Yield of 292 / %	ee / %
1	DCM	100	85:15	74	23
2	DCE	100	86:14	65	23
2	MeCN	70	94:6	60	9
4	Toluene	100	89:11	78	37
5	Benzene/DCM (ratio 2:1)	100	65:35	57	7
6	Hexane/DCM (ratio 5:1)	100	59:41	41	7

4.3.5 Addition of 4Å Molecular Sieves to the Oxidation of Benzyl Phenyl Sulfide **291q**

The use of additives in the sulfoxidation reaction has been widely reported. For example, the addition of either water or *iso*-propanol to the stoichiometric or catalytic systems of Kagan and co-workers was necessary to achieve any selectivity,^{151, 153} while water was also found to improve the efficiency of the catalytic system of Uemura *et al.*^{158, 159} Other additives such as 4Å molecular sieves have also given improvements these catalytic systems.

It was therefore decided that the oxidation of benzyl phenyl sulfide **291q** under the same conditions as before but with the addition of 4Å molecular sieves. Two reactions were conducted, using either dichloromethane or toluene as the solvent system, with 10mol % of catalyst and two equivalents of oxidant. After twenty-four hours the reactions were worked-up, with analysis of the crude product by ¹H NMR spectroscopy revealing that both reactions had gone to 100% completion. For the reaction run in dichloromethane, the sulfoxide **292q** and sulfone **293q** were present in a ratio of 78:22 (entry 1), while for the reaction run in toluene had a ratio of sulfoxide and sulfone of 50:50 (entry 3). Analysis of both the sulfoxide products by chiral HPLC showed that the enantiomeric excess was 32% and 11% in favour of the (*R*)-enantiomer, for dichloromethane and toluene, respectively. When compared to the analogous reactions run in these solvents without the addition of the molecular sieves, the additive appears to have significantly increased the rate of reaction in toluene (ratio **292:293** of 50:50 compared to 89:11) but at the detriment of the enantioselectivity of the sulfoxide product (11% ee compared to 37% ee, entry 3 and entry 4). In comparison, the addition of molecular sieves to dichloromethane appears not to have significantly affected the ratio of sulfoxide to sulfone (78:22 versus 85:15), but has given an improvement in selectivity (32% ee compared to 23% ee).



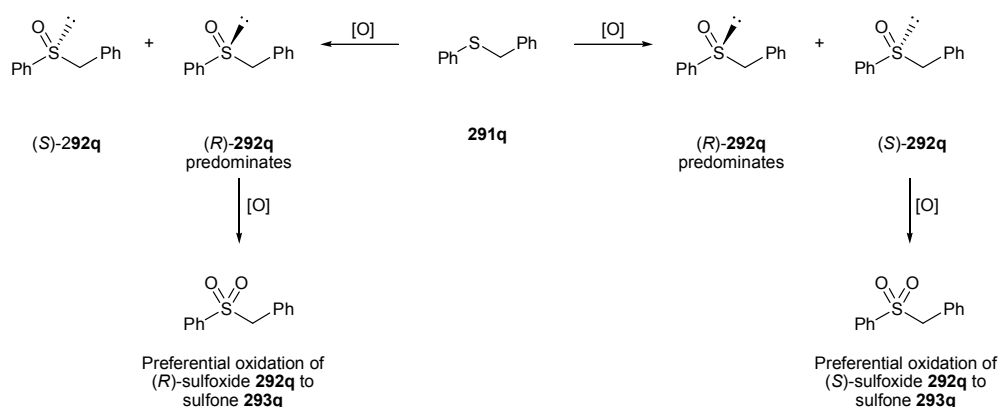
Scheme 175. Oxidation of benzyl phenyl sulfide **291q** under the standard conditions, with or without the addition of 4Å molecular sieves

Table 61

Entry	Solvent	4Å MS added	Conversion /%	Ratio 292:293	Yield of 292 /%	ee /%
1	DCM	Yes	100	78:22	59	32
2	DCM	No	100	85:15	74	23
3	Toluene	Yes	100	50:50	30	11
4	Toluene	No	100	89:11	60	37

4.3.6 Kinetic Resolution of Racemic Benzyl Phenyl Sulfoxide (*rac*)-292q

As has been shown in other catalytic systems, the kinetic resolution of the sulfoxide *via* oxidation of the sulfoxide to the sulfone, has been shown to either enhance or diminish the enantioselectivity of the sulfoxidation reaction. **Scheme 176** illustrates both the possible matched and mismatched systems. In the case of the matched system, the initial oxidation of sulfide **291q** forms the (*R*)-sulfoxide **292q** in excess. For the second process (the oxidation of the sulfoxide **292q** to the sulfone **293q**), the (*S*)-sulfoxide is oxidised preferentially, thus enhancing the enantiomeric excess of the remaining (*R*)-sulfoxide. In the case of the mismatched system, the second oxidative step favours the (*R*)-sulfoxide, such that, the enantiomeric excess of the remaining (*R*)-sulfoxide diminishes.



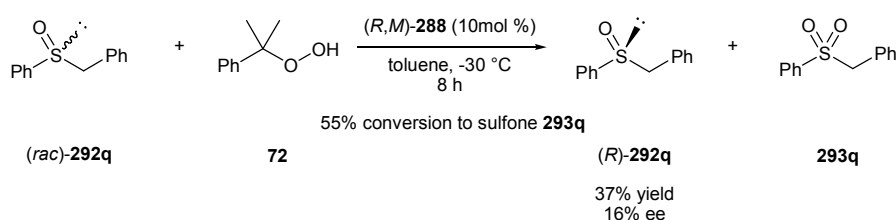
Mismatched system: The processes work against one another to diminish the enantiomeric excess of the remaining (*R*)-sulfoxide

Matched system: Both processes work cooperatively to enhance the enantiomeric excess of the remaining (*R*)-sulfoxide

Scheme 176. An illustration of possible matched/mismatched systems in the oxidation of sulfide **291q**

In order to demonstrate if there is any kinetic resolution of the sulfoxide in this reaction, a sample of racemic benzyl phenyl sulfoxide (*rac*)-292q was treated under

these optimised conditions. Thus, (*rac*)-**292q** in toluene was treated with one equivalent of cumene hydroperoxide **72** in the presence of (*R,M*)-**288** at -30 °C (Scheme 177). After 8 hours, the reaction was worked-up and the crude product analysed by ¹H NMR spectroscopy, which showed that 55% of the starting sulfoxide **292q** had been converted to the sulfone **293q**. After purification, the remaining sulfoxide **292q** was isolated in 37% yield. Analysis of this product *via* chiral HPLC revealed the enantiomeric excess to be 16% ee in favour of the (*R*)-enantiomer. This showed that the (*S*)-sulfoxide was being oxidised preferentially, and as the initial oxidation of the sulfide **291q** in this reaction favoured the (*R*)-sulfoxide **292q**, it suggested that the two processes were working in a co-operative fashion.

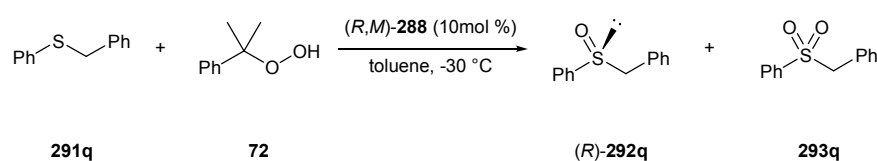


Scheme 177. Kinetic resolution of racemic benzyl phenyl sulfoxide (*rac*)-**292q** under the reaction conditions

4.3.7 Monitoring the Oxidation of Benzyl Phenyl Sulfide **291q** Catalysed by (*R,M*)-**288**

As was shown earlier (see Section 4.3.4, Table 60, entry 4), the oxidation of benzyl phenyl sulfide **291q** under these conditions produced a ratio of sulfoxide to sulfone of 89:11, suggesting that while kinetic resolution might be enhancing the enantioselectivity of this reaction, it wasn't a significant factor. However, if the reaction was run for a longer period of time, then the enantiomeric excess of the remaining sulfoxide in the reaction should increase. To test this, the reaction of benzyl phenyl sulfide **291q** with three equivalents of cumene hydroperoxide **72** was performed and aliquots of the reaction mixture were taken and analysed at both twenty four hours and thirty two hours (Scheme 178, Table 62). At twenty four hours the reaction had gone to 100% conversion, with all of the starting benzyl phenyl sulfide **291q** having reacted (entry 1). The ratio of sulfoxide **292q** to sulfone **293q** was determined to be 83:17. Following isolation of the (*R*)-sulfoxide **292q**, analysis by chiral HPLC showed it had formed in 35% ee. This compares favourably to the reaction where two equivalents of cumene hydroperoxide were employed in

the reaction (see Section 4.3.4, **Table 60**, entry 4), where a ratio **292:293** of 89:11 was obtained, and the (*R*)-sulfoxide formed in 37% ee. When an aliquot was taken at thirty two hours the ratio of sulfoxide to sulfone was found to be 33:67 in favour of the sulfone (entry 2). The analysis of the remaining sulfoxide revealed that the enantiomeric excess had increased to 47% ee, showing that the kinetic resolution of the sulfoxide **292q** to the sulfone **293q** was working to enhance the selectivity. Overall the enantioselectivity of this reaction was the best achieved yet but this was at the detriment to the maximum possible yield of sulfoxide **292q** from this reaction.



Scheme 178. Monitoring of the oxidation of benzyl phenyl sulfide **291q** by cumene hydroperoxide **72** in the presence of (*R,M*)-**288**

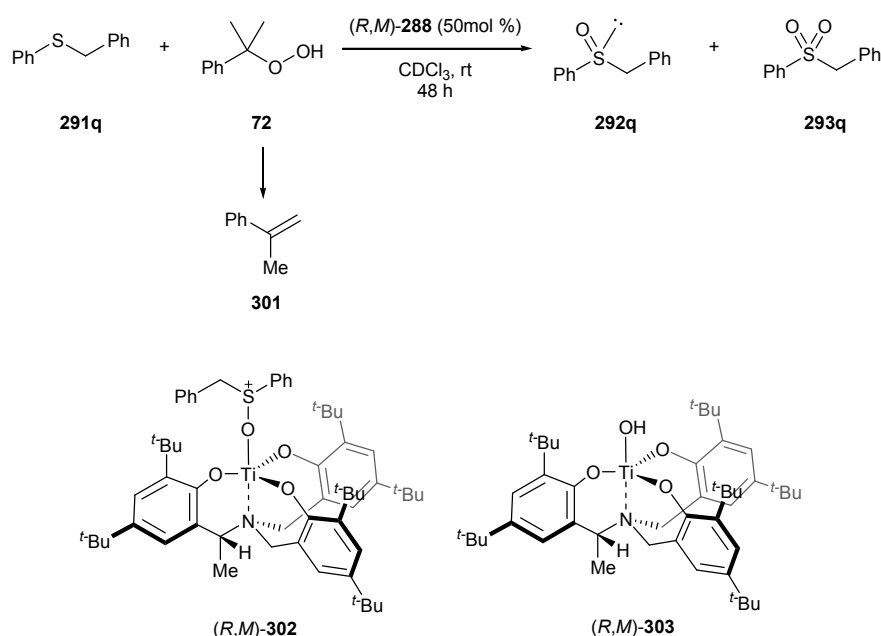
Table 62

Entry	Time /h	Conversion /%	Ratio 292:293	ee 292q /%
1	24	100	83:17	35
2	32	100	33:67	47

4.3.8 NMR Studies

A series of NMR experiments were performed to examine whether the structural integrity of the titanium complex remained intact during the course of the reaction. Firstly, two experiments were run in which complex (*R,M*)-**288** was treated with either 2.5 equivalents of sulfide **291q** or four equivalents of cumene hydroperoxide **72**. In both cases signals corresponding to (*R,M*)-**288** remained, suggesting that there was no degradation of the complex (see Appendix 7.1). Next, an NMR experiment was run where all the components of the reaction were present (two equivalents of sulfide **291q** and four equivalents of cumene hydroperoxide **72** with respect to (*R,M*)-**288**) (**Scheme 179**). Under these conditions the oxidation of the sulfide **291q** (A) to the sulfoxide **292q** (B) proceeded, although the reaction remained incomplete after forty-eight hours, probably due to a lack of agitating or mixing in the NMR tube (**Figure 62**). Similarly, new signals appeared at $\delta = 5.29$ ppm and $\delta = 5.01$ ppm and these were assigned to α -methyl styrene **301** (C), which presumably arose from the decomposition of cumene hydroperoxide **72** at room temperature. Importantly,

the signals corresponding to the benzylic protons in (R,M) -**288**, usually observed between $\delta = 4.15$ ppm and $\delta = 3.40$ ppm, were now replaced with a series of new signals between $\delta = 4.70$ ppm and $\delta = 3.05$ ppm. These signals were tentatively ascribed to one or more titanium complexes formed by displacement of the triflate ligand with benzyl phenyl sulfoxide. As confirmation, another NMR experiment was conducted, where titanium complex (R,M) -**288** was treated with two equivalents of benzyl phenyl sulfoxide (*rac*)-**292q** (see Appendix 7.1). This gave rise to an almost identical set of signals as was observed in the reaction mixture. Further confirmation was obtained by mass spectrometry with both samples shown to contain signals at 946.5 which corresponded to complex (R,M) -**302** ($C_{59}H_{80}NO_4STi$), where benzyl phenyl sulfoxide was now coordinated to the metal centre. Finally, the reaction mixture was quenched with addition of a saturated aqueous sodium sulfite solution, and this gave rise to a new titanium tris(phenolate) complex, with signals for the benzylic protons now observed between $\delta = 4.05$ ppm and $\delta = 3.15$ ppm (**Figure 63**). Mass spectrometry indicated this could be the titanium hydroxide compound (R,M) -**303** ($C_{46}H_{68}NO_4Ti$) with a signal observed at 746.5. No signal was observed for the μ -oxo-bridged dimer species. From these initial studies, it appears over the course of the reaction the structural integrity of the complex remains intact.



Scheme 179. Reaction of benzyl phenyl sulfide **291q** studied by ^1H NMR spectroscopy

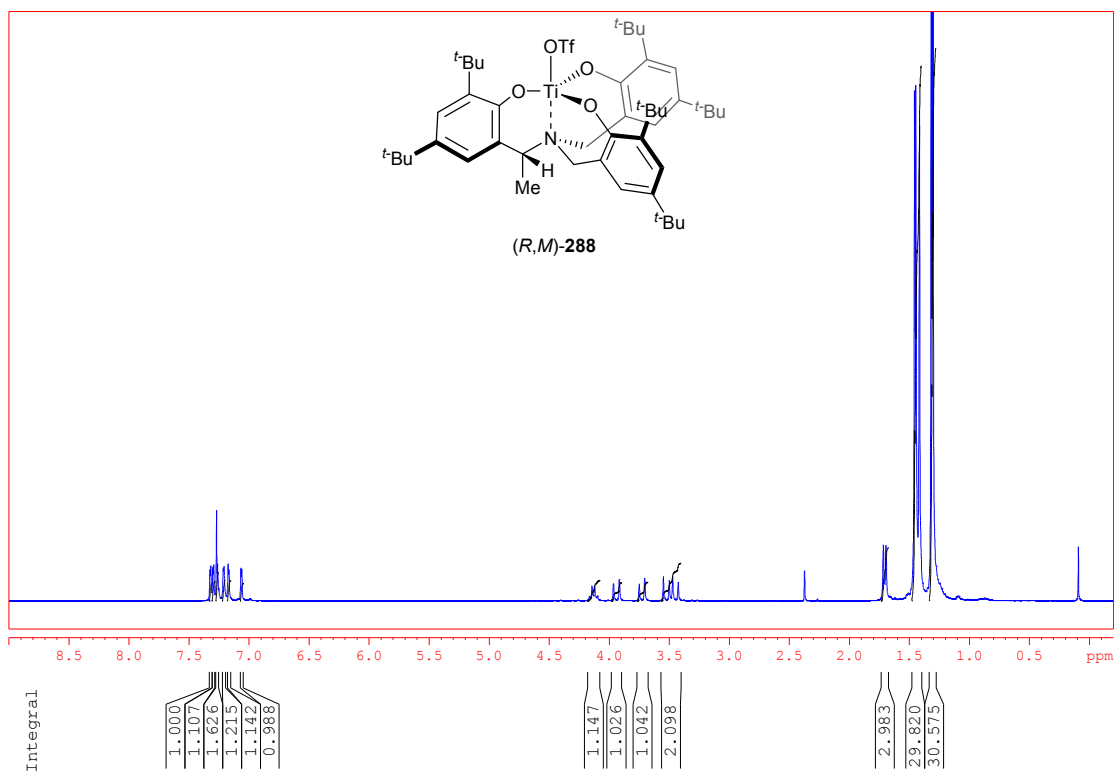


Figure 60. ¹H NMR (CDCl₃) spectrum of titanium complex **(R,M)-288**

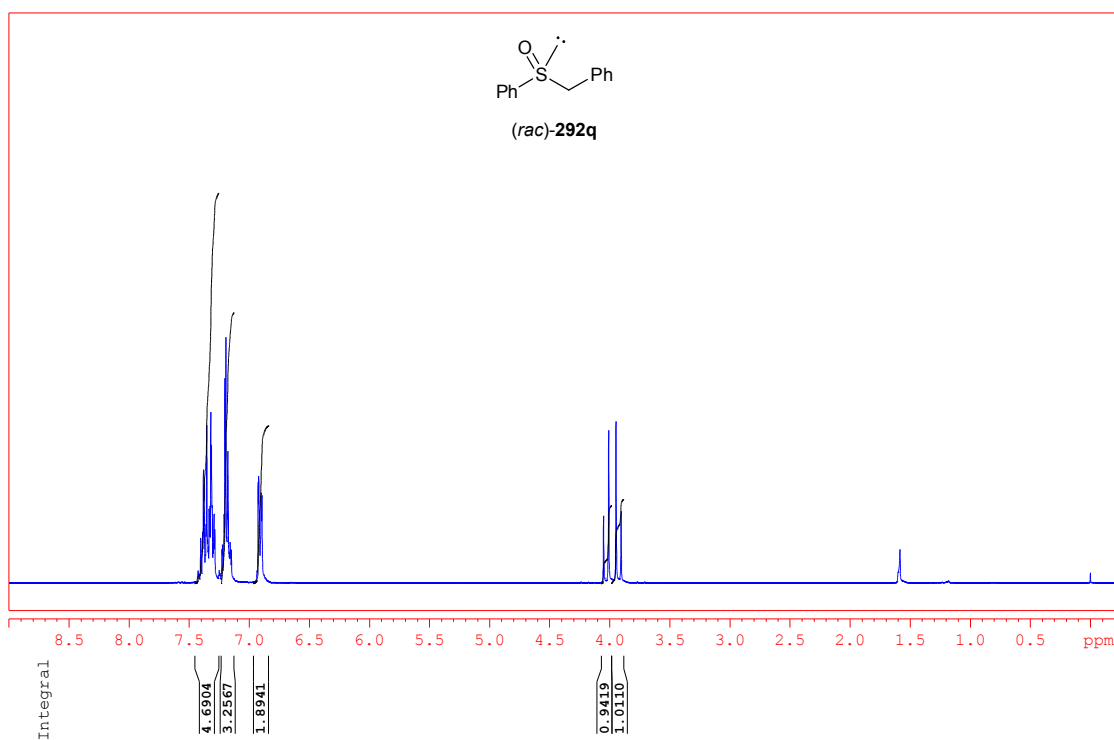


Figure 61. ¹H NMR (CDCl₃) spectrum of benzyl phenyl sulfoxide **(rac)-292q**

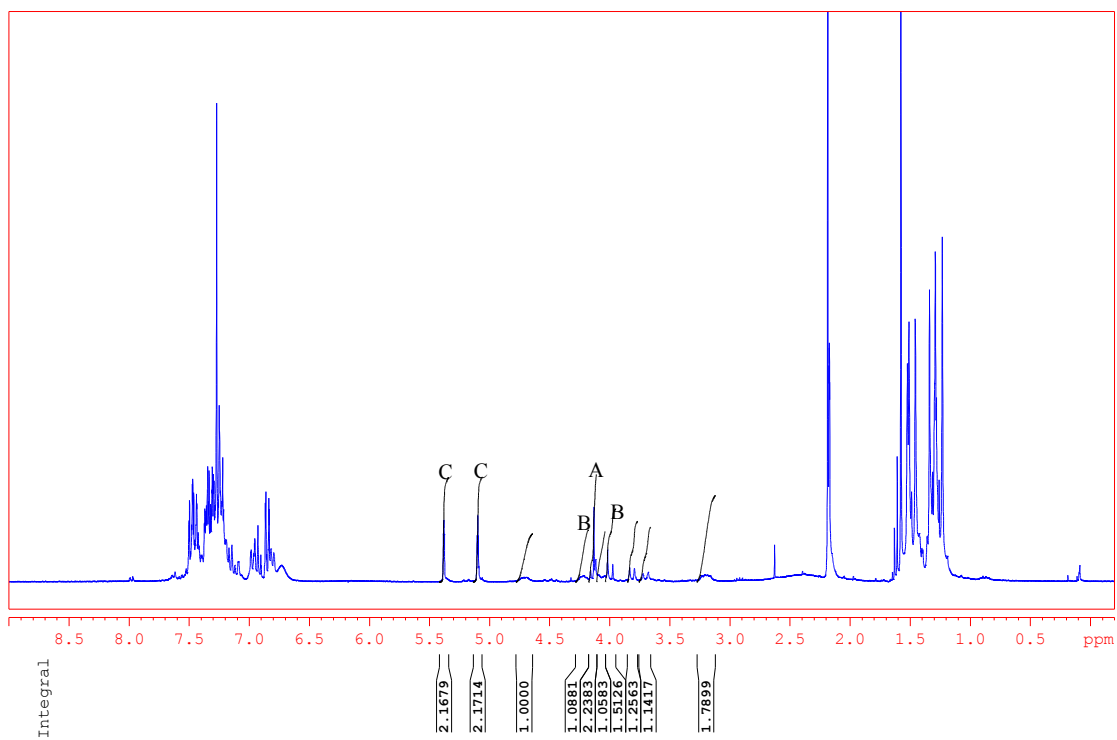


Figure 62. ^1H NMR (CDCl_3) spectrum of reaction after 48 hours

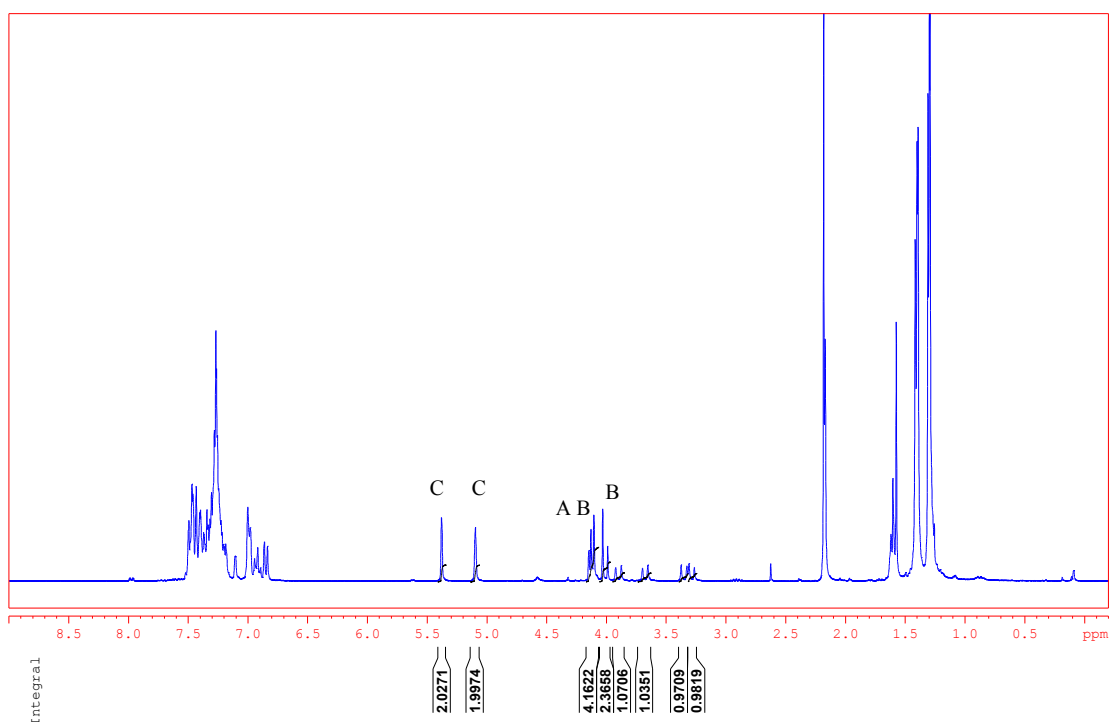


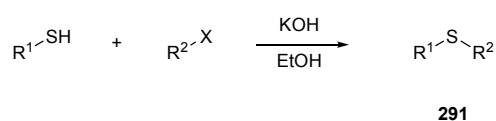
Figure 63. ^1H NMR (CDCl_3) spectrum of reaction after addition of a saturated aqueous sodium sulfite solution

4.4 SCREENING OF SULFIDES **291** IN THE REACTION CATALYSED BY (*R,M*)-**288**

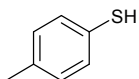
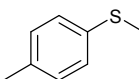
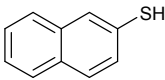
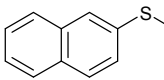
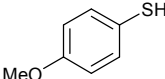
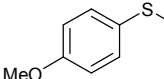
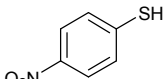
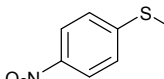
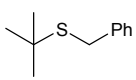
Before any screening of sulfides could commence, the synthesis of both these and their racemic sulfoxides would first need to be completed. A series of methyl aryl sulfides, **291a**, **291c**, **291d** and **291e**, were chosen, since these had extensively been used in other catalytic systems, as well benzyl-*tert*-butyl sulfide **291y**, the bulky nature of which has been shown to impede the oxidation of its corresponding sulfoxide in other catalytic systems.¹⁶⁹

4.4.1 Synthesis of Sulfides **291**

The synthesis of sulfides **291** was achieved by alkylation of the corresponding thiol. Treatment of the thiols in ethanol with potassium hydroxide followed by addition of the alkyl halide (methyl iodide or benzyl bromide) gave the desired sulfides in 82-98% yield.

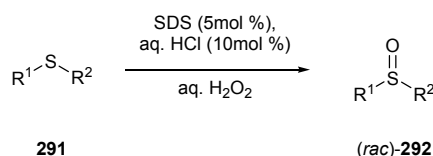


Scheme 180. Synthesis of sulfides **291**

Table 63					
Entry	R ¹ -SH	R ² -X	Sulfide	Yield /%	
1		MeI		291a	98
2		MeI		291c	96
3		MeI		291d	91
4		MeI		291e	82
5		BnBr		291y	79

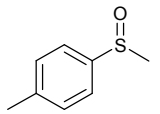
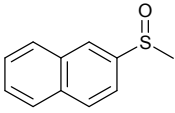
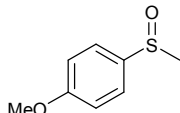
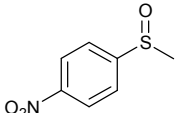
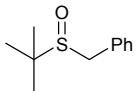
4.4.2 Synthesis of racemic sulfoxides (*rac*)-**292**

The synthesis of racemic sulfoxides (*rac*)-**292**, which were to be used for comparison with those isolated from the reactions involving the chiral titanium catalyst (*R,M*)-**288**, was completed. Following the same procedure as earlier, sulfides **291** were reacted with four equivalents of aqueous hydrogen peroxide, in the presence of sodium dodecyl sulphate and aqueous hydrochloric acid. Following purification the desired racemic sulfoxides (*rac*)-**292** were isolated in 78-92% yield (Scheme 181, Table 64).



Scheme 181. Oxidation of sulfides **291** to sulfoxides **292** by hydrogen peroxide in the presence of dodecyl hydrogen sulphate

Table 64

Entry	Sulfoxide	Yield /%
1		292a 87
2		292c 81
4		292d 84
3		292e 78
5		292y 92

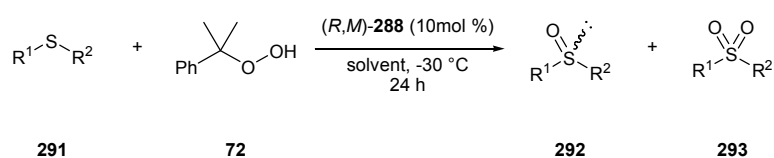
4.4.3 Screening of Sulfides **291** in the Sulfoxidation Reaction Catalysed by *(R,M)*-**288**

As has been shown earlier the oxidation of benzyl phenyl sulfide **291q** by cumene hydroperoxide **72** in the presence of *(R,M)*-**288** gave the desired (*R*)-sulfoxide **292q** in 74% yield and 23% ee when the reaction was run in dichloromethane, and 78% yield and 37% ee when run in toluene (**Table 65**, entries 1 and 2). For the reactions of other sulfides, the same conditions were also employed. In particular, the reaction time was kept at twenty-four hours, since monitoring these reactions by TLC proved to be difficult. For the oxidation of 4-methylthioanisole **291a**, the reaction was run in dichloromethane. Analysis of the crude product revealed the reaction had gone to completion, with the ratio of methyl-*p*-tolyl sulfoxide **292a** to methyl-*p*-tolyl sulfone **293a** of 28:72, showing a significant amount of over-oxidation had occurred. The desired sulfoxide **292a** was isolated in 14% yield, and following analysis by chiral HPLC, the enantioselectivity of reaction was determined to be 13% ee in favour of the (*R*)-enantiomer (entry 3).

The oxidation of methyl-2-naphthyl sulfide **291c** in dichloromethane proceeded to 100% conversion, with the ratio of desired of sulfoxide **292c** to sulfone **293c** 32:68 in favour of the sulfone **293**. Following purification methyl-2-naphthyl sulfoxide **292c** was isolated in 28% yield and 10% ee (entry 4). In contrast, when the reaction was repeated with toluene as the reaction solvent, the ratio of sulfoxide to sulfone was found to be 79:21, with the desired sulfoxide obtained in 61% yield and 20% ee (entry 5).

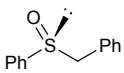
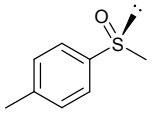
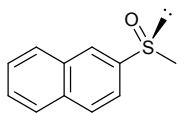
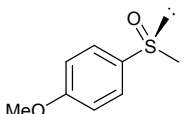
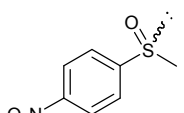
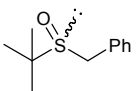
The oxidation of methyl-(4-methoxyphenyl)-sulfide **291d** in toluene proceeded in 88% conversion with a ratio of sulfoxide **292d** to sulfone **293d** of 90:10. Following purification the desired sulfoxide **292d** was isolated in 65% yield and 17% ee (entry 6). When the oxidation of methyl-(4-nitrophenyl)-sulfide **291e** by cumene hydroperoxide **72** was run in toluene, the reaction went to completion with a significant proportion of the crude product the sulfone **293e** (ratio sulfoxide **292e** to sulfone **293e**, 56:44). The desired methyl-(4-nitrophenyl)-sulfoxide was isolated in 47% yield. Following analysis *via* chiral HPLC the product was found to be racemic (entry 7). Finally, the oxidation of benzyl-*tert*-butyl sulfide **291y** went to 90%

conversion, the major product being the desired sulfoxide **292y** with only traces of the sulfone **293y**. This confirmed that the bulky *tert*-butyl did impede the oxidation of the newly formed sulfoxide **292y**. After isolation, *tert*-butylphenylmethyl sulfoxide **292y** was obtained in 71% yield, however, it was found that no enantioselective inducement had taken place, with the product being racemic (entry 8).



Scheme 182. Oxidation of sulfides **291** by cumene hydroperoxide **72**, catalysed by *(R,M)*-**288**

Table 65

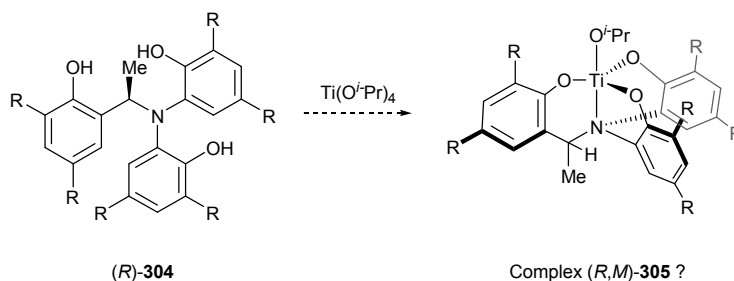
Entry	Sulfoxide	Solvent	Conversion /%	Ratio 292:293	Yield of 292 /%	ee /%
1		DCM	100	85:15	74	23(<i>R</i>)
2	292q	Toluene	100	89:11	78	37(<i>R</i>)
3		DCM	100	28:72	14	13(<i>R</i>)
4		DCM	100	32:68	28	10(<i>R</i>)
5	292c	Toluene	100	79:21	61	20(<i>R</i>)
7		Toluene	88	90:10	65	17(<i>R</i>)
6		Toluene	100	56:44	47	0
6	292e					
8		Toluene	90	trace sulfone	71	0
	292y					

4.5 CONCLUSION

Titanium triflate complex (*R,M*)-**288** has been shown to catalyse the oxidation of a range of sulfides by cumene hydroperoxide **72** giving the desired sulfoxides in moderate to good yields. For the reactions involving benzyl phenyl sulfide **291q**, 4-methylthioanisole **291a**, methyl-2-naphthyl sulfide **291c** and 4-methoxythioanisole **291d** modest levels of enantioselectivity were obtained, with the best result obtained in the reaction of benzyl phenyl sulfide **291q**, giving (*R*)-benzyl phenyl sulfoxide **292q** in 78% yield and 37% ee.

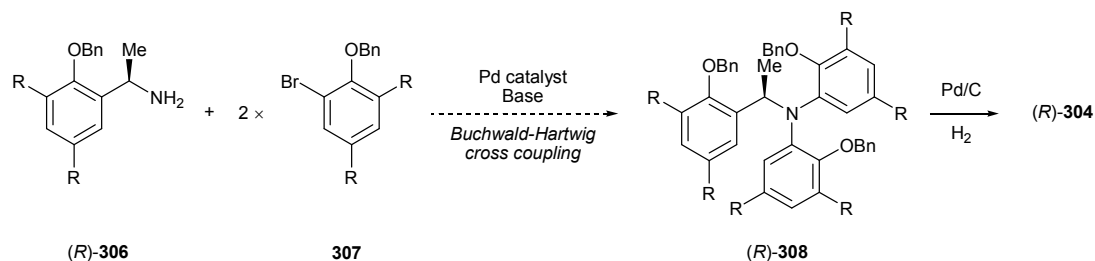
4.6 FUTURE WORK

Following the successful synthesis of ligands (*R*)-**254a** and (*R*)-**278** and their subsequent complexation to form the titanium *iso*-propoxide complexes (*R,M*)-**271** and (*R,M*)-**287**, together with the modest enantioselective inducement that complex (*R,M*)-**288** displayed in the sulfoxidation reaction, two areas of improvement in the ligand/complex design could be envisaged. Firstly, if the angle of the tilt of the aryl rings with respect to the titanium-nitrogen bond could be increased then this would be relayed to any coordinating substrate on the upper face of the complex. Secondly, if the *ortho*-substituents on the aryl rings could be increased in size or turned in further towards one another to create a smaller ‘pocket’, then this would further induce a chiral coordination sphere around the metal centre. One way in which this could be addressed is by removing the two benzylic methylene groups between the aryl rings and central nitrogen from the non-chiral arms to give a ligand such as (*R*)-**304** (Scheme 183).



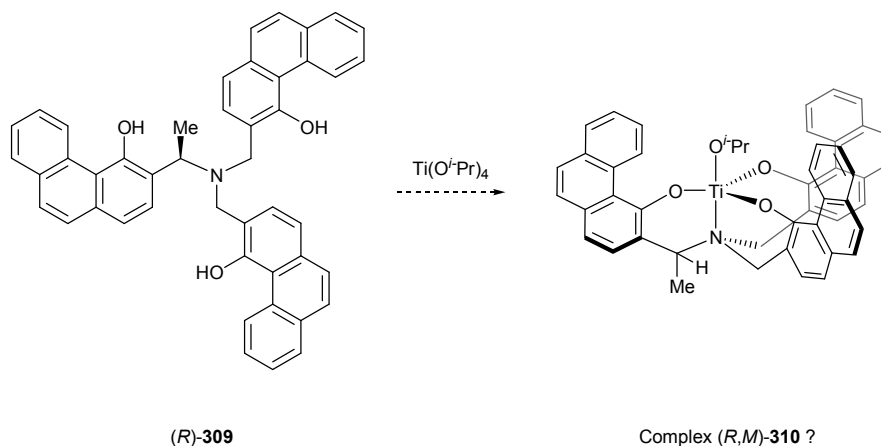
Scheme 183. Proposed ligand (*R*)-**304** and the possible titanium complex (*R,M*)-**305**

Synthesis of the ligand (*R*)-**304** could possibly be achieved by a Buchwald-Hartwig cross coupling of the primary amine (*R*)-**306** with the *ortho*-bromophenol compound **307** (Scheme 184). Under forcing conditions the bisarylation of the primary amine (*R*)-**306** to give the desired ligand precursor (*R*)-**308** might be possible.

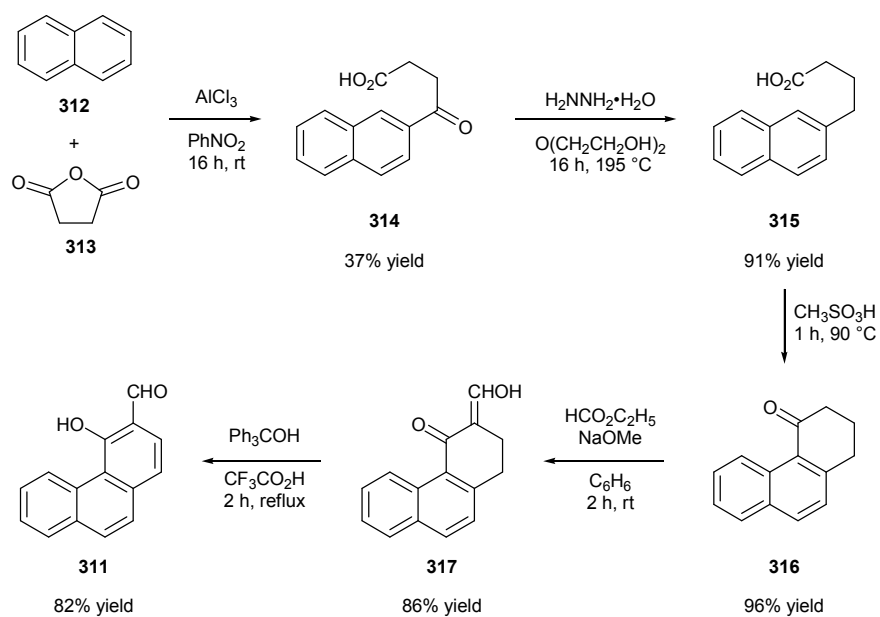


Scheme 184. Possible synthesis of ligand (*R*)-**304**

Another possible design would be to replace the aryl rings on the ligand with polyaromatics such as phenanthrenes, such as ligand (*R*)-**309** (Scheme 185). Upon coordination, the curved polyaromatic group would act to increase the tilt of the propeller function of the complex, whilst also creating more of a ‘pocket’ at the metal centre. Synthesis of 4-hydroxy-3-phenanthrenecarboxaldehyde **311**, from which the ligand could be synthesised as before, was published by Levy *et al.* in 2005 (Scheme 186).¹⁷⁰ The synthesis began with a Friedel-Crafts acylation of naphthalene to give **312** followed by a Wolff-Kishner reduction of **314** to give the acid **315** in 34% yield over the two steps. Subsequent cyclisation of the acid **315** with methanesulfonic acid gave 2,3-dihydrophenanthren-4(1*H*)-one **316** in 96% yield. Condensation of **316** with ethyl formate gave **317** in 86% yield; followed by oxidation with triphenylmethanol in trifluoroacetic acid gave the desired 4-hydroxy-3-phenanthrenecarboxaldehyde **311** in 82% yield, with an overall yield of 23% yield over the five steps.



Scheme 185. Proposed ligand (*R*)-**309** and the possible titanium complex (*R,M*)-**310**



Scheme 186. Synthesis of 4-hydro-3-phenanthrenecarboxaldehyde **311** from naphthalene **312**

Chapter 5:

Experimental

5 Experimental

5.1 GENERAL EXPERIMENTAL

Proton magnetic resonance spectra were either recorded at 250.13 MHz on a Bruker Avance 250 spectrometer, at 300.22 MHz on a Bruker Avance AC-300 spectrometer or at 399.78 MHz on a Bruker Avance WH-400 spectrometer. Chemical shifts δ are quoted in parts per million and are referenced to the residual solvent peak. Coupling constants (J) are quoted to the nearest 0.1 Hz. The multiplicities and general assignments of the spectroscopic data are denoted as: s, singlet; d, doublet; t, triplet; q, quartet; sept, septet; dd, doublet of doublets; ddd, doublet of doublet of doublets; dt, doublet of triplets; m, multiplet; app., apparent and br., broad.

Carbon magnetic resonance spectra were either recorded at 75.49 MHz on a Bruker Avance AC-300 spectrometer or at 100.52 MHz on a Bruker Avance WH-400. Chemical shifts δ are quoted in parts per million and are referenced to the residual solvent peak.

Infrared spectra were recorded on a Perkin Elmer 1600 series FT-IR spectrometer with internal background calibration for the range 600-4000 cm^{-1} , from thin films on NaCl plates (film), as KBr discs (KBr) or as Nujol mulls (Nujol). Selected absorptions are quoted as ν in cm^{-1} .

Capillary melting points were recorded on a Büchi 535 series instrument and are uncorrected.

Mass spectra including high resolution spectra were either recorded by the EPSRC National Mass Spectrometry Service Centre, Swansea, or by the mass spectrometry service of the University of Bath. Electron impact (EI) and chemical ionisation (CI) analyses were performed in positive ionisation mode.

Elemental analyses were performed with an Exeter Analytical, Inc. CE-400 elemental analyser at the University of Bath.

Optical rotations were recorded on an Optical Activity Ltd AA-10 automatic polarimeter with a path length of 1 dm. Concentrations are quoted in g/100mL.

High performance liquid chromatography was performed on a Perkin Elmer series 200 high performance liquid chromatography system, using different chiral columns, flow rates and *n*-hexane/*i*-PrOH solvent ratios, as specified.

Crystallographic measurements were recorded on a Nonius KappaCCD diffractometer with Mo-K α radiation ($\lambda = 0.71074 \text{ \AA}$). All structures were solved by direct methods and refined on all F_2 data using the SHELX-97 suite of programmes. Analytical thin layer chromatography was carried out using commercially available aluminium backed plates coated with Merck G/UV₂₅₄. Plates were visualised under UV light (at 254nm) or by staining potassium permanganate or ninhydrin followed by heating. Flash chromatography was carried out using Merck 60 H silica gel (35-70 μm). Samples were pre-absorbed onto silica or loaded as saturated solvents in an appropriate solvent.

Anhydrous tetrahydrofuran, toluene, dichloromethane, methanol, diethyl ether, hexane and acetonitrile were obtained from an Innovative Technology Pure Solv solvent purification system (SPS). Petrol refers to the fraction of petroleum ether boiling at 40-60 °C. Ether refers to diethyl ether. Solvents were evaporated on a Büchi Rotorvapor.

All chemicals were used as supplied unless otherwise stated, and were supplied by Acros Organics, Alfa Aesar, Avocado, Fisher Scientific, Fluka, Lancaster Synthesis, Sigma-Aldrich and Strem Chemicals. Reactions requiring anhydrous conditions were performed under nitrogen in oven dried glassware. 4 \AA molecular sieves (powdered and beads) were activated by drying in an oven at 150 °C. All temperatures quoted are external.

5.2 GENERAL PROCEDURES

5.2.1 General Procedure A: Preparation of Benzyl Protected Aldehydes

To a stirred solution of the 2-hydroxy-benzaldehyde (1 equiv.) in DMF was added benzyl bromide (1 equiv.) and potassium carbonate (3.8 equiv.). The solution was stirred under nitrogen at 60 °C for 20 h, after which the reaction mixture was filtered through Celite[®] and washed with DMF. The solvent was removed under reduced pressure to leave the crude product.

5.2.2 General Procedure B: Preparation of Imines

The appropriate aldehyde (1 equiv.) was dissolved in ethanol and to this was added 4Å molecular sieves and (*R*)-phenyl glycinol **237** (1 equiv.). The reaction mixture was stirred at room temperature under nitrogen for 20 h before being filtered through Celite[®], washed with ethanol and concentrated *in vacuo* to yield the crude product.

5.2.3 General Procedure C: Addition of Alkyl Lithium to Imines

A solution the imine (1 equiv.) in THF was cooled to -85 °C before the alkyl lithium was added dropwise. The solution was stirred at -85 °C for 4 hours before being slowly warmed to room temperature over 12 hours, after which, a saturated ammonium chloride solution was added. The layers were separated and the organic layer concentrated *in vacuo*. After the crude oil was taken up in diethyl ether it was washed with a saturated sodium hydrogen carbonate solution. The aqueous layer was extracted with diethyl ether (× 2) and the combined organic extracts were dried over magnesium sulphate and concentrated under reduced pressure to leave the crude product as an oil.

5.2.4 General Procedure D: Preparation of Primary Amines

Lead (IV) acetate (1 equiv.) was added to a solution of the relevant amine in dichloromethane and methanol (2:1 ratio DCM:MeOH) at 0 °C. After stirring for 5 minutes the reaction was neutralised by addition of a saturated sodium bicarbonate solution, before being filtered through Celite[®]. After separation of the two phases, the aqueous layer was extracted twice with dichloromethane before the combined organic layers were dried (MgSO₄), filtered and evaporated *in vacuo* yielding the crude imine as a yellow oil. The imine was immediately dissolved in a mixture of a 3M aqueous hydrochloric acid solution and tetrahydrofuran (3:1 ratio HCl:THF) and the resulting solution stirred at room temperature for 1 hour before heating to 80 °C for 4 hours. The crude reaction mixture was evaporated to leave an oil that was dissolved in diethyl ether and stirred with a 3M aqueous sodium hydroxide solution (1:1 ratio Et₂O:NaOH) for 15 minutes before the aqueous layer was separated and extracted with diethyl ether. The combined organic layers were dried (MgSO₄) and concentrated *in vacuo* to afford the crude product.

5.2.5 General Procedure E: Preparation of Benzyl Alcohols

A stirred solution of aldehyde (1 equiv.) in ethanol was cooled to 0 °C before sodium borohydride (1.4 equiv.) was added portionwise. The reaction mixture was stirred for 4 hours before being quenched with a 1M aqueous sodium hydroxide solution. The ethanol was removed *in vacuo* and the aqueous solution extracted with ethyl acetate (× 3). The combined organic extracts were washed with a 1M aqueous sodium hydroxide solution, water and brine. The organic layer was dried (MgSO₄), filtered and concentrated under reduced pressure to afford the product.

5.2.6 General Procedure F: Preparation of Benzyl Bromide Analogues

The appropriate benzyl alcohol (1 equiv.) was taken up in diethyl ether (*ca.* 0.1M) and phosphorus tribromide (1.1 equiv.) was added dropwise over 15 minutes. After stirring for a further 15 minutes the solution was cooled to 0 °C and the reaction quenched with saturated ammonium chloride solution. The two layers were

separated and the aqueous layer extracted with diethyl ether ($\times 3$). The combined organic extractions were dried (MgSO_4) and concentrated under reduced pressure to yield the desired product.

5.2.7 *General Procedure G: Preparation of Tertiary Amines via bis-N,N-alkylation*

To a stirred solution of amine, potassium carbonate and 4Å molecular sieves in DMF was added the benzyl bromide analogue. The reaction was stirred at room temperature and monitored by TLC until complete conversion to the tertiary amine was achieved (additional benzyl bromide analogue and potassium carbonate were added if required). The reaction mixture was filtered through Celite[®] and the organic solvents removed *in vacuo* to afford a crude oil that was purified by column chromatography.

5.2.8 *General Procedure H: Removal of Benzyl Protecting Groups*

A solution of the amine in ethyl acetate was added to 10% palladium on carbon and the resulting mixture was stirred vigorously under one atmosphere of hydrogen for 24 hours. Afterwards the mixture was passed through Celite[®] and concentrated under reduced pressure to afford the crude product.

5.2.9 *General Procedure I: Preparation of Sulfides*

To a stirred solution of the thiol in ethanol was added powdered potassium hydroxide (1 equiv.). The reaction mixture was stirred at room temperature until all the solids dissolved. Following this the alkyl halide (1 equiv.) was added. After stirring for 24 hours the ethanol was removed *in vacuo* and ethyl acetate and water were added. The layers were partitioned and the organic layer washed with water and brine, dried over magnesium sulphate, and concentrated under reduced pressure to afford the crude product.

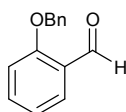
5.2.10 General Procedure J: Preparation of Racemic Sulfoxides

To a flask containing the sulfide and sodium dodecyl sulphate (0.05 equiv.) was added aqueous hydrogen peroxide (35%, 4 equiv.) and 1M aqueous hydrochloric acid (0.1 equiv.). The progress of the reaction was monitored by TLC. After complete disappearance of the starting material, the excess hydrogen peroxide was destroyed by the addition of saturated aqueous sodium sulphite solution to the reaction mixture. The reaction mixture was extracted with ethyl acetate ($\times 3$) and the combined organic layers dried over magnesium sulphate. After evaporation of the solvent under reduced pressure the crude product was obtained.

5.3 RESULTS AND DISCUSSION I

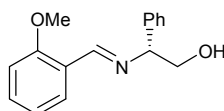
5.3.1 Synthesis of Chiral Amines (*R,R*)-**247** and (*R,R*)-**248**

2-(Benzyloxy)benzaldehyde, **245**¹⁷¹



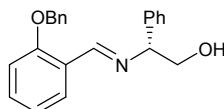
According to general procedure A, salicylaldehyde (5.00 mL, 46.9 mmol) in DMF (60 mL) was treated with benzyl bromide (5.58 mL, 46.9 mmol) and potassium carbonate (24.6 g, 178.2 mmol). The crude product was taken up in 5% ether in petrol and passed through a plug of silica to remove baseline impurities to give the product as a colourless oil (8.86 g, 41.7 mmol, 89% yield): $^1\text{H-NMR}$ (300MHz, CDCl_3) δ 10.59 (1H, s, CHO), 7.89-7.85 (1H, m, Ar-H), 7.57-7.51 (1H, m, Ar-H), 7.48-7.32 (5H, m, Ph), 7.08-7.01 (1H, m, Ar-H), 5.20 (2H, s, PhCH_2O); $^{13}\text{C-NMR}$ (75.5MHz, CDCl_3) δ 189.7, 161.0, 136.0, 135.8, 128.7, 128.4, 128.2, 127.2, 125.1, 121.0, 113.0, 70.4; $\nu_{\text{max}}/\text{cm}^{-1}$ (film) 1683 (C=O); MS (EI+) m/z (%) 235 (100, $[\text{M}+\text{Na}]^+$); HRMS m/z (EI+) $[\text{M}+\text{Na}]^+$ - $\text{C}_{14}\text{H}_{12}\text{NaO}_2$ requires 235.0734, found 235.0720.

The spectroscopic data is in agreement with the literature data

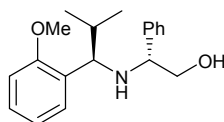
(*R*)-2-(2-Methoxybenzylideneamino)-2-phenylethanol, 241¹³⁹

According to general procedure B, 2-methoxybenzaldehyde (4.00 g, 29.4 mmol) in ethanol (50 mL) was treated with (*R*)-phenyl glycinol **237** (4.03 g, 29.4 mmol). The product was obtained as a yellow solid (7.50 g, 99% yield): mp 74-75 °C; $[\alpha]_D^{25} +14.8$ (*c* 1.69, CHCl₃); ¹H-NMR (300MHz, CDCl₃) δ 8.84 (1H, s, CH=N), 8.10 (1H, dd, *J* = 7.5 and 1.9 Hz, Ar-*H*), 7.48-7.24 (6H, m, Ph and Ar-*H*), 7.02 (1H, app. t, *J* = 7.5 Hz, Ar-*H*), 6.91 (1H, app. d, *J* = 8.3 Hz, Ar-*H*), 4.53 (1H, dd, *J* = 8.3 and 4.5 Hz, NCH(Ph)CH₂), 4.00-3.88 (2H, m, CH(Ph)CH_AH_B and CH(Ph)CH_AH_B), 3.85 (3H, s, OCH₃), 2.36 (1H, br s, OH); ¹³C-NMR (75.5MHz, CDCl₃) δ 158.9, 158.8, 141.1, 132.2, 128.5, 127.5, 127.3, 127.3, 124.3, 120.7, 110.9, 76.5, 67.8, 55.4; $\nu_{\max}/\text{cm}^{-1}$ (KBr) 3235 (OH); MS (EI+) *m/z* (%) 256 (100, [M+H]⁺); HRMS *m/z* (EI+) [M+H]⁺ - C₁₆H₁₈NO₂ requires 256.1338, found 241.1329.

The spectroscopic data is in agreement with the literature data

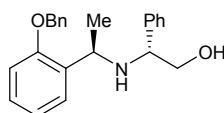
(*R*)-2-(2-(Benzyloxy)benzylideneamino)-2-phenylethanol, 246

According to general procedure B, aldehyde **245** (8.29 g, 39.1 mmol) in ethanol (100 mL) was treated with (*R*)-phenyl glycinol **237** (5.36g, 39.1 mmol). The product was obtained as a crude yellow solid (12.94 g, 97% yield): mp 78-80 °C; $[\alpha]_D^{25} -20.4$ (*c* 2.16, CHCl₃); ¹H-NMR (300MHz, CDCl₃) δ 8.80 (1H, s, CH=N), 8.03 (1H, dd, *J* = 7.5 and 1.9 Hz, Ar-*H*), 7.36-7.13 (6H, m, Ph and Ar-*H*), 6.92 (1H, app. t, *J* = 7.5 Hz, Ar-*H*), 6.85 (1H, app. d, *J* = 8.3 Hz, Ar-*H*), 5.02-4.98 (2H, m, PhCH₂O), 4.42 (1H, dd, *J* = 7.9 and 4.5 Hz, NCH(Ph)CH₂), 3.86 (1H, dd, *J* = 11.3 and 7.9 Hz, CH(Ph)CH_AH_B), 3.77 (1H, dd, *J* = 11.3 and 4.5 Hz, CH(Ph)CH_AH_B), 2.43 (1H, br s, OH); ¹³C-NMR (75.5MHz, CDCl₃) δ 158.6, 158.1, 140.9, 136.6, 132.1, 128.6, 128.5, 128.0, 127.7, 127.4, 127.3, 127.2, 124.8, 121.0, 112.5, 76.3, 70.3, 67.8; $\nu_{\max}/\text{cm}^{-1}$ (KBr) 3390 (OH); HRMS *m/z* (EI+) [M+H]⁺ - C₂₂H₂₂NO₂ requires 332.1651, found 332.1629.

[*R*]-2-([*R*]-1-[2-Methoxyphenyl]-2-methylpropylamino)-2-phenylethanol, 247¹³⁰

According to general procedure C, imine **241** (1.00 g, 3.91 mmol) in THF (70 mL) was treated with iso-propyl lithium (0.7M in hexanes, 20.10 mL, 14.10 mmol). The crude product was purified by column chromatography (SiO₂ 90:10 PE:EtOAc) to yield a yellow oil (0.69 g, 2.31 mmol, 59% yield, 92% de after purification): $[\alpha]_D^{25}$ -42.7 (*c* 0.38, CH₂Cl₂); ¹H-NMR (300MHz, CDCl₃) δ 7.25-7.00 (7H, m, 2 × Ar-*H* and Ph), 6.82 (1H, ddd, *J* = 8.3, 7.5 and 0.8 Hz, Ar-*H*), 6.67 (1H, dd, *J* = 8.3 and 0.8 Hz, Ar-*H*), 3.67 (1H, dd, *J* = 10.2 and 4.1 Hz, CH(Ph)CH_AH_B), 3.68-3.55 (6H, m, CH(Ph) CH_AH_B, CH(Ph)CH_AH_B, CH(i-Pr)N and OCH₃), 2.00 (1H, m, CH(CH₃)₂), 1.13 (3H, d, *J* = 6.4 Hz, (CH₃)CH(CH₃)), 0.73 (3H, d, *J* = 6.8 Hz, (CH₃)CH(CH₃)); ¹³C-NMR (75.5MHz, CDCl₃) δ 157.7, 142.8, 129.5, 128.5, 128.1, 127.5, 127.4, 120.6, 110.9, 64.6, 62.0, 55.2, 33.2, 20.9, 20.6; MS (EI+) *m/z* (%) 300 (100, [M+H]⁺); HRMS *m/z* (EI+) [M+H]⁺ - C₁₉H₂₆NO₂ requires 300.1963, found 300.1956.

The spectroscopic data is in agreement with the literature data

[*R*]-2-([*R*]-1-[2-(Benzyloxy)phenyl]ethylamino)-2-phenylethanol, 248

According to general procedure C, imine **246** (1.50 g, 4.53 mmol) in THF (100 mL) was treated with methyl lithium (1.6M in Et₂O, 10.2 mL, 16.31 mmol). The crude product was purified by column chromatography (SiO₂ 90:10 to 90:20 PE:EtOAc) to give a yellow oil (0.84 g, 2.42 mmol, 53% yield, >95% de after purification): $[\alpha]_D^{25}$ -28.7 (*c* 2.27, CH₂Cl₂); ¹H-NMR (300MHz, C₆D₆) δ 7.08 (1H, app. dt, *J* = 8.3 and 1.5 Hz, Ar-*H*), 7.03-6.83 (11H, m, 2 × Ph and Ar-*H*), 6.71 (1H, app. td, *J* = 7.5 and 1.1 Hz, Ar-*H*), 6.43 (1H, d, *J* = 8.3 and 1.1 Hz, Ar-*H*), 4.46 (1H, d, *J* = 11.7 Hz, PhCH_AH_BO), 4.40 (1H, d, *J* = 11.7 Hz, PhCH_AH_BO), 4.12 (1H, q, *J* = 6.4 Hz, CH(CH₃)N), 3.62 (1H, dd, *J* = 6.8 and 4.5 Hz, CH(Ph)CH₂), 3.54 (1H, dd, *J* = 10.5 and 4.5 Hz, CH(Ph)CH_AH_B), 3.34 (1H, dd, *J* = 10.5 and 6.8 Hz, CH(Ph)CH_AH_B), 2.32 (1H, br. s, OH), 1.23 (3H, d, *J* = 6.4 Hz, CH(CH₃)N); ¹³C-NMR (75.5MHz,

CDCl₃) δ 156.9, 141.3, 136.8, 133.9, 128.6, 128.2, 127.8, 127.6, 127.2, 127.1, 127.1, 120.9, 111.7, 69.8, 65.6, 61.4, 50.7, 21.1; $\nu_{\max}/\text{cm}^{-1}$ (film) 3323 (OH); MS (CI+, NH₃) m/z (%) 348 (15, [M+H]⁺), 106 (100, [M-NH₂CH(C₆H₅)CH₂OH and C₆H₅CH₂O]⁺); HRMS m/z (ES+) [M+H]⁺ - C₂₃H₂₆NO₂ requires 348.1958, found 348.1857.

5.3.2 Attempted Cleavage of Methyl Aryl Ether of (*R,R*)-**247**

Boron tribromide

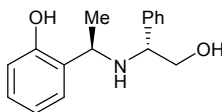
To a stirred solution of amine (*R,R*)-**247** (210 mg, 0.70 mmol) in DCM (20 mL) at -78 °C was added boron tribromide (1M solution in DCM, 2.80 mL, 2.80 mmol) and the mixture was allowed to warm to room temperature over 20 hours. The reaction mixture was quenched with the slow addition of a 1M sodium hydroxide solution (20 mL). The aqueous layer was separated and extracted with DCM (4 × 15 mL). The combined organic layers were dried over MgSO₄, filtered and the solvent removed to yield the crude product. The ¹H NMR spectrum revealed no reaction had occurred with only starting amine (*R,R*)-**247** present.

Aluminium bromide

Amine (*R,R*)-**247** (210 mg, 0.70 mmol) in toluene (0.5 mL) was added to a stirred solution of aluminium bromide (573 mg, 1.40 mmol) in toluene (6.5 mL) at room temperature. Stirring continued for 20 hours before the reaction mixture was added to saturated sodium bicarbonate solution (15 mL) at 0 °C. The mixture was filtered through Celite[®] before being extracted with EtOAc (4 × 15 mL). The combined organic layers were dried over MgSO₄, filtered and the solvent removed to yield the crude product. The ¹H NMR spectrum revealed no reaction had occurred with only starting amine (*R,R*)-**247** present.

5.3.3 Removal of Benzyl Protecting Group of (*R,R*)-**248**

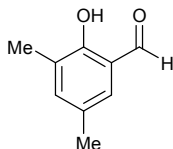
2-[(*R*)-1-[(*R*)-2-Hydroxy-1-phenylethylamino]ethyl]phenol, **253**



According to general procedure H, to 10% palladium on carbon was added to amine (*R,R*)-**248** (0.80 g, 2.30 mmol) dissolved in EtOAc (25 mL). After column chromatography (SiO₂, 80:20 PE:EtOAc) the title compound was obtained as a yellow oil (0.56 g, 1.56 mmol, 95% yield): $[\alpha]_D^{25}$ -65.5 (*c* 2.75, CH₂Cl₂); ¹H-NMR (300MHz, CDCl₃) δ 7.38-7.23 (5H, m, Ph), 7.10 (1H, app. td, *J* = 7.5 and 1.9 Hz, Ar-*H*), 6.92 (1H, app. d, *J* = 7.9, Ar-*H*), 6.78-6.72 (2H, m, 2 × Ar-*H*), 5.10 (1H, br. s, OH), 4.00 (1H, q, *J* = 6.8 Hz, CH(CH₃)N), 3.95 (1H, dd, *J* = 6.0 and 4.1 Hz, CH(Ph)CH₂), 3.89 (1H, dd, *J* = 10.9 and 4.1 Hz, CH(Ph)CH_AH_B), 3.75 (1H, dd, *J* = 10.9 and 6.0 Hz, CH(Ph)CH_AH_B), 1.46 (3H, d, *J* = 6.8 Hz, CH(CH₃)N); ¹³C-NMR (75.5MHz, CDCl₃) δ 157.0, 138.8, 128.7, 128.3, 127.8, 127.4, 127.3, 119.1, 116.8, 65.2, 60.8, 55.1, 20.4; ν_{\max} /cm⁻¹(film) 3305 (OH); MS (CI+, NH₃) *m/z* (%) 258 (20, [M+H]⁺), 138 (100, [M+H-CH(C₆H₅)CH₂OH]⁺); HRMS *m/z* (ES+) [M+H]⁺ - C₁₆H₂₀NO₂ requires 258.1489, found 258.1491.

5.3.4 Preparation of Chiral Amines (*R*)-**255a** and (*R*)-**255b**

2-Hydroxy-3,5-dimethylbenzaldehyde, **261**¹⁷²

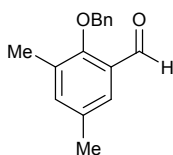


To a stirred solution of hexamethylenetetraamine (11.60 g, 82.7 mmol) dissolved in TFA (60 mL) under nitrogen was added 2,4-dimethylphenol (90% purity, 11.11 mL, 82.7 mmol). The reaction mixture was heated to reflux overnight. The solution was allowed to cool to room temperature before 3M aqueous hydrochloric acid (50 mL) was added and stirred for a further 30 minutes. The crude mixture was extracted with DCM (3 × 50 mL). The combined organic extractions were then washed with 3M aqueous hydrochloric acid (2 × 30 mL), brine (30 mL) and dried (MgSO₄). Removal of the solvent *in vacuo* yielded a yellow residue which was purified by flash

chromatography (SiO₂, 95:5 PE:EtOAc) to give a colourless oil (3.21 g, 21.4 mmol, 26% yield): ¹H-NMR (300MHz, CDCl₃) δ 11.08 (1H, s, ArOH), 9.81 (1H, s, CHO), 7.20 (1H, d, *J* = 1.5 Hz, Ar-*H*), 7.16 (1H, d, *J* = 1.5 Hz, Ar-*H*), 2.30 (3H, s, CH₃), 2.23 (3H, s, CH₃); ¹³C-NMR (75.5MHz, CDCl₃) δ 196.6, 157.9, 139.0, 130.0, 128.5, 126.5, 119.7, 20.2, 14.9; $\nu_{\max}/\text{cm}^{-1}$ (film) 3628(OH), 1651(C=O).

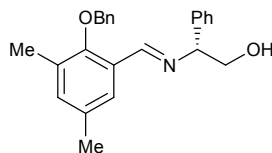
The spectroscopic data is in agreement with the literature data

2-(Benzyloxy)-3,5-dimethylbenzaldehyde, **256**



According to general procedure A, aldehyde **261** (2.32 g, 9.65 mmol) in DMF (12 mL) was treated with benzyl bromide (1.15 mL, 9.65 mmol) and potassium carbonate (5.07 g, 36.67 mmol). The crude product was taken up in 5% ether in petrol and passed through a plug of silica to remove baseline impurities to give the product as a white solid (2.18 g, 9.07 mmol, 94% yield): mp 37-40 °C; ¹H-NMR (300MHz, CDCl₃) δ 10.23 (1H, s, CHO), 7.49 (1H, d, *J* = 2.3 Hz, Ar-*H*), 7.36-7.44 (5H, m, Ph), 7.29 (1H, d, *J* = 2.3 Hz, Ar-*H*), 4.94 (2H, s, PhCH₂O), 2.33 (6H, app. s, Ar-CH₃); ¹³C-NMR (75.5MHz, CDCl₃) δ 190.4, 158.1, 138.4, 136.1, 134.0, 132.1, 129.1, 128.6, 128.5, 128.2, 126.3, 77.7, 20.0, 15.8; $\nu_{\max}/\text{cm}^{-1}$ (KBr) 1690 (C=O); MS (EI+) *m/z* (%) 240 (50, [M]⁺); HRMS *m/z* (ES+) [M+H]⁺ - C₁₆H₁₆O₂ requires 241.1223, found 241.1220.

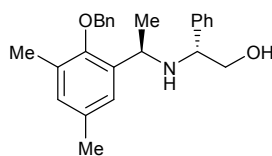
(*R*)-2-(2-(Benzyloxy)-3,5-dimethylbenzylideneamino)-2-phenylethanol, **262**



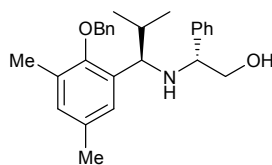
According to general procedure B, aldehyde **261** (7.00 g, 29.1 mmol) in ethanol (80 mL) was treated with (*R*)-phenyl glycinol **237** (4.00 g, 29.1 mmol). The product was obtained as a yellow solid (10.27 g, 28.5 mmol, 98%): mp 81 °C; $[\alpha]_D^{25}$ -6.0 (*c* 2.18, CHCl₃); ¹H-NMR (300MHz, CDCl₃) δ 8.64 (1H, s, CH=N), 7.71 (1H, d, *J* = 1.9 Hz, Ar-*H*), 7.42-7.27 (10H, m, 2 × Ph), 7.11 (1H, d, *J* = 1.9 Hz, Ar-*H*), 4.81 (1H, d, *J* =

10.9 Hz, PhCH_AH_BO), 4.77 (1H, d, $J = 10.9$ Hz, PhCH_AH_BO), 4.40 (1H, dd, $J = 7.9$ and 4.9 Hz, NCH(Ph)CH₂), 4.01 (1H, dd, $J = 10.9$ and 7.9 Hz, CH(Ph)CH_AH_B), 3.90 (1H, dd, $J = 10.9$ and 4.9 Hz, CH(Ph)CH_AH_B), 2.90 (1H, br s, OH), 2.33 (3H, s, Ar-CH₃), 2.30 (3H, s, Ar-CH₃); ¹³C-NMR (75.5MHz, CDCl₃) δ 159.3, 155.2, 140.7, 136.5, 134.6, 133.5, 131.0, 128.4, 128.3, 128.3, 128.0, 127.9, 127.2, 127.1, 125.4, 76.4, 76.4, 67.2, 20.6, 15.8; $\nu_{\max}/\text{cm}^{-1}$ (KBr) 3325 (OH); HRMS m/z (EI+) [M+H]⁺ - C₂₄H₂₆NO₂ requires 360.1964, found 360.1946.

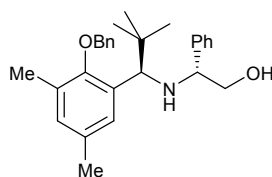
(*R*)-2-[(*R*)-1-(2-(Benzyloxy)-3,5-dimethylphenyl)ethylamino]-2-phenylethanol, 263a



According to general procedure C, imine **262** (1.00 g, 3.02 mmol) in THF (60 mL) was treated with methyl lithium (1.6M in Et₂O, 6.79 mL, 10.87 mmol). The crude product was purified by column chromatography (SiO₂, 90:10 PE:EtOAc) to give a yellow oil, which slowly solidified (0.55 g, 1.46 mmol, 49% yield, 94% de after purification): mp 72-73 °C; $[\alpha]_D^{25}$ -36.4 (c 1.32, CH₂Cl₂); ¹H-NMR (300MHz, CDCl₃) δ 7.23-7.02 (10H, m, 2 × Ph), 6.96 (1H, d, $J = 1.7$ Hz, Ar-*H*), 6.77 (1H, d, $J = 1.7$ Hz, Ar-*H*), 4.46 (1H, d, $J = 11.1$ Hz, PhCH_AH_BO), 4.35 (1H, d, $J = 11.1$ Hz, PhCH_AH_BO), 4.08 (1H, q, $J = 6.5$ Hz, CH(CH₃)N), 3.75 (1H, dd, $J = 8.0$ and 4.6 Hz, CH(Ph)CH_AH_B), 3.58 (1H, dd, $J = 10.7$ and 4.6 Hz, CH(Ph)CH_AH_B), 3.58 (1H, dd, $J = 10.7$ and 8.0 Hz, CH(Ph)CH_AH_B), 2.53 (1H, br s, OH), 2.16 (3H, s, Ar-CH₃), 2.14 (3H, s, Ar-CH₃), 1.20 (3H, d, $J = 6.5$ Hz, CH(CH₃)N); ¹³C-NMR (75.5MHz, CDCl₃) δ 151.9, 140.8, 138.3, 137.2, 133.7, 130.6, 130.5, 128.4, 128.2, 127.7, 127.4, 127.3, 127.1, 125.0, 75.0, 66.0, 61.4, 47.5, 21.9, 20.8, 16.3; $\nu_{\max}/\text{cm}^{-1}$ (KBr) 3385 (OH); MS (CI+, NH₃) m/z (%) 376 (100, [M+H]⁺), 286 (40, [M+NH₄-OCH₂(C₆H₅)]⁺); HRMS m/z (ES+) [M+H]⁺ - C₂₅H₃₀NO₂ requires 376.2271, found 376.2276.

(*R*)-2-[(*R*)-1-(2-(Benzyloxy)-3,5-dimethylphenyl)-2-methylpropylamino]-2-phenylethanol, 263b

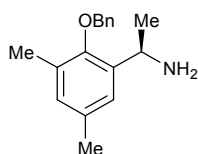
According to general procedure C, imine **262** (1.09 g, 3.28 mmol) in THF (60 mL) was treated with *iso*-propyl lithium (0.7M in hexanes, 16.9 mL, 11.81 mmol). The crude product was purified by column chromatography (SiO₂, 90:10 to 90:20 PE:EtOAc) to give a yellow oil (0.74 g, 1.97 mmol, 60% yield, 91% de after purification): $[\alpha]_D^{25}$ -47.6 (*c* 1.47, CH₂Cl₂); ¹H-NMR (300MHz, CDCl₃) δ 7.42-7.29 (5H, m, Ph), 7.25-7.14 (5H, m, Ph), 6.87 (1H, s, Ar-*H*), 6.85 (1H, s, Ar-*H*), 4.65 (1H, d, *J* = 11.3 Hz, PhCH_AH_BO), 4.47 (1H, d, *J* = 11.3 Hz, PhCH_AH_BO), 3.87 (1H, d, *J* = 6.8 Hz, CH(*i*-Pr)N), 3.78 (1H, dd, *J* = 10.2 and 4.5 Hz, CH(Ph)CH_AH_B), 3.72 (1H, dd, *J* = 5.7 and 4.5 Hz, CH(Ph)CH_AH_B), 3.54 (1H, dd, *J* = 10.2 and 5.7 Hz, CH(Ph)CH_AH_B), 2.25 (3H, s, Ar-CH₃), 2.24 (3H, s, Ar-CH₃), 2.00 (1H, app. sept, *J* = 6.8 Hz, CH(CH₃)₂), 1.02 (3H, d, *J* = 6.8 Hz, (CH₃)CH(CH₃)), 0.88 (3H, d, *J* = 6.8 Hz, (CH₃)CH(CH₃)); ¹³C-NMR (75.5MHz, CDCl₃) δ 153.3, 141.9, 137.6, 135.6, 133.2, 130.5, 128.4, 128.3, 127.8, 127.3, 127.2, 127.2, 126.0, 74.4, 65.0, 61.8, 33.4, 20.9, 19.8, 19.6, 16.6; ν_{\max} /cm⁻¹(film) 3418 (OH); MS (CI⁺, NH₃) *m/z* (%) 404 (100, [M+H]⁺); HRMS *m/z* (ES⁺) [M+H]⁺ - C₂₇H₃₄NO₂ requires 404.2584, found 404.2586.

(*R*)-2-[(*R*)-1-(2-(Benzyloxy)-3,5-dimethylphenyl)-2,2-dimethylpropylamino]-2-phenylethanol, 263c

According to general procedure C, imine **262** (1.09 g, 3.28 mmol) in THF (60 mL) was treated with *tert*-butyl lithium (1.7M in pentane, 6.95 mL, 11.81 mmol). The crude product was purified by column chromatography (SiO₂, 90:10 to 90:20 PE:EtOAc) to give a yellow oil (0.75 g, 1.80 mmol, 55% yield, 85% de after purification): ¹H-NMR (300MHz, CDCl₃) δ 7.52-7.32 (5H, m, Ph), 7.32-7.20 (5H, m, Ph), 6.94 (1H, d, *J* = 2.3 Hz, Ar-*H*), 6.90 (1H, d, *J* = 2.3 Hz, Ar-*H*), 4.66 (1H, d, *J*

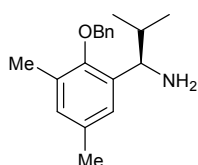
= 11.7 Hz, PhCH_AH_BO), 4.36 (1H, d, *J* = 11.7 Hz, PhCH_AH_BO), 4.07 (1H, s, CH(^tBu)N), 3.80 (1H, dd, *J* = 10.2 and 9.8 Hz, CH(Ph)CH_AH_B), 3.76 (1H, dd, *J* = 9.8 and 4.9 Hz, CH(Ph)CH_AH_B), 3.60 (1H, dd, *J* = 10.2 and 4.9 Hz, CH(Ph)CH_AH_B), 2.33 (3H, s, Ar-CH₃), 2.30 (3H, s, Ar-CH₃), 1.04 (9H, s, ^tBu); ¹³C-NMR (75.5MHz, CDCl₃) δ 153.8, 142.3, 137.9, 134.9, 132.4, 130.3, 130.0, 128.4, 128.3, 127.6, 127.3, 127.2, 126.9, 126.0, 73.6, 65.2, 63.2, 61.6, 36.3, 27.0, 20.9, 16.6; MS (CI+, NH₃) *m/z* (%) 418 (100, [M+H]⁺); HRMS *m/z* (ES+) [M+H]⁺ - C₂₈H₃₆NO₂ requires 418.2741, found 418.2744.

[*R*]-1-[2-(Benzyloxy)-3,5-dimethylphenyl]ethanamine, 255a



According to general procedure D, amine **263a** (0.50 g, 1.33 mmol) dissolved in DCM (5 mL) and MeOH (2.5 mL) was treated with lead (IV) acetate (0.59 g, 1.33 mmol). The crude product was purified by column chromatography (SiO₂, 50:49:1 DCM:EtOAc:Et₃N) to give a pale yellow oil (0.20 g, 0.78 mmol, 59% yield): $[\alpha]_D^{20} +8.81$ (*c* 1.14, CH₂Cl₂); ¹H-NMR (300MHz, CDCl₃) δ 7.51-7.32 (5H, m, Ph), 7.09 (1H, d, *J* = 1.5 Hz, Ar-*H*), 6.94 (1H, d, *J* = 1.5 Hz, Ar-*H*), 4.87 (1H, d, *J* = 11.3 Hz, PhCH_AH_BO), 4.82 (1H, d, *J* = 11.3 Hz, PhCH_AH_BO), 4.46 (1H, q, *J* = 6.8 Hz, CH(CH₃)N), 2.33 (3H, s, Ar-CH₃), 2.31 (3H, s, Ar-CH₃), 1.64 (2H, br s, NH₂), 1.38 (3H, d, *J* = 6.8 Hz, CH(CH₃)N); ¹³C-NMR (75.5MHz, CDCl₃) δ 152.0, 140.3, 137.4, 133.8, 130.8, 130.4, 128.5, 128.0, 127.7, 124.1, 75.2, 44.6, 24.5, 20.9, 16.4; $\nu_{\max}/\text{cm}^{-1}$ (film) 3367 and 3299 (NH₂); MS (CI+, NH₃) *m/z* (%) 256 (100, [M+H]⁺), 166 (70, [M+H-OCH₂(C₆H₅)]⁺); HRMS *m/z* (ES+) [M+H]⁺ - C₁₇H₂₂NO requires 256.1696, found 256.1698.

[*R*]-1-[2-(Benzyloxy)-3,5-dimethylphenyl]-2-methylpropan-1-amine, 255b

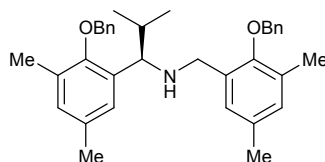


According to general procedure D, amine **263b** (3.33 g, 8.25 mmol) dissolved in DCM (40 mL) and MeOH (20 mL) was treated with lead (IV) acetate (3.66 g, 8.25

mmol). The crude product was purified by column chromatography (SiO₂, 50:49:1 DCM:EtOAc:Et₃N) to give a yellow oil (1.46 g, 5.20 mmol, 63% yield): $[\alpha]_D^{20}$ -5.9 (*c* 2.38, CH₂Cl₂); ¹H-NMR (300MHz, CDCl₃) δ 7.53-7.48 (2H, m, Ph), 7.46-7.33 (3H, m, Ph), 7.05 (1H, d, *J* = 1.5 Hz, Ar-*H*), 6.99 (1H, d, *J* = 1.5 Hz, Ar-*H*), 4.88 (1H, d, *J* = 11.3 Hz, PhCH_AH_BO), 4.83 (1H, d, *J* = 11.3 Hz, PhCH_AH_BO), 3.97 (1H, d, *J* = 7.9 Hz, CH(^{*t*}Pr)N), 2.35 (3H, s, Ar-CH₃), 2.32 (3H, s, Ar-CH₃), 1.93 (1H, app. sept, *J* = 6.8 Hz, CH(CH₃)₂), 1.42 (2H, br. s, NH₂), 1.03 (3H, d, *J* = 6.8 Hz, (CH₃)CH(CH₃)), 0.83 (3H, d, *J* = 6.8 Hz, (CH₃)CH(CH₃)); ¹³C-NMR (75.5MHz, CDCl₃) δ 152.5, 138.5, 137.6, 133.4, 130.4, 130.2, 128.4, 127.8, 127.5, 125.1, 74.9, 55.2, 34.7, 20.9, 20.3, 18.8, 16.4; ν_{\max} /cm⁻¹(film) 3376 and 3310 (NH₂); MS (CI+, NH₃) *m/z* (%) 284 (100, [M+H]⁺); HRMS *m/z* (ES+) [M+H]⁺ - C₁₉H₂₆NO requires 284.2009, found 284.2011.

5.3.5 Attempted Preparation of (*R*)-**266b** via Reductive Amination ((*R*)-**265b** Formed)

(*R*)-*N*-(2-(Benzyloxy)-3,5-dimethylbenzyl)-1-(2-(benzyloxy)-3,5-dimethylphenyl)-2-methylpropan-1-amine, **265b**



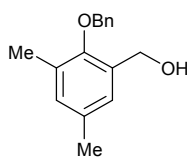
To a mixture of amine (*R*)-**255b** (150 mg, 0.47 mmol), aldehyde **256** (106 mg, 0.47 mmol) in DCE (6 mL) was added sodium triacetoxyborohydride (139 mg, 0.66 mmol). The reaction was then stirred at room temperature under a nitrogen atmosphere and monitored by TLC. When the reaction was deemed complete the reaction was quenched with saturated sodium bicarbonate (10 mL) and the crude product was extracted with EtOAc (3 × 15 mL). The organic layer was dried (MgSO₄), filtered and the solvent removed *in vacuo* to yield the crude product. The title compound was isolated after column chromatography (SiO₂, 75:24:1 PE:EtOAc:Et₃N) to give a pale yellow oil (191 mg, 0.37 mmol, 80% yield): $[\alpha]_D^{20}$ +9.6 (*c* 1.04, CH₂Cl₂); ¹H-NMR (300MHz, CDCl₃) δ 7.17 (1H, d, *J* = 1.9 Hz, Ar-*H*), 7.06 (1H, d, *J* = 2.3 Hz, Ar-*H*), 6.97 (1H, d, *J* = 1.9 Hz, Ar-*H*), 6.94 (1H, d, *J* = 2.3 Hz, Ar-*H*), 4.82 (1H, d, *J* = 10.9 Hz, PhCH_AH_BO), 4.79 (1H, d, *J* = 11.7 Hz,

PhCH_AH_BO), 4.76 (1H, d, $J = 10.9$ Hz, PhCH_AH_BO), 4.70 (1H, d, $J = 11.7$ Hz, PhCH_AH_BO), 3.95 (1H, d, $J = 6.8$ Hz, CH(^tPr)N), 3.72 (2H, s, NCH₂Ar), 2.36 (3H, s, Ar-CH₃), 2.33 (3H, s, Ar-CH₃), 2.31 (3H, s, Ar-CH₃), 2.30 (3H, s, Ar-CH₃), 1.97 (1H, app. sept, $J = 6.8$ Hz, CH(CH₃)₂), 1.03 (3H, d, $J = 6.8$ Hz, (CH₃)CH(CH₃)), 0.88 (3H, d, $J = 6.8$ Hz, (CH₃)CH(CH₃)); ¹³C-NMR (75.5MHz, CDCl₃) δ 153.9, 153.3, 137.7, 137.6, 135.8, 133.4, 133.4, 133.2, 130.8, 130.5, 130.4, 130.2, 129.0, 128.3, 128.1, 127.7, 127.6, 127.6, 127.3, 125.9, 74.8, 74.3, 53.3, 46.9, 34.2, 27.6, 22.6, 20.2, 19.0, 16.4, 16.2; MS (CI⁺, NH₃) m/z (%) 508 (100, [M+H]⁺); HRMS m/z (ES⁺) [M+H]⁺ - C₃₅H₄₂NO₂ requires 508.3210, found 508.3208.

To a mixture of secondary amine (*R*)-**265b** (13 mg, 0.026 mmol), aldehyde **256** (8 mg, 0.031 mmol) and acetic acid (1 μ L) in DCE (1 mL) was added sodium triacetoxyborohydride (8 mg, 0.036 mmol). The reaction was then stirred at room temperature under a nitrogen atmosphere and monitored by TLC for 48 hours after which it was quenched with saturated sodium bicarbonate (5 mL) and the crude product was extracted with EtOAc (3 \times 10 mL). The organic layer was dried (MgSO₄), filtered and the concentrated. The ¹H NMR spectrum showed that no tertiary amine had formed, only the slow reduction of the aldehyde **256** to the corresponding alcohol **268**.

5.3.6 Preparation of Benzyl Bromide **267**

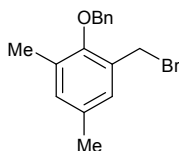
[2-(Benzyloxy)-3,5-dimethylphenyl]methanol, **268**



According to general procedure E, aldehyde **256** (4.50 g, 18.7 mmol) in ethanol (50 mL) was treated with sodium borohydride (0.99 g, 26.2 mmol). The product was obtained as a colourless oil (4.49 g, 18.5 mmol, 99% yield): ¹H-NMR (300MHz, CDCl₃) δ 7.50-7.30 (5H, m, Ph), 7.02 (1H, s, Ar-*H*), 6.98 (1H, s, Ar-*H*), 4.86 (2H, s, OCH₂Ph), 4.62 (2H, s, CH₂OH), 2.33 (3H, s, Ar-CH₃), 2.30 (3H, s, Ar-CH₃), 2.24 (1H, br s, OH); ¹³C-NMR (75.5MHz, CDCl₃) δ 153.0, 137.3, 133.8, 133.6, 131.6, 130.9, 128.6, 128.2, 128.0, 127.5, 75.5, 61.6, 20.7, 16.2; $\nu_{\max}/\text{cm}^{-1}$ (film) 3400 (OH);

MS (CI⁺, NH₃) *m/z* (%) 242 (100, [M+H]⁺); HRMS *m/z* (ES⁺) [M+NH₄]⁺ - C₁₆H₂₂NO₂ requires 260.1645, found 260.1643.

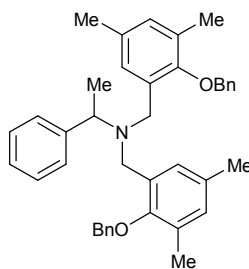
2-(Benzyloxy)-1-(bromomethyl)-3,5-dimethylbenzene, **267**



According to general procedure F, benzyl alcohol **268** (2.76 g, 11.40 mmol) in ether (120 mL) was treated with phosphorus tribromide (1.18 mL, 12.53 mmol). The product was isolated without the need for further purification as a pale yellow solid (3.37 g, 11.0 mmol, 97% yield): mp 58-60 °C; ¹H-NMR (300MHz, CDCl₃) δ 7.58-7.53 (2H, m, Ph), 7.48-7.36 (3H, m, Ph), 7.06 (1H, s, Ar-*H*), 7.00 (1H, s, Ar-*H*), 5.00 (2H, s, OCH₂Ph), 4.56 (2H, s, CH₂Br), 2.34 (3H, s, Ar-CH₃), 2.31 (3H, s, Ar-CH₃); ¹³C-NMR (75.5MHz, CDCl₃) δ 153.3, 137.3, 134.0, 132.9, 131.4, 130.9, 129.5, 128.6, 128.1, 127.9, 74.8, 28.9, 20.7, 16.3.

5.3.7 Synthesis of Chiral Ligand (*R*)-**254a**

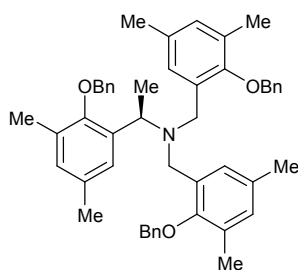
N,N-bis(2-(Benzyloxy)-3,5-dimethylbenzyl)-1-phenylethanamine, **270**



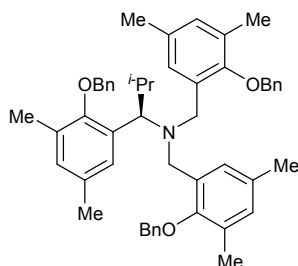
To a stirred solution of α -methyl benzylamine (50 μ L, 0.39 mmol), potassium carbonate (107 mg, 0.78 mmol) and 4Å molecular sieves (0.25 g) in DMF (2 mL) was added the benzyl bromide analogue **267** (0.24 g, 0.78 mmol). The reaction was stirred at room temperature overnight before being filtered through Celite[®] and the organic solvents removed *in vacuo* to leave a crude oil. After purification by column chromatography (SiO₂, 92:8 PE:Et₂O) the title compound was obtained as pale yellow oil (70 mg, 0.12 mmol, 31% yield): ¹H-NMR (300MHz, CDCl₃) δ 7.48-7.29 (17H, m, 3 × Ph and 2 × Ar-*H*), 6.93 (2H, d, *J* = 1.9 Hz, Ar-*H*), 4.73 (2H, d, *J* = 11.3 Hz, 2 × PhCH_AH_BO), 4.69 (2H, d, *J* = 11.3 Hz, 2 × PhCH_AH_BO), 4.00 (1H, q, *J* =

6.8 Hz, $CH(CH_3)N$), 3.79 (2H, d, $J = 14.3$ Hz, $2 \times ArCH_AH_BN$), 3.53 (2H, d, $J = 14.3$ Hz, $2 \times ArCH_AH_BN$), 2.37 (6H, s, $2 \times Ar-CH_3$), 2.30 (6H, s, $2 \times Ar-CH_3$), 1.44 (3H, d, $J = 6.8$ Hz, $CHCH_3$); ^{13}C -NMR (75.5MHz, $CDCl_3$) δ 153.6, 142.5, 137.5, 133.2, 133.0, 132.7, 130.4, 130.0, 128.4, 128.2, 128.1, 127.9, 127.9, 127.8, 126.5, 74.9, 57.1, 47.4, 21.0, 16.3, 14.6; MS (CI+, NH_3) m/z (%) 570 (30, $[M+H]^+$), 346 (80, $[M+H-C_{16}H_{17}O]^+$); HRMS m/z (ES+) $[M+H]^+$ - $C_{40}H_{44}NO_2$ requires 570.3367, found 570.3362.

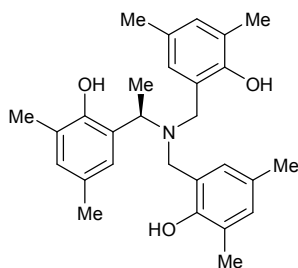
(*R*)-*N,N*-bis(2-(Benzyloxy)-3,5-dimethylbenzyl)-1-(2-(benzyloxy)-3,5-dimethylphenyl)ethanamine, **266a**



According to general procedure G, amine (*R*)-**255a** (0.55 g, 2.17 mmol), potassium carbonate (0.75 g, 5.42 mmol), 4Å MS (1.00 g) dissolved in DMF (11 mL) was reacted with bromide **267** (1.65 g, 5.42 mmol). The crude product was purified by column chromatography (SiO_2 , first column 90:10 to 70:30 PE:DCM; second column 95:5 PE:EtOAc) to give a pale yellow oil (0.92 g, 1.24 mmol, 57% yield): $[\alpha]_D^{25}$ -10.1 (c 2.17, CH_2Cl_2); 1H -NMR (300MHz, $CDCl_3$) δ 7.41 (2H, d, $J = 1.5$ Hz, $2 \times Ar-H$), 7.35-7.24 (13H, m, Ph), 7.23 (1H, d, $J = 1.9$ Hz, $Ar-H$), 7.11-7.06 (2H, m, Ph), 6.96 (1H, d, $J = 1.9$ Hz, $Ar-H$), 6.86 (2H, d, $J = 1.5$ Hz, $2 \times Ar-H$), 4.65 (2H, d, $J = 11.3$ Hz, $2 \times PhCH_AH_BO$), 4.59 (1H, q, $J = 7.2$ Hz, $CH(CH_3)N$), 4.57 (2H, d, $J = 11.3$ Hz, $2 \times PhCH_AH_BO$), 4.55 (2H, s, $PhCH_2O$), 3.82 (2H, d, $J = 15.4$ Hz, $2 \times CH_AH_BN$), 3.72 (2H, d, $J = 15.4$ Hz, $2 \times CH_AH_BN$), 2.31 (3H, s, $Ar-CH_3$), 2.30 (6H, s, $2 \times Ar-CH_3$), 2.27 (3H, s, $Ar-CH_3$), 2.23 (6H, s, $2 \times Ar-CH_3$), 1.45 (d, 3H, $J = 7.2$ Hz, $CH(CH_3)N$); ^{13}C -NMR (75.5MHz, $CDCl_3$) δ 152.8, 152.6, 137.3, 136.5, 133.8, 133.3, 133.1, 133.0, 130.6, 130.4, 130.3, 129.5, 128.5, 128.3, 128.2, 128.0, 127.7, 126.9, 126.6, 75.2, 73.6, 51.3, 48.1, 23.2, 23.2, 21.4, 19.8, 16.5, 16.1 (spectra run at 253 K); MS (CI+, NH_3) m/z (%) 704 (15, $[M+H]^+$); HRMS m/z (ES+) $[M+H]^+$ - $C_{49}H_{54}NO_3$ requires 704.4098, found 704.4108.

(*R*)-*N,N*-bis(2-(Benzyloxy)-3,5-dimethylbenzyl)-1-(2-(benzyloxy)-3,5-dimethylphenyl)-2-methylpropan-1-amine, 266b

According to general procedure G, amine (*R*)-**255b** (54 mg, 0.19 mmol), potassium carbonate (99 mg, 0.72 mmol), 4Å MS (100 mg) dissolved in DMF (2 mL) was reacted with bromide **267** (145 mg, 0.48 mmol). The crude product was purified by column chromatography (SiO₂, first column 90:10 to 70:30 PE:DCM; second column 95:5 PE:EtOAc) to give a white powder (73 mg, 0.10 mmol, 54% yield): mp 103-104 °C; $[\alpha]_D^{20}$ -25.2 (*c* 1.39, CH₂Cl₂); ¹H-NMR (300MHz, CDCl₃) δ 7.62 (2H, d, *J* = 1.5 Hz, 2 × Ar-*H*), 7.29-7.14 (13H, m, Ph), 7.03 (1H, d, *J* = 1.9 Hz, Ar-*H*), 7.00 (1H, d, *J* = 1.9 Hz, Ar-*H*), 6.85 (1H, d, *J* = 1.5 Hz, Ar-*H*), 6.81-6.76 (2H, m, Ph), 4.65 (2H, d, *J* = 10.9 Hz, 2 × PhCH_AH_BO), 4.55 (1H, d, *J* = 10.9 Hz, PhCH_AH_BO), 4.48 (2H, d, *J* = 10.9 Hz, 2 × PhCH_AH_BO), 4.45 (1H, d, *J* = 10.9 Hz, PhCH_AH_BO), 4.22 (1H, d, *J* = 11.3 Hz, CH(^{*t*}Pr)N), 3.70 (2H, d, *J* = 16.2 Hz, 2 × CH_AH_BN), 3.56 (2H, d, *J* = 16.2 Hz, 2 × CH_AH_BN), 2.55-2.40 (1H, m, (CH₃)CH(CH₃)), 2.31 (6H, s, 2 × Ar-CH₃), 2.27 (3H, s, Ar-CH₃), 2.21 (6H, s, 2 × Ar-CH₃), 2.19 (3H, s, Ar-CH₃), 1.52 (3H, d, *J* = 6.4 Hz, (CH₃)CH(CH₃)), 0.85 (d, *J* = 6.4 Hz, (CH₃)CH(CH₃)); ¹³C-NMR (75.5MHz, CDCl₃) δ 154.7, 152.9, 137.8, 137.2, 133.5, 133.1, 132.7, 130.6, 130.5, 130.3, 130.2, 129.4, 129.4, 128.3, 128.1, 127.8, 127.6, 127.3, 126.5, 75.0, 73.5, 61.8, 47.8, 29.4, 22.1, 21.3, 21.3, 21.1, 16.7, 16.1; MS (ES+) *m/z* (%) 732 (100, [M+H]⁺); HRMS *m/z* (ES+) [M+H]⁺ - C₅₁H₅₈NO₃ requires 732.4411, found 732.4408.

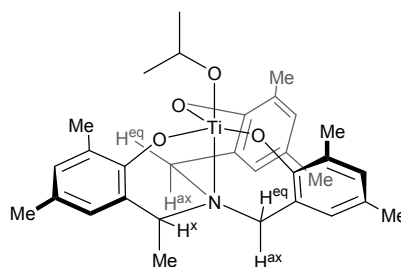
(*R*)-*N,N*-bis(2-(Hydroxy)-3,5-dimethylbenzyl)-1-(2-(hydroxy)-3,5-dimethylphenyl)ethylamine, 254a

According to general procedure H, to 10% palladium on carbon was added to amine (*R*)-**266a** (0.92 g, 1.07 mmol) dissolved in EtOAc (15 mL). The title compound was obtained as a white powder (0.45 g, 1.04 mmol, 98% yield): $[\alpha]_D^{25} -13.9$ (*c* 0.58, CHCl₃); ¹H-NMR (300 MHz, CDCl₃) δ 6.85 (1H, d, *J* = 1.5 Hz, Ar-*H*), 6.82 (3H, app. s, 3 \times Ar-*H*), 6.69 (2H, d, *J* = 1.9 Hz, 2 \times Ar-*H*), 4.49 (3H, br s, 3 \times OH), 4.34 (1H, q, *J* = 6.8 Hz, CH(CH₃)N), 3.87 (2H, d, *J* = 13.2 Hz, 2 \times ArCH_AH_BN), 3.51 (2H, d, *J* = 13.2 Hz, 2 \times ArCH_AH_BN), 2.22 (3H, s, Ar-CH₃), 2.21 (3H, s, Ar-CH₃), 2.18 (6H, s, 2 \times Ar-CH₃), 2.16 (6H, s, 2 \times Ar-CH₃), 1.49 (3H,d, *J* = 6.8 Hz, CH(CH₃)N); ¹³C-NMR (75.5MHz, CDCl₃) δ 151.2, 150.8, 131.0, 130.7, 128.8, 128.5, 128.1, 125.7, 125.5, 124.6, 124.5, 121.8, 53.2, 51.2, 20.5, 20.2, 15.9, 15.7, 8.7; MS (CI+, NH₃) *m/z* (%) 434 (15, [M+H]⁺), 286 (80, [M+H-C₁₀H₁₃O]⁺), 152 (100, [M+NH₄-C₁₉H₂₄NO₂]⁺); HRMS *m/z* (ES+) [M+H]⁺ - C₂₈H₃₆NO₃ requires 434.2690, found 434.2693.

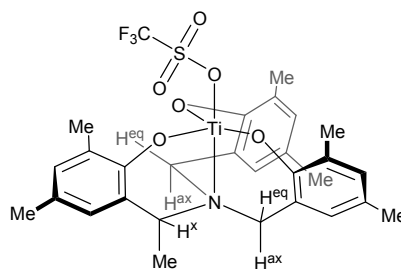
5.4 RESULTS AND DISCUSSION II

5.4.1 Preparation of Titanium Complexes (*R,M*)-271 and (*R,M*)-272

Titanium tris(phenolate) *iso*-propoxide complex, (*R,M*)-271



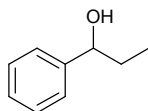
Titanium (IV) *iso*-propoxide (68 μL , 0.23 mmol) was added to a suspension of ligand (*R*)-254a (100 mg, 0.23 mmol) in toluene (3 mL) under an argon atmosphere. The resulting solution was heated to reflux and concentrated under vacuum to afford the crude product as a yellow-orange solid (121 mg, 0.23 mmol, 98% yield): $[\alpha]_D^{25}$ -28.2 (c 0.85, CHCl_3); $^1\text{H-NMR}$ (300MHz, CDCl_3) δ 6.90-6.82 (4H, m, $4 \times \text{Ar-H}$), 6.76 (1H, d, $J = 1.5$ Hz, Ar-*H*), 6.70 (1H, d, $J = 1.5$ Hz, Ar-*H*), 5.24 (1H, sept, $J = 6.0$ Hz, $\text{CH}(\text{CH}_3)_2$), 4.00 (1H, q, $J = 6.8$ Hz, $\text{CH}^x(\text{CH}_3)\text{N}$), 3.74 (1H, d, $J = 14.3$ Hz, $\text{CH}^{\text{eq}}\text{H}^{\text{ax}}\text{N}$), 3.53 (1H, d, $J = 13.2$ Hz, $\text{CH}^{\text{eq}}\text{H}^{\text{ax}}\text{N}$), 3.22-3.08 (2H, m, $2 \times \text{CH}^{\text{eq}}\text{H}^{\text{ax}}\text{N}$), 2.27 (6H, app s, $2 \times \text{Ar-CH}_3$), 2.26 (3H, s, Ar- CH_3), 2.24 (3H, s, Ar- CH_3), 2.23 (3H, s, Ar- CH_3), 2.21 (3H, s, Ar- CH_3), 1.53 (6H, d, $J = 6.0$ Hz, $\text{CH}(\text{CH}_3)_2$), 1.45 (3H, d, $J = 6.8$ Hz, $\text{CH}^x(\text{CH}_3)\text{N}$); $^{13}\text{C-NMR}$ (75.5MHz, toluene- d_8) δ 160.9, 160.9, 160.4, 131.0, 130.9, 130.7, 129.3, 129.1, 129.0, 128.5, 128.3, 128.1, 125.7, 125.7, 124.6, 124.4, 124.4, 123.9, 79.6, 54.1, 53.5, 51.3, 26.1, 26.0, 25.4, 21.2, 16.8, 16.6, 16.6, 9.0.

Titanium tris(phenolate) triflate complex, *(R,M)*-272

Titanium tris(phenolate) *iso*-propoxide complex, *(R,M)*-271 (80 mg, 0.15 mmol) in toluene (2 mL) was treated with trimethylsilyltriflate (27 μ L, 0.15 mmol) under an argon atmosphere. The resulting suspension was heated to reflux and concentrated under vacuum to a yield the crude product as a deep red solid (87 mg, 0.14 mmol, 95% yield): $^1\text{H-NMR}$ (300MHz, CDCl_3) δ 6.95-6.87 (4H, m, $4 \times \text{Ar-H}$), 6.83 (1H, d, $J = 1.5$ Hz, Ar-H), 6.77 (1H, d, $J = 1.5$ Hz, Ar-H), 4.11 (1H, q, $J = 6.8$ Hz, $\text{CH}^x(\text{CH}_3)\text{N}$), 3.88 (1H, d, $J = 14.3$ Hz, $\text{CH}^{\text{eq}}\text{H}^{\text{ax}}\text{N}$), 3.67 (1H, d, $J = 13.2$ Hz, $\text{CH}^{\text{eq}}\text{H}^{\text{ax}}\text{N}$), 3.49-3.35 (2H, m, $2 \times \text{CH}^{\text{eq}}\text{H}^{\text{ax}}\text{N}$), 2.29 (3H, s, Ar-CH_3), 2.26 (3H, s, Ar-CH_3), 2.24 (3H, s, Ar-CH_3), 2.24 (3H, s, Ar-CH_3), 2.23 (3H, s, Ar-CH_3), 2.21 (3H, s, Ar-CH_3), 1.60 (3H, d, $J = 6.8$ Hz, $\text{CH}^x(\text{CH}_3)\text{N}$); $^{13}\text{C-NMR}$ (75.5MHz, CDCl_3) δ 160.8, 160.6, 160.1, 132.1, 132.0, 131.6, 131.4, 131.2, 130.5, 127.3, 125.9, 125.4, 124.3, 124.2, 124.2, 122.4, 121.7, 117.5, 55.1, 54.3, 51.3, 21.0, 20.7, 20.6, 15.8, 15.6, 14.1, 10.0; HRMS m/z (EI+) $[\text{M}]^+$ - $\text{C}_{29}\text{H}_{32}\text{F}_3\text{NO}_6\text{STi}$ requires 627.1376, found 627.1375.

5.4.2 Addition of Diethyl Zinc to Benzaldehyde Catalysed by *(R,M)*-271 and *(R,M)*-272

1-Phenylpropan-1-ol, 275a¹⁷³



A solution of diethyl zinc in hexane (1M solution, 0.558 mL, 0.558 mmol) was added to a solution of catalyst (see **Table 66**) in DCM (1 mL). This solution was stirred for 10 minutes before being cooled to 0 $^{\circ}\text{C}$ and benzaldehyde (19 μ L, 0.186 mmol) was added. Stirring was continued at 0 $^{\circ}\text{C}$ for 6 hours, then at room temperature overnight. The solution was quenched by addition of aqueous 1 M hydrochloric acid (5 mL). The aqueous layer was extracted with EtOAc and the combined organic

layers were dried (MgSO_4), filtered and the solvent removed *in vacuo* to yield the crude product as a yellow oil. Column chromatography (SiO_2 , 80:20 PE:EtOAc) resulted in the product as a yellow oil. The enantiomeric excess of the alcohol **275a** was determined *via* chiral HPLC analysis over a Daicel Chiralcel OD-H column using a mixed *n*-hexane/*i*-PrOH (98:2) solvent system at a flow rate of 1 mL/min with the enantiomers of **275a** having retention times of 10 min (*R*) and 12 min (*S*) (detection at 254 nm). The configuration of the alcohol product was determined by the order of elution of the enantiomers compared with the literature.¹⁷³

$^1\text{H-NMR}$ (300MHz, CDCl_3) δ 7.37-7.25 (5H, m, Ph), 4.60 (1H, t, $J = 6.8$ Hz, *CHOH*), 1.90-1.70 (2H, m, CH_2), 0.92 (3H, t, $J = 7.2$ Hz, CH_3); $^{13}\text{C-NMR}$ (75.5MHz, CDCl_3) δ 144.5, 128.4, 127.5, 125.9, 76.0, 31.9, 10.1.

The spectroscopic data is in agreement with the literature data

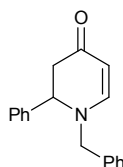
Table 66

Entry	Catalyst	Conversion /%	Isolated yield /%	ee ^a /%
1	none	trace	-	-
2	(<i>R</i>)- 254a (20mol %)	trace	-	-
3	(<i>rac</i>)- 194b (20mol %)	54	29	0
4	(<i>R,M</i>)- 271 (20mol %)	45	20	0
5	(<i>R,M</i>)- 272 (20mol %)	57	32	0
6	(<i>S</i>)-BINOL 13 (20mol %) Ti(<i>O</i> ^{<i>t</i>} Pr) ₄ (140mol %)	86	70	77(<i>S</i>)

^a Enantiomeric excess determined *via* chiral HPLC analysis

5.4.3 Aza-Diels Alder Reaction Catalysed by (*R,M*)-**272**

1-Benzyl-2-phenyl-2,3-dihydropyridin-4-one, **206a**¹⁴⁹



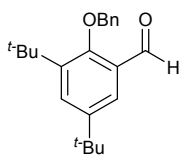
To a solution of titanium tris(phenolate) triflate (*R,M*)-**272** (28 mg, 0.046 mmol) in DCM (1 mL) was added *N*-benzylidene(phenyl)methanamine **204a** (43 μL , 0.23 mmol). The reaction mixture was cooled to -78 °C before Danishefsky's diene **205** (134 μL , 0.70 mmol) was added. After stirring at -78 °C for 4 hours the reaction mixture was warmed to room temperature and stirred overnight. The reaction

mixture was quenched with saturated ammonium chloride solution (8 mL) and the aqueous layer extracted with DCM (3 × 15 mL). The combined organic layers were dried (MgSO₄) and concentrated *in vacuo* to afford the crude product as a yellow oil. Column chromatography (SiO₂, 50:50 PE:EtOAc) resulted in the product as a yellow oil (24 mg, 0.09 mmol, 39% yield, 0% ee). The enantiomeric excess of the dihydropyridinone **206a** was determined *via* chiral HPLC analysis over a Daicel Chiralcel AD column using a mixed *n*-hexane/*i*-PrOH (97:3) solvent system at a flow rate of 1 mL/min with the enantiomers of **206a** having retention times of 70 min (*R*) and 79 min (*S*) (detection at 225 nm): ¹H-NMR (300MHz, CDCl₃) δ 7.36-7.19 (9H, m, 8 × Ar-*H* and CH=CHN), 7.13-7.07 (2H, m, 2 × Ar-*H*), 5.06 (1H, d, *J* = 7.5 Hz, CH=CHN), 4.47 (1H, dd, *J* = 7.9 and 7.5 Hz, NCH(Ph)), 4.32 (1H, d, *J* = 15.1 Hz, CH_AH_BPh), 4.09 (1H, d, *J* = 15.1 Hz, CH_AH_BPh), 2.82 (1H, dd, *J* = 16.6 and 7.5 Hz, NCH(Ph)CH_AH_B), 2.65 (1H, dd, *J* = 16.6 and 7.9 Hz, NCH(Ph)CH_AH_B); ¹³C-NMR (75.5MHz, CDCl₃) δ 190.3, 154.2, 138.6, 135.9, 129.0, 128.9, 128.3, 128.2, 127.7, 127.1, 98.7, 60.7, 57.2, 43.7; HRMS *m/z* (ES+) [M+H]⁺ - C₁₈H₁₈NO requires 264.1388, found 264.1366.

The spectroscopic data is in agreement with the literature data

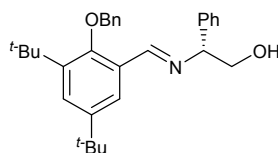
5.4.4 Attempted *aza-Diels Alder Reaction Catalysed by (R)-254a*

To a solution of ligand (*R*)-**254a** (26 mg, 0.060 mmol) in DCM (1 mL) was added borane dimethylsulfide (1M solution in DCM, 60 μL, 0.60 mmol) and stirred at room temperature for 30 minutes. To this was added *N*-benzylidene(phenyl)methanamine **204a** (58 μL, 0.30 mmol). The reaction mixture was cooled to -78 °C before Danishefsky's diene **205** (174 μL, 0.90 mmol) was added. After stirring at -78 °C for 4 hours the reaction mixture was warmed to room temperature and stirred overnight. The reaction mixture was quenched with saturated ammonium chloride solution (8 mL) and the aqueous layer extracted with DCM (3 × 15 mL). The combined organic layers were dried (MgSO₄) and concentrated *in vacuo* to afford the crude product as a yellow oil. The ¹H NMR spectrum revealed there to be starting imine **204a** present with only trace amounts of the desired product.

5.4.5 Synthesis of Chiral Amine (*R*)-2792-(Benzyloxy)-3,5-di-*tert*-butylbenzaldehyde, **282**¹⁷⁴

According to general procedure A, 3,5-di-*tert*-butyl-2-hydroxybenzaldehyde (40.0 g, 171 mmol) in DMF (200 mL) was treated with benzyl bromide (20.3 mL, 171 mmol) and potassium carbonate (89.3 g, 650 mmol). The product was isolated without the need for further purification as a pale brown solid (55.2 g, 170 mmol, 99% yield): mp 95-98 °C [Lit.¹⁷⁴ mp 96-97 °C]; ¹H-NMR (300MHz, CDCl₃) δ 10.39 (1H, s, CHO), 7.80 (1H, d, *J* = 2.6 Hz, Ar-*H*), 7.71 (1H, d, *J* = 2.6 Hz, Ar-*H*), 7.56-7.35 (5H, m, Ph), 5.08 (2H, s, PhCH₂O), 1.50 (9H, s, *t*-Bu), 1.38 (9H, s, *t*-Bu); ¹³C-NMR (75.5MHz, CDCl₃) δ 190.7, 159.6, 146.5, 143.0, 136.5, 130.9, 129.2, 128.6, 128.1, 126.9, 124.0, 80.3, 35.3, 34.7, 31.3, 30.9; ν_{max}/cm⁻¹(Nujol) 1691 (C=O).

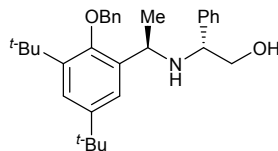
The spectroscopic data is in agreement with the literature data

[*R*]-2-(2-(Benzyloxy)-3,5-di-*tert*-butylbenzylideneamino)-2-phenylethanol, **283**

According to general procedure B, aldehyde **282** (35.0 g, 108 mmol) in ethanol (540 mL) was treated with (*R*)-phenyl glycinol **237** (14.8 g, 108 mmol). The product was obtained as a yellow solid (43.9 g, 99.0 mmol, 92%): mp 95-100 °C; [α]_D²⁵ -21.5 (*c* 1.44, CH₂Cl₂); ¹H-NMR (300MHz, CDCl₃) δ 8.73 (1H, s, CH=N), 7.98 (1H, d, *J* = 2.5 Hz, Ar-*H*), 7.53 (1H, d, *J* = 2.5 Hz, Ar-*H*), 7.44-7.25 (10H, m, 2 × Ph), 5.00 (1H, d, *J* = 12.0 Hz, PhCH_AH_BO), 4.81 (1H, d, *J* = 12.0 Hz, PhCH_AH_BO), 4.45 (1H, dd, *J* = 8.3 and 4.5 Hz, NCH(Ph)CH₂), 4.01 (1H, dd, *J* = 11.0 and 8.4 Hz, CH(Ph)CH_AH_B), 3.90 (1H, dd, *J* = 11.0 and 4.5 Hz, CH(Ph)CH_AH_B), 2.40 (1H, br s, OH), 1.48 (9H, s, *t*-Bu), 1.40 (9H, s, *t*-Bu); ¹³C-NMR (75.5MHz, CDCl₃) δ 160.6, 156.7, 146.2, 142.2, 140.8, 137.1, 128.9, 128.5, 128.5, 127.7, 127.5, 127.4, 127.2, 126.9, 122.9, 78.1, 76.2, 67.6, 35.3, 34.7, 31.4, 31.0; ν_{max}/cm⁻¹ (KBr) 3246 (OH), 1632 (C=N); MS (CI⁺, NH₃) *m/z* (%) 444 (100, [M+H]⁺), 354 (35, [M+NH₄-O

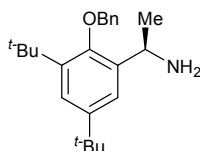
$\text{CH}_2\text{C}_6\text{H}_5]^+$); HRMS m/z (ES+) $[\text{M}+\text{H}]^+$ - $\text{C}_{16}\text{H}_{16}\text{O}_2$ requires 241.1223, found 241.1220.

(*R*)-2-[(*R*)-1-(2-(Benzyloxy)-3,5-di-*tert*-butylphenyl)ethylamino]-2-phenylethanol, 284



According to general procedure C, imine **283** (10.0 g, 22.6 mmol) in THF (400 mL) was treated with methyl lithium (1.6M in Et_2O , 50.8 mL, 81.4 mmol). The crude product was purified by column chromatography (80:20 PE:EtOAc) to yield the desired product as a yellow solid (4.57 g, 9.94 mmol, 44% yield, >95% de after purification): mp 103-105 °C; $[\alpha]_D^{25}$ -31.6 (c 0.98, CH_2Cl_2); $^1\text{H-NMR}$ (300 MHz, CDCl_3) δ 7.38-7.28 (5H, m, Ph), 7.26-7.12 (7H, m, Ph and $2 \times \text{Ar-H}$), 4.73 (1H, d, $J = 13.5$ Hz, $\text{PhCH}_A\text{H}_B\text{O}$), 4.67 (1H, d, $J = 13.5$ Hz, $\text{PhCH}_A\text{H}_B\text{O}$), 4.31 (1H, q, $J = 6.4$ Hz, $\text{CH}(\text{CH}_3)\text{N}$), 3.77 (1H, dd, $J = 7.9$ and 4.7 Hz, $\text{CH}(\text{Ph})\text{CH}_A\text{H}_B$), 3.71 (1H, dd, $J = 10.3$ and 4.7 Hz, $\text{CH}(\text{Ph})\text{CH}_A\text{H}_B$), 3.54 (1H, dd, $J = 10.3$ and 7.9 Hz, $\text{CH}(\text{Ph})\text{CH}_A\text{H}_B$), 2.42 (2H, br s, NH and OH), 1.46 (3H, d, $J = 6.4$ Hz, $\text{CH}(\text{CH}_3)\text{N}$), 1.42 (9H, s, *t*-Bu), 1.31 (9H, s, *t*-Bu); $^{13}\text{C-NMR}$ (75.5MHz, CDCl_3) δ 152.9, 146.3, 141.8, 141.0, 138.5, 137.5, 128.5, 128.5, 128.3, 127.4, 127.0, 126.5, 123.2, 121.9, 76.2, 65.8, 61.7, 48.0, 35.5, 34.7, 31.5, 31.3, 22.8; $\nu_{\text{max}}/\text{cm}^{-1}$ (KBr) 3200 (OH); MS (CI+, NH_3) m/z (%) 460 (55, $[\text{M}+\text{H}]^+$), 138 (100, $[\text{M}-\text{C}_{23}\text{H}_{30}\text{O}]^+$); HRMS m/z (ES+) $[\text{M}+\text{H}]^+$ - $\text{C}_{31}\text{H}_{42}\text{NO}_2$ requires 460.3210, found 460.3209.

(*R*)-1-(2-(Benzyloxy)-3,5-di-*tert*-butylphenyl)ethanamine, 279

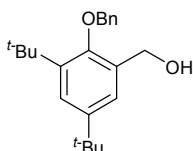


According to general procedure D, amine **284** (3.24 g, 7.05 mmol) dissolved in DCM (40 mL) and MeOH (20 mL) was treated with lead (IV) acetate (3.13 g, 7.05 mmol). The crude product was purified by column chromatography (SiO_2 , 50:49:1 DCM:EtOAc: Et_3N) to give a pale yellow oil (1.57 g, 4.62 mmol, 66% yield): mp 94-96 °C; $[\alpha]_D^{25}$ +5.2 (c 1.55, CH_2Cl_2); $^1\text{H-NMR}$ (300 MHz, CDCl_3) δ 7.55-7.52 (2H,

m, Ph), 7.48-7.30 (5H, m, Ph and $2 \times$ Ar-*H*), 5.02 (1H, d, $J = 12.2$ Hz, PhCH_AH_BO), 4.92 (1H, d, $J = 12.2$ Hz, PhCH_AH_BO), 4.55 (1H, q, $J = 6.6$ Hz, CH(CH₃)N), 1.68 (2H, br s, NH₂), 1.47 (9H, s, ^tBu), 1.45 (3H, d, $J = 6.6$ Hz, CH(CH₃)N), 1.35 (9H, s, ^tBu); ¹³C-NMR (75.5MHz, CDCl₃) δ 152.7, 146.3, 141.9, 140.4, 137.8, 128.5, 127.6, 126.6, 123.0, 121.2, 76.3, 44.3, 35.5, 34.7, 31.6, 31.4, 25.4; $\nu_{\max}/\text{cm}^{-1}$ (KBr) 3379 and 3305 (NH₂); MS (CI⁺, NH₃) m/z (%) 340 (50, [M+H]⁺), 250 (50, [M+NH₄-OCH₂C₆H₅]⁺), 233 (100, [M+H-OCH₂C₆H₅]⁺); HRMS m/z (ES⁺) [M+H]⁺ - C₂₃H₃₄NO requires 340.2635, found 340.2637.

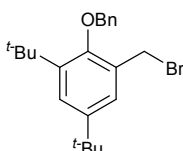
5.4.6 Preparation of Benzyl Bromide **280**

[2-(Benzyloxy)-3,5-di-*tert*-butylphenyl]methanol, **285**



According to general procedure E, aldehyde **282** (15.0 g, 46.2 mmol) in ethanol (300 mL) was treated with sodium borohydride (2.45 g, 64.7 mmol). The product was obtained as a white solid (14.8 g, 45.3 mmol, 98% yield): mp 73-78 °C; ¹H-NMR (300MHz, CDCl₃) δ 7.57 (1H, s, Ar-*H*), 7.54 (1H, s, Ar-*H*), 7.49-7.34 (5H, m, Ph), 5.04 (2H, s, PhCH₂O), 4.81 (2H, s, CH₂OH), 2.25 (1H, br s, OH), 1.49 (9H, s, ^tBu), 1.38 (9H, s, ^tBu); ¹³C-NMR (75.5MHz, CDCl₃) δ 153.8, 146.2, 142.0, 137.6, 133.7, 128.5, 127.7, 126.8, 124.8, 124.2, 75.8, 61.6, 35.4, 34.5, 31.5, 31.2; $\nu_{\max}/\text{cm}^{-1}$ (Nujol) 3234 (OH); MS (CI⁺, NH₃) m/z (%) 344 (100, [M+NH₄]⁺), 326 (80, [M+H]⁺), 309 (70, [M+H-OH]⁺); HRMS m/z (ES⁺) [M+NH₄]⁺ - C₂₂H₃₄NO₂ requires 344.2584, found 344.2583.

2-(Benzyloxy)-1-(bromomethyl)-3,5-di-*tert*-butylbenzene, **280**

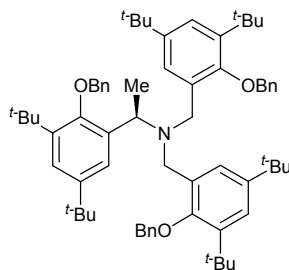


According to general procedure F, benzyl alcohol **282** (4.24 g, 13.0 mmol) in ether (130 mL) was treated with phosphorus tribromide (1.34 mL, 14.3 mmol). The product was isolated without the need for further purification as a white solid (4.79

g, 12.3 mmol, 95% yield): mp 97-99°C; $^1\text{H-NMR}$ (300MHz, CDCl_3) δ 7.60 (1H, s, Ar-*H*), 7.58 (1H, s, Ar-*H*), 7.49-7.43 (2H, m, Ph), 7.41-7.35 (3H, m, Ph), 5.16 (2H, s, PhCH_2O), 4.62 (2H, s, CH_2Br), 1.47 (9H, s, ^tBu), 1.37 (9H, s, ^tBu); $^{13}\text{C-NMR}$ (75.5MHz, CDCl_3) δ 154.2, 146.5, 142.5, 137.6, 130.9, 128.5, 127.7, 127.3, 126.8, 125.3, 75.2, 35.6, 34.6, 31.4, 31.2, 30.1; MS (CI^+ , NH_3) m/z (%) 406, 408 (15, $[\text{M}+\text{NH}_4]^+$), 326 (100, $[\text{M}-\text{Br}+\text{H}_2\text{O}]^+$).

5.4.7 Synthesis of Chiral Ligand (*R*)-**278**

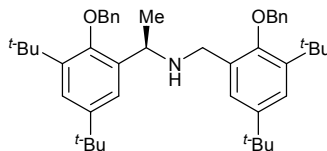
(*R*)-*N,N*-bis(2-(Benzyloxy)-3,5-di-*tert*-butylbenzyl)-1-(2-(benzyloxy)-3,5-di-*tert*-butylphenyl)ethanamine, **286**



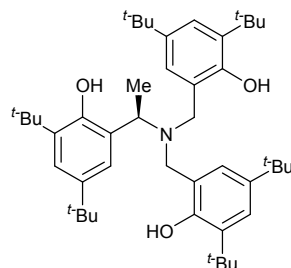
According to general procedure G, amine (*R*)-**279** (0.82 g, 2.42 mmol), potassium carbonate (1.67 g, 12.10 mmol), 4Å MS (4.00 g) dissolved in DMF (12 mL) was reacted with bromide **280** (3.29 g, 8.48 mmol). *To the reaction mixture was also added sodium iodide (0.36 g, 2.42 mmol)*. The crude product was purified by column chromatography (SiO_2 , 85:15 Petrol: CH_2Cl_2) to afford the title compound as a white powder (1.49 g, 1.56 mmol, 64% yield): mp 81-82 °C; $[\alpha]_D^{25} +9.3$ (c 1.08, CH_2Cl_2); $^1\text{H-NMR}$ (300 MHz, CDCl_3) δ 7.74 (2H, d, $J = 2.5$ Hz, Ar-*H*), 7.61 (1H, d, $J = 2.5$ Hz, 2 × Ar-*H*), 7.28-7.24 (4H, m, Ph), 7.21-7.10 (12H, m, 3 × Ar-*H* and Ph), 6.99-6.93 (2H, m, Ph), 4.63 (2H, d, $J = 12.1$ Hz, 2 × $\text{PhCH}_A\text{H}_B\text{O}$), 4.59 (1H, d, $J = 12.1$ Hz, $\text{PhCH}_A\text{H}_B\text{O}$), 4.56 (2H, d, $J = 12.1$ Hz, 2 × $\text{PhCH}_A\text{H}_B\text{O}$), 4.44 (1H, d, $J = 12.1$ Hz, $\text{PhCH}_A\text{H}_B\text{O}$), 4.09 (1H, q, $J = 6.8$ Hz, $\text{CH}(\text{CH}_3)\text{N}$), 3.75 (2H, d, $J = 15.1$ Hz, 2 × $\text{CH}_A\text{H}_B\text{N}$), 3.61 (2H, d, $J = 15.1$ Hz, 2 × $\text{CH}_A\text{H}_B\text{N}$), 1.28 (18H, s, 2 × ^tBu), 1.26 (9H, s, ^tBu), 1.19 (9H, s, ^tBu), 1.18 (18H, s, 2 × ^tBu), 1.14 (3H, d, $J = 6.8$ Hz, $\text{CH}(\text{CH}_3)\text{N}$); $^{13}\text{C-NMR}$ (75.5MHz, CDCl_3) δ 153.9, 153.5, 145.8, 141.7, 141.3, 137.9, 137.8, 137.7, 133.8, 128.3, 128.2, 127.3, 127.1, 127.0, 126.6, 124.6, 122.9, 122.7, 122.3, 75.6, 74.6, 56.8, 51.0, 35.4, 35.3, 34.6, 34.6, 31.7, 31.7, 31.4, 31.3,

20.1; MS (CI+, NH₃) *m/z* (%) 957 (25, [M+H]⁺), 649 (25, [M+H-C₂₂H₂₉O]⁺); HRMS *m/z* (ES+) [M+H]⁺ - C₆₇H₉₀NO₃ requires 956.6915, found 956.6921.

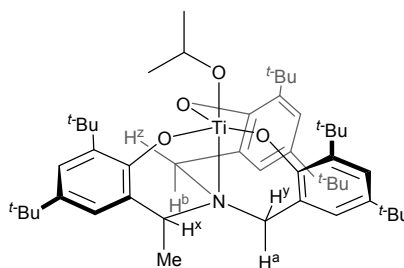
(*R*)-N-(2-(Benzyloxy)-3,5-di-*tert*-butylbenzyl)-1-(2-(benzyloxy)-3,5-di-*tert*-butylphenyl)ethanamine, **287**



According to general procedure G, amine (*R*)-**279** (80 mg, 0.24 mmol), potassium carbonate (100 mg, 0.72 mmol), 4Å MS (400 mg) dissolved in DMF (1.6 mL) was reacted with bromide **280** (230 mg, 0.59 mmol). Analysis of the ¹H NMR spectrum of the crude mixture revealed that the ratio of tertiary amine (*R*)-**286** to secondary amine (*R*)-**287** was 2:1. The crude mixture was purified by column chromatography (SiO₂, 85:15 Petrol:CH₂Cl₂) to afford both tertiary amine (*R*)-**286** (70 mg, 0.07 mmol, 30% yield) and the title compound as a white powder (26 mg, 0.04 mmol, 18% yield): mp 103-104 °C; ¹H-NMR (300 MHz, CDCl₃) δ 7.47 (1H, d, *J* = 2.3 Hz, Ar-*H*), 7.36-7.20 (13H, m, 3 × Ar-*H* and Ph), 5.05 (1H, d, *J* = 12.1 Hz, PhCH_AH_BO), 4.83 (2H, s, PhCH₂O), 4.80 (1H, d, *J* = 12.1 Hz, PhCH_AH_BO), 4.24 (1H, q, *J* = 6.4 Hz, CH(CH₃)N), 3.87 (1H, d, *J* = 15.0 Hz, CH_AH_BN), 3.57 (1H, d, *J* = 15.0 Hz, CH_AH_BN), 1.40 (9H, s, *t*-Bu), 1.39 (9H, s, *t*-Bu), 1.37 (3H, d, *J* = 6.4 Hz, CH(CH₃)N), 1.32 (9H, s, *t*-Bu), 1.28 (9H, s, *t*-Bu); ¹³C-NMR (75.5MHz, CDCl₃) δ 154.0, 153.7, 146.3, 145.8, 141.9, 141.6, 138.0, 137.9, 128.4, 127.4, 127.4, 127.4, 126.8, 126.6, 125.1, 123.2, 122.9, 121.8, 76.0, 75.2, 50.8, 47.0, 35.4, 35.4, 34.7, 34.5, 31.6, 31.5, 31.3, 31.2, 23.8; MS (CI+, NH₃) *m/z* (%) 648 (20, [M+H]⁺), 558 (35, [M+H-CH₂(C₆H₅)]⁺); HRMS *m/z* (ES+) [M+H]⁺ - C₄₅H₆₂NO₂ requires 648.4775, found 648.4778.

(*R*)-*N,N*-bis(2-(Hydroxy)-3,5-di-*tert*-butylbenzyl)-1-(2-(hydroxy)-3,5-di-*tert*-butylphenyl)ethylamine, 278

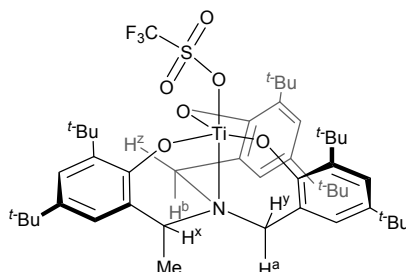
According to general procedure D, 10% palladium on carbon was added to amine (*R*)-**286** (1.69 g, 1.77 mmol) dissolved in EtOAc (20 mL). The title compound was obtained as a white powder (1.17 g, 1.71 mmol, 98% yield): mp 177-178 °C; $[\alpha]_D^{25}$ -58.2 (*c* 0.98, CH₂Cl₂); ¹H-NMR (300 MHz, CDCl₃) δ 7.24 (1H, d, *J* = 2.3 Hz, Ar-*H*), 7.23 (2H, d, *J* = 2.4 Hz, 2 × Ar-*H*), 7.11 (1H, d, *J* = 2.3 Hz, Ar-*H*), 6.98 (2H, d, *J* = 2.4 Hz, 2 × Ar-*H*), 6.59 (3H, br s, 3 × OH), 4.28 (1H, q, *J* = 6.8 Hz, CH(CH₃)N), 3.93 (2H, d, *J* = 13.5 Hz, 2 × CH_AH_BN), 3.49 (2H, d, *J* = 13.5 Hz, 2 × CH_AH_BN), 1.53 (3H, d, *J* = 6.8 Hz, CH(CH₃)N), 1.39 (9H, s, ^tBu), 1.38 (18H, s, 2 × ^tBu), 1.28 (9H, s, ^tBu), 1.26 (18H, s, 2 × ^tBu); ¹³C-NMR (75.5MHz, CDCl₃) δ 151.6, 151.0, 142.0, 141.5, 136.7, 136.4, 125.6, 125.6, 123.9, 123.6, 122.0, 121.7, 52.0, 51.4, 35.0, 34.9, 34.4, 34.2, 31.7, 31.6, 29.7, 29.7, 8.0; $\nu_{\max}/\text{cm}^{-1}$ (Nujol) 3521 (OH); MS (CI+, NH₃) *m/z* (%) 686 (10, [M+H]⁺), 454 (40, [M+H-C₁₆H₂₅O]⁺), 233 (100, [M+H-C₃₀H₄₆NO₂]⁺); HRMS *m/z* (ES+) [M+H]⁺ - C₄₆H₇₂NO₃ requires 686.5507, found 686.5509.

5.4.8 Preparation of Titanium Complexes (*R,M*)-287 and (*R,M*)-288**Titanium tris(phenolate) *iso*-propoxide complex, (*R,M*)-287**

Titanium (IV) *iso*-propoxide (0.30 mL, 1.05 mmol) was added to a suspension of ligand (*R*)-**278** (720 mg, 1.05 mmol) in toluene (20 mL) under an argon atmosphere. The resulting yellow solution was heated to reflux for 1 hour and concentrated under

vacuum to afford the crude product as a yellow powder which was recrystallised from hexane to afford the title compound as a yellow solid (534 mg, 0.68 mmol, 65% yield): $[\alpha]_D^{20}$ -124.2 (*c* 0.91, CHCl₃); ¹H-NMR (400 MHz, CDCl₃) δ 7.23 (1H, d, *J* = 2.4 Hz, Ar-*H*), 7.21 (1H, d, *J* = 2.4 Hz, Ar-*H*), 7.17 (1H, d, *J* = 2.4 Hz, Ar-*H*), 7.14 (1H, d, *J* = 1.8 Hz, Ar-*H*), 7.06 (1H, d, *J* = 2.1 Hz, Ar-*H*), 6.95 (1H, d, *J* = 2.4 Hz, Ar-*H*), 5.25 (1H, sept, *J* = 6.0 Hz, CH(CH₃)₂), 4.00 (1H, q, *J* = 6.9, CH^x(CH₃)N), 3.77 (1H, d, *J* = 14.0 Hz, CH^fH^bN), 3.56 (1H, d, *J* = 13.3 Hz, CH^pH^aN), 3.22 (1H, d, *J* = 14.0 Hz, CH^zH^bN), 3.17 (1H, d, *J* = 13.3 Hz, CH^yH^aN), 1.54 (3H, d, *J* = 6.9 Hz, CH^x(CH₃)N), 1.51 (6H, d, *J* = 6.0 Hz, CH(CH₃)₂), 1.48 (18H, s, 2 × ^tBu), 1.44 (9H, s, ^tBu), 1.30 (9H, s, ^tBu), 1.29 (9H, s, ^tBu), 1.28 (9H, s, ^tBu); ¹³C-NMR (75.5MHz, CDCl₃) δ 161.0, 160.8, 160.5, 142.2, 141.9, 141.9, 135.0, 134.9, 134.8, 128.0, 124.9, 124.3, 124.2, 124.1, 122.7, 122.6, 122.5, 121.7, 79.5, 54.4, 53.5, 51.6, 35.0, 35.0, 34.9, 34.6, 34.3, 34.3, 31.7, 31.7, 31.7, 29.7, 29.6, 29.5, 26.6, 26.4, 9.6; MS (EI) *m/z* (%) 789 (100, [M]⁺); HRMS *m/z* (EI) [M]⁺ - C₄₉H₇₅NO₄Ti requires 789.5170, found 789.5174.

Titanium tris(phenolate) triflate complex, (*R,M*)-288



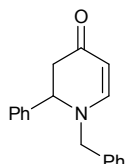
Titanium tris(phenolate) *iso*-propoxide complex, (*R,M*)-287 (500 mg, 0.63 mmol) in toluene (7 mL) was treated with trimethylsilyltriflate (0.11 mL, 0.63 mmol) under an argon atmosphere. The resulting suspension was heated to reflux and concentrated under vacuum to yield the product as a red solid (551 mg, 0.63 mmol, 99% yield): ¹H-NMR (300 MHz, CDCl₃) δ 7.31 (1H, d, *J* = 2.3 Hz, Ar-*H*), 7.29 (1H, d, *J* = 2.3 Hz, Ar-*H*), 7.25 (1H, d, *J* = 2.3 Hz, Ar-*H*), 7.20 (1H, d, *J* = 2.3 Hz, Ar-*H*), 7.16 (1H, d, *J* = 2.3 Hz, Ar-*H*), 7.05 (1H, d, *J* = 2.3 Hz, Ar-*H*), 4.13 (1H, q, *J* = 6.8 Hz, 1H, CH^x(CH₃)N), 3.93 (1H, d, *J* = 14.7 Hz, CH^fH^bN), 3.72 (1H, d, *J* = 13.9 Hz, CH^pH^aN), 3.51 (1H, d, *J* = 14.7 Hz, CH^zH^bN), 3.44 (1H, d, *J* = 13.9 Hz, CH^yH^aN), 1.69 (3H, d, *J* = 6.8 Hz, CH^x(CH₃)N), 1.45 (9H, s, ^tBu), 1.43 (9H, s, ^tBu), 1.40 (9H, s, ^tBu), 1.31 (9H, s, ^tBu), 1.30 (9H, s, ^tBu), 1.29 (9H, s, ^tBu); ¹³C-NMR (75.5MHz,

CDCl₃) δ 161.9, 161.6, 161.2, 145.3, 145.0, 145.0, 135.9, 135.8, 135.7, 126.3, 124.6, 124.0, 123.9, 123.8, 123.6, 123.1, 121.9, 55.3, 54.7, 51.8, 35.0, 35.0, 34.9, 34.8, 34.8, 34.6, 31.6, 31.5, 31.5, 29.6, 29.5, 29.5, 10.4; MS (EI) m/z (%) 879 (20, [M]⁺); HRMS m/z (EI) [M]⁺ - C₄₇H₆₈NO₆SF₃Ti requires 879.4193, found 879.4188; CHN found C, 64.7, H, 7.38, N, 1.31 - C₄₇H₆₈NO₆SF₃Ti requires C, 64.15, H, 7.79, N, 1.59.

5.5 RESULTS AND DISCUSSION III

5.5.1 Aza-Diels Alder Reaction Catalysed by (*rac*)-**195b** and (*R,M*)-**288**

1-Benzyl-2-phenyl-2,3-dihydropyridin-4-one, **206a**



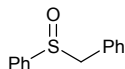
To a solution of the titanium catalyst (0.1 equiv.) in DCM (1 mL) was added *N*-benzylidene(phenyl)methanamine **204a**. The reaction mixture was cooled to 0 °C before Danishefsky's diene **205** (3 equiv.) was added. After stirring at 0 °C for 4 hours the reaction mixture was warmed to room temperature and stirred overnight. The reaction mixture was quenched with saturated ammonium chloride solution (8 mL) and the aqueous layer extracted with DCM (3 × 15 mL). The combined organic layers were dried (MgSO₄) and concentrated *in vacuo* to afford the crude product as a yellow oil. Column chromatography (SiO₂, 50:50 PE:EtOAc) resulted in the product as a yellow oil. The enantiomeric excess of the product was determined by chiral HPLC as described earlier.

The reaction of benzylidene(phenyl)methanamine **204a** (50 μL, 0.27 mmol) and Danishefsky's diene **205** (170 μL, 0.81 mmol) in the presence of titanium tris(phenolate) triflate (*rac*)-**195b** (26 mg, 0.027 mmol) yielded the title compound (42 mg, 0.16 mmol, 60% yield): Data as before.

The reaction of benzylidene(phenyl)methanamine **204a** (43 μL, 0.23 mmol) and Danishefsky's diene **205** (150 μL, 0.69 mmol) in the presence of titanium tris(phenolate) triflate (*R,M*)-**288** (20 mg, 0.023 mmol) yielded the title compound (25 mg, 0.10 mmol, 41% yield, 0% ee): Data as before.

5.5.2 Synthesis of Racemic Benzyl Phenyl Sulfoxide (*rac*)-292q

Benzyl phenyl sulfoxide, (*rac*)-292q¹⁶⁶



According to general procedure J, benzyl phenyl sulfide (400 mg, 2.0 mmol) was treated with aqueous hydrogen peroxide (0.66 mL, 8.0 mmol), SDS (29 mg, 0.1 mmol) and 1M aqueous hydrochloric acid (0.2 mL, 0.2 mmol). The product was isolated after column chromatography (SiO₂, 70:30 to 50:50 PE:EtOAc) as a white powder (387 mg, 1.8 mmol, 90% yield): ¹H-NMR (300MHz, CDCl₃) δ 7.42-7.26 (5H, m, 5 × Ar-H), 7.24-7.13 (3H, m, 3 × Ar-H), 6.93-6.88 (2H, m, 2 × Ar-H), 4.02 (1H, d, *J* = 12.4 Hz, CH_AH_BPh), 3.93 (1H, d, *J* = 12.4 Hz, CH_AH_BPh); ¹³C-NMR (75.5MHz, CDCl₃) δ 142.7, 131.1, 130.3, 129.1, 128.8, 128.4, 128.2, 124.4, 63.5; HRMS *m/z* (ES+) [M+Na]⁺ - C₁₃H₁₂NaOS requires 239.0507, found 239.0486.

The spectroscopic data is in agreement with the literature data

5.5.3 Screening of (*rac*)-195b in the Oxidation of Benzyl Phenyl Sulfide 291q

A solution of the catalyst and benzyl phenyl sulfide (50 mg, 0.25 mmol) in dichloromethane (3 mL) under nitrogen was stirred at the required temperature before cumene hydroperoxide (88% in cumene) was added (**Table 67**). The reaction was stirred at the temperature stated for 24 hours before the reaction was quenched with the addition of saturated aqueous sodium sulphite (8 mL) to the reaction mixture. The reaction mixture was extracted with dichloromethane (× 3) and the combined organic layers dried over magnesium sulphate. After evaporation of the solvent under reduced pressure the crude product was analysed by ¹H NMR spectroscopy.

Table 67

Entry	Catalyst	Conditions	Temp /°C	Conversion ^a /%	Ratio ^a 292:293
3	none	CHP 72 (2 eq.)	-30	<5	no sulfone
1	(<i>rac</i>)- 195b (10mol %)	CHP 72 (1 eq.)	-30	16	no sulfone
2	(<i>rac</i>)- 195b (10mol %)	CHP 72 (2 eq.)	-30	29	no sulfone
4	(<i>rac</i>)- 195b (10mol %)	CHP 72 (2 eq.)	rt	61	93:7

^a Conversion and ratio of **292:293** measured *via* ¹H NMR spectroscopic analysis

5.5.4 Screening of (*R,M*)-**287** and (*R,M*)-**288** in the Oxidation of Benzyl Phenyl Sulfide **291q**

A solution of the catalyst (20 mg, equivalent to 0.023 mmol for (*R,M*)-**288** or 0.025 mmol for (*R,M*)-**287**) and benzyl phenyl sulfide (46 or 51 mg, equivalent to 0.23 or 0.25 mmol respectively) in dichloromethane (3 mL) under nitrogen was stirred at -30 °C before cumene hydroperoxide (88% in cumene) or *tert*-butyl hydroperoxide (5M in decane) was added (see **Table 68**). The reaction was stirred for 24 hours before the reaction was quenched with the addition of saturated aqueous sodium sulphite (8 mL) to the reaction mixture. The reaction mixture was extracted with dichloromethane (× 3) and the combined organic layers dried over magnesium sulphate. After evaporation of the solvent under reduced pressure the crude product was analysed by ¹H NMR spectroscopy. The crude product was purified *via* column chromatography (SiO₂, 70:30 to 50:50 PE:EtOAc) to yield the product as an off-white solid. The enantiomeric excess of benzyl phenyl sulfoxide **292q** was determined *via* chiral HPLC analysis. The sample was run through a Daicel Chiralcel OD-H column using a mixed *n*-hexane/*i*-PrOH (90:10) solvent system at a flow rate of 1 mL/min with the enantiomers of **292q** having retention times of 13 min (*R*) and 15 min (*S*) (detection at 254 nm). The configuration of the sulfoxide was determined by the order of elution of the enantiomers compared with the literature,¹⁶⁸ and by comparison of the optical rotation with the literature - for entry 1, (*R*)-benzyl phenyl sulfoxide **292q**, 23% ee: $[\alpha]_D^{25} +42$ (*c* 0.51, acetone) [Lit.¹⁶⁷ $[\alpha]_D^{24} -91$ (*c* 1.0, acetone) for (*S*)-**292q**, 36% ee].

Table 68

Entry	Catalyst	Oxidant	Conv. ^a /%	Ratio ^a 292:293	Mass of 292q /mg	Yield of 292q /%	ee ^b /%
1	(<i>R,M</i>)- 288 (10mol %)	CHP 72 (2 eq.)	100	85:15	37	74	23(<i>R</i>)
2	(<i>R,M</i>)- 287 (10mol %)	CHP 72 (2 eq.)	63	90:10	25	46	18(<i>R</i>)
3	(<i>R,M</i>)- 288 (10mol %)	TBHP 290 (2 eq.)	25	trace sulfone	8	16	3(<i>R</i>)
4	(<i>R,M</i>)- 288 (10mol %)	CHP 72 (2 eq.)	100 ^c	91:9	40	80	23(<i>R</i>)
5	(<i>R,M</i>)- 288 (5mol %)	CHP 72 (2 eq.)	25	no sulfone	-	-	-
6	(<i>R,M</i>)- 288 (50mol %)	CHP 72 (2 eq.)	90 ^d	91:9	-	-	10(<i>R</i>)
7	(<i>R,M</i>)- 288 (10mol %)	CHP 72 (1 eq.)	54	97:3	14	28	8(<i>R</i>)

^a Conversion and ratio of **292:293** measured *via* ¹H NMR spectroscopic analysis; ^b Enantiomeric excess determined *via* chiral HPLC analysis; ^c Reaction run at -78 °C for 10 hours, then -30 °C for 14 hours; ^d Reaction run for 18 hours

5.5.5 Solvent Screen in the Oxidation of Benzyl Phenyl Sulfide **291q** Catalysed by (*R,M*)-**288**

(*R,M*)-**288** (15 or 20 mg, equivalent to 0.017 or 0.023 mmol respectively) and benzyl phenyl sulfide (34 or 46 mg, equivalent to 0.17 or 0.23 mmol respectively) were dissolved in the desired solvent (2.25 or 3 mL) under nitrogen and stirred at -30 °C before cumene hydroperoxide (88% in cumene, 2 equiv.) was added (**Table 69**). The reaction was stirred for 24 hours before the reaction was quenched with the addition of saturated aqueous sodium sulphite (8 mL) to the reaction mixture. The reaction mixture was extracted with dichloromethane (× 3) and the combined organic layers dried over magnesium sulphate. After evaporation of the solvent under reduced pressure the crude product was analysed by ¹H NMR spectroscopy. The crude product was purified *via* column chromatography (SiO₂, 70:30 to 50:50 PE:EtOAc) to yield the product as an off-white powder. The enantiomeric excess of benzyl phenyl sulfoxide **292q** was determined *via* chiral HPLC analysis as described earlier.

Table 69

Entry	Solvent	Mass of 291 /mg	Conv. ^a /%	Ratio ^a 292:293	Mass of 292q /mg	Yield of 292q /%	ee ^b /%
1	DCM	46	100	85:15	37	74	23(R)
2	DCE	34	100	86:14	24	65	23(R)
3	MeCN	46	70	94:6	30	60	9(R)
4	Toluene	46	100	89:11	39	78	37(R)
5	Benzene/DCM (ratio 2:1)	34	100	65:35	21	57	7(R)
6	Hexane/DCM (ratio 5:1)	34	100	59:41	15	41	7(R)

^a Conversion and ratio of **292:293** measured *via* ¹H NMR spectroscopic analysis; ^b Enantiomeric excess determined *via* chiral HPLC analysis

5.5.6 Addition of 4Å Molecular Sieves to the Oxidation of Benzyl Phenyl Sulfide **291q**

(*R,M*)-**288** (15 mg, 0.017 mmol), 4Å molecular sieves (125 mg) and benzyl phenyl sulfide (34 mg, 0.17 mmol) were dissolved in the desired solvent (2.25 mL) under nitrogen and stirred at -30 °C before cumene hydroperoxide (88% in cumene, 57 μL, 0.34 mmol) was added. The reaction was stirred for 24 hours before the reaction was quenched with the addition of saturated aqueous sodium sulphite (8 mL) to the reaction mixture. The reaction mixture was extracted with dichloromethane (× 3) and the combined organic layers dried over magnesium sulphate. After evaporation of the solvent under reduced pressure the crude product was analysed by ¹H NMR spectroscopy (**Table 70**). The crude product was purified *via* column chromatography (SiO₂, 70:30 to 50:50 Petrol:EtOAc) to yield the product as an off-white powder. The enantiomeric excess of benzyl phenyl sulfoxide **292q** was determined *via* chiral HPLC analysis as described earlier.

Table 70

Entry	Solvent	Conversion ^a /%	Ratio ^a 292:293	Mass of 292q /mg	Yield of 293q /%	ee ^b /%
1	DCM	100	78:22	22	59	32(R)
2	Toluene	100	50:50	11	30	11(R)

^a Conversion and ratio of **292:293** measured *via* ¹H NMR spectroscopic analysis; ^b Enantiomeric excess determined *via* chiral HPLC analysis

5.5.7 Kinetic Resolution of Racemic Benzyl Phenyl Sulfoxide (*rac*)-**292q**

A solution of (*R,M*)-**288** (15 mg, 0.017 mmol) and benzyl phenyl sulfoxide (*rac*)-**292q** (37 mg, 0.170 mmol) in toluene (3 mL) under nitrogen was stirred at -30 °C before cumene hydroperoxide (88% in cumene, 28 μ L, 0.170 mmol) was added. The reaction was stirred at -30 °C for 8 hours before the reaction was quenched with the addition of saturated aqueous sodium sulphite (8 mL) to the reaction mixture. The reaction mixture was extracted with dichloromethane (\times 3) and the combined organic layers dried over magnesium sulphate to leave the crude product. Analysis of the crude mixture by ^1H NMR spectroscopy revealed that the reaction had gone to 55% completion. The remaining benzyl phenyl sulfoxide was isolated after column chromatography (SiO_2 , 70:30 to 50:50 PE:EtOAc) as a off-white solid (14 mg, 0.065 mmol, 37% yield, 16% ee): Data as before.

5.5.8 Monitoring the Oxidation of Benzyl Phenyl Sulfide **291q** Catalysed by (*R,M*)-**288**

(*R,M*)-**288** (15 mg, 0.017 mmol) and benzyl phenyl sulfide (34 mg, 0.17 mmol) were dissolved in toluene (2.25 mL) under nitrogen and stirred at -30 °C before cumene hydroperoxide (88% in cumene, 3 equiv.) was added. The reaction was stirred over 32 hours with aliquots (*ca.* 0.3 mL) taken after 24 hours and 32 hours. Each aliquot was diluted with dichloromethane (10 mL) and quenched with the addition of saturated aqueous sodium sulphite (8 mL). The layers were separated and the aqueous layer extracted with dichloromethane (\times 2). The combined organic layers dried over magnesium sulphate. After evaporation of the solvent under reduced pressure the crude product was analysed by ^1H NMR spectroscopy (**Table 71**). The crude product was purified *via* small scale column chromatography (SiO_2 , 70:30 PE:EtOAc) to yield the product as an off-white powder. The enantiomeric excess of benzyl phenyl sulfoxide **292q** was determined *via* chiral HPLC analysis as described earlier.

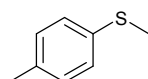
Table 71

Entry	Time /h	Conversion ^a /%	Ratio ^a 292:293	ee ^b /%
1	24	100	83:17	35
2	32	100	33:67	47

^a Conversion and ratio of **292:293** measured *via* ¹H NMR spectroscopic analysis; ^b Enantiomeric excess determined *via* chiral HPLC analysis

5.5.9 Synthesis of Sulfides 291

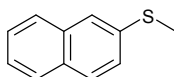
4-Methylthioanisole **291a**¹⁷⁵



According to general procedure I, 4-methylbenzenethiol (0.50 g, 4.58 mmol) in ethanol (30 mL) was treated with methyl iodide (0.29 mL, 4.58 mmol) and potassium hydroxide (0.26 g, 4.58 mmol). The product was isolated without the need for further purification as a colourless oil (0.62 g, 4.49 mmol, 98% yield): ¹H-NMR (300MHz, CDCl₃) δ 7.21 (2H, d, *J* = 8.3 Hz, 2 × Ar-*H*), 7.12 (2H, d, *J* = 8.3 Hz, 2 × Ar-*H*), 2.48 (3H, s, SCH₃), 2.34 (3H, s, CH₃); ¹³C-NMR (75.5MHz, CDCl₃) δ 135.0, 134.6, 129.5, 127.2, 20.8, 16.5

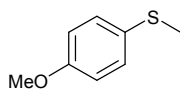
The spectroscopic data is in agreement with the literature data

Methyl-2-naphthyl sulfide **291c**¹⁷⁶



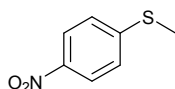
According to general procedure I, 2-naphthalenethiol (0.57 g, 3.56 mmol) in ethanol (22 mL) was treated with methyl iodide (0.22 mL, 3.56 mmol) and potassium hydroxide (0.20 g, 3.56 mmol). The product was isolated without the need for further purification as a white powder (0.59 g, 3.42 mmol, 96% yield): ¹H-NMR (300MHz, CDCl₃) δ 7.90-7.79 (3H, m, 3 × Ar-*H*), 7.73 (1H, d, *J* = 1.9 Hz, Ar-*H*), 7.61-7.48 (3H, m, 3 × Ar-*H*), 2.64 (3H, s, SCH₃); ¹³C-NMR (75.5MHz, CDCl₃) δ 136.8, 133.7, 131.1, 128.0, 127.5, 126.6, 126.3, 125.4, 125.0, 123.1, 15.4.

The spectroscopic data is in agreement with the literature data

4-Methoxythioanisole 291d¹⁷⁷

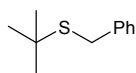
According to general procedure I, 4-methoxybenzenethiol (0.71 g, 5.06 mmol) in ethanol (30 mL) was treated with methyl iodide (0.32 mL, 5.06 mmol) and potassium hydroxide (0.28 g, 5.06 mmol). Following purification by column chromatography (SiO₂, 95:5 PE:EtOAc) the product was isolated as a pale yellow solid (0.71 g, 4.60 mmol, 91% yield): ¹H-NMR (300MHz, CDCl₃) δ 7.28 (2H, d, *J* = 9.0 Hz, 2 × Ar-*H*), 6.87 (2H, d, *J* = 9.0 Hz, 2 × Ar-*H*), 3.80 (3H, s, OCH₃), 2.45 (3H, s, SCH₃); ¹³C-NMR (75.5MHz, CDCl₃) δ 158.1, 130.1, 128.7, 114.5, 55.3, 18.0.

The spectroscopic data is in agreement with the literature data

Methyl-(4-nitrophenyl)-sulfide 291e¹⁷⁸

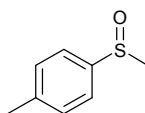
According to general procedure I, 4-nitrobenzenethiol (0.83 g, 4.28 mmol) in ethanol (30 mL) was treated with methyl iodide (0.27 mL, 4.28 mmol) and potassium hydroxide (0.24 g, 4.28 mmol). Following purification by column chromatography (SiO₂, 95:5 PE:EtOAc) the product was isolated as a yellow solid (0.59 g, 3.51 mmol, 82% yield): ¹H-NMR (300MHz, CDCl₃) δ 8.01 (2H, d, *J* = 9.0 Hz, 2 × Ar-*H*), 7.19 (2H, d, *J* = 9.0 Hz, 2 × Ar-*H*), 2.48 (3H, s, SCH₃); ¹³C-NMR (75.5MHz, CDCl₃) δ 148.7, 144.3, 124.6, 123.5, 14.4.

The spectroscopic data is in agreement with the literature data

Benzyl-*tert*-butyl sulfide 291y¹⁷⁹

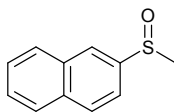
According to general procedure I, *tert*-butyl thiol (1.00 mL, 9.34 mmol) in ethanol (45 mL) was treated with benzyl bromide (1.12 mL, 9.34 mmol) and potassium hydroxide (0.53 g, 9.34 mmol). The product was isolated after column chromatography (SiO₂, 85:15 Petrol:EtOAc) as a colourless oil (1.33 g, 7.38 mmol, 79% yield): ¹H-NMR (300MHz, CDCl₃) δ 7.30-7.10 (5H, m, 5 × Ar-*H*), 3.70 (2H, s, CH₂Ph), 1.29 (9H, s, *t*-Bu); ¹³C-NMR (75.5MHz, CDCl₃) δ 138.6, 128.9, 128.4, 126.7, 42.8, 33.4, 30.9.

The spectroscopic data is in agreement with the literature data

5.5.10 Synthesis of racemic sulfoxides (*rac*)-292**(*rac*)-Methyl-*p*-tolyl sulfoxide, (*rac*)-292a**¹⁶⁶

According to general procedure J, 4-methylthioanisole **291a** (412 mg, 3.0 mmol) was treated with aqueous hydrogen peroxide (0.99 mL, 11.9 mmol), SDS (43 mg, 0.15 mmol) and 1M aqueous hydrochloric acid (0.30 mL, 0.30 mmol). The product was isolated after column chromatography (SiO₂, 70:30 to 50:50 PE:EtOAc) as a colourless oil (399 mg, 2.6 mmol, 87% yield): ¹H-NMR (300MHz, CDCl₃) δ 7.43 (2H, d, *J* = 8.3 Hz, 2 × Ar-*H*), 7.22 (2H, d, *J* = 8.3 Hz, 2 × Ar-*H*), 2.59 (3H, s, SCH₃), 2.30 (3H, s, CH₃); ¹³C-NMR (75.5MHz, CDCl₃) δ 142.1, 141.1, 129.7, 123.2, 43.6, 21.0; HRMS *m/z* (ES⁺) [M+H]⁺ - C₈H₁₁OS requires 155.0531, found 155.0527.

The spectroscopic data is in agreement with the literature data

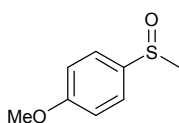
(*rac*)-Methyl-2-naphthyl sulfoxide, (*rac*)-292c¹⁸⁰

According to general procedure J, methyl-2-naphthyl sulfide **291c** (464 mg, 2.7 mmol) was treated with aqueous hydrogen peroxide (0.9 mL, 10.7 mmol), SDS (38

mg, 0.13 mmol) and 1M aqueous hydrochloric acid (0.27 mL, 0.27 mmol). The product was isolated after column chromatography (SiO₂, 70:30 to 50:50 PE:EtOAc) as a white powder (410 mg, 2.15 mmol, 81% yield): ¹H-NMR (300MHz, CDCl₃) δ 8.11 (1H, d, *J* = 1.5 Hz, Ar-*H*), 7.88-7.76 (3H, m, 3 × Ar-*H*), 7.52-7.43 (3H, m, 3 × Ar-*H*), 2.67 (3H, s, SCH₃); ¹³C-NMR (75.5MHz, CDCl₃) δ 142.4, 134.0, 132.5, 129.2, 128.1, 127.7, 127.4, 126.9, 123.6, 119.1, 43.4; HRMS *m/z* (ES+) [M+H]⁺ - C₁₁H₁₁OS requires 191.0531, found 191.0527.

The spectroscopic data is in agreement with the literature data

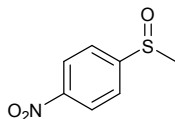
[*rac*]-Methyl-(4-methoxyphenyl)-sulfoxide, [*rac*]-292d¹⁶⁶



According to general procedure J, 4-methoxythioanisole **291d** (128 mg, 0.83 mmol) was treated with aqueous hydrogen peroxide (0.27 mL, 3.32 mmol), SDS (12 mg, 0.04 mmol) and 1M aqueous hydrochloric acid (0.08 mL, 0.08 mmol). The product was isolated after column chromatography (SiO₂, 70:30 to 50:50 PE:EtOAc) as a colourless oil (118 mg, 0.70 mmol, 84% yield): ¹H-NMR (300MHz, CDCl₃) δ 7.55 (2H, d, *J* = 8.7 Hz, 2 × Ar-*H*), 6.98 (2H, d, *J* = 8.7 Hz, 2 × Ar-*H*), 3.80 (3H, s, OCH₃), 2.65 (3H, s, SCH₃); ¹³C-NMR (75.5MHz, CDCl₃) δ 161.8, 136.4, 125.3, 114.7, 55.4, 43.8; HRMS *m/z* (ES+) [M+H]⁺ - C₈H₁₁O₂S requires 171.0480, found 171.0475.

The spectroscopic data is in agreement with the literature data

[*rac*]-Methyl-(4-nitrophenyl)-sulfoxide, [*rac*]-292e¹⁶⁶

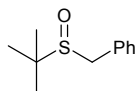


According to general procedure J, methyl-(4-nitrophenyl)-sulfide **291e** (123 mg, 0.73 mmol) was treated with aqueous hydrogen peroxide (0.24 mL, 2.91 mmol), SDS (11 mg, 0.04 mmol) and 1M aqueous hydrochloric acid (0.07 mL, 0.07 mmol). The product was isolated after column chromatography (SiO₂, 70:30 to 50:50 PE:EtOAc) as a pale yellow solid (105 mg, 0.57 mmol, 78% yield): ¹H-NMR (300MHz, CDCl₃) δ 8.35 (2H, d, *J* = 8.7 Hz, 2 × Ar-*H*), 7.81 (2H, d, *J* = 8.7 Hz, 2 × Ar-*H*), 2.77 (3H, s,

SCH_3); ^{13}C -NMR (75.5MHz, CDCl_3) δ 153.2, 149.3, 126.6, 124.3, 43.7; HRMS m/z (ES+) $[\text{M}+\text{H}]^+$ - $\text{C}_7\text{H}_8\text{NO}_3\text{S}$ requires 186.0225, found 186.0216.

The spectroscopic data is in agreement with the literature data

***[rac]*-tert-Butylphenylmethyl sulfoxide, *[rac]*-292y¹⁶⁹**



According to general procedure J, benzyl-*tert*-butyl sulfide **291y** (0.99 g, 4.93 mmol) was treated with aqueous hydrogen peroxide (1.64 mL, 19.7 mmol), SDS (71 mg, 0.25 mmol) and 1M aqueous hydrochloric acid (0.47 mL, 0.47 mmol). The product was isolated after column chromatography (SiO_2 , 70:30 to 50:50 PE:EtOAc) as a white powder (0.89 g, 4.55 mmol, 92% yield): ^1H -NMR (300MHz, CDCl_3) δ 7.37-7.30 (5H, m, $5 \times \text{Ar-H}$), 3.83 (1H, d, $J = 12.8$ Hz, $\text{CH}_A\text{H}_B\text{Ph}$), 3.63 (1H, d, $J = 12.8$ Hz, $\text{CH}_A\text{H}_B\text{Ph}$), 1.32 (9H, s, ^tBu); ^{13}C -NMR (75.5MHz, CDCl_3) δ 138.6, 128.9, 128.4, 126.7, 42.8, 33.4, 30.9; HRMS m/z (ES+) $[\text{M}+\text{H}]^+$ - $\text{C}_{11}\text{H}_{17}\text{OS}$ requires 197.1000, found 197.0994.

The spectroscopic data is in agreement with the literature data

5.5.11 Screening of Sulfides **291** in the Sulfoxidation Reaction

(*R,M*)-**288** (15 or 20 mg, equivalent to 0.017 or 0.023 mmol respectively) and sulfide **291** (0.17 or 0.23 mmol respectively) were dissolved in either DCM or toluene (2.25 or 3 mL) under nitrogen and stirred at -30 °C before cumene hydroperoxide (88% in cumene, 2 equiv.) was added. The reaction was stirred for 24 hours before the reaction was quenched with the addition of saturated aqueous sodium sulphite (8 mL) to the reaction mixture. The reaction mixture was extracted with dichloromethane ($\times 3$) and the combined organic layers dried over magnesium sulphate. After evaporation of the solvent under reduced pressure the crude product was analysed by ^1H NMR spectroscopy (**Table 72**). The crude product was purified *via* column chromatography (SiO_2 , 70:30 to 50:50 PE:EtOAc) to yield the desired product. The enantiomeric excesses of the sulfoxide products **292** were determined *via* chiral HPLC analysis. For (*R*)-**292a**, (*R*)-**292c** and (*R*)-**292d**, the configuration of

the sulfoxide was determined by the order of elution of the enantiomers compared with the literature.¹⁶⁸

For methyl-*p*-tolyl sulfoxide **292a**, the sample was run through a Daicel Chiralcel OD-H column using a mixed *n*-hexane/*i*-PrOH (90:10) solvent system at a flow rate of 1 mL/min with the enantiomers of **292a** having retention times of 40 min (*R*) and 45 min (*S*) (detection at 254 nm).

For methyl-2-naphthyl sulfoxide **292c**, the sample was run through a Daicel Chiralcel OD-H column using a mixed *n*-hexane/*i*-PrOH (90:10) solvent system at a flow rate of 1 mL/min with the enantiomers of **292c** having retention times of 19 min (*R*) and 21 min (*S*) (detection at 254 nm).

For methyl-(4-methoxyphenyl)-sulfoxide **292d**, the sample was run through a Daicel Chiralcel OD-H column using a mixed *n*-hexane/*i*-PrOH (95:5) solvent system at a flow rate of 0.5 mL/min with the enantiomers of **292d** having retention times of 71 min (*R*) and 76 min (*S*) (detection at 220 nm).

For methyl-(4-nitrophenyl)-sulfoxide **292e**, the sample was run through a Daicel Chiralcel OJ column using a mixed *n*-hexane/*i*-PrOH (90:10) solvent system at a flow rate of 1 mL/min with the enantiomers of **292e** having retention times of 56 min (*R*) and 67 min (*S*) (detection at 254 nm).

For *tert*-butylphenylmethyl sulfoxide **292y**, the sample was run through a Daicel Chiralcel OD-H column using a mixed *n*-hexane/*i*-PrOH (90:10) solvent system at a flow rate of 1 mL/min with the enantiomers of **292y** having retention times of 25 min (*R*) and 30 min (*S*) (detection at 225 nm).

Table 72

Entry	Sulfoxide	Solvent	Mass of sulfide /mg	Conv. ^a /%	Ratio ^a 292:293	Mass of sulfoxide /mg	Yield of 292 /%	ee ^b /%
1	292q	DCM	46	100	85:15	37	74	23(<i>R</i>)
2		Toluene	46	100	89:11	39	78	37(<i>R</i>)
3	292a	DCM	32	100	28:72	15	14	13(<i>R</i>)
4	292c	DCM	40	100	32:68	12	28	10(<i>R</i>)
5		Toluene	30	100	79:21	20	61	20(<i>R</i>)
6	292d	Toluene	26	88	90:10	19	65	17(<i>R</i>)
7	292e	Toluene	29	100	56:44	15	47	0
8	292y	Toluene	34	90	trace sulfone	24	71	0

^a Conversion and ratio of **292:293** measured *via* ¹H NMR spectroscopic analysis; ^b Enantiomeric excess determined *via* chiral HPLC analysis

Chapter 6:

References

6 References

1. N. Hall, *The Age of The Molecule*, Royal Society of Chemistry, 1999.
2. G. Haniotakis, W. Francke, K. Mori, H. Redlich and V. Schurig, *J. Chem. Ecol.*, 1986, **12**, 1559-1568.
3. K. Mori, T. Uesmatsu, K. Yanagi and M. Minobe, *Tetrahedron*, 1985, **41**, 2751-2758.
4. T. Eriksson, S. Björkman and P. Höglund, *Eur. J. Clin. Pharmacol.*, 2001, **57**, 365-376.
5. S. Steijker, W. H. J. Kruit and G. Stoter, *Eur. J. Cancer*, 2004, **40**, 2377-2382.
6. K. R. Prasad and P. Anbarasan, *Synlett*, 2006, **13**, 2087-2088.
7. K. R. Prasad and P. Anbarasan, *Tetrahedron: Asymmetry*, 2006, **17**, 850-853.
8. E. Tayama and H. Tanaka, *Tetrahedron Lett.*, 2007, **48**, 4183-4185.
9. Y. Zhao, A. W. Mitra, M. L. Snapper and A. H. Hoveyda, *Angew. Chem. Int. Edit.*, 2007, **46**, 8471-8474.
10. S. Yamada and K. Yamashita, *Tetrahedron Lett.*, 2008, **49**, 32-35.
11. D. Giacomini, P. Galletti, A. Quintavalla, G. Gucciardo and F. Paradisi, *Chem. Commun.*, 2007, 4038-4040.
12. Y. Gnas and F. Glorius, *Synthesis*, 2006, **12**, 1899-1930.
13. D. A. Evans, J. Bartroli and T. L. Shih, *J. Am. Chem. Soc.*, 1981, **103**, 2127-2129.
14. S. D. Bull, S. G. Davies, S. Jones and H. Sanganee, *J. Chem. Soc., Perkin Trans. 1*, 1999, 387-398.
15. M. Gruber-Khadjawi, T. Purkathofer, W. Skranc and H. Griengl, *Adv. Synth. Catal.*, 2007, **349**, 1445-1450.
16. P. I. Dalko and L. Moisan, *Angew. Chem. Int. Edit.*, 2004, **43**, 5138-5175.
17. B. List and J. W. Yang, *Science*, 2006, **313**, 1584-1586.
18. J. Seayad and B. List, *Org. Biomol. Chem.*, 2005, **3**, 719-724.
19. K. A. Ahrendt, C. J. Borths and D. W. C. MacMillan, *J. Am. Chem. Soc.*, 2000, **122**, 4243-4244.
20. E. J. Corey, F. Xu and M. C. Noe, *J. Am. Chem. Soc.*, 1997, **119**, 12414-12415.

21. U.-H. Dolling, P. Davis and E. J. J. Grabowski, *J. Am. Chem. Soc.*, 1984, **106**, 446-447.
22. M. J. O'Donnell, W. D. Bennett and S. Wu, *J. Am. Chem. Soc.*, 1989, **111**, 2353-2355.
23. B. Lygo and P. G. Wainwright, *Tetrahedron Lett.*, 1997, **38**, 8595-8598.
24. E. J. Corey and M. J. Grogan, *Org. Lett.*, 1999, **1**, 157-160.
25. P. Vachal and E. N. Jacobsen, *J. Am. Chem. Soc.*, 2002, **124**, 10012-10014.
26. P. Ahlberg, *The Royal Swedish Academy of Sciences, Press Release*, 2001.
27. B. D. Vineyard, W. S. Knowles, M. J. Sabacky, G. L. Bachman and O. J. Weinkauff, *J. Am. Chem. Soc.*, 1977, **99**, 5946-5952.
28. A. Miyashita, A. Yasuda, H. Takaya, K. Toriumi, T. Ito, T. Souchi and R. Noyori, *J. Am. Chem. Soc.*, 1980, **102**, 7932-7934.
29. T. Ohta, H. Takaya, M. Kitamura, K. Nagai and R. Noyori, *J. Org. Chem.*, 1987, **52**, 3174-3176.
30. T. Katsuki and K. B. Sharpless, *J. Am. Chem. Soc.*, 1980, **102**, 5974-5976.
31. J. K. Whitesell, *Chem. Rev.*, 1989, **89**, 1581-1590.
32. L. H. Gade, P. Renner, H. Memmler, F. Fecher, C. H. Galka, M. Laubender, S. Radojevic, M. McPartlin and J. W. Lauher, *Chem. Eur. J.*, 2001, **7**, 2563-2580.
33. C. Moberg, *Angew. Chem. Int. Edit.*, 1998, **37**, 248-268.
34. S. E. Gibson and M. P. Castaldi, *Chem. Commun.*, 2006, 3045-3062.
35. S. T. Handy, *Curr. Org. Chem.*, 2000, **4**, 363-395.
36. J. M. Brunel, *Chem. Rev.*, 2005, **105**, 857-897.
37. C. Moberg, *Angew. Chem. Int. Edit.*, 2006, **45**, 4721-4723.
38. J. I. Hong, K. W. Lee, D. H. Lee, S. Hwang, O. S. Lee and D. S. Chung, *Org. Lett.*, 2003, **5**, 1431-1433.
39. S. G. Kim, K. H. Kim, J. Jung, S. K. Shin and K. H. Ahn, *J. Am. Chem. Soc.*, 2002, **124**, 591-596.
40. S. G. Kim, K. H. Kim, Y. K. Kim, S. K. Shin and K. H. Ahn, *J. Am. Chem. Soc.*, 2003, **125**, 13819-13824.
41. R. Welti and F. Diederich, *Helv. Chim. Acta*, 2003, **86**, 494-503.
42. G. Heinrichs, L. Vial, J. Lacour and S. Kubik, *Chem. Commun.*, 2003, 1252-1253.

43. S. R. Waldvogel, R. Fröhlich and C. A. Schalley, *Angew. Chem. Int. Edit.*, 2000, **39**, 2472-2475.
44. M. C. Schopohl, C. Siering, O. Kataeva and S. R. Waldvogel, *Angew. Chem. Int. Edit.*, 2003, **42**, 2620-2633.
45. W. A. Nugent, *J. Am. Chem. Soc.*, 1992, **114**, 2768-2769.
46. W. A. Nugent and R. L. Harlow, *J. Am. Chem. Soc.*, 1994, **116**, 6142-6148.
47. B. W. McClelland, W. A. Nugent and M. G. Finn, *J. Org. Chem.*, 1998, **63**, 6656-6666.
48. W. A. Nugent, *J. Am. Chem. Soc.*, 1998, **120**, 7139-7140.
49. F. Di Furia, G. Licini, G. Modena, R. Motterle and W. A. Nugent, *J. Org. Chem.*, 1996, **61**, 5175-5177.
50. M. Bonchio, G. Licini, G. Modena, O. Bortolini, S. Moro and W. A. Nugent, *J. Am. Chem. Soc.*, 1999, **121**, 6258-6268.
51. M. Bonchio, G. Licini, F. Di Furia, S. Mantovani, G. Modena and W. A. Nugent, *J. Org. Chem.*, 1999, **64**, 1326-1330.
52. N. Mase, T. Ohno, N. Hoshikawa, K. Ohishi, H. Morimoto, H. Yoda and K. Takabe, *Tetrahedron Lett.*, 2003, **44**, 4073-4075.
53. H. Lütjens, G. Wahl, F. Möller, P. Knochel and J. Sundermeyer, *Organometallics*, 1997, **16**, 5869-5878.
54. S. K. Armstrong and S. Clunas, *Synthesis*, 2000, 281-288.
55. G. Bringmann, R. M. Pfeifer, C. Rummey, K. Hartner and M. Breuning, *J. Org. Chem.*, 2003, **68**, 6859-6863.
56. G. Bringmann, M. Breuning, R. M. Pfeifer and P. Schreiber, *Tetrahedron: Asymmetry*, 2003, **14**, 2225-2228.
57. T. Fang, D. M. Du, S. F. Lu and J. X. Xu, *Org. Lett.*, 2005, **7**, 2081-2084.
58. T. Fang, J. Xu and D. M. Du, *Synlett*, 2006, 1559-1563.
59. D. M. Du, T. Fang, J. Xu and S.-W. Zheng, *Org. Lett.*, 2006, **8**, 1327-1330.
60. C. J. Tokar, P. B. Kettler and W. B. Tolman, *Organometallics*, 1992, **11**, 2737-2739.
61. M. C. Keyes, B. M. Chamberlain, S. A. Caltagirone, J. A. Halfen and W. B. Tolman, *Organometallics*, 1998, **17**, 1984-1992.
62. B. Burns, J. R. Studley and M. Wills, *Tetrahedron Lett.*, 1993, **34**, 7105-7106.

63. C. Bolm, N. Meyer, G. Raabe, T. Weyhermuller and E. Bothe, *Chem. Commun.*, 2000, 2435-2436.
64. B. J. Postnikova and E. V. Anslyn, *Tetrahedron Lett.*, 2004, **45**, 501-504.
65. L. H. Gade, *Acc. Chem. Res.*, 2002, **35**, 575-582.
66. F. Lake and C. Moberg, *Eur. J. Org. Chem.*, 2002, 3179-3188.
67. J. Zhou and Y. Tang, *Chem. Soc. Rev.*, 2005, **34**, 664-676.
68. T. Katsuki, K. Kawasaki and S. Tsumura, *Synlett*, 1995, 1245-1246.
69. T. H. Chan and G. Z. Zheng, *Can. J. Chem.*, 1997, **75**, 629-633.
70. K. Kawasaki and T. Katsuki, *Tetrahedron*, 1997, **53**, 6337-6350.
71. Y. Kohmura and T. Katsuki, *Synlett*, 1999, 1231-1234.
72. Y. Kohmura and T. Katsuki, *Tetrahedron Lett.*, 2000, **41**, 3941-3945.
73. S. Bellemin-Laponnaz and L. H. Gade, *Angew. Chem. Int. Edit.*, 2002, **41**, 3473-3475.
74. C. Foltz, B. Strecker, G. Marconi, S. Bellemin-Laponnaz, H. Wadepohl and L. H. Gade, *Chem. Commun.*, 2005, 5115-5117.
75. C. Dro, S. Bellemin-Laponnaz, R. Welter and L. H. Gade, *Angew. Chem. Int. Edit.*, 2004, 4479-4482.
76. C. Foltz, M. Enders, S. Bellemin-Laponnaz, H. Wadepohl and L. H. Gade, *Chem. Eur. J.*, 2007, 5994-6008.
77. B. D. Ward, S. Bellemin-Laponnaz and L. H. Gade, *Angew. Chem. Int. Edit.*, 2005, 1668-1671.
78. L. Lukešová, B. D. Ward, S. Bellemin-Laponnaz, H. Wadepohl and L. H. Gade, *Dalton Trans.*, 2007, 920-922.
79. L. Lukešová, B. D. Ward, S. Bellemin-Laponnaz, H. Wadepohl and L. H. Gade, *Organometallics*, 2007, 4652-4657.
80. S. G. Kim and K. H. Ahn, *Tetrahedron Lett.*, 2001, **42**, 4175-4177.
81. C. Bolm, T. H. Chuang and J. M. Fang, *Synth. Commun.*, 2000, **30**, 1627-1641.
82. J. Zhou, M. C. Ye, Z. Z. Huang and Y. Tang, *J. Org. Chem.*, 2004, **69**, 1309-1320.
83. J. Zhou and Y. Tang, *Org. Biomol. Chem.*, 2004, **2**, 429-433.
84. M. C. Ye, J. Zhou and Y. Tang, *J. Org. Chem.*, 2006, **71**, 3576-3582.
85. L. K. Ding and W. J. Irwin, *J. Chem. Soc., Perkin Trans. 1*, 1976, 2382-2386.
86. J. Marco-Contelles, *Angew. Chem. Int. Edit.*, 2004, **43**, 2198-2200.

87. R. Shintani and G. C. Fu, *Angew. Chem. Int. Edit.*, 2003, **42**, 4082-4085.
88. M. J. Burk, J. E. Feaster and R. L. Harlow, *Tetrahedron: Asymmetry*, 1991, **2**, 569-592.
89. M. T. Powell, A. M. Porte and K. Burgess, *Chem. Commun.*, 1998, 2161-2162.
90. M. T. Powell, A. M. Porte, J. Reibenspies and K. Burgess, *Tetrahedron*, 2001, **57**, 5027-5038.
91. G. Helmchen and S. Kudis, *Angew. Chem. Int. Edit.*, 1998, **37**, 3047-3050.
92. B. M. Trost and R. C. Bunt, *J. Am. Chem. Soc.*, 1994, **116**, 4089-4090.
93. B. M. Trost and D. L. Van Vranken, *Chem. Rev.*, 1996, **96**, 395-422.
94. T. Hayashi, M. Kawatsura and Y. Uozumi, *Chem. Commun.*, 1997, 561-562.
95. M. Stolorz, C. Floriani, G. Gervasio and D. Viterbo, *J. Chem. Soc., Dalton Trans.*, 1997, 1119-1121.
96. A. Suárez, A. Pizzano, I. Fernández and N. Khair, *Tetrahedron: Asymmetry*, 2001, **12**, 633-642.
97. K. Ishihara, Y. Karumi, S. Kondo and H. Yamamoto, *J. Org. Chem.*, 1998, **63**, 5692-5695.
98. S. D. Pastor and S. P. Shum, *Tetrahedron: Asymmetry*, 1998, **9**, 543-546.
99. S. D. Pastor, S. P. Shum, A. D. DeBellis, P. A. Odorisio, L. Burke, F. H. Clarke, G. Rihs, B. Piatek and R. K. Rodebaugh, *Inorg. Chem.*, 2003, **42**, 5097-5106.
100. T. C. H. Lam, W. L. Mak, W. L. Wong, H. L. Kwong, H. H. Y. Sung, S. M. F. Lo, I. D. Williams and W. H. Leung, *Organometallics*, 2004, **23**, 1247-1252.
101. G. Zemplén and A. Kunz, *Chem. Ber.*, 1922, **55**, 979-992.
102. K. Hultsch, *Chem. Ber.*, 1949, **82**, 16-25.
103. J. Hwang, K. Govindaswamy and S. A. Koch, *Chem. Commun.*, 1998, 1667-1668.
104. M. Kol, M. Shamis, I. Goldberg, Z. Goldschmidt, S. Alfi and E. Hayut-Salant, *Inorg. Chem. Commun.*, 2001, **4**, 177-179.
105. V. Ugrinova, G. A. Ellis and S. N. Brown, *Chem. Commun.*, 2004, 468-469.
106. S. D. Bull, M. G. Davidson, A. L. Johnson, D. E. J. E. Robinson and M. F. Mahon, *Chem. Commun.*, 2003, 1750-1751.
107. M. Mba, L. J. Prins and G. Licini, *Org. Lett.*, 2007, **9**, 21-24.

108. K. Nomura, W. Wang and M. Fujiki, *Macromol. Rapid Commun.*, 2004, **25**, 504-507.
109. Y. Kim and J. G. Verkade, *Organometallics*, 2002, **21**, 2395-2399.
110. S. A. Cortes, M. A. Muñoz Hernández, H. Nakai, I. Casto-Rodríguez, K. Meyer, A. R. Fout, D. L. Miller, J. C. Huffman and D. J. Mindiola, *Inorg. Chem. Commun.*, 2005, **8**, 903-907.
111. K. C. Fortner, J. P. Bigi and S. N. Brown, *Inorg. Chem.*, 2005, **44**, 2803-2814.
112. L. Michalczyk, S. De Gala and J. W. Bruno, *Organometallics*, 2001, **20**, 5547-5556.
113. Y. Kim, G. K. Jnaneshwara and J. G. Verkade, *Inorg. Chem.*, 2003, **42**, 1437-1447.
114. A. L. Johnson, M. G. Davidson and M. F. Mahon, *Dalton Trans.*, 2007, 5405-5411.
115. S. Gendler, S. Segal, I. Goldberg, Z. Goldschmidt and M. Kol, *Inorg. Chem.*, 2006, **45**, 4783-4790.
116. M. G. Davidson, C. L. Doherty, A. L. Johnson and M. F. Mahon, *Chem. Commun.*, 2003, 1832-1833.
117. R. J. Motekaitis, A. E. Martell, S. A. Koch, J. W. Hwang, D. A. Quarless and M. J. Welch, *Inorg. Chem.*, 1998, **37**, 5902-5911.
118. S. Groysman, I. Goldberg and M. Kol, *Organometallics*, 2003, **22**, 3793-3795.
119. S. Groysman, I. Goldberg, M. Kol, E. Genizi and Z. Goldschmidt, *Adv. Synth. Catal.*, 2005, **347**, 409-415.
120. S. Groysman, S. Segal, M. Shamis, I. Goldberg, M. Kol, Z. Goldschmidt and E. Hayut-Salant, *J. Chem. Soc., Dalton Trans.*, 2002, 3425-3426.
121. C. Redshaw, M. A. Rowan, D. M. Homden, S. H. Dale, M. R. J. Elsegood, S. Matsui and S. Matsuura, *Chem. Commun.*, 2006, 3329-3331.
122. Y. Kim and J. G. Verkade, *Phosphorus, Sulfur Silicon Relat. Elem.*, 2004, **179**, 729-732.
123. A. J. Chmura, C. J. Chuck, M. G. Davidson, M. D. Jones, M. D. Lunn, S. D. Bull and M. F. Mahon, *Angew. Chem. Int. Edit.*, 2007, **46**, 2280-2283.
124. A. Chandrasekaran, R. O. Day and R. R. Holmes, *J. Am. Chem. Soc.*, 2000, **122**, 1066-1072.

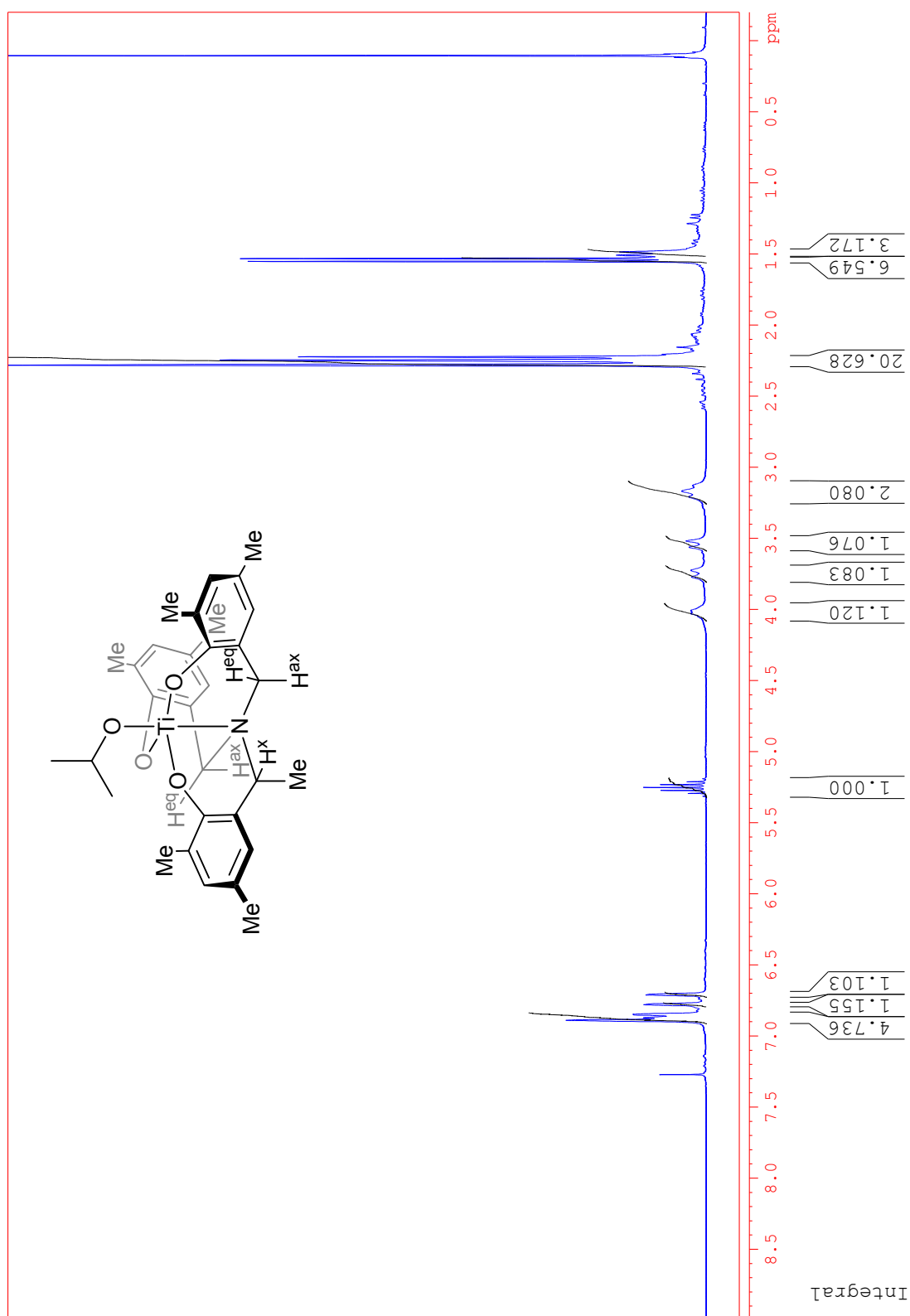
125. N. V. Timosheva, A. Chandrasekaran, R. O. Day and R. R. Holmes, *Organometallics*, 2000, **19**, 5614-5622.
126. N. V. Timosheva, A. Chandrasekaran, R. O. Day and R. R. Holmes, *Organometallics*, 2001, **20**, 2231-2237.
127. N. V. Timosheva, A. Chandrasekaran, R. O. Day and R. R. Holmes, *J. Am. Chem. Soc.*, 2002, **124**, 7035-7040.
128. P. Foster, J. C. W. Chien and M. D. Rausch, *Organometallics*, 1996, **15**, 2404-2409.
129. Y. Kim, E. Hong, M. H. Lee, J. Kim, Y. Han and Y. Do, *Organometallics*, 1999, **18**, 36-39.
130. D. E. J. E. Robinson, PhD thesis, University of Bath, 2004.
131. D. L. Van Vranken, S. J. Stadel and J. W. Ziller, *Tetrahedron Lett.*, 1999, **40**, 5811-5812.
132. P. Wyatt, C. P. Butts, V. Patel and B. Voysey, *J. Chem. Soc., Perkin Trans. I*, 2000, 4222-4223.
133. J. W. Canary, C. S. Allen, J. M. Castagneto, Y. H. Chiu, P. J. Toscano and Y. Wang, *Inorg. Chem.*, 1998, **37**, 6257-6262.
134. J. W. Canary, C. S. Allen, J. M. Castagneto and Y. Wang, *J. Am. Chem. Soc.*, 1995, **117**, 8484-8485.
135. P. J. Kocięński, *Protecting Groups*, 3rd edn., Thieme, 2004.
136. Z. Y. Chang and R. M. Coates, *J. Org. Chem.*, 1990, **55**, 3475-3483.
137. D. Delorme, C. Berthelette, R. Lavoie and E. Roberts, *Tetrahedron: Asymmetry*, 1998, **9**, 3963-3966.
138. K. Higashiyama, T. Yamauchi and H. Takahashi, *Chem. Pharm. Bull.*, 1998, **46**, 384-389.
139. G. Bernardinelli, D. Fernandez, R. Gosmini, P. Meier, A. Ripa, P. Schüpfer, B. Treptow and E. P. Kündig, *Chirality*, 2000, **12**, 529-539.
140. E. P. Kündig, C. Botuha, G. Lemercier, P. Romanens, L. Saudan and S. Thibault, *Helv. Chim. Acta*, 2004, **87**, 561-579.
141. M. J. Wu and L. N. Pridgen, *J. Org. Chem.*, 1991, **56**, 1340-1344.
142. L. A. Saudan, G. Bernardinelli and E. P. Kündig, *Synlett*, 2000, 483-486.
143. L. F. Lindoy, G. V. Meehan and N. Svenstrup, *Synthesis*, 1998, 1029-1032.
144. Y. Ogata, A. Kawasaki and F. Sugiura, *Tetrahedron*, 1968, **24**, 5001-5010.

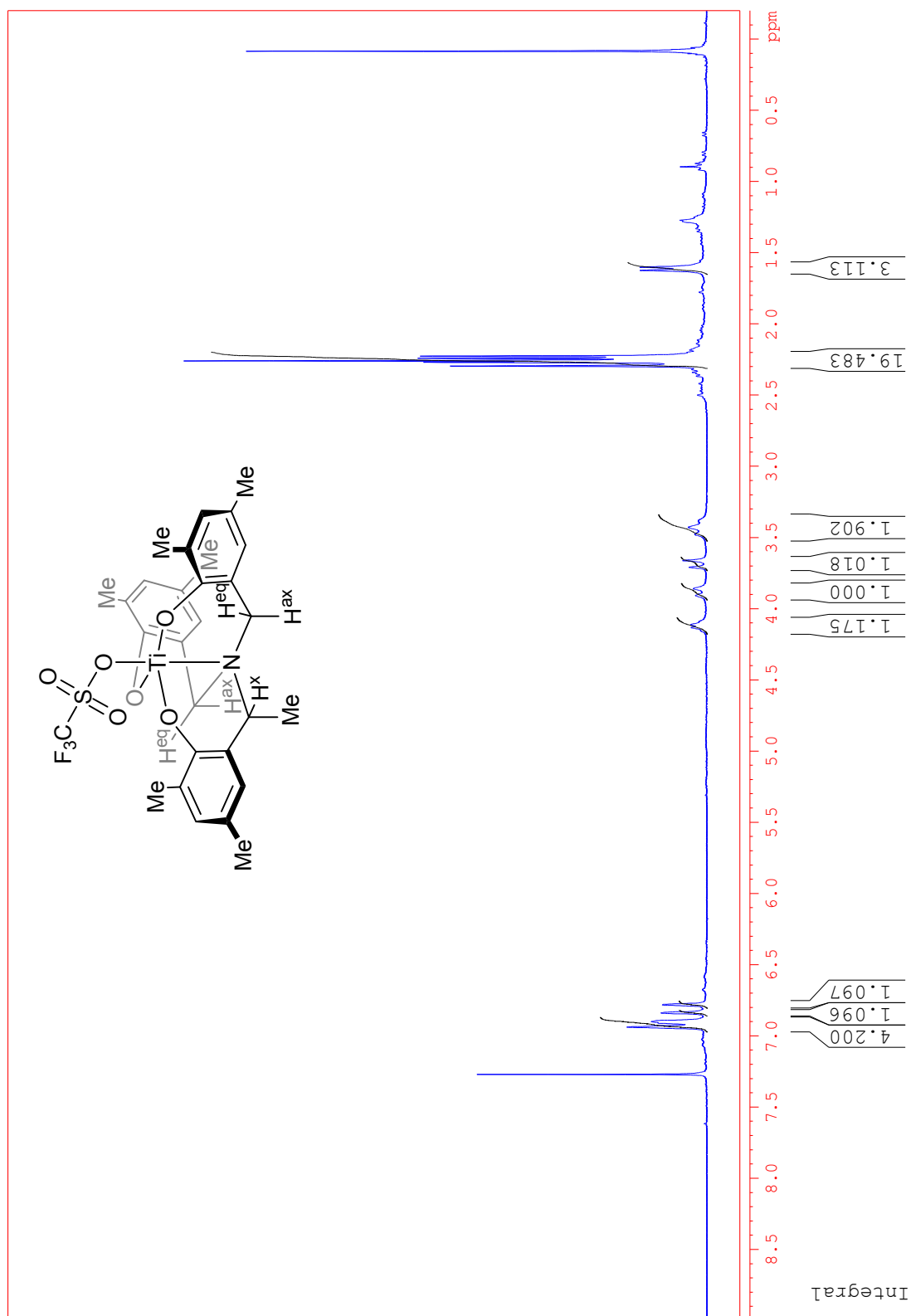
145. F.-Y. Zhang and A. S. C. Chan, *Tetrahedron: Asymmetry*, 1997, **8**, 3651-3655.
146. D. J. Ramón and M. Yus, *Chem. Rev.*, 2006, **106**, 2126-2208.
147. F.-Y. Zhang, C.-W. Yip, R. Cao and A. S. C. Chan, *Tetrahedron: Asymmetry*, 1997, **8**, 585-589.
148. T. Nakai and M. Mori, *Tetrahedron Lett.*, 1997, **38**, 6233-6236.
149. K. Hattori and H. Yamamoto, *Tetrahedron*, 1993, **49**, 1749-1760.
150. G. Modena, F. Di Furia and R. Seraglia, *Synthesis*, 1984, 325-326.
151. P. Pitchen and H. B. Kagan, *Tetrahedron Lett.*, 1984, **25**, 1049-1052.
152. P. Pitchen, E. Duñach, M. N. Deshmukh and H. B. Kagan, *J. Am. Chem. Soc.*, 1984, **106**, 8188-8193.
153. J. M. Brunel and H. B. Kagan, *Synlett*, 1996, 404-406.
154. H. Ando, T. Shuetake, H. Chikamatsu and K. Yamamoto, *J. Chem. Soc., Chem. Commun.*, 1989, 754-755.
155. M. I. Donnoli, S. Superchi and C. Rosini, *J. Org. Chem.*, 1998, **63**, 9392-9395.
156. S. Superchi and C. Rosini, *Tetrahedron: Asymmetry*, 1997, **8**, 349-352.
157. Y. Yamanoi and I. Imamoto, *J. Org. Chem.*, 1997, **62**, 8560-8564.
158. N. Komatsu, Y. Nishibayashi, T. Sugita and S. Uemura, *Tetrahedron Lett.*, 1992, **33**, 5391-5394.
159. N. Komatsu, M. Hashizume, T. Sugita and S. Uemura, *J. Org. Chem.*, 1993, **58**, 4529-4533.
160. M. T. Reetz, C. Merk, G. Naberfeld, R. J., N. Griebenow and R. Goddard, *Tetrahedron Lett.*, 1997, **38**, 5273-5276.
161. C. Bolm and O. A. G. Dabard, *Synlett*, 1999, 360-362.
162. A. K. Yudin, L. J. P. Martyn and S. Pandiaraju, *J. Organomet. Chem.*, 2000, **603**, 98-104.
163. B. Saito and T. Katsuki, *Tetrahedron Lett.*, 2001, **42**, 8333-8336.
164. B. Saito and T. Katsuki, *Tetrahedron Lett.*, 2001, **42**, 3873-3876.
165. H. Firouzabadi, N. Iranpoor, A. A. Jafari and R. E., *Adv. Synth. Catal.*, 2006, **348**, 434-438.
166. M. H. Ali and W. C. Stevens, *Synthesis*, 1997, 764-768.
167. G. Glahsl and R. Hermann, *J. Chem. Soc., Perkin Trans. 1*, 1988, 1753-1757.
168. J. Legros and C. Bolm, *Chem. Eur. J.*, 2005, **11**, 1086-1092.

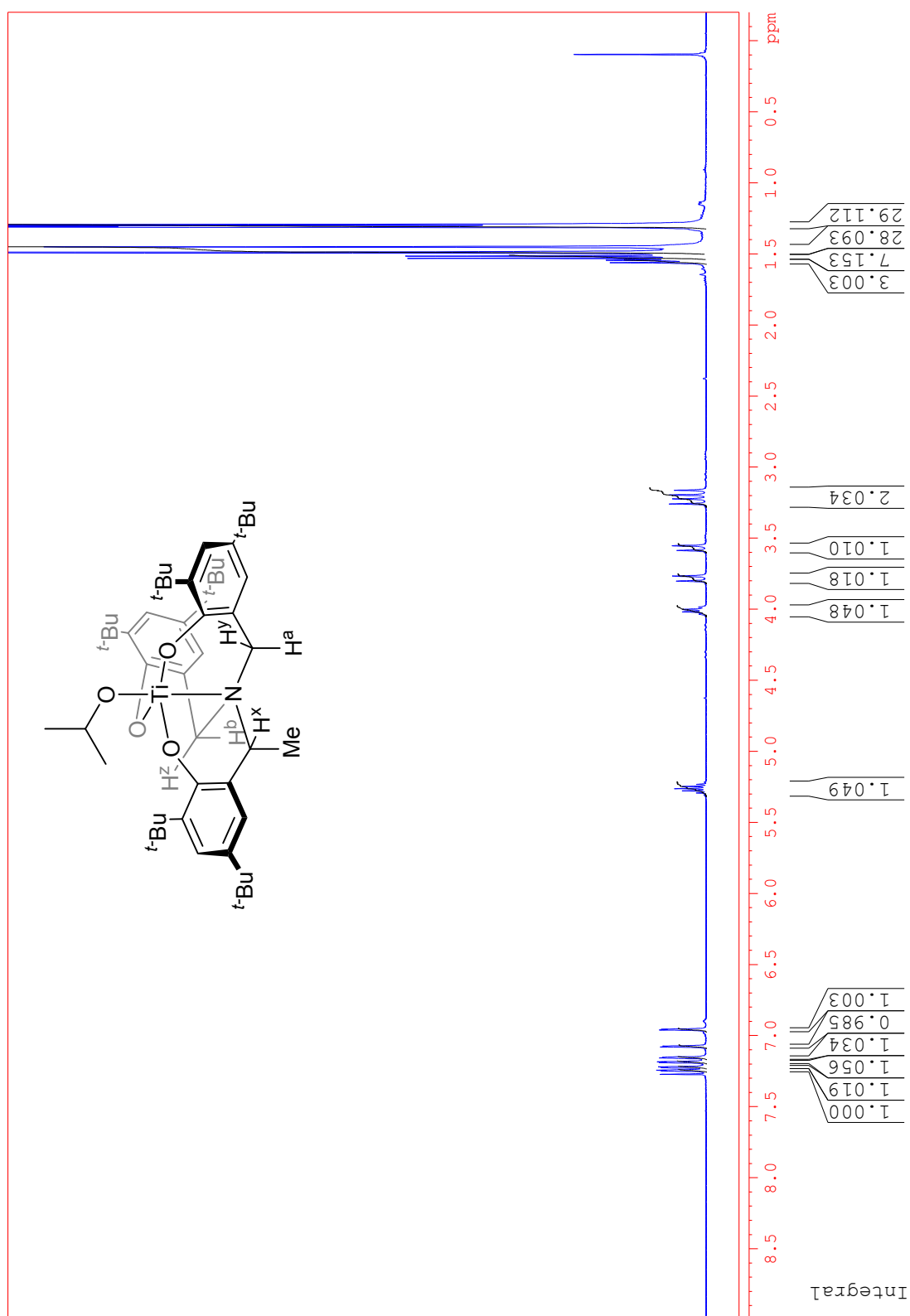
169. P. Kelly, S. E. Lawrence and A. R. Maguire, *Eur. J. Org. Chem.*, 2006, 4500-4509.
170. A. V. Wiznycia, J. Desper and C. J. Levy, *Chem. Commun.*, 2005, 4693-4695.
171. B. Lesch and S. Bräse, *Angew. Chem. Int. Edit.*, 2004, **43**, 115-118.
172. P. D. Knight, P. N. O'Shaughnessy, I. J. Munslow, B. S. Kimberley and P. Scott, *J. Organomet. Chem.*, 2003, **683**, 103-113.
173. H. Du and K. Ding, *Org. Lett.*, 2003, **5**, 1091-1093.
174. M. Karhu, *J. Chem. Soc., Perkin Trans. 1*, 1979, 1661-1664.
175. G. Hua and J. D. Woollins, *Tetrahedron Lett.*, 2007, **48**, 3677-3679.
176. S. Perumal, S. Selvaraj and M. J. E. Hewlins, *Magn. Reson. Chem.*, 1999, **37**, 445-446.
177. F. S. Allaire and J. W. Lyga, *Synth. Commun.*, 2001, **31**, 1857-1861.
178. D. J. Pasto, F. Cottard and L. Jumelle, *J. Am. Chem. Soc.*, 1994, **116**, 8978-8984.
179. G. A. Olah, Q. Wang, N. J. Trivedi and G. K. S. Prakash, *Synthesis*, 1992, 465-466.
180. A. Lattanzi, S. Piccirillo and A. Scettri, *Eur. J. Org. Chem.*, 2006, 713-718.

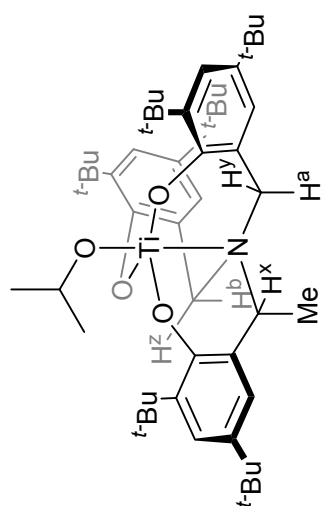
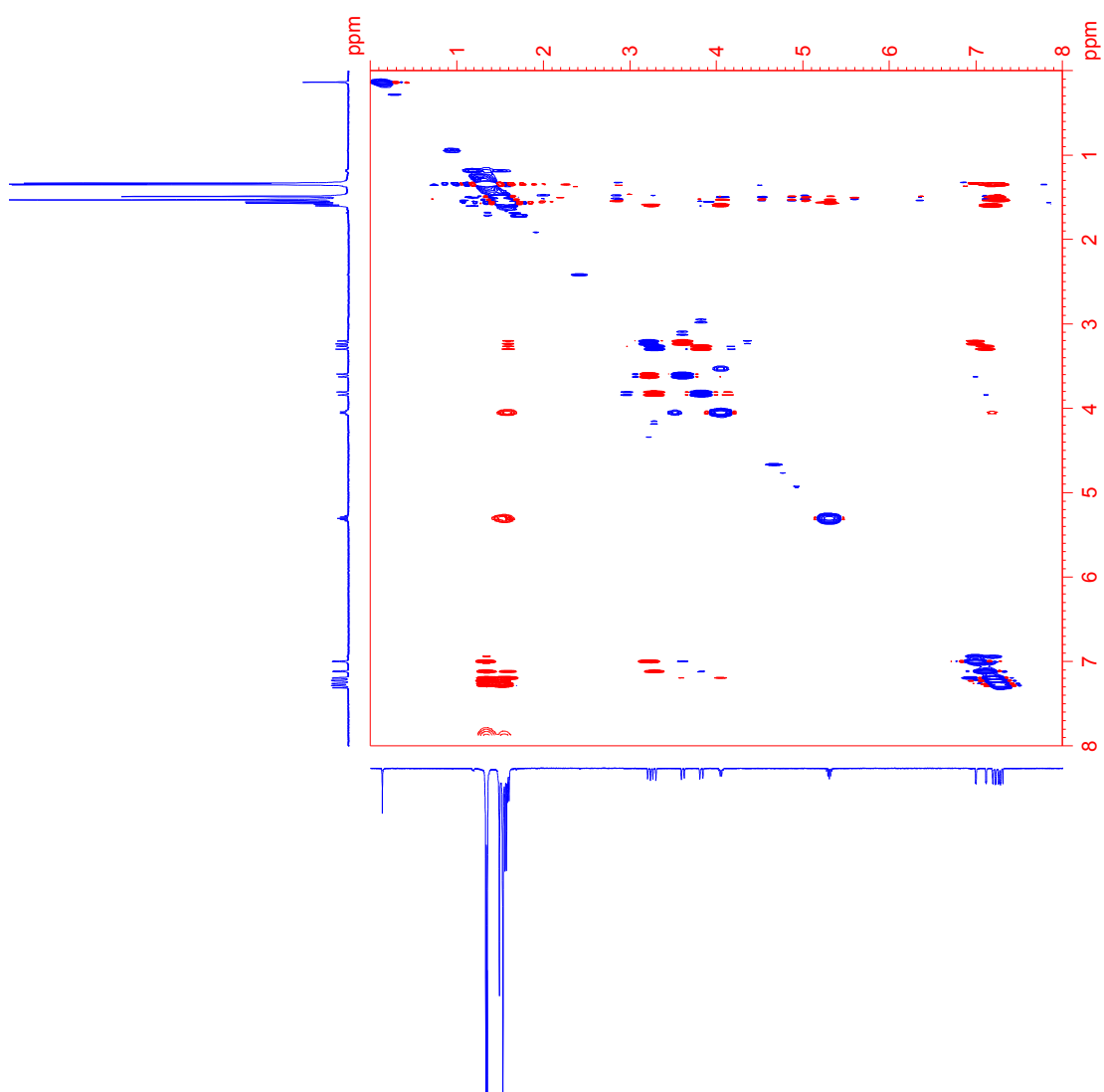
7 Appendix

7.1 **SELECTED NMR SPECTRA**

Titanium *iso*-propoxide complex (R,M)-271 ^1H NMR spectrum (300 MHz, CDCl_3)

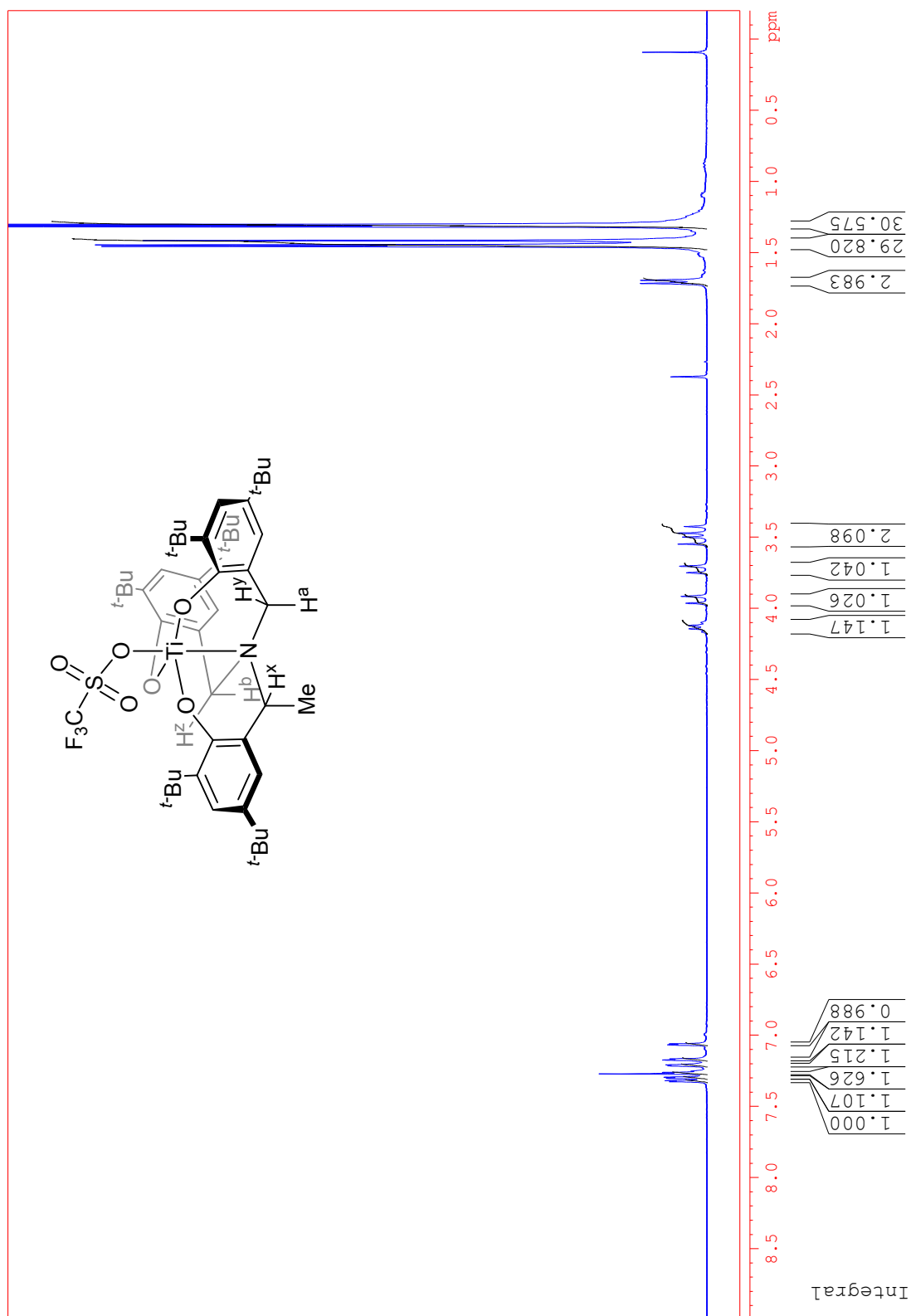
Titanium triflate complex (*R,M*)-272 ^1H NMR spectrum (300 MHz, CDCl_3)

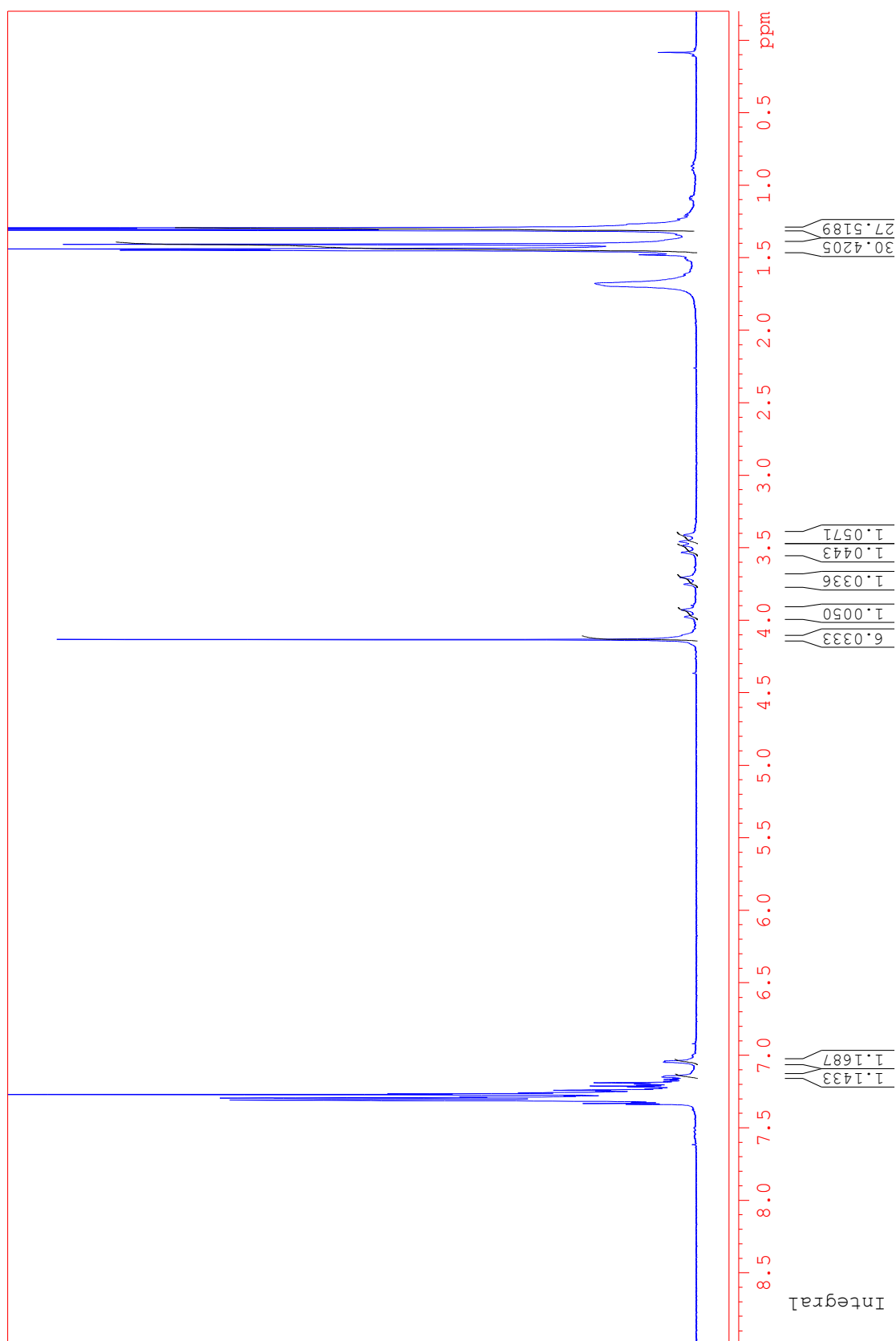
Titanium *iso*-propoxide complex (*R,M*)-287 ^1H NMR spectrum (300 MHz, CDCl_3)



Titanium *iso*-propoxide complex (*R,M*)-287

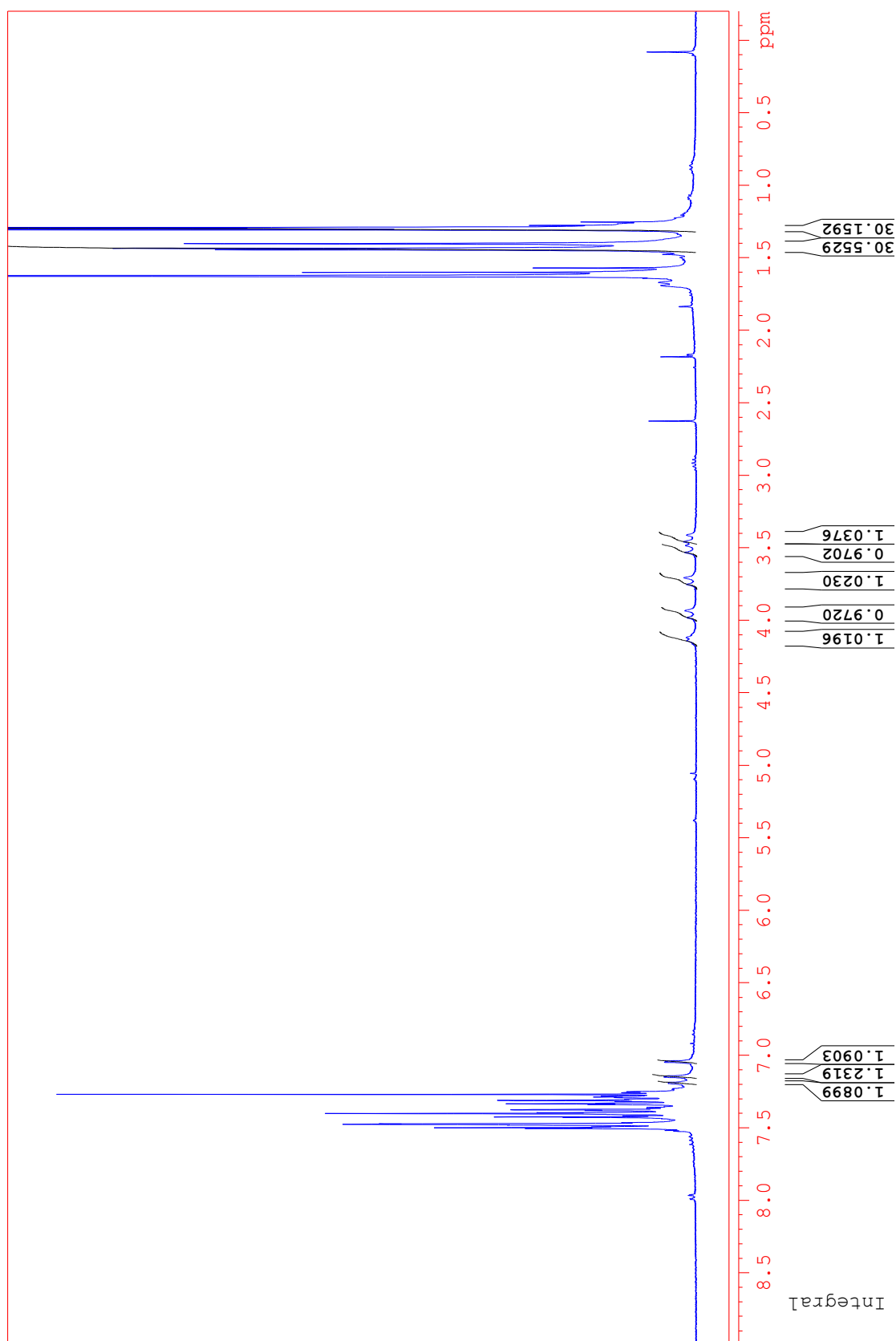
NOE NMR spectrum (400 MHz, CDCl₃)

Titanium triflate complex (*R,M*)-288 ^1H NMR spectrum (300 MHz, CDCl_3)



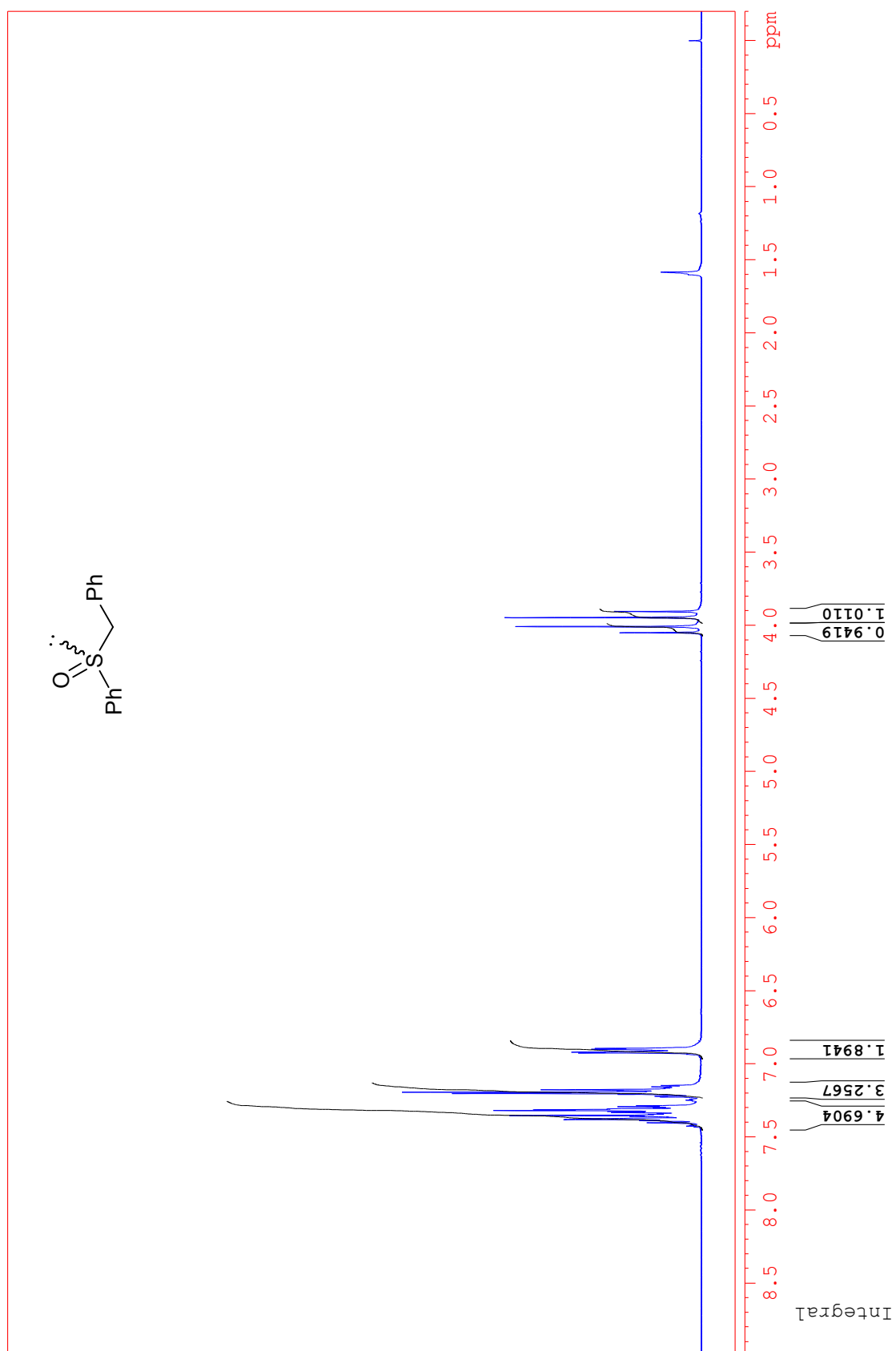
Titanium triflate complex (*R,M*)-288 + benzyl phenyl sulfide 291q (2.5 equiv.)

¹H NMR spectrum (300 MHz, CDCl₃)



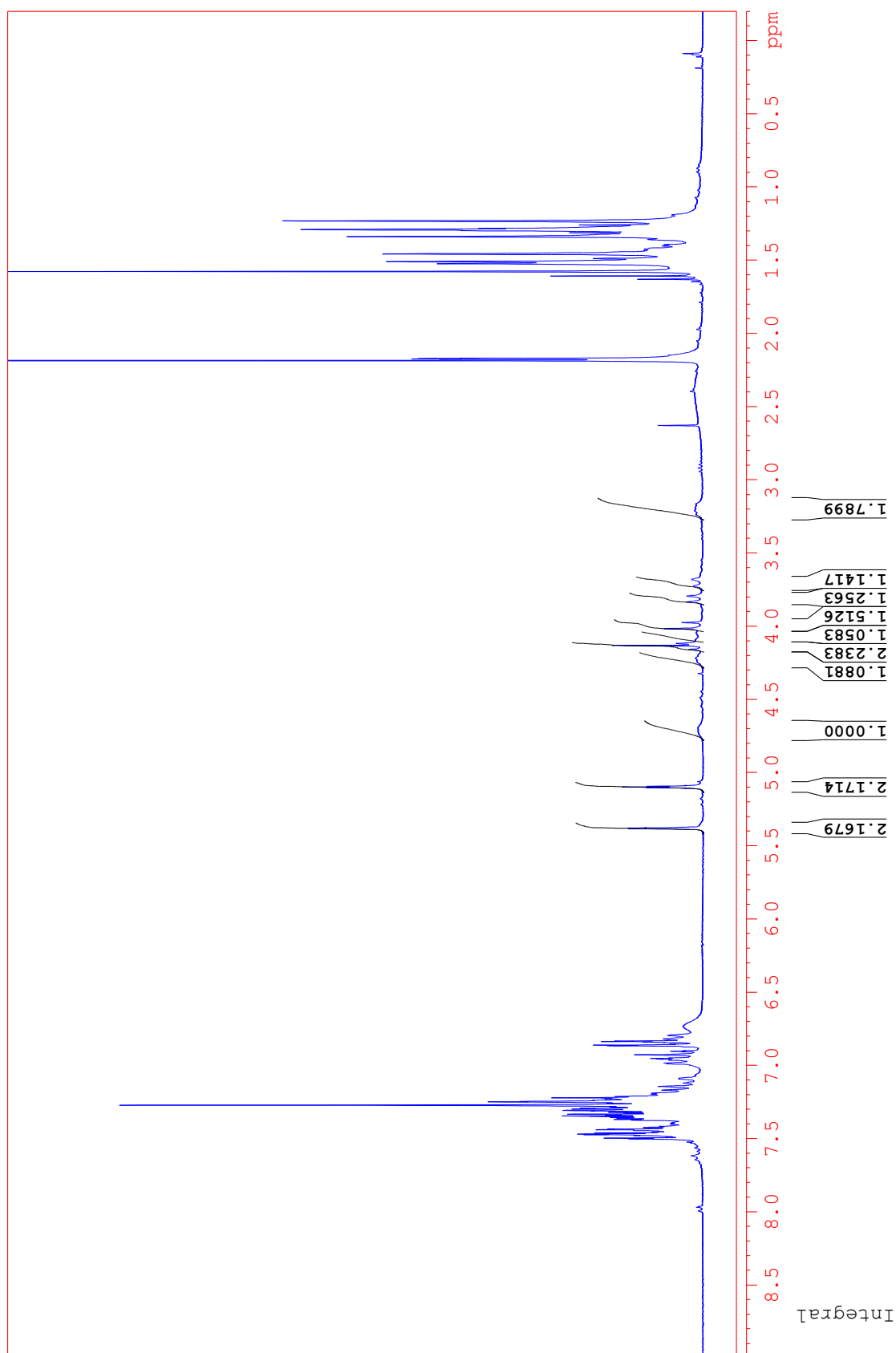
Titanium triflate complex (*R,M*)-288 + cumene hydroperoxide 72 (4 equiv.)

^1H NMR spectrum (300 MHz, CDCl_3)



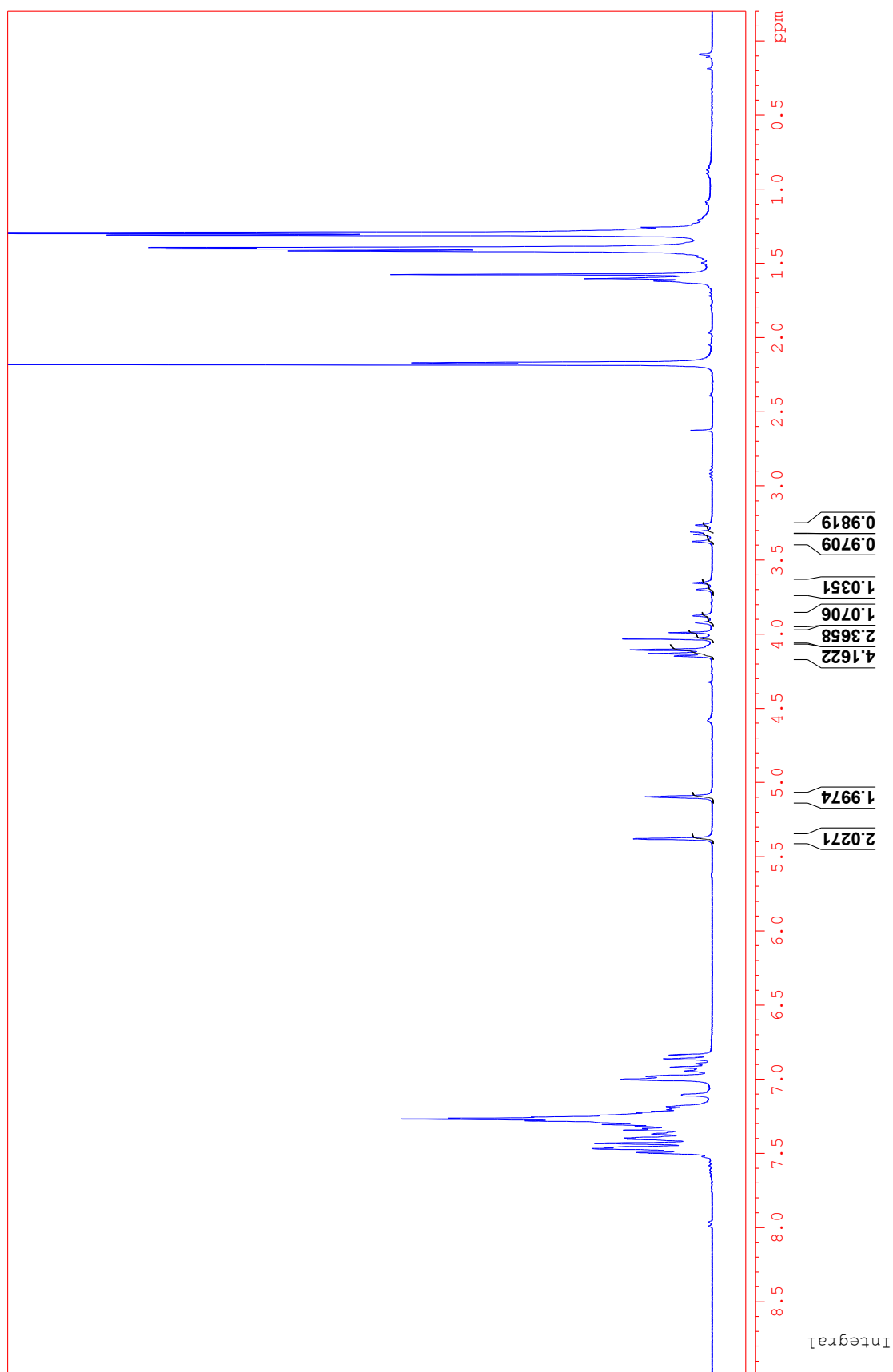
Benzyl phenyl sulfoxide (*rac*)-292q

^1H NMR spectrum (300 MHz, CDCl_3)



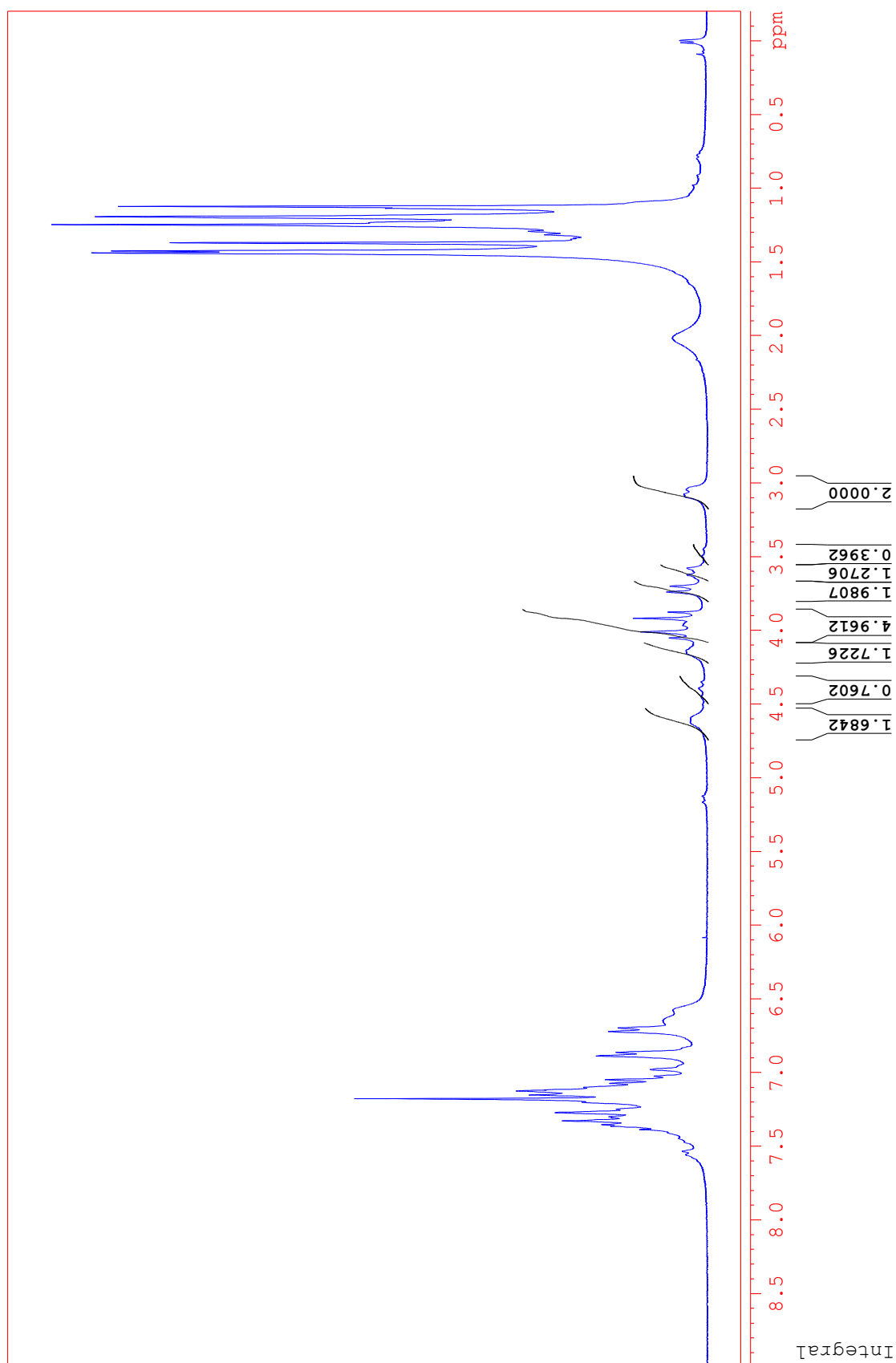
Sulfoxidation reaction after 48 hours [benzyl phenyl sulfide **291q**, cumene hydroperoxide **72** (2 equiv.) and (R,M)-**288** (0.5 equiv.)]

^1H NMR spectrum (300 MHz, CDCl_3)



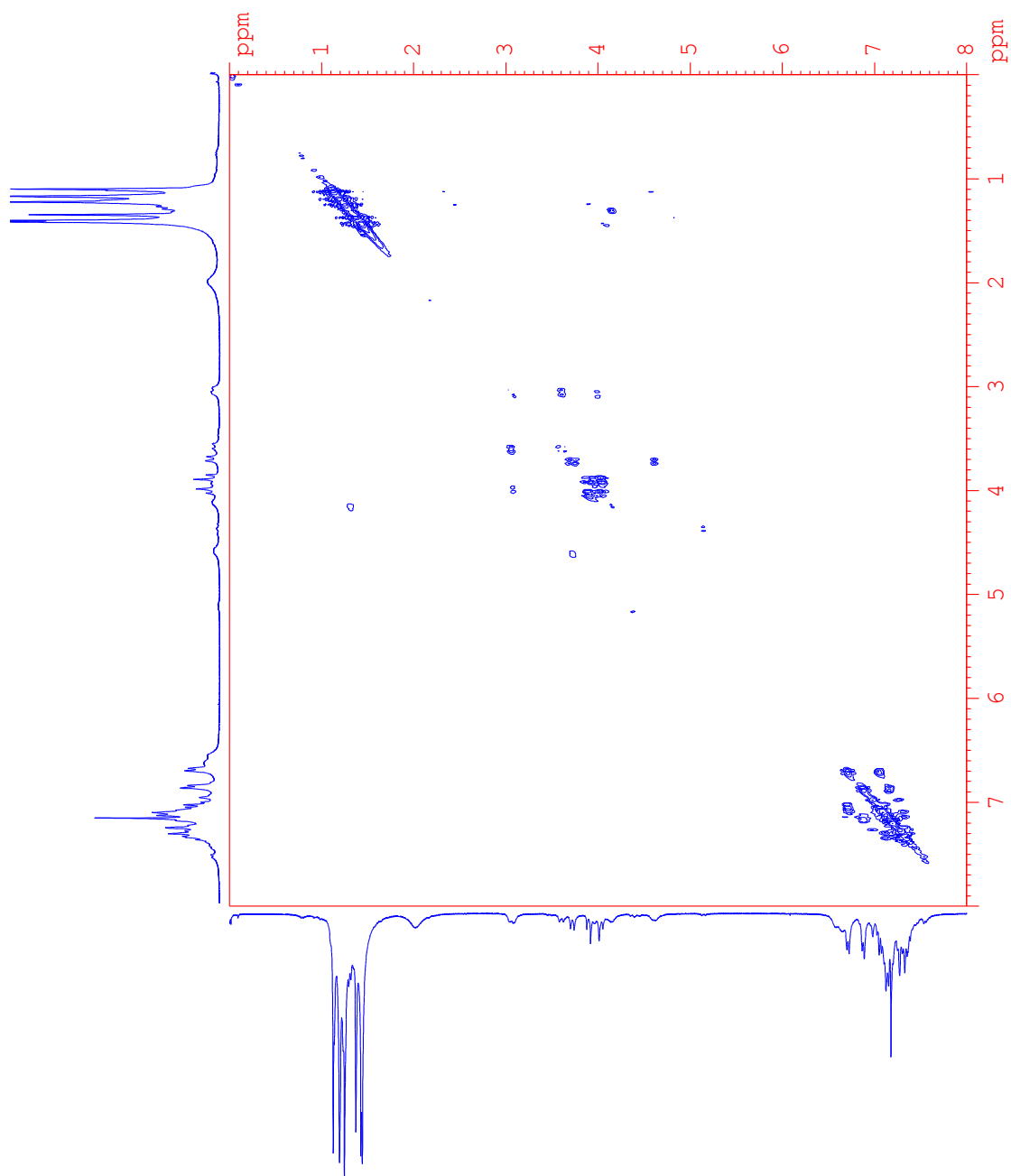
Sulfoxidation reaction after addition of $\text{Na}_2\text{SO}_{3(\text{aq})}$

^1H NMR spectrum (300 MHz, CDCl_3)



Titanium triflate complex (*R,M*)-288 + benzyl phenyl sulfoxide (*rac*)-292q (2 equiv.)

^1H NMR spectrum (300 MHz, CDCl_3)



Titanium triflate complex (*R,M*)-288 + benzyl phenyl sulfoxide (*rac*)-292q (2 equiv.)

COSY NMR spectrum (300 MHz, CDCl₃)

7.2 CRYSTAL STRUCTURE DATA FOR (*R,M*)-271 AND THE CO-CRYSTALLISED TRIMETALLIC AMINE (TRISPHENOLATE)-OXO-ALKOXIDE COMPLEX

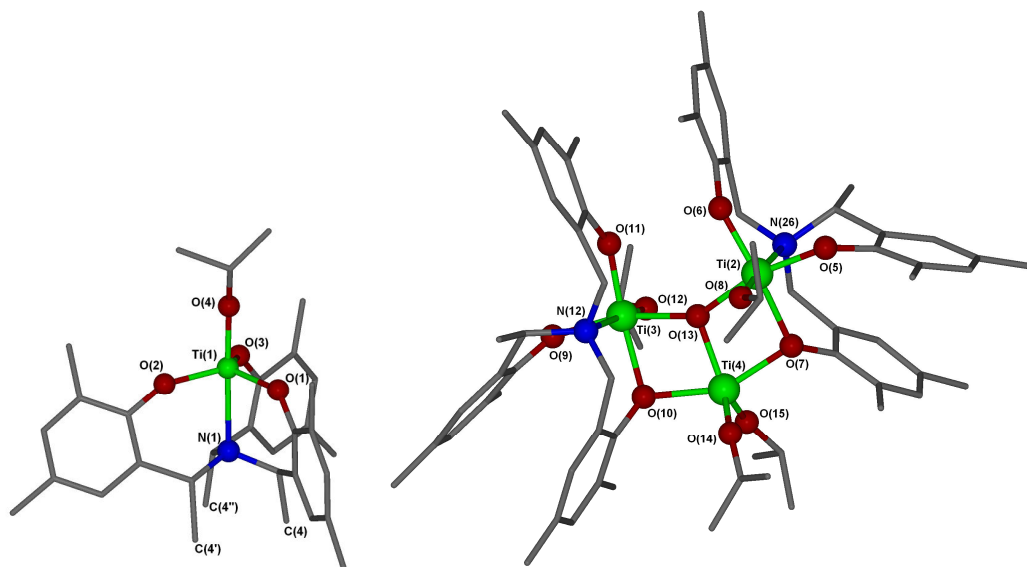


Figure 64. Crystal structure of (*R,M*)-271 and the co-crystallised trimetallic amine (trisphenolate)-oxo-alkoxide complex

Table 73. Crystal data and structural refinement

Empirical formula	C _{49.50} H ₆₆ N _{1.50} O _{7.50} Ti ₂	
Formula weight	897.84	
Temperature	150(2) K	
Wavelength	0.71073 Å	
Crystal system	Monoclinic	
Space group	P2 ₁	
Unit cell dimensions	a = 12.0620(2) Å	α = 90°
	b = 31.1510(5) Å	β = 105.5180(10)°
	c = 13.3950(2) Å	γ = 90°
Volume	4849.61(13) Å ³	
Z	4	
Density (calculated)	1.230 Mg/m ³	
Absorption coefficient	0.380 mm ⁻¹	
F(000)	1910	
Crystal size	0.20 x 0.20 x 0.15 mm ³	
Theta range for data collection	3.57 to 27.65°.	
Index ranges	-15 ≤ h ≤ 15, -40 ≤ k ≤ 40, -17 ≤ l ≤ 16	
Reflections collected	59337	
Independent reflections	19464 [R(int) = 0.0995]	
Completeness to theta = 27.65°	91.1 %	
Max. and min. transmission	0.9452 and 0.9279	

Refinement method	Full-matrix least-squares on F ²
Data / restraints / parameters	19464 / 2 / 1141
Goodness-of-fit on F ²	1.064
Final R indices [$I > 2\sigma(I)$]	R1 = 0.0914, wR2 = 0.2259
R indices (all data)	R1 = 0.1218, wR2 = 0.2466
Absolute structure parameter	-0.01(3)
Largest diff. peak and hole	1.063 and -0.770 e.Å ⁻³

Table 74. Atomic coordinates ($\times 10^4$) and equivalent isotropic displacement parameters ($\text{\AA}^2 \times 10^3$)

	x	y	z	U(eq) ⁶
Ti(1)	8322(1)	5958(1)	8572(1)	44(1)
Ti(2)	5052(1)	2664(1)	5400(1)	29(1)
Ti(3)	6507(1)	3656(1)	6844(1)	28(1)
Ti(4)	6583(1)	2709(1)	7710(1)	32(1)
O(1)	8146(5)	5485(2)	7721(4)	52(1)
O(2)	8079(5)	6485(2)	7925(4)	53(1)
O(3)	9284(6)	5930(2)	9905(4)	59(2)
O(4)	7014(5)	5909(2)	8914(5)	68(2)
O(5)	4132(4)	2215(2)	4722(4)	36(1)
O(6)	4620(4)	3074(1)	4360(3)	32(1)
O(7)	5334(4)	2338(1)	6823(3)	29(1)
O(8)	6347(4)	2472(2)	5119(4)	38(1)
O(9)	7356(4)	4135(1)	7456(3)	32(1)
O(10)	7474(4)	3263(2)	8032(3)	33(1)
O(11)	5835(4)	3885(1)	5533(3)	31(1)
O(12)	5331(4)	3763(2)	7422(4)	33(1)
O(13)	5958(4)	3059(1)	6491(3)	28(1)
O(14)	7757(4)	2354(2)	7840(5)	49(1)
O(15)	6087(5)	2678(2)	8825(4)	56(2)
N(1)	10133(5)	6007(2)	8138(4)	37(1)
N(12)	8155(4)	3543(2)	6200(4)	28(1)
N(26)	3315(5)	2869(2)	5822(4)	30(1)
C(1)	10497(7)	5568(2)	7912(6)	43(2)
C(2)	9994(9)	6298(2)	7209(6)	50(2)
C(3)	11028(7)	6198(2)	9035(6)	45(2)
C(4)	11740(20)	5541(11)	7810(30)	101(11)

⁶ U(eq) is defined as one third of the trace of the orthogonalized U^{ij} tensor.

Table 74 (cont)

	x	y	z	U(eq)
C(4')	11100(30)	6294(7)	6730(20)	54(9)
C(4")	12120(30)	6301(12)	8770(30)	78(14)
C(5)	5817(10)	5848(5)	8680(11)	100(4)
C(6)	5495(14)	5512(6)	9350(20)	175(10)
C(7)	5205(12)	6272(6)	8603(14)	125(6)
C(11)	8534(9)	5332(2)	6947(6)	57(2)
C(12)	9695(9)	5372(2)	6965(6)	49(2)
C(13)	10056(11)	5215(3)	6130(7)	67(3)
C(14)	9233(13)	5023(3)	5269(7)	75(3)
C(15)	8114(13)	4988(3)	5311(8)	79(4)
C(16)	7718(9)	5132(2)	6099(7)	59(2)
C(17)	9647(18)	4876(4)	4344(9)	125(7)
C(18)	6512(10)	5082(4)	6121(10)	88(4)
C(21)	8673(7)	6824(2)	7720(6)	46(2)
C(22)	9676(7)	6752(2)	7415(5)	44(2)
C(23)	10317(9)	7103(2)	7245(6)	54(2)
C(24)	9978(9)	7519(3)	7385(6)	53(2)
C(25)	8969(10)	7579(2)	7654(6)	62(3)
C(26)	8310(8)	7238(3)	7841(6)	54(2)
C(27)	10687(10)	7901(3)	7209(8)	75(3)
C(28)	7188(11)	7299(3)	8124(9)	84(3)
C(31)	10378(8)	5802(3)	10352(6)	54(2)
C(32)	11273(8)	5906(2)	9967(6)	49(2)
C(33)	12394(9)	5761(3)	10430(7)	62(2)
C(34)	12588(10)	5488(3)	11312(8)	71(3)
C(35)	11677(11)	5396(3)	11694(7)	69(3)
C(36)	10574(10)	5531(3)	11258(7)	65(3)
C(37)	13781(13)	5309(4)	11768(10)	116(6)
C(38)	9586(13)	5425(4)	11677(8)	88(4)
C(51)	3305(6)	1955(2)	4921(5)	34(2)
C(52)	2403(6)	2138(2)	5231(5)	34(1)
C(53)	1622(7)	1865(2)	5503(5)	39(2)
C(54)	1705(7)	1424(2)	5463(6)	44(2)
C(55)	2576(7)	1255(2)	5093(6)	45(2)
C(56)	3384(6)	1512(2)	4808(5)	38(2)
C(57)	2278(5)	2624(2)	5183(5)	32(1)
C(58)	885(11)	1140(3)	5821(8)	75(3)
C(59)	4331(7)	1318(3)	4385(8)	56(2)
C(59)	4331(7)	1318(3)	4385(8)	56(2)
C(60)	1152(7)	2768(2)	5383(6)	45(2)

Table 74 (cont)

	x	y	z	U(eq)
C(61)	3724(6)	3326(2)	3911(5)	32(1)
C(62)	2943(6)	3445(2)	4448(5)	29(1)
C(63)	1994(6)	3702(2)	3954(5)	35(1)
C(64)	1841(6)	3842(2)	2944(5)	37(2)
C(65)	2649(6)	3731(2)	2437(5)	36(2)
C(66)	3613(6)	3477(2)	2890(5)	32(1)
C(67)	3183(5)	3331(2)	5589(5)	30(1)
C(68)	836(6)	4131(3)	2433(6)	47(2)
C(69)	4524(6)	3364(2)	2355(5)	38(2)
C(71)	4534(5)	2143(2)	7262(4)	27(1)
C(72)	3623(5)	2384(2)	7382(5)	33(1)
C(73)	2866(6)	2207(2)	7903(5)	37(2)
C(74)	2995(6)	1784(3)	8260(6)	42(2)
C(75)	3904(6)	1545(2)	8061(6)	42(2)
C(76)	4665(6)	1715(2)	7544(6)	38(2)
C(77)	3453(5)	2837(2)	6967(5)	31(1)
C(78)	2183(8)	1590(4)	8826(8)	68(3)
C(79)	5598(7)	1443(3)	7339(7)	53(2)
C(81)	6751(9)	2154(3)	4570(9)	72(3)
C(82)	6389(12)	2257(7)	3436(9)	145(8)
C(83)	8091(9)	2148(4)	4934(10)	88(4)
C(91)	8454(6)	4246(2)	7869(5)	33(1)
C(92)	9286(6)	4134(2)	7386(5)	32(1)
C(93)	10427(7)	4239(2)	7859(6)	39(2)
C(94)	10751(6)	4453(2)	8810(6)	39(2)
C(95)	9890(7)	4574(2)	9257(6)	43(2)
C(96)	8742(6)	4483(2)	8818(5)	37(2)
C(97)	8921(6)	3941(2)	6283(5)	33(1)
C(98)	11998(7)	4552(3)	9332(8)	63(3)
C(99)	7820(8)	4631(3)	9280(7)	54(2)
C(100)	9949(7)	3887(3)	5824(6)	44(2)
C(101)	8642(6)	3265(2)	8445(5)	36(2)
C(102)	9372(6)	3192(2)	7805(5)	35(2)
C(103)	10530(6)	3174(2)	8220(5)	35(2)
C(104)	11047(6)	3235(2)	9278(6)	42(2)
C(105)	10316(7)	3321(2)	9896(6)	44(2)
C(106)	9128(7)	3345(3)	9516(5)	41(2)
C(107)	8813(6)	3152(2)	6661(5)	31(1)
C(108)	12331(7)	3209(3)	9701(7)	58(2)
C(109)	8344(7)	3448(3)	10173(6)	59(2)

Table 74 (cont)

	x	y	z	U(eq)
C(111)	6118(6)	3993(2)	4658(5)	33(1)
C(112)	7061(5)	3799(2)	4406(5)	30(1)
C(113)	7366(6)	3917(2)	3524(5)	38(2)
C(114)	6715(7)	4233(3)	2857(6)	45(2)
C(115)	5791(6)	4415(3)	3106(6)	43(2)
C(116)	5449(6)	4302(2)	3981(5)	34(1)
C(117)	7654(6)	3433(2)	5063(5)	32(1)
C(118)	7077(9)	4362(3)	1884(7)	64(2)
C(119)	4414(6)	4492(2)	4211(6)	40(2)
C(121)	4986(6)	4131(2)	7893(6)	44(2)
C(122)	3819(9)	4292(3)	7198(8)	69(3)
C(123)	4900(9)	4012(4)	8958(7)	67(3)
C(141)	8614(13)	2053(4)	8257(12)	125(7)
C(142)	8809(11)	1717(4)	7704(11)	96(4)
C(143)	9407(7)	2180(3)	9262(7)	60(2)
C(151)	5729(9)	2481(4)	9653(6)	67(3)
C(152)	5442(9)	2840(5)	10307(9)	94(4)
C(153)	6631(13)	2183(5)	10247(9)	105(5)

Table 75. Bond lengths

Bond	Length /Å	Bond	Length /Å
Ti(1)-O(4)	1.763(6)	N(1)-C(3)	1.507(9)
Ti(1)-O(1)	1.841(6)	N(1)-C(2)	1.511(9)
Ti(1)-O(2)	1.844(6)	N(12)-C(107)	1.495(8)
Ti(1)-O(3)	1.853(6)	N(12)-C(117)	1.520(8)
Ti(1)-N(1)	2.411(7)	N(12)-C(97)	1.533(8)
Ti(2)-O(8)	1.803(5)	N(26)-C(67)	1.473(8)
Ti(2)-O(6)	1.859(5)	N(26)-C(77)	1.501(8)
Ti(2)-O(5)	1.864(4)	N(26)-C(57)	1.518(8)
Ti(2)-O(13)	1.998(4)	C(1)-C(12)	1.503(12)
Ti(2)-O(7)	2.104(4)	C(1)-C(4)	1.55(3)
Ti(2)-N(26)	2.398(5)	C(1)-H(1A)	0.9900
Ti(2)-Ti(4)	3.1533(15)	C(1)-H(1B)	0.9900
Ti(3)-O(12)	1.819(4)	C(2)-C(22)	1.511(11)
Ti(3)-O(11)	1.868(4)	C(2)-C(4')	1.62(3)
Ti(3)-O(9)	1.869(4)	C(2)-H(2A)	0.9900
Ti(3)-O(13)	1.988(4)	C(2)-H(2B)	0.9900
Ti(3)-O(10)	2.097(4)	C(3)-C(4")	1.49(4)
Ti(3)-N(12)	2.395(5)	C(3)-C(32)	1.508(11)
Ti(3)-Ti(4)	3.1620(16)	C(3)-H(3A)	0.9900
Ti(4)-O(15)	1.755(5)	C(3)-H(3B)	0.9900
Ti(4)-O(14)	1.769(5)	C(4)-H(4A)	0.9800
Ti(4)-O(13)	1.940(4)	C(4)-H(4B)	0.9800
Ti(4)-O(7)	2.015(4)	C(4)-H(4C)	0.9800
Ti(4)-O(10)	2.018(5)	C(4')-H(4'A)	0.9800
O(1)-C(11)	1.333(11)	C(4')-H(4'B)	0.9800
O(2)-C(21)	1.344(10)	C(4')-H(4'C)	0.9800
O(3)-C(31)	1.355(11)	C(4")-H(4"A)	0.9800
O(4)-C(5)	1.406(13)	C(4")-H(4"B)	0.9800
O(5)-C(51)	1.365(8)	C(4")-H(4"C)	0.9800
O(6)-C(61)	1.341(8)	C(5)-C(6)	1.49(2)
O(7)-C(71)	1.396(7)	C(5)-C(7)	1.50(2)
O(8)-C(81)	1.397(9)	C(5)-H(5)	1.0000
O(9)-C(91)	1.337(8)	C(6)-H(6A)	0.9800
O(10)-C(101)	1.369(8)	C(6)-H(6B)	0.9800
O(11)-C(111)	1.347(8)	C(6)-H(6C)	0.9800
O(12)-C(121)	1.423(8)	C(7)-H(7A)	0.9800
O(14)-C(141)	1.397(10)	C(7)-H(7B)	0.9800
O(15)-C(151)	1.431(10)	C(7)-H(7C)	0.9800
N(1)-C(1)	1.492(9)	C(11)-C(12)	1.399(14)

Table 75 (cont)

Bond	Length /Å	Bond	Length /Å
C(11)-C(16)	1.432(12)	C(34)-C(37)	1.512(16)
C(12)-C(13)	1.393(11)	C(35)-C(36)	1.368(15)
C(13)-C(14)	1.437(16)	C(35)-H(35)	0.9500
C(13)-H(13)	0.9500	C(36)-C(38)	1.484(16)
C(14)-C(15)	1.370(17)	C(37)-H(37A)	0.9800
C(14)-C(17)	1.525(14)	C(37)-H(37B)	0.9800
C(15)-C(16)	1.347(15)	C(37)-H(37C)	0.9800
C(15)-H(15)	0.9500	C(38)-H(38A)	0.9800
C(16)-C(18)	1.471(16)	C(38)-H(38B)	0.9800
C(17)-H(17A)	0.9800	C(38)-H(38C)	0.9800
C(17)-H(17B)	0.9800	C(51)-C(52)	1.386(10)
C(17)-H(17C)	0.9800	C(51)-C(56)	1.393(10)
C(18)-H(18A)	0.9800	C(52)-C(53)	1.387(10)
C(18)-H(18B)	0.9800	C(52)-C(57)	1.522(10)
C(18)-H(18C)	0.9800	C(53)-C(54)	1.381(11)
C(21)-C(26)	1.386(11)	C(53)-H(53)	0.9500
C(21)-C(22)	1.395(12)	C(54)-C(55)	1.380(12)
C(22)-C(23)	1.392(12)	C(54)-C(58)	1.499(12)
C(23)-C(24)	1.387(12)	C(55)-C(56)	1.391(11)
C(23)-H(23)	0.9500	C(55)-H(55)	0.9500
C(24)-C(25)	1.370(14)	C(56)-C(59)	1.529(11)
C(24)-C(27)	1.520(13)	C(57)-C(60)	1.521(10)
C(25)-C(26)	1.388(13)	C(57)-H(57)	1.0000
C(25)-H(25)	0.9500	C(58)-H(58A)	0.9800
C(26)-C(28)	1.512(15)	C(58)-H(58B)	0.9800
C(27)-H(27A)	0.9800	C(58)-H(58C)	0.9800
C(27)-H(27B)	0.9800	C(59)-H(59A)	0.9800
C(27)-H(27C)	0.9800	C(59)-H(59B)	0.9800
C(28)-H(28A)	0.9800	C(59)-H(59C)	0.9800
C(28)-H(28B)	0.9800	C(60)-H(60A)	0.9800
C(28)-H(28C)	0.9800	C(60)-H(60B)	0.9800
C(31)-C(32)	1.354(13)	C(60)-H(60C)	0.9800
C(31)-C(36)	1.445(12)	C(61)-C(62)	1.380(9)
C(32)-C(33)	1.403(12)	C(61)-C(66)	1.419(9)
C(33)-C(34)	1.422(14)	C(62)-C(63)	1.408(9)
C(33)-H(33)	0.9500	C(62)-C(67)	1.520(9)
C(34)-C(35)	1.363(16)	C(63)-C(64)	1.386(10)

Table 75 (cont)

Bond	Length /Å	Bond	Length /Å
C(63)-H(63)	0.9500	C(83)-H(83A)	0.9800
C(64)-C(65)	1.373(10)	C(83)-H(83B)	0.9800
C(64)-C(68)	1.519(10)	C(83)-H(83C)	0.9800
C(65)-C(66)	1.402(10)	C(91)-C(92)	1.377(10)
C(65)-H(65)	0.9500	C(91)-C(96)	1.430(10)
C(66)-C(69)	1.506(10)	C(92)-C(93)	1.391(10)
C(67)-H(67A)	0.9900	C(92)-C(97)	1.546(9)
C(67)-H(67B)	0.9900	C(93)-C(94)	1.397(10)
C(68)-H(68A)	0.9800	C(93)-H(93)	0.9500
C(68)-H(68B)	0.9800	C(94)-C(95)	1.383(11)
C(68)-H(68C)	0.9800	C(94)-C(98)	1.512(10)
C(69)-H(69A)	0.9800	C(95)-C(96)	1.381(10)
C(69)-H(69B)	0.9800	C(95)-H(95)	0.9500
C(69)-H(69C)	0.9800	C(96)-C(99)	1.485(11)
C(71)-C(72)	1.375(9)	C(97)-C(100)	1.533(10)
C(71)-C(76)	1.383(10)	C(97)-H(97)	1.0000
C(72)-C(73)	1.402(9)	C(98)-H(98A)	0.9800
C(72)-C(77)	1.513(10)	C(98)-H(98B)	0.9800
C(73)-C(74)	1.394(11)	C(98)-H(98C)	0.9800
C(73)-H(73)	0.9500	C(99)-H(99A)	0.9800
C(74)-C(75)	1.408(11)	C(99)-H(99B)	0.9800
C(74)-C(78)	1.517(11)	C(99)-H(99C)	0.9800
C(75)-C(76)	1.394(10)	C(100)-H(10A)	0.9800
C(75)-H(75)	0.9500	C(100)-H(10B)	0.9800
C(76)-C(79)	1.491(11)	C(100)-H(10C)	0.9800
C(77)-H(77A)	0.9900	C(101)-C(102)	1.403(10)
C(77)-H(77B)	0.9900	C(101)-C(106)	1.418(10)
C(78)-H(78A)	0.9800	C(102)-C(103)	1.360(10)
C(78)-H(78B)	0.9800	C(102)-C(107)	1.506(9)
C(78)-H(78C)	0.9800	C(103)-C(104)	1.400(10)
C(79)-H(79A)	0.9800	C(103)-H(103)	0.9500
C(79)-H(79B)	0.9800	C(104)-C(105)	1.388(11)
C(79)-H(79C)	0.9800	C(104)-C(108)	1.503(10)
C(81)-C(82)	1.498(18)	C(105)-C(106)	1.389(10)
C(81)-C(83)	1.558(15)	C(105)-H(105)	0.9500
C(81)-H(81)	1.0000	C(106)-C(109)	1.489(11)
C(82)-H(82A)	0.9800	C(107)-H(10D)	0.9900
C(82)-H(82B)	0.9800	C(107)-H(10E)	0.9900
C(82)-H(82C)	0.9800	C(108)-H(10F)	0.9800

Table 75 (cont)

Bond	Length /Å	Bond	Length /Å
C(108)-H(10G)	0.9800	C(121)-H(121)	1.0000
C(108)-H(10H)	0.9800	C(122)-H(12A)	0.9800
C(109)-H(10I)	0.9800	C(122)-H(12B)	0.9800
C(109)-H(10J)	0.9800	C(122)-H(12C)	0.9800
C(109)-H(10K)	0.9800	C(123)-H(12D)	0.9800
C(111)-C(112)	1.405(10)	C(123)-H(12E)	0.9800
C(111)-C(116)	1.418(9)	C(123)-H(12F)	0.9800
C(112)-C(113)	1.378(10)	C(141)-C(142)	1.338(17)
C(112)-C(117)	1.500(9)	C(141)-C(143)	1.482(15)
C(113)-C(114)	1.416(10)	C(141)-H(141)	1.0000
C(113)-H(113)	0.9500	C(142)-H(14A)	0.9800
C(114)-C(115)	1.369(11)	C(142)-H(14B)	0.9800
C(114)-C(118)	1.536(11)	C(142)-H(14C)	0.9800
C(115)-C(116)	1.387(10)	C(143)-H(14D)	0.9800
C(115)-H(115)	0.9500	C(143)-H(14E)	0.9800
C(116)-C(119)	1.487(10)	C(143)-H(14F)	0.9800
C(117)-H(11A)	0.9900	C(151)-C(153)	1.489(16)
C(117)-H(11B)	0.9900	C(151)-C(152)	1.516(16)
C(118)-H(11C)	0.9800	C(151)-H(151)	1.0000
C(118)-H(11D)	0.9800	C(152)-H(15A)	0.9800
C(118)-H(11E)	0.9800	C(152)-H(15B)	0.9800
C(119)-H(11F)	0.9800	C(152)-H(15C)	0.9800
C(119)-H(11G)	0.9800	C(153)-H(15D)	0.9800
C(119)-H(11H)	0.9800	C(153)-H(15E)	0.9800
C(121)-C(123)	1.505(12)	C(153)-H(15F)	0.9800
C(121)-C(122)	1.550(12)		

Table 76. Bond angles

Bond	Angle /°	Bond	Angle /°
O(4)-Ti(1)-O(1)	97.4(3)	O(9)-Ti(3)-O(10)	90.26(19)
O(4)-Ti(1)-O(2)	99.1(3)	O(13)-Ti(3)-O(10)	73.53(18)
O(1)-Ti(1)-O(2)	116.4(3)	O(12)-Ti(3)-N(12)	175.44(19)
O(4)-Ti(1)-O(3)	96.9(3)	O(11)-Ti(3)-N(12)	84.85(19)
O(1)-Ti(1)-O(3)	119.9(3)	O(9)-Ti(3)-N(12)	82.22(18)
O(2)-Ti(1)-O(3)	118.3(3)	O(13)-Ti(3)-N(12)	91.85(18)
O(4)-Ti(1)-N(1)	178.3(3)	O(10)-Ti(3)-N(12)	80.82(18)
O(1)-Ti(1)-N(1)	82.1(2)	O(12)-Ti(3)-Ti(4)	87.94(15)
O(2)-Ti(1)-N(1)	82.6(2)	O(11)-Ti(3)-Ti(4)	131.57(15)
O(3)-Ti(1)-N(1)	82.0(2)	O(9)-Ti(3)-Ti(4)	128.65(15)
O(8)-Ti(2)-O(6)	99.0(2)	O(13)-Ti(3)-Ti(4)	35.87(12)
O(8)-Ti(2)-O(5)	95.0(2)	O(10)-Ti(3)-Ti(4)	38.87(13)
O(6)-Ti(2)-O(5)	98.0(2)	N(12)-Ti(3)-Ti(4)	92.82(13)
O(8)-Ti(2)-O(13)	91.2(2)	O(15)-Ti(4)-O(14)	109.1(3)
O(6)-Ti(2)-O(13)	96.50(19)	O(15)-Ti(4)-O(13)	127.1(3)
O(5)-Ti(2)-O(13)	163.1(2)	O(14)-Ti(4)-O(13)	123.7(2)
O(8)-Ti(2)-O(7)	95.2(2)	O(15)-Ti(4)-O(7)	95.7(2)
O(6)-Ti(2)-O(7)	162.67(19)	O(14)-Ti(4)-O(7)	98.8(2)
O(5)-Ti(2)-O(7)	90.6(2)	O(13)-Ti(4)-O(7)	76.42(18)
O(13)-Ti(2)-O(7)	73.18(17)	O(15)-Ti(4)-O(10)	98.5(2)
O(8)-Ti(2)-N(26)	176.0(2)	O(14)-Ti(4)-O(10)	98.5(2)
O(6)-Ti(2)-N(26)	84.59(19)	O(13)-Ti(4)-O(10)	76.36(18)
O(5)-Ti(2)-N(26)	82.57(19)	O(7)-Ti(4)-O(10)	152.65(18)
O(13)-Ti(2)-N(26)	90.26(18)	O(15)-Ti(4)-Ti(2)	126.13(18)
O(7)-Ti(2)-N(26)	81.64(17)	O(14)-Ti(4)-Ti(2)	108.2(2)
O(8)-Ti(2)-Ti(4)	84.67(16)	O(13)-Ti(4)-Ti(2)	37.44(12)
O(6)-Ti(2)-Ti(4)	132.65(15)	O(7)-Ti(4)-Ti(2)	41.10(13)
O(5)-Ti(2)-Ti(4)	128.90(16)	O(10)-Ti(4)-Ti(2)	112.76(13)
O(13)-Ti(2)-Ti(4)	36.17(12)	O(15)-Ti(4)-Ti(3)	112.3(2)
O(7)-Ti(2)-Ti(4)	39.01(12)	O(14)-Ti(4)-Ti(3)	124.32(18)
N(26)-Ti(2)-Ti(4)	94.36(13)	O(13)-Ti(4)-Ti(3)	36.91(12)
O(12)-Ti(3)-O(11)	98.0(2)	O(7)-Ti(4)-Ti(3)	112.03(13)
O(12)-Ti(3)-O(9)	93.8(2)	O(10)-Ti(4)-Ti(3)	40.72(13)
O(11)-Ti(3)-O(9)	99.0(2)	Ti(2)-Ti(4)-Ti(3)	74.35(4)
O(12)-Ti(3)-O(13)	91.40(19)	C(11)-O(1)-Ti(1)	139.5(6)
O(11)-Ti(3)-O(13)	95.74(19)	C(21)-O(2)-Ti(1)	140.3(5)
O(9)-Ti(3)-O(13)	163.49(19)	C(31)-O(3)-Ti(1)	136.4(5)
O(12)-Ti(3)-O(10)	97.1(2)	C(5)-O(4)-Ti(1)	153.0(8)
O(11)-Ti(3)-O(10)	161.71(19)	C(51)-O(5)-Ti(2)	136.2(4)

Table 76 (cont)

Bond	Angle /°	Bond	Angle /°
C(61)-O(6)-Ti(2)	140.3(4)	C(4)-C(1)-H(1A)	102.2
C(71)-O(7)-Ti(4)	119.5(4)	N(1)-C(1)-H(1B)	109.1
C(71)-O(7)-Ti(2)	129.0(4)	C(12)-C(1)-H(1B)	109.1
Ti(4)-O(7)-Ti(2)	99.89(18)	C(4)-C(1)-H(1B)	6.4
C(81)-O(8)-Ti(2)	142.0(6)	H(1A)-C(1)-H(1B)	107.8
C(91)-O(9)-Ti(3)	139.0(4)	C(22)-C(2)-N(1)	112.9(6)
C(101)-O(10)-Ti(4)	121.5(4)	C(22)-C(2)-C(4')	110.6(10)
C(101)-O(10)-Ti(3)	127.4(4)	N(1)-C(2)-C(4')	113.5(12)
Ti(4)-O(10)-Ti(3)	100.41(19)	C(22)-C(2)-H(2A)	109.0
C(111)-O(11)-Ti(3)	140.0(4)	N(1)-C(2)-H(2A)	109.0
C(121)-O(12)-Ti(3)	133.6(4)	C(4')-C(2)-H(2A)	7.0
Ti(4)-O(13)-Ti(3)	107.2(2)	C(22)-C(2)-H(2B)	109.0
Ti(4)-O(13)-Ti(2)	106.39(19)	N(1)-C(2)-H(2B)	109.0
Ti(3)-O(13)-Ti(2)	146.4(2)	C(4')-C(2)-H(2B)	101.0
C(141)-O(14)-Ti(4)	161.3(9)	H(2A)-C(2)-H(2B)	107.8
C(151)-O(15)-Ti(4)	157.7(7)	C(4'')-C(3)-N(1)	112.7(16)
C(1)-N(1)-C(3)	109.7(6)	C(4'')-C(3)-C(32)	109.7(15)
C(1)-N(1)-C(2)	110.9(5)	N(1)-C(3)-C(32)	111.2(6)
C(3)-N(1)-C(2)	108.5(6)	C(4'')-C(3)-H(3A)	104.2
C(1)-N(1)-Ti(1)	109.0(4)	N(1)-C(3)-H(3A)	109.4
C(3)-N(1)-Ti(1)	109.5(4)	C(32)-C(3)-H(3A)	109.4
C(2)-N(1)-Ti(1)	109.1(5)	C(4'')-C(3)-H(3B)	4.2
C(107)-N(12)-C(117)	104.7(5)	N(1)-C(3)-H(3B)	109.4
C(107)-N(12)-C(97)	112.7(5)	C(32)-C(3)-H(3B)	109.4
C(117)-N(12)-C(97)	109.0(5)	H(3A)-C(3)-H(3B)	108.0
C(107)-N(12)-Ti(3)	111.8(4)	C(1)-C(4)-H(4A)	109.5
C(117)-N(12)-Ti(3)	104.4(4)	C(1)-C(4)-H(4B)	109.5
C(97)-N(12)-Ti(3)	113.4(4)	H(4A)-C(4)-H(4B)	109.5
C(67)-N(26)-C(77)	104.8(5)	C(1)-C(4)-H(4C)	109.5
C(67)-N(26)-C(57)	110.2(5)	H(4A)-C(4)-H(4C)	109.5
C(77)-N(26)-C(57)	113.1(5)	H(4B)-C(4)-H(4C)	109.5
C(67)-N(26)-Ti(2)	105.2(4)	C(2)-C(4')-H(4'A)	109.5
C(77)-N(26)-Ti(2)	111.0(4)	C(2)-C(4')-H(4'B)	109.5
C(57)-N(26)-Ti(2)	111.9(4)	H(4'A)-C(4')-H(4'B)	109.5
N(1)-C(1)-C(12)	112.6(6)	C(2)-C(4')-H(4'C)	109.5
N(1)-C(1)-C(4)	114.4(13)	H(4'A)-C(4')-H(4'C)	109.5
C(12)-C(1)-C(4)	108.9(14)	H(4'B)-C(4')-H(4'C)	109.5
N(1)-C(1)-H(1A)	109.1	C(3)-C(4'')-H(4''A)	109.5
C(12)-C(1)-H(1A)	109.1	C(3)-C(4'')-H(4''B)	109.5

Table 76 (cont)

Bond	Angle /°	Bond	Angle /°
H(4"A)-C(4")-H(4"B)	109.5	C(11)-C(16)-C(18)	120.3(10)
C(3)-C(4")-H(4"C)	109.5	C(14)-C(17)-H(17A)	109.5
H(4"A)-C(4")-H(4"C)	109.5	C(14)-C(17)-H(17B)	109.5
H(4"B)-C(4")-H(4"C)	109.5	H(17A)-C(17)-H(17B)	109.5
O(4)-C(5)-C(6)	112.2(13)	C(14)-C(17)-H(17C)	109.5
O(4)-C(5)-C(7)	110.6(12)	H(17A)-C(17)-H(17C)	109.5
C(6)-C(5)-C(7)	117.1(14)	H(17B)-C(17)-H(17C)	109.5
O(4)-C(5)-H(5)	105.3	C(16)-C(18)-H(18A)	109.5
C(6)-C(5)-H(5)	105.3	C(16)-C(18)-H(18B)	109.5
C(7)-C(5)-H(5)	105.3	H(18A)-C(18)-H(18B)	109.5
C(5)-C(6)-H(6A)	109.5	C(16)-C(18)-H(18C)	109.5
C(5)-C(6)-H(6B)	109.5	H(18A)-C(18)-H(18C)	109.5
H(6A)-C(6)-H(6B)	109.5	H(18B)-C(18)-H(18C)	109.5
C(5)-C(6)-H(6C)	109.5	O(2)-C(21)-C(26)	120.3(8)
H(6A)-C(6)-H(6C)	109.5	O(2)-C(21)-C(22)	119.0(7)
H(6B)-C(6)-H(6C)	109.5	C(26)-C(21)-C(22)	120.6(8)
C(5)-C(7)-H(7A)	109.5	C(23)-C(22)-C(21)	119.0(7)
C(5)-C(7)-H(7B)	109.5	C(23)-C(22)-C(2)	121.8(8)
H(7A)-C(7)-H(7B)	109.5	C(21)-C(22)-C(2)	119.1(7)
C(5)-C(7)-H(7C)	109.5	C(24)-C(23)-C(22)	121.0(9)
H(7A)-C(7)-H(7C)	109.5	C(24)-C(23)-H(23)	119.5
H(7B)-C(7)-H(7C)	109.5	C(22)-C(23)-H(23)	119.5
O(1)-C(11)-C(12)	120.8(7)	C(25)-C(24)-C(23)	118.5(8)
O(1)-C(11)-C(16)	117.5(9)	C(25)-C(24)-C(27)	120.7(8)
C(12)-C(11)-C(16)	121.7(9)	C(23)-C(24)-C(27)	120.7(10)
C(13)-C(12)-C(11)	118.8(9)	C(24)-C(25)-C(26)	122.4(8)
C(13)-C(12)-C(1)	123.4(9)	C(24)-C(25)-H(25)	118.8
C(11)-C(12)-C(1)	117.8(7)	C(26)-C(25)-H(25)	118.8
C(12)-C(13)-C(14)	119.6(11)	C(21)-C(26)-C(25)	118.4(9)
C(12)-C(13)-H(13)	120.2	C(21)-C(26)-C(28)	118.6(9)
C(14)-C(13)-H(13)	120.2	C(25)-C(26)-C(28)	122.9(8)
C(15)-C(14)-C(13)	118.4(9)	C(24)-C(27)-H(27A)	109.5
C(15)-C(14)-C(17)	123.4(12)	C(24)-C(27)-H(27B)	109.5
C(13)-C(14)-C(17)	118.1(13)	H(27A)-C(27)-H(27B)	109.5
C(16)-C(15)-C(14)	124.5(10)	C(24)-C(27)-H(27C)	109.5
C(16)-C(15)-H(15)	117.7	H(27A)-C(27)-H(27C)	109.5
C(14)-C(15)-H(15)	117.7	H(27B)-C(27)-H(27C)	109.5
C(15)-C(16)-C(11)	117.0(11)	C(26)-C(28)-H(28A)	109.5
C(15)-C(16)-C(18)	122.7(10)	C(26)-C(28)-H(28B)	109.5

Table 76 (cont)

Bond	Angle /°	Bond	Angle /°
H(28A)-C(28)-H(28B)	109.5	C(53)-C(52)-C(57)	123.6(6)
C(26)-C(28)-H(28C)	109.5	C(54)-C(53)-C(52)	122.4(7)
H(28A)-C(28)-H(28C)	109.5	C(54)-C(53)-H(53)	118.8
H(28B)-C(28)-H(28C)	109.5	C(52)-C(53)-H(53)	118.8
C(32)-C(31)-O(3)	122.8(8)	C(55)-C(54)-C(53)	117.7(7)
C(32)-C(31)-C(36)	119.4(9)	C(55)-C(54)-C(58)	121.3(8)
O(3)-C(31)-C(36)	117.7(10)	C(53)-C(54)-C(58)	121.0(8)
C(31)-C(32)-C(33)	121.8(8)	C(54)-C(55)-C(56)	122.3(7)
C(31)-C(32)-C(3)	117.4(7)	C(54)-C(55)-H(55)	118.9
C(33)-C(32)-C(3)	120.8(9)	C(56)-C(55)-H(55)	118.9
C(32)-C(33)-C(34)	119.0(11)	C(55)-C(56)-C(51)	117.9(7)
C(32)-C(33)-H(33)	120.5	C(55)-C(56)-C(59)	121.4(7)
C(34)-C(33)-H(33)	120.5	C(51)-C(56)-C(59)	120.7(7)
C(35)-C(34)-C(33)	117.9(9)	N(26)-C(57)-C(60)	113.1(5)
C(35)-C(34)-C(37)	123.1(11)	N(26)-C(57)-C(52)	114.8(5)
C(33)-C(34)-C(37)	119.0(13)	C(60)-C(57)-C(52)	111.6(6)
C(34)-C(35)-C(36)	124.3(9)	N(26)-C(57)-H(57)	105.4
C(34)-C(35)-H(35)	117.8	C(60)-C(57)-H(57)	105.4
C(36)-C(35)-H(35)	117.8	C(52)-C(57)-H(57)	105.4
C(35)-C(36)-C(31)	117.5(10)	C(54)-C(58)-H(58A)	109.5
C(35)-C(36)-C(38)	123.9(10)	C(54)-C(58)-H(58B)	109.5
C(31)-C(36)-C(38)	118.7(10)	H(58A)-C(58)-H(58B)	109.5
C(34)-C(37)-H(37A)	109.5	C(54)-C(58)-H(58C)	109.5
C(34)-C(37)-H(37B)	109.5	H(58A)-C(58)-H(58C)	109.5
H(37A)-C(37)-H(37B)	109.5	H(58B)-C(58)-H(58C)	109.5
C(34)-C(37)-H(37C)	109.5	C(56)-C(59)-H(59A)	109.5
H(37A)-C(37)-H(37C)	109.5	C(56)-C(59)-H(59B)	109.5
H(37B)-C(37)-H(37C)	109.5	H(59A)-C(59)-H(59B)	109.5
C(36)-C(38)-H(38A)	109.5	C(56)-C(59)-H(59C)	109.5
C(36)-C(38)-H(38B)	109.5	H(59A)-C(59)-H(59C)	109.5
H(38A)-C(38)-H(38B)	109.5	H(59B)-C(59)-H(59C)	109.5
C(36)-C(38)-H(38C)	109.5	C(57)-C(60)-H(60A)	109.5
H(38A)-C(38)-H(38C)	109.5	C(57)-C(60)-H(60B)	109.5
H(38B)-C(38)-H(38C)	109.5	H(60A)-C(60)-H(60B)	109.5
O(5)-C(51)-C(52)	119.2(6)	C(57)-C(60)-H(60C)	109.5
O(5)-C(51)-C(56)	119.4(6)	H(60A)-C(60)-H(60C)	109.5
C(52)-C(51)-C(56)	121.4(6)	H(60B)-C(60)-H(60C)	109.5
C(51)-C(52)-C(53)	118.1(7)	O(6)-C(61)-C(62)	120.3(6)
C(51)-C(52)-C(57)	118.2(6)	O(6)-C(61)-C(66)	118.9(6)

Table 76 (cont)

Bond	Angle /°	Bond	Angle /°
C(62)-C(61)-C(66)	120.8(6)	C(73)-C(72)-C(77)	120.6(6)
C(61)-C(62)-C(63)	119.3(6)	C(74)-C(73)-C(72)	120.9(7)
C(61)-C(62)-C(67)	119.2(6)	C(74)-C(73)-H(73)	119.5
C(63)-C(62)-C(67)	121.2(6)	C(72)-C(73)-H(73)	119.5
C(64)-C(63)-C(62)	121.1(6)	C(73)-C(74)-C(75)	117.1(7)
C(64)-C(63)-H(63)	119.4	C(73)-C(74)-C(78)	121.4(7)
C(62)-C(63)-H(63)	119.4	C(75)-C(74)-C(78)	121.5(8)
C(65)-C(64)-C(63)	118.4(6)	C(76)-C(75)-C(74)	122.9(7)
C(65)-C(64)-C(68)	120.9(6)	C(76)-C(75)-H(75)	118.5
C(63)-C(64)-C(68)	120.6(7)	C(74)-C(75)-H(75)	118.5
C(64)-C(65)-C(66)	123.0(6)	C(71)-C(76)-C(75)	117.3(6)
C(64)-C(65)-H(65)	118.5	C(71)-C(76)-C(79)	122.3(6)
C(66)-C(65)-H(65)	118.5	C(75)-C(76)-C(79)	120.4(7)
C(65)-C(66)-C(61)	117.2(6)	N(26)-C(77)-C(72)	113.8(5)
C(65)-C(66)-C(69)	123.6(6)	N(26)-C(77)-H(77A)	108.8
C(61)-C(66)-C(69)	119.2(6)	C(72)-C(77)-H(77A)	108.8
N(26)-C(67)-C(62)	114.9(5)	N(26)-C(77)-H(77B)	108.8
N(26)-C(67)-H(67A)	108.5	C(72)-C(77)-H(77B)	108.8
C(62)-C(67)-H(67A)	108.5	H(77A)-C(77)-H(77B)	107.7
N(26)-C(67)-H(67B)	108.5	C(74)-C(78)-H(78A)	109.5
C(62)-C(67)-H(67B)	108.5	C(74)-C(78)-H(78B)	109.5
H(67A)-C(67)-H(67B)	107.5	H(78A)-C(78)-H(78B)	109.5
C(64)-C(68)-H(68A)	109.5	C(74)-C(78)-H(78C)	109.5
C(64)-C(68)-H(68B)	109.5	H(78A)-C(78)-H(78C)	109.5
H(68A)-C(68)-H(68B)	109.5	H(78B)-C(78)-H(78C)	109.5
C(64)-C(68)-H(68C)	109.5	C(76)-C(79)-H(79A)	109.5
H(68A)-C(68)-H(68C)	109.5	C(76)-C(79)-H(79B)	109.5
H(68B)-C(68)-H(68C)	109.5	H(79A)-C(79)-H(79B)	109.5
C(66)-C(69)-H(69A)	109.5	C(76)-C(79)-H(79C)	109.5
C(66)-C(69)-H(69B)	109.5	H(79A)-C(79)-H(79C)	109.5
H(69A)-C(69)-H(69B)	109.5	H(79B)-C(79)-H(79C)	109.5
C(66)-C(69)-H(69C)	109.5	O(8)-C(81)-C(82)	109.5(10)
H(69A)-C(69)-H(69C)	109.5	O(8)-C(81)-C(83)	108.9(9)
H(69B)-C(69)-H(69C)	109.5	C(82)-C(81)-C(83)	108.5(10)
C(72)-C(71)-C(76)	122.0(6)	O(8)-C(81)-H(81)	110.0
C(72)-C(71)-O(7)	118.4(6)	C(82)-C(81)-H(81)	110.0
C(76)-C(71)-O(7)	119.5(5)	C(83)-C(81)-H(81)	110.0
C(71)-C(72)-C(73)	119.4(7)	C(81)-C(82)-H(82A)	109.5
C(71)-C(72)-C(77)	120.0(6)	C(81)-C(82)-H(82B)	109.5

Table 76 (cont)

Bond	Angle /°	Bond	Angle /°
H(82A)-C(82)-H(82B)	109.5	H(98B)-C(98)-H(98C)	109.5
C(81)-C(82)-H(82C)	109.5	C(96)-C(99)-H(99A)	109.5
H(82A)-C(82)-H(82C)	109.5	C(96)-C(99)-H(99B)	109.5
H(82B)-C(82)-H(82C)	109.5	H(99A)-C(99)-H(99B)	109.5
C(81)-C(83)-H(83A)	109.5	C(96)-C(99)-H(99C)	109.5
C(81)-C(83)-H(83B)	109.5	H(99A)-C(99)-H(99C)	109.5
H(83A)-C(83)-H(83B)	109.5	H(99B)-C(99)-H(99C)	109.5
C(81)-C(83)-H(83C)	109.5	C(97)-C(100)-H(10A)	109.5
H(83A)-C(83)-H(83C)	109.5	C(97)-C(100)-H(10B)	109.5
H(83B)-C(83)-H(83C)	109.5	H(10A)-C(100)-H(10B)	109.5
O(9)-C(91)-C(92)	120.3(6)	C(97)-C(100)-H(10C)	109.5
O(9)-C(91)-C(96)	118.7(6)	H(10A)-C(100)-H(10C)	109.5
C(92)-C(91)-C(96)	121.0(6)	H(10B)-C(100)-H(10C)	109.5
C(91)-C(92)-C(93)	118.9(6)	O(10)-C(101)-C(102)	119.9(6)
C(91)-C(92)-C(97)	119.4(6)	O(10)-C(101)-C(106)	120.8(7)
C(93)-C(92)-C(97)	121.4(6)	C(102)-C(101)-C(106)	119.3(7)
C(92)-C(93)-C(94)	121.9(7)	C(103)-C(102)-C(101)	120.1(6)
C(92)-C(93)-H(93)	119.1	C(103)-C(102)-C(107)	123.0(7)
C(94)-C(93)-H(93)	119.1	C(101)-C(102)-C(107)	116.9(6)
C(95)-C(94)-C(93)	117.8(6)	C(102)-C(103)-C(104)	122.6(7)
C(95)-C(94)-C(98)	120.9(7)	C(102)-C(103)-H(103)	118.7
C(93)-C(94)-C(98)	121.4(7)	C(104)-C(103)-H(103)	118.7
C(96)-C(95)-C(94)	122.9(7)	C(105)-C(104)-C(103)	116.7(7)
C(96)-C(95)-H(95)	118.6	C(105)-C(104)-C(108)	122.7(7)
C(94)-C(95)-H(95)	118.6	C(103)-C(104)-C(108)	120.6(8)
C(95)-C(96)-C(91)	117.5(7)	C(104)-C(105)-C(106)	123.3(7)
C(95)-C(96)-C(99)	122.4(7)	C(104)-C(105)-H(105)	118.3
C(91)-C(96)-C(99)	120.0(6)	C(106)-C(105)-H(105)	118.3
N(12)-C(97)-C(100)	114.8(5)	C(105)-C(106)-C(101)	117.9(7)
N(12)-C(97)-C(92)	113.3(5)	C(105)-C(106)-C(109)	123.4(7)
C(100)-C(97)-C(92)	111.8(6)	C(101)-C(106)-C(109)	118.7(7)
N(12)-C(97)-H(97)	105.3	N(12)-C(107)-C(102)	113.3(5)
C(100)-C(97)-H(97)	105.3	N(12)-C(107)-H(10D)	108.9
C(92)-C(97)-H(97)	105.3	C(102)-C(107)-H(10D)	108.9
C(94)-C(98)-H(98A)	109.5	N(12)-C(107)-H(10E)	108.9
C(94)-C(98)-H(98B)	109.5	C(102)-C(107)-H(10E)	108.9
H(98A)-C(98)-H(98B)	109.5	H(10D)-C(107)-H(10E)	107.7
C(94)-C(98)-H(98C)	109.5	C(104)-C(108)-H(10F)	109.5
H(98A)-C(98)-H(98C)	109.5	C(104)-C(108)-H(10G)	109.5

Table 76 (cont)

Bond	Angle /°	Bond	Angle /°
H(10F)-C(108)-H(10G)	109.5	H(11D)-C(118)-H(11E)	109.5
C(104)-C(108)-H(10H)	109.5	C(116)-C(119)-H(11F)	109.5
H(10F)-C(108)-H(10H)	109.5	C(116)-C(119)-H(11G)	109.5
H(10G)-C(108)-H(10H)	109.5	H(11F)-C(119)-H(11G)	109.5
C(106)-C(109)-H(10I)	109.5	C(116)-C(119)-H(11H)	109.5
C(106)-C(109)-H(10J)	109.5	H(11F)-C(119)-H(11H)	109.5
H(10I)-C(109)-H(10J)	109.5	H(11G)-C(119)-H(11H)	109.5
C(106)-C(109)-H(10K)	109.5	O(12)-C(121)-C(123)	109.0(7)
H(10I)-C(109)-H(10K)	109.5	O(12)-C(121)-C(122)	108.8(6)
H(10J)-C(109)-H(10K)	109.5	C(123)-C(121)-C(122)	111.6(7)
O(11)-C(111)-C(112)	120.8(6)	O(12)-C(121)-H(121)	109.2
O(11)-C(111)-C(116)	119.5(6)	C(123)-C(121)-H(121)	109.2
C(112)-C(111)-C(116)	119.7(6)	C(122)-C(121)-H(121)	109.2
C(113)-C(112)-C(111)	120.7(6)	C(121)-C(122)-H(12A)	109.5
C(113)-C(112)-C(117)	120.7(6)	C(121)-C(122)-H(12B)	109.5
C(111)-C(112)-C(117)	118.3(6)	H(12A)-C(122)-H(12B)	109.5
C(112)-C(113)-C(114)	119.7(7)	C(121)-C(122)-H(12C)	109.5
C(112)-C(113)-H(113)	120.1	H(12A)-C(122)-H(12C)	109.5
C(114)-C(113)-H(113)	120.2	H(12B)-C(122)-H(12C)	109.5
C(115)-C(114)-C(113)	119.0(7)	C(121)-C(123)-H(12D)	109.5
C(115)-C(114)-C(118)	122.2(7)	C(121)-C(123)-H(12E)	109.5
C(113)-C(114)-C(118)	118.8(7)	H(12D)-C(123)-H(12E)	109.5
C(114)-C(115)-C(116)	123.1(7)	C(121)-C(123)-H(12F)	109.5
C(114)-C(115)-H(115)	118.5	H(12D)-C(123)-H(12F)	109.5
C(116)-C(115)-H(115)	118.5	H(12E)-C(123)-H(12F)	109.5
C(115)-C(116)-C(111)	117.8(6)	C(142)-C(141)-O(14)	121.6(11)
C(115)-C(116)-C(119)	122.0(6)	C(142)-C(141)-C(143)	123.1(10)
C(111)-C(116)-C(119)	120.2(6)	O(14)-C(141)-C(143)	114.3(9)
C(112)-C(117)-N(12)	114.6(5)	C(142)-C(141)-H(141)	93.3
C(112)-C(117)-H(11A)	108.6	O(14)-C(141)-H(141)	93.3
N(12)-C(117)-H(11A)	108.6	C(143)-C(141)-H(141)	93.3
C(112)-C(117)-H(11B)	108.6	C(141)-C(142)-H(14A)	109.5
N(12)-C(117)-H(11B)	108.6	C(141)-C(142)-H(14B)	109.5
H(11A)-C(117)-H(11B)	107.6	H(14A)-C(142)-H(14B)	109.5
C(114)-C(118)-H(11C)	109.5	C(141)-C(142)-H(14C)	109.5
C(114)-C(118)-H(11D)	109.5	H(14A)-C(142)-H(14C)	109.5
H(11C)-C(118)-H(11D)	109.5	H(14B)-C(142)-H(14C)	109.5
C(114)-C(118)-H(11E)	109.5	C(141)-C(143)-H(14D)	109.5
H(11C)-C(118)-H(11E)	109.5	C(141)-C(143)-H(14E)	109.5

Table 76 (cont)

Bond	Angle /°	Bond	Angle /°
H(14D)-C(143)-H(14E)	109.5	C(151)-C(152)-H(15B)	109.5
C(141)-C(143)-H(14F)	109.5	H(15A)-C(152)-H(15B)	109.5
H(14D)-C(143)-H(14F)	109.5	C(151)-C(152)-H(15C)	109.5
H(14E)-C(143)-H(14F)	109.5	H(15A)-C(152)-H(15C)	109.5
O(15)-C(151)-C(153)	110.7(8)	H(15B)-C(152)-H(15C)	109.5
O(15)-C(151)-C(152)	107.2(9)	C(151)-C(153)-H(15D)	109.5
C(153)-C(151)-C(152)	113.5(9)	C(151)-C(153)-H(15E)	109.5
O(15)-C(151)-H(151)	108.5	H(15D)-C(153)-H(15E)	109.5
C(153)-C(151)-H(151)	108.5	C(151)-C(153)-H(15F)	109.5
C(152)-C(151)-H(151)	108.5	H(15D)-C(153)-H(15F)	109.5
C(151)-C(152)-H(15A)	109.5	H(15E)-C(153)-H(15F)	109.5

Table 77. Anisotropic displacement parameters ($\text{\AA}^2 \times 10^3$) for (R,M)-**271**. The anisotropic displacement factor exponent takes the form: $-2\pi^2 [h^2 a^{*2} U^{11} + \dots + 2 h k a^* b^* U^{12}]$

	U^{11}	U^{22}	U^{33}	U^{23}	U^{13}	U^{12}
Ti(1)	49(1)	47(1)	39(1)	-1(1)	14(1)	5(1)
Ti(2)	26(1)	35(1)	23(1)	-2(1)	5(1)	1(1)
Ti(3)	26(1)	37(1)	20(1)	0(1)	4(1)	0(1)
Ti(4)	27(1)	45(1)	23(1)	6(1)	2(1)	-1(1)
O(1)	57(4)	50(3)	48(3)	-7(3)	14(3)	-4(3)
O(2)	60(4)	51(3)	46(3)	2(2)	11(3)	16(3)
O(3)	79(4)	70(4)	29(3)	-6(3)	20(3)	2(3)
O(4)	49(4)	88(5)	72(5)	-5(4)	23(3)	1(3)
O(5)	23(2)	47(3)	36(3)	-9(2)	6(2)	-4(2)
O(6)	27(2)	45(3)	24(2)	2(2)	7(2)	1(2)
O(7)	21(2)	41(2)	27(2)	3(2)	7(2)	1(2)
O(8)	38(3)	42(3)	37(3)	2(2)	18(2)	8(2)
O(9)	27(2)	44(3)	26(2)	-7(2)	9(2)	-4(2)
O(10)	28(2)	49(3)	17(2)	1(2)	0(2)	-4(2)
O(11)	24(2)	41(2)	26(3)	5(2)	4(2)	2(2)
O(12)	21(2)	49(3)	29(3)	-6(2)	5(2)	-1(2)
O(13)	26(2)	35(2)	21(2)	1(2)	3(2)	0(2)
O(14)	20(2)	54(3)	66(4)	11(3)	-3(2)	5(2)
O(15)	61(3)	89(4)	17(2)	2(3)	7(2)	-28(3)
N(1)	49(4)	38(3)	19(3)	-1(2)	2(3)	3(3)
N(12)	26(3)	35(3)	22(3)	2(2)	3(2)	-1(2)
N(26)	32(3)	43(3)	14(3)	-2(2)	5(2)	0(2)
C(1)	57(5)	39(4)	33(4)	1(3)	12(4)	3(3)
C(2)	77(6)	45(4)	22(4)	2(3)	1(4)	-2(4)
C(3)	49(5)	42(4)	33(4)	-2(3)	-7(3)	-1(3)
C(4)	57(17)	85(19)	150(30)	-20(20)	6(18)	4(14)
C(4')	100(20)	38(13)	45(16)	-5(10)	65(17)	8(12)
C(4'')	37(18)	80(20)	90(30)	7(19)	-36(17)	-25(15)
C(5)	55(7)	138(12)	99(10)	-22(9)	8(6)	-7(7)
C(6)	97(12)	110(12)	350(30)	37(16)	124(17)	-3(9)
C(7)	62(8)	169(15)	133(14)	23(11)	6(8)	28(9)
C(11)	97(7)	35(4)	31(4)	3(3)	2(4)	-1(4)
C(12)	90(7)	30(3)	33(4)	-1(3)	27(4)	1(4)
C(13)	124(9)	41(4)	55(6)	-4(4)	57(6)	-5(5)
C(14)	164(12)	36(4)	31(5)	-9(3)	37(6)	-5(6)
C(15)	144(12)	50(5)	31(5)	-3(4)	4(6)	-13(6)
C(16)	86(7)	36(4)	41(5)	7(3)	-9(5)	-5(4)
C(17)	280(20)	69(7)	50(7)	-22(5)	82(10)	-29(10)
C(18)	82(8)	67(6)	81(8)	-2(5)	-37(6)	-2(5)

Table 77 (cont)

	U^{11}	U^{22}	U^{33}	U^{23}	U^{13}	U^{12}
C(21)	54(5)	43(4)	30(4)	0(3)	-8(3)	4(3)
C(22)	63(5)	44(4)	14(3)	2(3)	-9(3)	6(3)
C(23)	81(6)	43(4)	30(4)	0(3)	0(4)	-4(4)
C(24)	78(6)	47(4)	24(4)	4(3)	-6(4)	1(4)
C(25)	101(8)	35(4)	31(4)	-4(3)	-18(5)	8(4)
C(26)	63(5)	59(5)	26(4)	0(3)	-12(4)	19(4)
C(27)	114(9)	44(5)	50(6)	4(4)	-6(6)	-12(5)
C(28)	115(10)	58(6)	76(8)	2(5)	22(7)	32(6)
C(31)	70(6)	48(4)	29(4)	-6(3)	-11(4)	12(4)
C(32)	58(5)	41(4)	39(4)	0(3)	0(4)	3(3)
C(33)	65(6)	62(5)	43(5)	-6(4)	-14(4)	10(4)
C(34)	89(8)	56(5)	49(6)	2(4)	-15(5)	20(5)
C(35)	113(9)	47(5)	31(5)	4(4)	-10(5)	13(5)
C(36)	113(9)	50(5)	35(5)	-2(4)	23(5)	-2(5)
C(37)	140(12)	97(9)	64(8)	5(6)	-55(8)	41(8)
C(38)	155(12)	70(7)	50(6)	-7(5)	45(7)	-3(7)
C(51)	30(3)	49(4)	22(4)	-1(3)	1(3)	-3(3)
C(52)	32(3)	50(4)	16(3)	-6(3)	2(3)	-5(3)
C(53)	45(4)	49(4)	24(4)	-4(3)	8(3)	-10(3)
C(54)	49(4)	50(4)	31(4)	-2(3)	7(3)	-13(3)
C(55)	57(5)	41(4)	32(4)	-6(3)	-1(4)	-9(3)
C(56)	31(4)	53(4)	24(4)	-2(3)	-3(3)	-3(3)
C(57)	25(3)	50(4)	16(3)	1(3)	-3(2)	-4(3)
C(58)	109(9)	58(5)	59(6)	-6(4)	26(6)	-32(5)
C(59)	48(5)	49(5)	71(6)	-13(4)	17(4)	3(4)
C(60)	45(4)	49(4)	39(4)	-1(3)	6(3)	-4(3)
C(61)	43(4)	27(3)	23(3)	1(2)	6(3)	0(3)
C(62)	32(3)	33(3)	24(3)	-2(2)	11(3)	-5(2)
C(63)	34(3)	35(3)	36(4)	1(3)	11(3)	3(3)
C(64)	40(4)	36(3)	28(4)	1(3)	-1(3)	3(3)
C(65)	37(4)	47(4)	17(3)	4(3)	-2(3)	-6(3)
C(66)	36(4)	39(3)	19(3)	-3(2)	4(3)	-5(3)
C(67)	22(3)	43(3)	26(3)	-8(3)	11(3)	1(2)
C(68)	34(4)	65(5)	39(4)	9(4)	4(3)	10(3)
C(69)	34(4)	55(4)	22(4)	-3(3)	4(3)	-6(3)
C(71)	14(3)	58(4)	11(3)	-3(3)	7(2)	-5(2)
C(72)	16(3)	56(4)	25(4)	-5(3)	5(3)	-6(3)
C(73)	26(3)	59(4)	26(4)	2(3)	5(3)	-3(3)
C(74)	23(3)	70(5)	33(4)	2(3)	4(3)	-4(3)
C(75)	37(4)	54(4)	32(4)	12(3)	5(3)	-4(3)

Table 77 (cont)

	U^{11}	U^{22}	U^{33}	U^{23}	U^{13}	U^{12}
C(76)	29(3)	50(4)	32(4)	1(3)	4(3)	-2(3)
C(77)	20(3)	49(4)	24(3)	-2(3)	5(3)	0(2)
C(78)	48(5)	94(7)	59(6)	26(5)	11(4)	-8(5)
C(79)	41(4)	54(5)	63(6)	15(4)	13(4)	8(3)
C(81)	80(7)	51(5)	103(9)	-20(5)	59(7)	-3(5)
C(82)	90(10)	270(20)	56(8)	-75(10)	-18(7)	72(12)
C(83)	64(7)	124(10)	87(8)	2(7)	38(6)	38(6)
C(91)	33(4)	41(4)	23(3)	2(3)	4(3)	-4(3)
C(92)	35(4)	38(3)	20(3)	-1(2)	5(3)	-6(3)
C(93)	45(4)	39(4)	36(4)	2(3)	16(3)	3(3)
C(94)	26(3)	47(4)	35(4)	-1(3)	-7(3)	6(3)
C(95)	45(4)	48(4)	33(4)	-3(3)	4(3)	-2(3)
C(96)	43(4)	38(3)	25(4)	-3(3)	3(3)	-5(3)
C(97)	32(3)	39(3)	25(4)	0(3)	4(3)	2(3)
C(98)	44(5)	68(6)	65(6)	-23(5)	-10(4)	5(4)
C(99)	56(5)	70(5)	39(5)	-17(4)	19(4)	-17(4)
C(100)	42(4)	52(4)	39(4)	0(3)	14(3)	-8(3)
C(101)	36(4)	39(4)	25(4)	6(3)	-3(3)	-3(3)
C(102)	43(4)	29(3)	29(4)	3(3)	4(3)	-2(3)
C(103)	26(3)	45(4)	28(4)	2(3)	0(3)	-1(3)
C(104)	34(4)	45(4)	37(4)	4(3)	-9(3)	2(3)
C(105)	40(4)	57(5)	26(4)	2(3)	-5(3)	-2(3)
C(106)	40(4)	64(5)	14(3)	2(3)	0(3)	-2(3)
C(107)	28(3)	38(3)	28(4)	3(3)	7(3)	0(3)
C(108)	38(4)	78(6)	46(5)	-5(4)	-10(4)	0(4)
C(109)	41(5)	109(7)	24(4)	-5(4)	2(3)	-4(4)
C(111)	35(4)	38(3)	21(3)	1(3)	-1(3)	-5(3)
C(112)	27(3)	44(3)	17(3)	-1(2)	2(3)	-2(2)
C(113)	40(4)	47(4)	25(4)	0(3)	6(3)	-2(3)
C(114)	47(4)	59(5)	27(4)	11(3)	8(3)	3(3)
C(115)	38(4)	55(4)	32(4)	12(3)	0(3)	3(3)
C(116)	31(3)	40(4)	27(4)	6(3)	1(3)	-2(3)
C(117)	36(4)	38(3)	22(3)	-5(3)	11(3)	-1(3)
C(118)	70(6)	94(7)	31(5)	21(4)	19(4)	11(5)
C(119)	32(4)	42(4)	38(4)	3(3)	-1(3)	1(3)
C(121)	36(4)	53(4)	44(5)	-14(3)	14(3)	1(3)
C(122)	63(6)	76(6)	67(6)	-7(5)	14(5)	31(5)
C(123)	59(6)	102(8)	41(5)	-19(5)	15(4)	9(5)
C(141)	114(11)	94(9)	114(11)	-29(8)	-59(9)	70(8)
C(142)	82(8)	92(8)	101(10)	6(7)	0(7)	37(7)

Table 77 (cont)

	U^{11}	U^{22}	U^{33}	U^{23}	U^{13}	U^{12}
C(143)	38(4)	71(6)	67(6)	27(5)	7(4)	8(4)
C(151)	59(6)	120(8)	25(4)	8(5)	19(4)	-10(5)
C(152)	58(6)	164(13)	74(8)	9(7)	43(6)	24(7)
C(153)	137(12)	139(11)	63(8)	37(8)	69(8)	25(9)

7.3 CRYSTAL STRUCTURE DATA FOR (R,M)-287

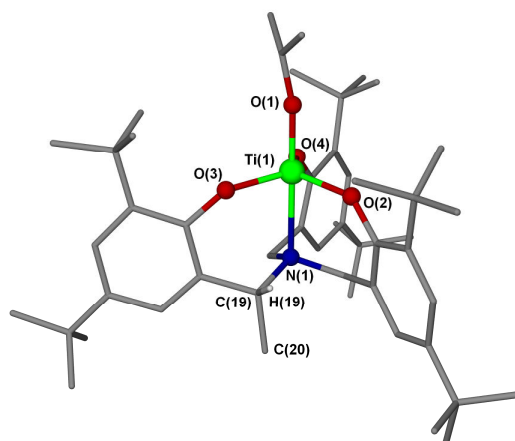


Figure 65. Crystal structure of (R,M)-287

Table 78. Crystal data and structural refinement

Empirical formula	C ₅₅ H ₈₉ NO ₄ Ti	
Formula weight	876.17	
Temperature	150(2) K	
Wavelength	0.71073 Å	
Crystal system	Tetragonal	
Space group	P4 ₃	
Unit cell dimensions	a = 14.5840(2) Å	α = 90°
	b = 14.5840(2) Å	β = 90°
	c = 25.3740(4) Å	γ = 90°
Volume	5396.87(13) Å ³	
Z	4	
Density (calculated)	1.078 Mg/m ³	
Absorption coefficient	0.200 mm ⁻¹	
F(000)	1920	
Crystal size	0.40 x 0.30 x 0.25 mm ³	
Theta range for data collection	3.69 to 27.48°	
Index ranges	-18 ≤ h ≤ 15, -18 ≤ k ≤ 14, -30 ≤ l ≤ 32	
Reflections collected	21199	
Independent reflections	11331 [R(int) = 0.0279]	
Completeness to theta = 27.48°	98.6 %	
Max. and min. transmission	0.9517 and 0.9243	
Refinement method	Full-matrix least-squares on F ²	
Data / restraints / parameters	11331 / 1 / 573	
Goodness-of-fit on F ²	1.024	
Final R indices [I > 2σ(I)]	R1 = 0.0560, wR2 = 0.1464	
R indices (all data)	R1 = 0.0709, wR2 = 0.1578	

Absolute structure parameter	0.02(3)
Largest diff. peak and hole	0.531 and -0.371 e.Å ⁻³

Table 79. Atomic coordinates ($\times 10^4$) and equivalent isotropic displacement parameters ($\text{\AA}^2 \times 10^3$)

	x	y	z	U(eq) ⁷
Ti(1)	2536(1)	7502(1)	7499(1)	26(1)
O(1)	1607(1)	7231(1)	7068(1)	35(1)
N(1)	3757(1)	7872(1)	8066(1)	26(1)
C(1)	813(4)	7183(6)	6780(2)	125(3)
O(2)	3467(1)	7447(1)	7006(1)	33(1)
C(2)	119(3)	6564(4)	7001(2)	73(1)
O(3)	2140(1)	8652(1)	7684(1)	34(1)
C(3)	819(3)	7397(4)	6254(2)	76(1)
O(4)	2364(1)	6556(1)	7974(1)	35(1)
C(4)	4347(2)	7716(2)	6919(1)	29(1)
C(5)	4939(2)	7713(2)	7353(1)	30(1)
C(6)	5846(2)	7991(2)	7287(1)	32(1)
C(7)	6182(2)	8265(2)	6797(1)	35(1)
C(8)	5564(2)	8239(2)	6373(1)	33(1)
C(9)	4654(2)	7972(2)	6417(1)	30(1)
C(10)	4006(2)	7949(2)	5938(1)	34(1)
C(11)	3235(2)	8640(3)	6009(1)	46(1)
C(12)	3628(2)	6975(2)	5868(1)	45(1)
C(13)	4512(2)	8202(2)	5425(1)	41(1)
C(14)	7166(2)	8588(2)	6716(1)	43(1)
C(15)	7726(3)	8566(5)	7217(2)	91(2)
C(16)	7160(3)	9575(3)	6495(2)	54(1)
C(17)	7636(3)	7963(3)	6302(2)	63(1)
C(18)	4591(2)	7384(2)	7874(1)	31(1)
C(19)	3905(2)	8899(2)	8064(1)	30(1)
C(20)	4817(2)	9192(2)	8317(1)	40(1)
C(21)	2220(2)	9259(2)	8090(1)	29(1)
C(22)	3087(2)	9385(2)	8312(1)	29(1)
C(23)	3179(2)	9963(2)	8745(1)	32(1)
C(24)	2426(2)	10436(2)	8954(1)	32(1)
C(25)	1585(2)	10320(2)	8714(1)	31(1)
C(26)	1444(2)	9728(2)	8282(1)	30(1)
C(27)	495(2)	9614(2)	8029(1)	34(1)
C(28)	156(2)	8626(2)	8106(2)	48(1)

⁷ U(eq) is defined as one third of the trace of the orthogonalized U_{ij} tensor.

Table 79 (cont)

	x	y	z	U(eq)
C(29)	541(2)	9845(2)	7437(1)	43(1)
C(30)	-217(2)	10254(2)	8278(1)	44(1)
C(31)	2568(2)	11050(2)	9438(1)	36(1)
C(32)	2819(4)	10415(3)	9908(2)	82(2)
C(33)	1715(3)	11593(3)	9582(2)	71(1)
C(34)	3346(3)	11704(3)	9339(2)	74(1)
C(35)	3552(2)	7549(2)	8608(1)	31(1)
C(36)	2832(2)	6069(2)	8339(1)	32(1)
C(37)	3477(2)	6521(2)	8651(1)	30(1)
C(38)	4028(2)	6037(2)	8995(1)	33(1)
C(39)	3933(2)	5093(2)	9061(1)	37(1)
C(40)	3231(2)	4664(2)	8766(1)	37(1)
C(41)	2677(2)	5117(2)	8410(1)	32(1)
C(42)	1902(2)	4622(2)	8113(1)	37(1)
C(43)	979(2)	5072(3)	8233(2)	48(1)
C(44)	1829(2)	3605(2)	8288(2)	47(1)
C(45)	2084(3)	4623(2)	7515(2)	50(1)
C(46)	4540(2)	4534(2)	9431(2)	44(1)
C(47)	5259(4)	5113(3)	9711(3)	93(2)
C(48)	5012(3)	3758(4)	9128(2)	82(1)
C(49)	3932(3)	4105(3)	9875(2)	60(1)
C(50)	1229(4)	7623(4)	9267(2)	96(2)
C(51)	1595(4)	7124(4)	9716(2)	82(2)
C(52)	1330(4)	6127(4)	9702(2)	81(1)
C(53)	1600(4)	5516(4)	10143(2)	88(2)
C(54)	1375(5)	4558(4)	10127(3)	122(3)
C(55)	1571(6)	3946(5)	10542(4)	148(4)

Table 80. Bond lengths

Bond	Length /Å	Bond	Length /Å
Ti(1)-O(1)	1.7861(19)	C(12)-H(12B)	0.9800
Ti(1)-O(3)	1.836(2)	C(12)-H(12C)	0.9800
Ti(1)-O(2)	1.848(2)	C(13)-H(13A)	0.9800
Ti(1)-O(4)	1.848(2)	C(13)-H(13B)	0.9800
Ti(1)-N(1)	2.351(2)	C(13)-H(13C)	0.9800
O(1)-C(1)	1.371(4)	C(14)-C(15)	1.511(5)
N(1)-C(35)	1.486(3)	C(14)-C(16)	1.545(5)
N(1)-C(18)	1.491(3)	C(14)-C(17)	1.552(5)
N(1)-C(19)	1.513(3)	C(15)-H(15A)	0.9800
C(1)-C(3)	1.372(7)	C(15)-H(15B)	0.9800
C(1)-C(2)	1.467(6)	C(15)-H(15C)	0.9800
C(1)-H(1)	1.0000	C(16)-H(16A)	0.9800
O(2)-C(4)	1.360(3)	C(16)-H(16B)	0.9800
C(2)-H(2A)	0.9800	C(16)-H(16C)	0.9800
C(2)-H(2B)	0.9800	C(17)-H(17A)	0.9800
C(2)-H(2C)	0.9800	C(17)-H(17B)	0.9800
O(3)-C(21)	1.363(3)	C(17)-H(17C)	0.9800
C(3)-H(3A)	0.9800	C(18)-H(18A)	0.9900
C(3)-H(3B)	0.9800	C(18)-H(18B)	0.9900
C(3)-H(3C)	0.9800	C(19)-C(22)	1.522(4)
O(4)-C(36)	1.353(3)	C(19)-C(20)	1.538(4)
C(4)-C(5)	1.398(4)	C(19)-H(19)	1.0000
C(4)-C(9)	1.401(4)	C(20)-H(20A)	0.9800
C(5)-C(6)	1.394(4)	C(20)-H(20B)	0.9800
C(5)-C(18)	1.496(4)	C(20)-H(20C)	0.9800
C(6)-C(7)	1.396(4)	C(21)-C(22)	1.396(4)
C(6)-H(6)	0.9500	C(21)-C(26)	1.409(4)
C(7)-C(8)	1.404(4)	C(22)-C(23)	1.391(4)
C(7)-C(14)	1.525(4)	C(23)-C(24)	1.402(4)
C(8)-C(9)	1.389(4)	C(23)-H(23)	0.9500
C(8)-H(8)	0.9500	C(24)-C(25)	1.380(4)
C(9)-C(10)	1.541(4)	C(24)-C(31)	1.533(4)
C(10)-C(11)	1.522(4)	C(25)-C(26)	1.409(4)
C(10)-C(12)	1.533(4)	C(25)-H(25)	0.9500
C(10)-C(13)	1.541(4)	C(26)-C(27)	1.535(4)
C(11)-H(11A)	0.9800	C(27)-C(30)	1.532(4)
C(11)-H(11B)	0.9800	C(27)-C(28)	1.536(4)
C(11)-H(11C)	0.9800	C(27)-C(29)	1.541(5)
C(12)-H(12A)	0.9800	C(28)-H(28A)	0.9800

Table 80 (cont)

Bond	Length /Å	Bond	Length /Å
C(28)-H(28B)	0.9800	C(43)-H(43C)	0.9800
C(28)-H(28C)	0.9800	C(44)-H(44A)	0.9800
C(29)-H(29A)	0.9800	C(44)-H(44B)	0.9800
C(29)-H(29B)	0.9800	C(44)-H(44C)	0.9800
C(29)-H(29C)	0.9800	C(45)-H(45A)	0.9800
C(30)-H(30A)	0.9800	C(45)-H(45B)	0.9800
C(30)-H(30B)	0.9800	C(45)-H(45C)	0.9800
C(30)-H(30C)	0.9800	C(46)-C(47)	1.523(5)
C(31)-C(34)	1.504(5)	C(46)-C(48)	1.532(6)
C(31)-C(33)	1.519(5)	C(46)-C(49)	1.566(6)
C(31)-C(32)	1.554(5)	C(47)-H(47A)	0.9800
C(32)-H(32A)	0.9800	C(47)-H(47B)	0.9800
C(32)-H(32B)	0.9800	C(47)-H(47C)	0.9800
C(32)-H(32C)	0.9800	C(48)-H(48A)	0.9800
C(33)-H(33A)	0.9800	C(48)-H(48B)	0.9800
C(33)-H(33B)	0.9800	C(48)-H(48C)	0.9800
C(33)-H(33C)	0.9800	C(49)-H(49A)	0.9800
C(34)-H(34A)	0.9800	C(49)-H(49B)	0.9800
C(34)-H(34B)	0.9800	C(49)-H(49C)	0.9800
C(34)-H(34C)	0.9800	C(50)-C(51)	1.452(8)
C(35)-C(37)	1.507(4)	C(50)-H(50A)	0.9800
C(35)-H(35A)	0.9900	C(50)-H(50B)	0.9800
C(35)-H(35B)	0.9900	C(50)-H(50C)	0.9800
C(36)-C(37)	1.394(4)	C(51)-C(52)	1.505(7)
C(36)-C(41)	1.419(4)	C(51)-H(51A)	0.9900
C(37)-C(38)	1.381(4)	C(51)-H(51B)	0.9900
C(38)-C(39)	1.393(4)	C(52)-C(53)	1.484(7)
C(38)-H(38)	0.9500	C(52)-H(52A)	0.9900
C(39)-C(40)	1.416(4)	C(52)-H(52B)	0.9900
C(39)-C(46)	1.526(4)	C(53)-C(54)	1.435(9)
C(40)-C(41)	1.380(4)	C(53)-H(53A)	0.9900
C(40)-H(40)	0.9500	C(53)-H(53B)	0.9900
C(41)-C(42)	1.538(4)	C(54)-C(55)	1.410(10)
C(42)-C(43)	1.528(5)	C(54)-H(54A)	0.9900
C(42)-C(45)	1.540(5)	C(54)-H(54B)	0.9900
C(42)-C(44)	1.552(4)	C(55)-H(55A)	0.9800
C(43)-H(43A)	0.9800	C(55)-H(55B)	0.9800
C(43)-H(43B)	0.9800	C(55)-H(55C)	0.9800

Table 81. Bond angles

Bond	Angle /°	Bond	Angle /°
O(1)-Ti(1)-O(3)	96.90(9)	O(2)-C(4)-C(9)	121.7(2)
O(1)-Ti(1)-O(2)	97.67(10)	C(5)-C(4)-C(9)	121.3(2)
O(3)-Ti(1)-O(2)	116.35(10)	C(6)-C(5)-C(4)	119.4(3)
O(1)-Ti(1)-O(4)	97.52(9)	C(6)-C(5)-C(18)	121.4(2)
O(3)-Ti(1)-O(4)	118.19(10)	C(4)-C(5)-C(18)	119.2(2)
O(2)-Ti(1)-O(4)	120.60(10)	C(5)-C(6)-C(7)	121.5(3)
O(1)-Ti(1)-N(1)	179.51(9)	C(5)-C(6)-H(6)	119.2
O(3)-Ti(1)-N(1)	82.64(8)	C(7)-C(6)-H(6)	119.2
O(2)-Ti(1)-N(1)	82.40(8)	C(6)-C(7)-C(8)	116.8(2)
O(4)-Ti(1)-N(1)	82.84(8)	C(6)-C(7)-C(14)	122.5(3)
C(1)-O(1)-Ti(1)	168.1(4)	C(8)-C(7)-C(14)	120.6(3)
C(35)-N(1)-C(18)	108.4(2)	C(9)-C(8)-C(7)	123.9(3)
C(35)-N(1)-C(19)	110.1(2)	C(9)-C(8)-H(8)	118.0
C(18)-N(1)-C(19)	110.8(2)	C(7)-C(8)-H(8)	118.0
C(35)-N(1)-Ti(1)	109.99(15)	C(8)-C(9)-C(4)	117.0(3)
C(18)-N(1)-Ti(1)	107.98(16)	C(8)-C(9)-C(10)	121.9(3)
C(19)-N(1)-Ti(1)	109.52(15)	C(4)-C(9)-C(10)	121.1(2)
C(3)-C(1)-O(1)	120.1(4)	C(11)-C(10)-C(12)	111.2(3)
C(3)-C(1)-C(2)	121.1(4)	C(11)-C(10)-C(13)	107.2(3)
O(1)-C(1)-C(2)	114.2(4)	C(12)-C(10)-C(13)	107.2(3)
C(3)-C(1)-H(1)	97.2	C(11)-C(10)-C(9)	110.2(2)
O(1)-C(1)-H(1)	97.2	C(12)-C(10)-C(9)	109.4(2)
C(2)-C(1)-H(1)	97.2	C(13)-C(10)-C(9)	111.6(2)
C(4)-O(2)-Ti(1)	142.24(18)	C(10)-C(11)-H(11A)	109.5
C(1)-C(2)-H(2A)	109.5	C(10)-C(11)-H(11B)	109.5
C(1)-C(2)-H(2B)	109.5	H(11A)-C(11)-H(11B)	109.5
H(2A)-C(2)-H(2B)	109.5	C(10)-C(11)-H(11C)	109.5
C(1)-C(2)-H(2C)	109.5	H(11A)-C(11)-H(11C)	109.5
H(2A)-C(2)-H(2C)	109.5	H(11B)-C(11)-H(11C)	109.5
H(2B)-C(2)-H(2C)	109.5	C(10)-C(12)-H(12A)	109.5
C(21)-O(3)-Ti(1)	139.43(18)	C(10)-C(12)-H(12B)	109.5
C(1)-C(3)-H(3A)	109.5	H(12A)-C(12)-H(12B)	109.5
C(1)-C(3)-H(3B)	109.5	C(10)-C(12)-H(12C)	109.5
H(3A)-C(3)-H(3B)	109.5	H(12A)-C(12)-H(12C)	109.5
C(1)-C(3)-H(3C)	109.5	H(12B)-C(12)-H(12C)	109.5
H(3A)-C(3)-H(3C)	109.5	C(10)-C(13)-H(13A)	109.5
H(3B)-C(3)-H(3C)	109.5	C(10)-C(13)-H(13B)	109.5
C(36)-O(4)-Ti(1)	140.38(18)	H(13A)-C(13)-H(13B)	109.5
O(2)-C(4)-C(5)	117.0(2)	C(10)-C(13)-H(13C)	109.5

Table 81 (cont)

Bond	Angle /°	Bond	Angle /°
H(13A)-C(13)-H(13C)	109.5	C(19)-C(20)-H(20B)	109.5
H(13B)-C(13)-H(13C)	109.5	H(20A)-C(20)-H(20B)	109.5
C(15)-C(14)-C(7)	112.9(3)	C(19)-C(20)-H(20C)	109.5
C(15)-C(14)-C(16)	109.3(4)	H(20A)-C(20)-H(20C)	109.5
C(7)-C(14)-C(16)	109.3(3)	H(20B)-C(20)-H(20C)	109.5
C(15)-C(14)-C(17)	108.5(4)	O(3)-C(21)-C(22)	117.9(2)
C(7)-C(14)-C(17)	109.0(3)	O(3)-C(21)-C(26)	120.5(2)
C(16)-C(14)-C(17)	107.7(3)	C(22)-C(21)-C(26)	121.6(3)
C(14)-C(15)-H(15A)	109.5	C(23)-C(22)-C(21)	119.0(3)
C(14)-C(15)-H(15B)	109.5	C(23)-C(22)-C(19)	122.2(2)
H(15A)-C(15)-H(15B)	109.5	C(21)-C(22)-C(19)	118.8(2)
C(14)-C(15)-H(15C)	109.5	C(22)-C(23)-C(24)	121.5(3)
H(15A)-C(15)-H(15C)	109.5	C(22)-C(23)-H(23)	119.2
H(15B)-C(15)-H(15C)	109.5	C(24)-C(23)-H(23)	119.2
C(14)-C(16)-H(16A)	109.5	C(25)-C(24)-C(23)	117.9(3)
C(14)-C(16)-H(16B)	109.5	C(25)-C(24)-C(31)	123.1(3)
H(16A)-C(16)-H(16B)	109.5	C(23)-C(24)-C(31)	119.1(3)
C(14)-C(16)-H(16C)	109.5	C(24)-C(25)-C(26)	123.2(3)
H(16A)-C(16)-H(16C)	109.5	C(24)-C(25)-H(25)	118.4
H(16B)-C(16)-H(16C)	109.5	C(26)-C(25)-H(25)	118.4
C(14)-C(17)-H(17A)	109.5	C(21)-C(26)-C(25)	116.7(2)
C(14)-C(17)-H(17B)	109.5	C(21)-C(26)-C(27)	121.8(3)
H(17A)-C(17)-H(17B)	109.5	C(25)-C(26)-C(27)	121.5(2)
C(14)-C(17)-H(17C)	109.5	C(30)-C(27)-C(28)	107.5(3)
H(17A)-C(17)-H(17C)	109.5	C(30)-C(27)-C(26)	111.9(2)
H(17B)-C(17)-H(17C)	109.5	C(28)-C(27)-C(26)	109.8(2)
N(1)-C(18)-C(5)	114.3(2)	C(30)-C(27)-C(29)	107.3(3)
N(1)-C(18)-H(18A)	108.7	C(28)-C(27)-C(29)	110.0(3)
C(5)-C(18)-H(18A)	108.7	C(26)-C(27)-C(29)	110.2(2)
N(1)-C(18)-H(18B)	108.7	C(27)-C(28)-H(28A)	109.5
C(5)-C(18)-H(18B)	108.7	C(27)-C(28)-H(28B)	109.5
H(18A)-C(18)-H(18B)	107.6	H(28A)-C(28)-H(28B)	109.5
N(1)-C(19)-C(22)	110.4(2)	C(27)-C(28)-H(28C)	109.5
N(1)-C(19)-C(20)	113.5(2)	H(28A)-C(28)-H(28C)	109.5
C(22)-C(19)-C(20)	112.1(2)	H(28B)-C(28)-H(28C)	109.5
N(1)-C(19)-H(19)	106.8	C(27)-C(29)-H(29A)	109.5
C(22)-C(19)-H(19)	106.8	C(27)-C(29)-H(29B)	109.5
C(20)-C(19)-H(19)	106.8	H(29A)-C(29)-H(29B)	109.5
C(19)-C(20)-H(20A)	109.5	C(27)-C(29)-H(29C)	109.5

Table 81 (cont)

Bond	Angle /°	Bond	Angle /°
H(29A)-C(29)-H(29C)	109.5	O(4)-C(36)-C(41)	121.4(3)
H(29B)-C(29)-H(29C)	109.5	C(37)-C(36)-C(41)	120.0(3)
C(27)-C(30)-H(30A)	109.5	C(38)-C(37)-C(36)	120.6(3)
C(27)-C(30)-H(30B)	109.5	C(38)-C(37)-C(35)	120.8(2)
H(30A)-C(30)-H(30B)	109.5	C(36)-C(37)-C(35)	118.6(3)
C(27)-C(30)-H(30C)	109.5	C(37)-C(38)-C(39)	121.6(3)
H(30A)-C(30)-H(30C)	109.5	C(37)-C(38)-H(38)	119.2
H(30B)-C(30)-H(30C)	109.5	C(39)-C(38)-H(38)	119.2
C(34)-C(31)-C(33)	109.1(3)	C(38)-C(39)-C(40)	116.4(3)
C(34)-C(31)-C(24)	109.8(3)	C(38)-C(39)-C(46)	123.0(3)
C(33)-C(31)-C(24)	112.8(3)	C(40)-C(39)-C(46)	120.6(3)
C(34)-C(31)-C(32)	109.2(4)	C(41)-C(40)-C(39)	124.0(3)
C(33)-C(31)-C(32)	108.6(4)	C(41)-C(40)-H(40)	118.0
C(24)-C(31)-C(32)	107.3(3)	C(39)-C(40)-H(40)	118.0
C(31)-C(32)-H(32A)	109.5	C(40)-C(41)-C(36)	117.2(3)
C(31)-C(32)-H(32B)	109.5	C(40)-C(41)-C(42)	121.8(3)
H(32A)-C(32)-H(32B)	109.5	C(36)-C(41)-C(42)	121.0(3)
C(31)-C(32)-H(32C)	109.5	C(43)-C(42)-C(41)	110.4(3)
H(32A)-C(32)-H(32C)	109.5	C(43)-C(42)-C(45)	110.3(3)
H(32B)-C(32)-H(32C)	109.5	C(41)-C(42)-C(45)	110.9(2)
C(31)-C(33)-H(33A)	109.5	C(43)-C(42)-C(44)	107.0(3)
C(31)-C(33)-H(33B)	109.5	C(41)-C(42)-C(44)	111.0(3)
H(33A)-C(33)-H(33B)	109.5	C(45)-C(42)-C(44)	107.1(3)
C(31)-C(33)-H(33C)	109.5	C(42)-C(43)-H(43A)	109.5
H(33A)-C(33)-H(33C)	109.5	C(42)-C(43)-H(43B)	109.5
H(33B)-C(33)-H(33C)	109.5	H(43A)-C(43)-H(43B)	109.5
C(31)-C(34)-H(34A)	109.5	C(42)-C(43)-H(43C)	109.5
C(31)-C(34)-H(34B)	109.5	H(43A)-C(43)-H(43C)	109.5
H(34A)-C(34)-H(34B)	109.5	H(43B)-C(43)-H(43C)	109.5
C(31)-C(34)-H(34C)	109.5	C(42)-C(44)-H(44A)	109.5
H(34A)-C(34)-H(34C)	109.5	C(42)-C(44)-H(44B)	109.5
H(34B)-C(34)-H(34C)	109.5	H(44A)-C(44)-H(44B)	109.5
N(1)-C(35)-C(37)	113.4(2)	C(42)-C(44)-H(44C)	109.5
N(1)-C(35)-H(35A)	108.9	H(44A)-C(44)-H(44C)	109.5
C(37)-C(35)-H(35A)	108.9	H(44B)-C(44)-H(44C)	109.5
N(1)-C(35)-H(35B)	108.9	C(42)-C(45)-H(45A)	109.5
C(37)-C(35)-H(35B)	108.9	C(42)-C(45)-H(45B)	109.5
H(35A)-C(35)-H(35B)	107.7	H(45A)-C(45)-H(45B)	109.5
O(4)-C(36)-C(37)	118.7(2)	C(42)-C(45)-H(45C)	109.5

Table 81 (cont)

Bond	Angle /°	Bond	Angle /°
H(45A)-C(45)-H(45C)	109.5	H(50B)-C(50)-H(50C)	109.5
H(45B)-C(45)-H(45C)	109.5	C(50)-C(51)-C(52)	111.8(5)
C(39)-C(46)-C(47)	113.0(3)	C(50)-C(51)-H(51A)	109.3
C(39)-C(46)-C(48)	110.3(3)	C(52)-C(51)-H(51A)	109.3
C(47)-C(46)-C(48)	109.6(4)	C(50)-C(51)-H(51B)	109.3
C(39)-C(46)-C(49)	109.1(3)	C(52)-C(51)-H(51B)	109.3
C(47)-C(46)-C(49)	105.9(4)	H(51A)-C(51)-H(51B)	107.9
C(48)-C(46)-C(49)	108.8(3)	C(53)-C(52)-C(51)	119.7(5)
C(46)-C(47)-H(47A)	109.5	C(53)-C(52)-H(52A)	107.4
C(46)-C(47)-H(47B)	109.5	C(51)-C(52)-H(52A)	107.4
H(47A)-C(47)-H(47B)	109.5	C(53)-C(52)-H(52B)	107.4
C(46)-C(47)-H(47C)	109.5	C(51)-C(52)-H(52B)	107.4
H(47A)-C(47)-H(47C)	109.5	H(52A)-C(52)-H(52B)	106.9
H(47B)-C(47)-H(47C)	109.5	C(54)-C(53)-C(52)	120.2(6)
C(46)-C(48)-H(48A)	109.5	C(54)-C(53)-H(53A)	107.3
C(46)-C(48)-H(48B)	109.5	C(52)-C(53)-H(53A)	107.3
H(48A)-C(48)-H(48B)	109.5	C(54)-C(53)-H(53B)	107.3
C(46)-C(48)-H(48C)	109.5	C(52)-C(53)-H(53B)	107.3
H(48A)-C(48)-H(48C)	109.5	H(53A)-C(53)-H(53B)	106.9
H(48B)-C(48)-H(48C)	109.5	C(55)-C(54)-C(53)	123.3(9)
C(46)-C(49)-H(49A)	109.5	C(55)-C(54)-H(54A)	106.5
C(46)-C(49)-H(49B)	109.5	C(53)-C(54)-H(54A)	106.5
H(49A)-C(49)-H(49B)	109.5	C(55)-C(54)-H(54B)	106.5
C(46)-C(49)-H(49C)	109.5	C(53)-C(54)-H(54B)	106.5
H(49A)-C(49)-H(49C)	109.5	H(54A)-C(54)-H(54B)	106.5
H(49B)-C(49)-H(49C)	109.5	C(54)-C(55)-H(55A)	109.5
C(51)-C(50)-H(50A)	109.5	C(54)-C(55)-H(55B)	109.5
C(51)-C(50)-H(50B)	109.5	H(55A)-C(55)-H(55B)	109.5
H(50A)-C(50)-H(50B)	109.5	C(54)-C(55)-H(55C)	109.5
C(51)-C(50)-H(50C)	109.5	H(55A)-C(55)-H(55C)	109.5
H(50A)-C(50)-H(50C)	109.5	H(55B)-C(55)-H(55C)	109.5

Table 82. Anisotropic displacement parameters ($\text{\AA}^2 \times 10^3$) for (R,M)-**287**. The anisotropic displacement factor exponent takes the form: $-2\pi^2 [h^2 a^{*2} U^{11} + \dots + 2 h k a^* b^* U^{12}]$

	U^{11}	U^{22}	U^{33}	U^{23}	U^{13}	U^{12}
Ti(1)	24(1)	27(1)	25(1)	-2(1)	-3(1)	-2(1)
O(1)	31(1)	43(1)	32(1)	-6(1)	-7(1)	-5(1)
N(1)	26(1)	26(1)	27(1)	-2(1)	-1(1)	-1(1)
C(1)	71(3)	245(8)	60(3)	65(4)	-42(3)	-101(4)
O(2)	29(1)	40(1)	29(1)	-3(1)	-2(1)	-5(1)
C(2)	44(2)	117(4)	57(2)	15(2)	-15(2)	-39(2)
O(3)	32(1)	34(1)	35(1)	-6(1)	-8(1)	2(1)
C(3)	69(3)	97(3)	62(3)	27(2)	-31(2)	-31(3)
O(4)	31(1)	37(1)	36(1)	2(1)	-2(1)	-6(1)
C(4)	27(1)	29(1)	30(2)	-5(1)	0(1)	0(1)
C(5)	25(1)	29(1)	34(2)	2(1)	-1(1)	2(1)
C(6)	29(1)	37(1)	31(1)	1(1)	-5(1)	0(1)
C(7)	28(1)	41(2)	35(2)	8(1)	0(1)	-1(1)
C(8)	36(2)	33(1)	28(2)	3(1)	3(1)	-1(1)
C(9)	33(1)	29(1)	29(1)	-1(1)	-3(1)	5(1)
C(10)	36(1)	39(2)	28(2)	-1(1)	-2(1)	3(1)
C(11)	38(2)	56(2)	44(2)	5(2)	-5(1)	14(1)
C(12)	52(2)	43(2)	41(2)	-5(1)	-6(2)	-11(2)
C(13)	48(2)	49(2)	26(2)	0(1)	-1(1)	3(1)
C(14)	32(2)	58(2)	39(2)	10(2)	0(1)	-8(1)
C(15)	38(2)	185(6)	50(3)	30(3)	-10(2)	-40(3)
C(16)	47(2)	59(2)	56(2)	5(2)	8(2)	-12(2)
C(17)	37(2)	69(3)	81(3)	4(2)	13(2)	5(2)
C(18)	28(1)	32(1)	32(2)	0(1)	-4(1)	2(1)
C(19)	31(1)	27(1)	32(1)	2(1)	-4(1)	-4(1)
C(20)	32(1)	37(2)	51(2)	0(1)	-4(1)	-7(1)
C(21)	36(1)	24(1)	25(1)	0(1)	3(1)	-2(1)
C(22)	32(1)	23(1)	33(1)	3(1)	-3(1)	-2(1)
C(23)	33(1)	26(1)	37(2)	0(1)	-5(1)	-3(1)
C(24)	42(2)	23(1)	31(2)	-2(1)	-2(1)	-1(1)
C(25)	33(1)	28(1)	33(2)	-1(1)	1(1)	2(1)
C(26)	31(1)	26(1)	33(2)	2(1)	-2(1)	-2(1)
C(27)	25(1)	38(2)	39(2)	-4(1)	-1(1)	0(1)
C(28)	35(2)	48(2)	60(2)	0(2)	-1(2)	-13(1)
C(29)	35(2)	56(2)	38(2)	-3(1)	-5(1)	6(1)
C(30)	28(1)	57(2)	48(2)	-7(2)	-1(1)	6(1)
C(31)	43(2)	31(1)	34(2)	-5(1)	-6(1)	4(1)
C(32)	126(4)	73(3)	47(3)	-5(2)	-23(3)	25(3)
C(33)	80(3)	71(3)	62(3)	-28(2)	-13(2)	22(2)

Table 82 (cont)

	U^{11}	U^{22}	U^{33}	U^{23}	U^{13}	U^{12}
C(34)	75(3)	59(2)	89(4)	-25(2)	-5(2)	-13(2)
C(35)	36(1)	31(1)	25(1)	-1(1)	0(1)	-5(1)
C(36)	32(1)	32(1)	31(2)	1(1)	3(1)	-1(1)
C(37)	30(1)	29(1)	32(2)	-1(1)	3(1)	-5(1)
C(38)	34(1)	33(1)	33(2)	2(1)	-3(1)	-8(1)
C(39)	35(2)	33(1)	43(2)	6(1)	-4(1)	-4(1)
C(40)	37(2)	27(1)	47(2)	3(1)	-2(1)	-6(1)
C(41)	28(1)	31(1)	37(2)	-3(1)	2(1)	-5(1)
C(42)	35(2)	35(2)	41(2)	-1(1)	-1(1)	-12(1)
C(43)	32(2)	57(2)	54(2)	-3(2)	-1(1)	-9(1)
C(44)	53(2)	36(2)	54(2)	0(1)	-6(2)	-16(1)
C(45)	54(2)	51(2)	43(2)	-10(2)	2(2)	-15(2)
C(46)	38(2)	36(2)	59(2)	9(1)	-10(2)	-4(1)
C(47)	80(3)	65(3)	134(5)	42(3)	-71(3)	-21(2)
C(48)	66(3)	80(3)	99(4)	11(3)	1(3)	26(2)
C(49)	63(2)	55(2)	63(3)	17(2)	-16(2)	-3(2)
C(50)	97(4)	107(4)	84(4)	4(3)	23(3)	25(3)
C(51)	82(3)	80(3)	85(4)	-1(3)	26(3)	13(3)
C(52)	81(3)	99(4)	62(3)	-2(3)	10(2)	2(3)
C(53)	88(3)	91(4)	84(4)	7(3)	31(3)	19(3)
C(54)	127(5)	97(4)	143(6)	47(4)	72(5)	41(4)
C(55)	155(7)	106(5)	184(8)	50(5)	94(7)	39(5)